



National Library
of Canada

Bibliothèque nationale
du Canada

Canadian Theses Service

Services des thèses canadiennes

Ottawa, Canada
K1A 0N4

CANADIAN THESES

THÈSES CANADIENNES

NOTICE

The quality of this microfiche is heavily dependent upon the quality of the original thesis submitted for microfilming. Every effort has been made to ensure the highest quality of reproduction possible.

If pages are missing, contact the university which granted the degree.

Some pages may have indistinct print especially if the original pages were typed with a poor typewriter ribbon or if the university sent us an inferior photocopy.

Previously copyrighted materials (journal articles, published tests, etc.) are not filmed.

Reproduction in full or in part of this film is governed by the Canadian Copyright Act, R.S.C. 1970, c. C-30. Please read the authorization forms which accompany this thesis.

**THIS DISSERTATION
HAS BEEN MICROFILMED
EXACTLY AS RECEIVED**

AVIS

La qualité de cette microfiche dépend grandement de la qualité de la thèse soumise au microfilmage. Nous avons tout fait pour assurer une qualité supérieure de reproduction.

S'il manque des pages, veuillez communiquer avec l'université qui a conféré le grade.

La qualité d'impression de certaines pages peut laisser à désirer, surtout si les pages originales ont été dactylographiées à l'aide d'un ruban usé ou si l'université nous a fait parvenir une photocopie de qualité inférieure.

Les documents qui font déjà l'objet d'un droit d'auteur (articles de revue, examens publiés, etc.) ne sont pas microfilmés.

La reproduction, même partielle, de ce microfilm est soumise à la Loi canadienne sur le droit d'auteur, SRC 1970, c. C-30. Veuillez prendre connaissance des formules d'autorisation qui accompagnent cette thèse.

**LA THÈSE A ÉTÉ
MICROFILMÉE TELLE QUE
NOUS L'AVONS REÇUE**

Canada



National Library of Canada / Bibliothèque nationale du Canada

Ottawa, Canada
K1A 0N4

TC -

0-315-22934-9

CANADIAN THESES ON MICROFICHE SERVICE - SERVICE DES THÈSES CANADIENNES SUR MICROFICHE

PERMISSION TO MICROFILM - AUTORISATION DE MICROFILMER

• Please print or type - Écrire en lettres moulées ou dactylographier

AUTHOR - AUTEUR

Full Name of Author - Nom complet de l'auteur

JOHN SAMUEL

Date of Birth - Date de naissance

JUNE 07, 1953

Canadian Citizen - Citoyen canadien

Yes / Oui

No / Non

Country of Birth - Lieu de naissance

INDIA

Permanent Address - Résidence fixe

KANNYEL THEKKATHIL, THAMALLAKKAL
KARUVATTA, HARIPAD, KERALA
INDIA

THESIS - THÈSE /

Title of Thesis - Titre de la thèse

RADIOHALOGENATED PYRIMIDINE NUCLEOSIDES
AS POTENTIAL NON-INVASIVE DIAGNOSTIC AGENTS
FOR HERPES SIMPLEX ENCEPHALITIS

Degree for which thesis was presented /
Grade pour lequel cette thèse fut présentée

DOCTOR OF PHILOSOPHY

Year this degree conferred /
Année d'obtention de ce grade

FALL 1985

University - Université

UNIVERSITY OF ALBERTA

Name of Supervisor - Nom du directeur de thèse

LEONARD I WIEBE

AUTHORIZATION - AUTORISATION

THE UNIVERSITY OF ALBERTA

RADIOHALOGENATED PYRIMIDINE NUCLEOSIDES AS POTENTIAL
NON-INVASIVE DIAGNOSTIC AGENTS FOR HERPES SIMPLEX ENCEPHALITIS

by

(C)

JOHN SAMUEL

A THESIS

SUBMITTED TO THE FACULTY OF GRADUATE STUDIES AND RESEARCH
IN PARTIAL FULFILMENT OF THE REQUIREMENTS FOR THE DEGREE

OF DOCTOR OF PHILOSOPHY

IN

PHARMACEUTICAL SCIENCES

FACULTY OF PHARMACY AND PHARMACEUTICAL SCIENCES

EDMONTON, ALBERTA

FALL 1985

THE UNIVERSITY OF ALBERTA

RELEASE FORM

NAME OF AUTHOR JOHN SAMUEL

TITLE OF THESIS RADIOHALOGENATED PYRIMIDINE NUCLEOSIDES AS
POTENTIAL NON-INVASIVE DIAGNOSTIC AGENTS FOR
HERPES SIMPLEX ENCEPHALITIS

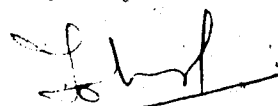
DEGREE FOR WHICH THESIS WAS PRESENTED DOCTOR OF PHILOSOPHY

YEAR THIS DEGREE GRANTED FALL 1985

Permission is hereby granted to THE UNIVERSITY OF ALBERTA LIBRARY to reproduce single copies of this thesis and to lend or sell such copies for private, scholarly or scientific research purposes only.

The author reserves other publication rights, and neither the thesis nor extensive extracts from it may be printed or otherwise reproduced without the author's written permission.

(SIGNED)



PERMANENT ADDRESS:

KANNIYEL THEKKATHIL
THAMALLACKAL, KARUVATTA
HARIPAD, KERALA, INDIA

DATED

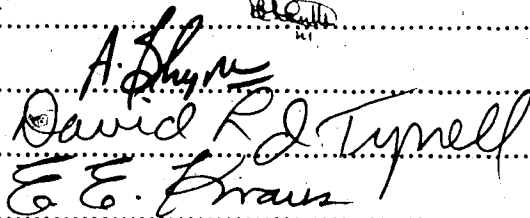
Oct 9, 1985

THE UNIVERSITY OF ALBERTA
FACULTY OF GRADUATE STUDIES AND RESEARCH

The undersigned certify that they have read, and recommend to the Faculty of Graduate Studies and Research, for acceptance, a thesis entitled Radiohalogenated Pyrimidine Nucleosides as Potential Non-Invasive Diagnostic Agents for Herpes Simplex Encephalitis submitted by John Samuel in partial fulfilment of the requirements for the degree of Doctor of Philosophy in Pharmaceutical Sciences.



Supervisor



External Examiner

Date Oct 8, 1988

DEDICATION

To
my parents

ABSTRACT

Herpes simplex encephalitis (HSE) is considered to be the most common fatal encephalitis in North America. At present brain biopsy is the only definitive means of diagnosing HSE. The aim of this study was to develop radiolabeled nucleoside analogs as biochemical probes for the non-invasive diagnosis of HSE.

[¹³¹I, ¹²⁵I, and ¹²³I]-(*E*)-5-(2-iodovinyl)-2'-deoxyuridine (IVdU) were synthesised by the reaction of (*E*)-5-(2-carboxyvinyl)-2'-deoxyuridine with radioactive iodide in the presence of chloramine-T. [¹³¹I]-IVdU was also prepared using the cuprous ion catalysed halogen isotope exchange method. [¹²³I]-(*E*)-5-(2-bromovinyl)-2'-deoxyuridine (BVdU) was synthesised by the reaction of (*E*)-5-(2-carboxyvinyl)-2'-deoxyuridine with [¹²³I]-NH₄Br in the presence chloramine-T and by direct neutron activation of BVdU containing natural abundance bromine.

In vitro uptake studies for [¹³¹I]-IVdU demonstrated its selective uptake in a deoxythymidine kinase positive herpes simplex virus type 1 (HSV-1)-infected cells. The uptake was dependent upon the duration of exposure of cells to [¹³¹I]-IVdU, the infecting dose of the virus, and the concentration of [¹³¹I]-IVdU. *In vivo* tissue distribution studies on [¹²⁵I]-IVdU showed a 5.4 to 6.4 times higher uptake in a HSV-1-infected rabbit brain relative to an uninfected brain at 1 hour after an intravenous injection of [¹²⁵I]-IVdU. The brain to blood ratio of radioactivity in infected rabbits was about 0.5. *In vivo* pharmacokinetic and metabolic studies of [¹³¹I]-IVdU in dogs showed its rapid metabolic degradation (biological half-life of about 3 minutes) to the corresponding base [¹³¹I]-(*E*)-5-(2-iodovinyl)uracil and [¹³¹I]-iodide. The renal excretion of radioactivity was extremely slow (8% of the total radioactivity injected was recovered from urine in 8 h). Diagnostic imaging in the planar and SPECT mode was performed using [¹³¹I]-IVdU and [¹²³I]-IVdU respectively in a HSE rabbit model. Neither planar nor tomographic images differentiated the HSV-1-infected brain from an uninfected brain.

In vitro uptake studies of

[5-¹³³I]-1-(2-deoxy-2-fluoro- β -D-ribofuranosyl)-5-iodouracil,

[2-¹⁴C]-1-(2-deoxy-2-fluoro- β -D-ribofuranosyl)-5-chlorouracil,

[2-¹⁴C]-1-(2-deoxy-2-fluoro- β -D-ribofuranosyl)-5-fluorouracil, and

[5-¹³³I]-1-(2-deoxy-2-fluoro- β -D-arabinofuranosyl)-5-iodouracil have exhibited selective

uptake in deoxythymidine kinase positive HSV-1-infected cells, suggesting that they deserve

further biological evaluation as potential non-invasive diagnostic agents for HSE.

ACKNOWLEDGEMENTS

I express my sincere thanks to :

Prof. Leonard I. Wiebe, Prof. Edward E. Knaus, and Prof. D. Lorne Tyrrell, my supervisors for their excellent guidance and constant encouragement throughout the course of these investigations ,

Dr. M. John Gill and Dr. Dorothy R. Tovell for their enthusiastic participation in this collaborative project,

Prof. Brian C. Lentle for making available the facilities for diagnostic imaging and Mr. James Thornton for assistance with imaging procedures;

Dr. Paul Reese for drawing majority of the figures and Ms. Siew Tang for typing assistance,

Dr. Richard Flanagan, Mr. Peter Ford, Mr. Takashi Iwashina, Mr. Graeme Boniface, Dr. Hemant Misra, Dr. John Mercer, Dr. Doug Abrams, Dr. Yip Lee, and Ms. Diane Jette for their helping hand at various stages of this work, and

Alberta Heritage Foundation for Medical Research for financial support in the form of a studentship.

Table of Contents

Chapter	Page
I. INTRODUCTION	1
A. Radionuclide Brain Imaging	1
B. Herpes Simplex Encephalitis	5
C. Nucleoside Analogs as Selective anti-HSV Drugs	16
II. MATERIALS AND METHODS	28
A. General	28
Chemicals and solvents	28
Radioisotopes	28
Instrumental analysis	29
Chromatography	30
Radioactivity measurements	30
B. Chemical Synthesis	31
5-Chloromercuri-2'-deoxyuridine	31
(E)-5-(2-Carboethoxyvinyl)-2'-deoxyuridine	31
(E)-5-(2-Carboxyvinyl)-2'-deoxyuridine	32
(E)-5-(2-Iodovinyl)-2'-deoxyuridine	32
(E)-5-(2-Bromovinyl)-2'-deoxyuridine	33
(E)-5-(2-Carboxyvinyl)-2'-deoxyuridine-3',5'-diacetate	34
(E)-5-(2-Iodovinyl)-2'-deoxyuridine-3',5'-diacetate	35
5-Formyl uracil	35
(E)-5-(2-Carboxyvinyl)uracil	35
(E)-5-(2-Iodovinyl)uracil	36
C. Radiochemical Synthesis	36
¹³¹ I, ¹²⁵ I, ¹²³ I-(E)-5-(2-Iodovinyl)-2'-deoxyuridine	36
¹³¹ I-(E)-5-(2-Iodovinyl)-2'-deoxyuridine-3',5'-diacetate	37

[¹²⁵ I]-5-(2-Bromovinyl)-2'-deoxyuridine (BVdU)	38
D. Quantitative Uptake Studies of Radiolabeled Nucleosides in HSV-1-Infected Cells <i>In Vitro</i>	38
Cells	38
Viruses	39
Radiolabeled nucleosides	39
Quantitation of cellular uptake of radiolabeled nucleosides by primary rabbit kidney (PRK) cells	40
E. Tissue Distribution of [¹³¹ I]-IVdU in a Herpes Simplex Encephalitis Animal Model	40
Animal model	40
Quantitative tissue distribution of [¹³¹ I]-IVdU	41
F. Pharmacokinetics and Metabolism of [¹³¹ I]-IVdU in Dogs	41
Quantitative radio high-pressure liquid chromatography (r-HPLC)	41
Metabolism of [¹³¹ I]-IVdU in blood <i>in vitro</i>	42
Metabolism of [¹³¹ I]-IVdU in blood <i>in vivo</i>	42
G. Diagnostic Imaging	43
Planar imaging	43
SPECT	43
III. RESULTS AND DISCUSSION	44
A. The Problem and the Approach	44
B. Chemical Synthesis	46
C. Radiochemical Syntheses	53
D. Quantitative Uptake Studies of ¹³¹ I-Labeled (E)-5-(2-Iodovinyl)-2'-deoxyuridine in Herpes Simplex Virus-Infected Cells <i>In Vitro</i>	60
Time-response curve for cellular uptake of [¹³¹ I]-IVdU	61
Effect of increasing infecting dose of virus on [¹³¹ I]-IVdU uptake	65
Dose-response curve for [¹³¹ I]-IVdU uptake	66

E. Tissue Distribution of [¹²⁵ I]-IVdU in a Herpes Simplex Encephalitis Animal Model	66
F. Pharmacokinetics and Metabolism of [¹³¹ I]-(E)-5-(2-Iodovinyl)-2'-deoxyuridine in Dogs	73
Metabolism of [¹³¹ I]-IVdU in blood <i>in vitro</i>	73
Metabolism of [¹³¹ I]-IVdU in dog <i>in vivo</i>	76
G. Diagnostic Imaging	84
H. Quantitative Uptake Studies of Radiolabeled Nucleosides in Herpes Simplex Virus-Infected Cells <i>In Vitro</i>	92
IV. SUMMARY AND CONCLUSIONS	104
REFERENCES	108
APPENDIX	125
A. Yield Calculation for the ⁸¹ Br(n,γ) ⁸² Br Nuclear Reaction	125

List of Tables

Table	Page
.1 Human Herpesviruses	8
.2 Deoxythymidine Kinase Isoenzymes of Various Origins	10
.3 Assessment of Different Non-Invasive Diagnostic Tests for HSE	14
.4 <i>In Vitro</i> Anti-HSV Activities of Some Second Generation Nucleoside Analogs	18
.5 Inhibition Constants (K_i) of Some Antiviral Nucleosides for Deoxythymidine Kinases of Various Origins	20
.6 Inhibition Constants of Some Antiviral Nucleoside Triphosphates for DNA Polymerases of Various Origins	23
.7 Radiochemical Synthesis of IVdU	57
.8 Preparation of [^{125}I]-BVdU	59
.9 Tissue Distribution of [^{125}I]-IVdU (Expressed As % Injected Dose Per Gram Tissue) in a Rabbit Model 1 Hour After i.v Injection of 0.74 MBq of [^{125}I]-IDdU (Mean of Two Animals with Range)	68
.10 Tissue Distribution of [^{125}I]-IVdU (Expressed as % Injected Dose per Gram Tissue) in a Rabbit Model 6 Hours After i.v Injection of 0.74 MBq of [^{125}I]-IVdU (Mean of Two Animals with Range)	69
.11 Tissue Distribution of [^{125}I]-IVdU (Expressed as Tissue to Blood Ratio) in a Rabbit Model 1 Hour After i.v Injection of 0.74 MBq of [^{125}I]-IVdU (Mean of Two Animals with Range)	70
.12 Tissue Distribution of [^{125}I]-IVdU (Expressed as Tissue to Blood Ratio) in a Rabbit Model 6 Hours After i.v Injection 0.74 MBq of [^{125}I]-IVdU (Mean of Two Animals with Range)	71
.13 Recovery of Radioactivity from Urine for Various Times After i.v Injection of [^{131}I]-IVdU (Mean of Two Experiment with Range)	80
.14 <i>In Vitro</i> Anti-HSV Activity of Some 5-Halogenated 1-(2-deoxy-2-fluoro- β -D-arabinofuranosyl)-uracils	96
.15 Percent Uptake of Radiolabeled Nucleoside Analogs in HSV-1 (TK ⁻)-Infected cells at 4 h and 24 h	102

List of Figures

Figure	Page
1 Diagram of a Virion of Herpes Simplex Virus.	6
2 Some Second Generation Nucleoside Analogs with Antiherpes Activity.	17
3 Selective Metabolic Trapping of (<i>E</i>)-5-(2-Halovinyl)-2'-deoxyuridines in Herpes Simplex Virus-Infected Cells.	45
4 Chemical Structure for (<i>E</i>)-5-(2-Halovinyl)-2'-deoxyuridines.	47
5 General Synthetic Route for the Synthesis of IVdU and BVdU.	48
6 Reaction Mechanism for Coupling of Dilithium Palladium Tetrachloride with 5-Chloromercuri Nucleosides.	49
7 Synthesis of IVdU and BVdU using the Chloramine-T Method.	51
8 Synthesis of IVdU-3',5'-diacetate.	52
9 Synthesis of (<i>E</i>)-5-(2-iodovinyl)uracil.	54
10 Synthesis of Radiohalogenated IVdU and BVdU.	56
11 Time-Response Curve for [¹³¹ I]-IVdU Uptake in HSV-1 (TK ⁺) (n=3) and Mock-Infected (n=2) PRK cells. (Mean and Range).	62
12 Effect of Increasing the Titer of the Infecting Dose on the Uptake of [¹³¹ I]-IVdU in HSV-1 (TK ⁺) (n=3), HSV-1 (TK ⁻) (n=2), Mock-Infected Cells (n=3) (Mean and Range).	63
13 Effect of Increasing Concentrations of [¹³¹ I]-IVdU on its Uptake in HSV-1 (TK ⁺) (n=3), HSV-1 (TK ⁻) (n=2), Mock-Infected Cells (n=2) (Mean and Range).	64
14 A Typical Radio High-Pressure Liquid Chromatogram of Plasma Sample Containing [¹³¹ I]-IVdU and its Metabolites.	74
15 Metabolites of [¹³¹ I]-IVdU in Blood <i>In Vitro</i>	76
16 Metabolites of [¹³¹ I]-IVdU (specific activity, 1665 MBq /mmol) in Dogs <i>In Vivo</i> (n=2).	78
17 Metabolites of [¹³¹ I]-IVdU (specific activity, 37 TBq /mmol) in Dog <i>In Vivo</i> (n=1).	79
18 Schematic Presentation of the Metabolism of [¹³¹ I]-IVdU in Dogs <i>in vivo</i>	82
19 Planar Whole Body Image of an Uninfected Rabbit 1 h After an Intravenous Injection of [¹³¹ I]-IVdU.	85

Figure	Page
.20 Planar Image (Head) of an HSV-1-infected Rabbit 1 h After an Intravenous Injection of [¹³¹ I]-IVdU.	86
.21 Chemical Structures for 1-(2-deoxy-2-fluoro-β-D-ribofuranosyl)-5-halouracils and 1-(2-deoxy-2-fluoro-β-D-arabinofuranosyl)-5-halouracils.	94
.22 <i>In Vitro</i> Uptake of [5- ¹³¹ I]-FIRU in HSV-1 (TK ⁺) (n=5), HSV-1 (TK ⁻) (n=4), and Mock-Infected Cells (n=4)	98
.23 <i>In Vitro</i> Uptake of [2- ¹⁴ C]-FCRU in HSV-1 (TK ⁺) (n=5), HSV-1 (TK ⁻) (n=4), and Mock-Infected Cells (n=4)	99
.24 <i>In Vitro</i> Uptake of [2- ¹⁴ C]-FFRU in HSV-1 (TK ⁺) (n=5), HSV-1 (TK ⁻) (n=4), and Mock-Infected Cells (n=4)	100
.25 <i>In Vitro</i> Uptake of [5- ¹³¹ I]-FIAU in HSV-1 (TK ⁺) (n=5), HSV-1 (TK ⁻) (n=4), and Mock-Infected Cells (n=4)	101

List of Plates

Plate	Page
.1 SPECT Images of an Uninfected Rabbit 30 min after Intracarotid Injection of [¹²³ I]-IVdU	89
.2 SPECT Images of an HSV-1-Infected Rabbit 30 min after Intracarotid Injection of [¹²³ I]-IVdU	91

List of Abbreviations

ACG	9-(2-hydroxyethoxymethyl)guanine
ACG-MP	9-(2-hydroxyethoxymethyl)guanine-5'-monophosphate
ACG-TP	9-(2-hydroxyethoxymethyl)guanine-5'-triphosphate
ara-A	9- β -D-arabinofuranosyl adenine
ara-AMP	9- β -D-arabinofuranosyl adenine-5'-monophosphate
ATP	adenosine-5'-triphosphate
BBB	blood-brain barrier
BME	Basal Medium Eagle's
Bq	Becquerel(s)
BVdU	(<i>E</i>)-5-(2-bromovinyl)-2'-deoxyuridine.
BVdU-DP	(<i>E</i>)-5-(2-bromovinyl)-2'-deoxyuridine-5'-diphosphate
BVdU-MP	(<i>E</i>)-5-(2-bromovinyl)-2'-deoxyuridine-5'-monophosphate
BVdU-TP	(<i>E</i>)-5-(2-bromovinyl)-2'-deoxyuridine-5'-triphosphate
BVU	(<i>E</i>)-5-(2-bromovinyl)uracil
C	cytosine
°C	degree Celsius
cm	centimeter(s)
CMV	cytomegalovirus
CNS	central nervous system
CPM	counts per minute
CSF	cerebrospinal fluid
CT	computed tomography
CTP	cytidine-5'-triphosphate
dATP	deoxyadenosine-5'-triphosphate
dC	deoxycytidine
dCMP	deoxycytidine-5'-monophosphate

dCTP	deoxycytidine-5'-triphosphate
dGDP	deoxyguanosine-5'-diphosphate
dGTP	deoxyguanosine-5'-triphosphate
DHPG	9-[(1,3-dihydroxy-2-propoxy)methyl]guanine
DMF	dimethyl formamide
DNA	deoxyribonucleic acid
dT	deoxythymidine
dTDP	deoxythymidine-5'-diphosphate
dTMP	deoxythymidine-5'-monophosphate
DTPA	diethylene triamine pentacetic acid
dTTP	deoxythymidine-5'-triphosphate
dU	deoxyuridine
dUTP	deoxyuridine-5'-triphosphate
EBV	Epstein-Barr virus
EEG	electroencephalography
ECT	emission computed tomography
FDG	2-deoxy-2-fluoro-D-glucose
FDG-6-P	2-deoxy-2-fluoro-D-glucose-6-phosphate
FBAU	1-(2-deoxy-2-fluoro- β -D-arabinofuranosyl)-5-bromouracil
FBRU	1-(2-deoxy-2-fluoro- β -D-ribofuranosyl)-5-bromouracil
FCAU	1-(2-deoxy-2-fluoro- β -D-arabinofuranosyl)-5-chlorouracil
FCRU	1-(2-deoxy-2-fluoro- β -D-ribofuranosyl)-5-chlorouracil
FFAU	1-(2-deoxy-2-fluoro- β -D-arabinofuranosyl)-5-fluorouracil
FFRU	1-(2-deoxy-2-fluoro- β -D-ribofuranosyl)-5-fluorouracil
FIAC	1-(2-deoxy-2-fluoro- β -D-arabinofuranosyl)-5-iodocytosine
FIAC-MP	1-(2-deoxy-2-fluoro- β -D-arabinofuranosyl)-5-iodocytosine-5'-monophosphate

FIAC-TP	1-(2-deoxy-2-fluoro- β -D-arabinofuranosyl)-5-iodocytosine-5'-triphosphate
FIAU	1-(2-deoxy-2-fluoro- β -D-arabinofuranosyl)-5-iodouracil
FIAU-MP	1-(2-deoxy-2-fluoro- β -D-arabinofuranosyl)-5-iodouracil-5'-monophosphate
FIRU	1-(2-deoxy-2-fluoro- β -D-ribofuranosyl)-5-iodouracil
FMAU	1-(2-deoxy-2-fluoro- β -D-arabinofuranosyl)-5-methyluracil
G	guanine
g	gram(s)
GBq	gigaBecquerel
GDP	guanosine-5'-diphosphate
GMP	guanosine-5'-monophosphate
GTP	guanosine-5'-triphosphate
h	hour(s)
^1H NMR	proton magnetic resonance spectra
HPLC	high-pressure liquid chromatography
hrms	high resolution mass spectra
HSE	herpes simplex encephalitis
HSV	herpes simplex virus
HSV-1	herpes simplex virus type 1
HSV-2	herpes simplex virus type 2
Hz	hertz
id	internal diameter
ID ₅₀	inhibitory dose-50
IdU	5-iodo-2'-deoxyuridine
i.v	intravenous
IVdU	(<i>E</i>)-5-(2-iodovinyl)-2'-deoxyuridine

IVdU-DP	(<i>E</i>)-5-(2-iodovinyl)-2'-deoxyuridine-5'-diphosphate
IVdU-MP	(<i>E</i>)-5-(2-iodovinyl)-2'-deoxyuridine-5'-monophosphate
IVdU-TP	(<i>E</i>)-5-(2-iodovinyl)-2'-deoxyuridine-5'-triphosphate
IVU	(<i>E</i>)-5-(2-iodovinyl)uracil
KBq	kiloBecquerel
<i>K_i</i>	inhibition constant
L	litre(s)
M	molar
MBq	megaBecquerel
MEM	Minimum Essential Medium
mg	milligram(s)
min	minute(s)
mL	millilitre(s)
mM	millimolar
μ M	micromolar
mmol	millimole(s)
μ mol	micromole(s)
mol	mole(s)
mp	melting point
MS	mass spectra
MW	molecular weight
N	normal
n	neutron(s)
<i>n</i>	number(s)
NBS	N-bromosuccinimide
NCA	no-carrier-added
NIS	N-iodosuccinimide

NIAID	National Institute of Allergy and Infectious Diseases
ng	nanogram(s)
nmol	nanomole(s)
NMR	nuclear magnetic resonance
nmol	nanomole(s)
P	partition coefficient (octanol : water)
PBS	phosphate buffered saline
PFU	plaque forming unit(s)
pI	isoelectric point
PET	positron emission tomography
PRK-	primary rabbit kidney
RDP	ribonucleoside diphosphate
R _f	retardation factor
r-HPLC	radio high-pressure liquid chromatography
RIPA	radioimmune precipitation assay
s	second(s)
S	sedimentation coefficient
SPECT	single photon emission computed tomography
TBq	TeraBecquerel
TD ₅₀	toxic dose-50
TK	deoxythymidine kinase
TK ⁺	deoxythymidine kinase positive
TK ⁻	deoxythymidine kinase negative
TLC	thin layer chromatography
TLRC	thin layer radio chromatography
TS	thymidylate synthetase
UV	ultraviolet spectra

UTP

uridine-5'-triphosphate

VZV

varicella-zoster virus

I. INTRODUCTION

A. Radionuclide Brain Imaging

The imaging of brain using radionuclides originated in 1948, when George Moore at the University of Minnesota reported the detection of brain tumors with [^{131}I]-diiodofluorescein using a Gieger-Muller counter (1). Advances in the subsequent years included the development of the rectilinear scanners, which preceded the introduction of scintillation camera (2-4). In 1958 Anger, at the University of California at Berkeley, introduced an imaging system with no moving parts (5). This was a major contribution to neuronuclear medicine since dynamic rapid-sequence flow studies of the brain could now be done. When $^{99\text{m}}\text{Tc}$ -labeled pertechnetate became available as a radiopharmaceutical for brain imaging in 1964 (6), radionuclide brain scans became widely used in the late 1960s and early 1970s. A variety of lesions involving breakdown of the blood-brain barrier (BBB) could be detected non-invasively by this method. However, these images suffered from poor spatial resolution and provided little anatomical or functional detail.

The concept of emission tomography (ECT) for three dimensional scans was introduced by Kuhl and Edward in 1963 (7). An idea ahead its time, this methodology had little immediate impact in the medical field, probably due to the lack of appropriate radiopharmaceuticals and inadequate instrumentation. However, the same principle of reconstruction tomography found an important application in X-ray transmission computed tomography (CT) in 1973 (8, 9). The brain images obtained by CT were superior to conventional radionuclide brain images with respect to spatial resolution. In the late 1970s, CT became the best method for evaluation of many neurological disorders, resulting in a dramatic decline in the number of radionuclide studies of brain. However, with recent developments in the design of radiopharmaceuticals for functional imaging of brain and advances in radiation detection systems, ECT has reemerged as an important brain imaging technique.

The physical principles of tomography have been reviewed (10, 11). Tomographic imaging requires the acquisition of a series of images at different angular orientations with respect to the target organ. These images are then processed using a filtered back projection algorithm to obtain tomographic images showing the distribution of the radionuclide in the tissue section of interest (11). There are two types of ECT *viz* positron emission tomography (PET) and single photon emission computed tomography (SPECT). They differ with respect to the type of radionuclide used and the detection system required for imaging. PET imaging requires the use of positron emitting radionuclides such as ^{11}C , ^{13}N , ^{15}O and ^{18}F . This imaging technique detects annihilation radiation by coincidence counting. SPECT can be performed using γ -ray emitting nuclides such as $^{99\text{m}}\text{Tc}$ and ^{123}I . The detection system operates in the single photon mode. The inherent advantages and disadvantages of PET and SPECT have been reviewed (12). The annihilation coincidence detection used in PET offers higher spatial resolution than that obtained by single photon detection used in SPECT. A PET unit requires, in most instances, facilities for on-site production of the radionuclides and preparation of the radiopharmaceuticals, since medically useful positron emitting nuclides have extremely short half-lives. PET programs require a large financial investment, thereby limiting their availability to medical research institutions. Since the cost factor for SPECT is more favourable than for PET, at present it is the most commonly used ECT in general hospitals.

Radiopharmaceuticals used in brain imaging may be classified into two major groups : non-specific agents used for the evaluation of vascularity of brain and metabolic analogs used for functional imaging. The non-specific agents include macromolecules such as $^{99\text{m}}\text{Tc}$ - or ^{125}I -labeled human serum albumin and small molecules such as [$^{99\text{m}}\text{Tc}$]- diethylene triamine pentaacetic acid (DTPA) and [$^{99\text{m}}\text{Tc}$]-glucoheptonate. These radiopharmaceuticals are used to detect brain lesions associated with increased regional vascularity and/or permeability using tomographic or planar brain imaging techniques. Radiopharmaceuticals for the evaluation of brain function are designed as probes for regional cerebral metabolism. They include probes for energy metabolism, neurotransmitters and their analogs, and centrally acting drugs. These

studies require imaging in the tomographic (PET or SPECT) mode.

Transport of molecules across the blood-brain barrier (BBB) is one of the important factors to be considered in the design of radiopharmaceuticals for brain imaging. The BBB, a unique microanatomic feature of brain, constitutes a barrier to the passage of compounds not required for brain metabolism and thus limits the movement of potentially toxic substances from blood to brain (13). Chemicals entering the brain cells do so either by carrier mediated transport (eg: glucose) or by passive diffusion across the lipid bilayer by virtue of their high lipid solubility (eg: oxygen). The rationale for the use of non-specific radiopharmaceuticals is based on their inability to cross the intact BBB. Several pathological conditions of the central nervous system (CNS) are associated with regional breakdown of the BBB.

Radiopharmaceuticals used in the evaluation of the BBB will be useful to delineate such areas using a diagnostic brain scan.

The ability to cross the BBB is an essential requirement of radiopharmaceuticals designed as probes of brain metabolism. An excellent example of a radiopharmaceutical entering the brain by carrier mediated transport is [^{18}F]-2-deoxy-2-fluoro-D-glucose (FDG) (14). The hexose carrier in the BBB has stringent stereochemical requirements for all positions of the substrate except for C₂ (15, 16). 2-Deoxy-2-fluoro-D-glucose therefore satisfies the structural requirements for the transport across the BBB. The design of [^{18}F]-fluoro analogs as radiopharmaceuticals, which retain the BBB transport characteristics of the natural substrates has also been successfully applied to aminoacid derivatives (eg: [^{18}F]-6-fluoro-L-dopa) (17, 18).

An alternate approach to facilitate the BBB transport of radiopharmaceuticals is to increase their lipophilicity. The brain capillary permeability of a compound is related to its octanol/water partition coefficient (P) and molecular weight (19). For compounds with molecular weight below 400, increasing lipophilicity will improve the brain capillary permeability. Dischino *et al* have reported a parabolic relationship between log P (partition coefficient for octanol/water) values and brain extractability for a group of ^{11}C -labeled

compounds and have suggested an optimal log P range of 0.9 to 2.5 for radiopharmaceuticals designed to cross the BBB by virtue of their lipid solubility (20).

The design of metabolic analogs as biochemical probes for cerebral function is one important approach to the development of radiopharmaceuticals for brain imaging. The biochemical rationale behind the development of [^{18}F]-FDG as a non-invasive probe for quantitation of regional cerebral glucose metabolism illustrates such an approach (21, 22). Brain meets its energy requirements exclusively from D-glucose. Hence, the rate of cerebral glucose metabolism could serve as an important index for neurological investigations. FDG is a good substrate for hexokinase (23) and therefore will be phosphorylated to the 6-phosphate (FDG-6-P). FDG-6-P is not subject to metabolism by the enzymes glucose-6-phosphate dehydrogenase and glucose phosphate isomerase, unlike glucose-6-phosphate (24, 25). There is very little glucose-6-phosphatase activity in the brain (26, 27). Hexose-6-phosphates exhibit very low permeability across the plasma membrane. Therefore FDG-6-P, once formed, is trapped in cerebral tissue. This metabolic trapping of [^{18}F]-FDG can be monitored non-invasively by PET and can be used as an index of regional cerebral glucose metabolism. Pharmacokinetic models of FDG utilization could be used for the tomographic quantitation of regional cerebral glucose metabolic rate (28). The clinical applications of [^{18}F]-FDG have been recently reviewed (14, 29).

A similar principle has been used to study dopamine metabolism in brain (17, 18). Dopamine does not cross the BBB and is produced in brain by decarboxylation of its immediate precursor L-dopa. This amino acid crosses the BBB by an active transport process. [$6\text{-}^{18}\text{F}$]-L-dopa possesses transport characteristics similar to dopa and is a substrate for a cerebral aromatic acid decarboxylase. PET studies using this compound in normal human subjects suggests its potential as a probe for quantitative regional cerebral metabolism of dopamine (18). Drugs acting on the CNS such as chlorpromazine and flunitrazepam labeled with ^{14}C have been used in PET studies for non-invasive mapping of specific receptors in brain (30, 31).

Besides ECT and CT another important tomographic mode of imaging - nuclear magnetic resonance (NMR) imaging - has recently become available as a non-invasive tool for neurological investigations (32, 33). The full potential of ECT and NMR in brain imaging remains to be explored. Therefore it is difficult to project the relative importance of these three imaging modalities for the future. The greatest strength of CT is its ability to show intracranial morphology with high resolution. It is quite likely that NMR imaging may provide this in the near future. One desirable feature of NMR imaging is that it does not use ionising radiation. ECT is advantageous since it provides information on regional brain biochemistry and therefore is of value in understanding the biochemical aspects of diseases and objective monitoring of therapy. The tracer technique used in ECT would seem to be superior to other imaging modalities with respect to flexibility of studying specific biochemical pathways by determining biochemical components that contribute to an observed disturbance. Since each of these imaging methods have different advantages, it is expected that the information derived would be complementary and would be helpful in acquiring the overall pathophysiological picture of the CNS.

B. Herpes Simplex Encephalitis

Herpes simplex virus (HSV), the causative organism for herpes simplex encephalitis (HSE), belongs to the family of herpetoviridae, commonly known as the herpesvirus group (34). The core of the herpesviruses consists of a single molecule of double stranded DNA with a molecular weight (MW) of about 100×10^6 , wrapped around an associated protein (Fig 1). This DNA-protein core is enclosed in a protein capsid shell with an icosahedral symmetry. The tegument surrounding the capsid consists of asymmetrically distributed globular material. A lipid bilayer membrane envelops the tegument and is studded with glycoprotein projections. There are two main immunological variants of HSV, type 1 and type 2. The common clinical manifestations of HSV-1 are herpes labialis (cold sore), gingivostomatitis, and keratoconjunctivitis. The most common site of HSV-2 infection is the genital organs and the

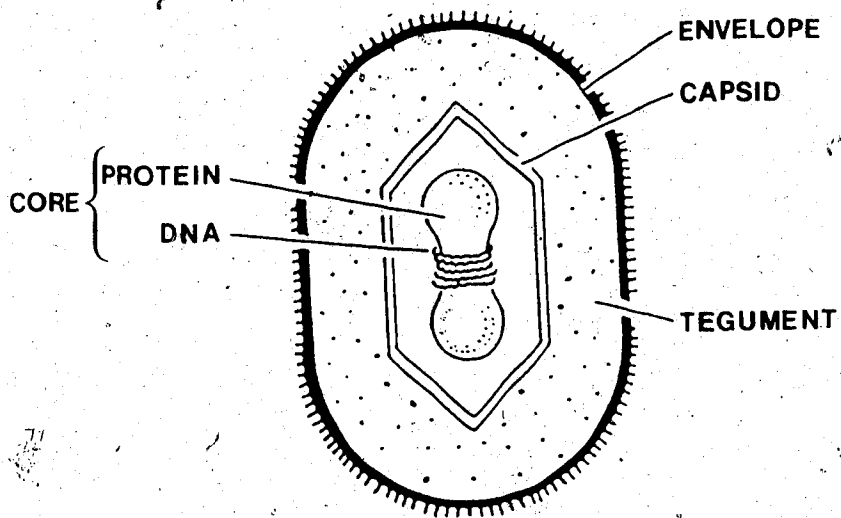


Fig. 1 Diagram of a Virion of Herpes Simplex Virus.

infection is usually transmitted venereally. In addition to HSV, the major human pathogens of herpesviruses are varicella-zoster virus (VZV), cytomegalovirus (CMV), and Epstein-Barr virus (EBV). Some characteristic of herpesviruses including the human diseases caused by them are shown in Table 1.

The pathogenesis of HSV infections has been extensively reviewed (35-39). Following a primary infection, both HSV-1 and HSV-2 establish latent infection in the neurons of the sensory ganglia innervating the site of primary infection. The infected ganglia becomes a reservoir of latent virus, which upon reactivation, may establish a recurrent infection. The details of the mechanisms for latency and recurrence have not been fully elucidated, and some aspects are still the subject of opposing views. The virus is believed to reach the ganglia by centripetal axonal migration (36, 40-42). However, some reports indicate that under certain circumstances the virus may reach the site of latency as a result of viremia (43, 44). During the latent state, the infectious virus cannot be isolated from cell-free ganglia homogenates. Ritchie and Timbury have discussed the possibility of insertion of the viral genome into the host DNA during latency (45). A variety of stimuli including sunlight, emotional stress, menstruation, and surgical procedures have been reported to be associated with the reactivation of the latent virus (38, 46). The mechanism(s) of reactivation by these stimuli is (are) not yet clear. Hill and Blyth have suggested that the reactivation process is mediated through an increased synthesis of prostaglandins (47-49). However, there is no definitive evidence supporting this theory.

HSV induces synthesis of many virus-specific proteins in the infected cells. Among these, the enzymes deoxythymidine kinase (TK) and DNA polymerase have received considerable attention as potential targets for the design of antiviral drugs. TK is a 'salvage pathway' enzyme that catalyzes the phosphorylation of deoxythymidine (dT) to the corresponding 5'-monophosphate (dTMP). TK isoenzymes of various origins have been extensively studied (50-53). Human cells contain two types of TK enzymes : deoxythymidine kinase F (TK-F) found primarily in the cytosol fraction and deoxythymidine kinase A (TK-A)

Table 1. Human Herpesviruses.

Virus	Molecular Weight (10 ⁶) (Approximate)	DNA G + C Content (%)	Site of Latency	Human Disease(s)
HSV-1	100	70	Neurons	Herpes Labialis, Keratoconjunctivitis, Herpes Encephalitis
HSV-2	100	69	Neurons	Genital herpes, Neonatal Herpes
VZV	80-100	46	Neurons	Chicken Pox, Shingles
CMV	130-150	58.5	Epithelial or White Blood Cells	Cytomegalic Inclusion Disease
EBV	110-115	57-59	Lymphocytes	Infectious Mononucleosis, Burkitt's Lymphoma, Nasopharyngeal Carcinoma

G = Guanine
C = Cytosine

localized mainly in the mitochondrial matrix (50). TK-A does not play a significant role in the generation of dT phosphates for nuclear DNA synthesis. HSV-1- and HSV-2-encoded TK isoenzymes are distinctively different from human TKs. The HSV-1- and HSV-2-induced TK enzymes differ antigenically from the human enzymes. With respect to molecular weight (MW), isoelectric point (pI), phosphate donor specificities and substrate specificities, the virus-encoded enzymes differ from TK-F, but resemble TK-A (Table 2) (50, 53-58). However, HSV-induced TKs have larger sedimentation coefficients (S) than the mitochondrial enzyme. Unlike TK-A, the viral enzymes are not subject to feed back inhibition by deoxycytidine triphosphate (dCTP). The broad substrate specificities of HSV-encoded enzymes is of special interest for the design of selective antiviral agents (59-61).

The virus-induced TK enzymes play a very important role in the DNA replication of HSV. The dTMP produced by TK is a precursor of dTTP, which is one of the four deoxyribonucleoside triphosphates required for DNA synthesis. dTTP is also required as an allosteric effector for the reduction of guanosine diphosphate (GDP) to deoxyguanosine diphosphate (dGDP) by the host enzyme ribonucleoside diphosphate (RDP) reductase (62, 63). dGDP is the precursor of deoxyguanosine triphosphate (dGTP). The intracellular concentration of dGTP is usually significantly lower than that of the other three deoxyribonucleoside triphosphates dATP, dCTP, and dTTP and therefore is a critical factor controlling the rate of DNA synthesis. Kit *et al* have pointed out that the major role of TK enzymes in the rapid synthesis of DNA may in fact be its indirect stimulation of the biosynthesis of dGTP (50). An HSV-1-induced RDP reductase has been recently isolated (64, 65). This enzyme appear to be not subject to significant allosteric modulation and therefore unlikely to be influenced by TK activity. The virus-encoded TK is considered to be important in relation to the pathogenesis and latency of HSV-1 and HSV-2. TK-deficient (TK⁻) mutants of HSV have been reported to be less pathogenic as compared to the TK-positive (TK⁺) strains (66). The expression of the TK gene is also observed to be an essential requirement for the establishment of HSV infection in sensory ganglia and therefore the latent stage of infection

Table 2. Deoxythymidine Kinase Isoenzymes of Various Origins

Enzyme	Molecular Weight	Isoelectric Point (pI)	Sedimentation Coefficient (S)	Phosphate Donor	Feed back Inhibitors	Natural Substrates
Human Cytosolic (TK-F)	90,000	9.7	5.2	ATP	dTTP	dT, dU
Human Mitochondrial (TK-A)	70,000	5.6	4.5	ATP, UTP CTP, GTP	dTTP dCTP	dT, dU
HSV-1	70,000	6.0-6.5	5.2	ATP, UTP CTP, GTP	dTTP	dT, dU, dC
HSV-2	70,000	6.3	4.9	ATP, UTP CTP, GTP	dTTP	dT, dU, dC

(67, 68).

The enzyme responsible for the incorporation of nucleotides into the growing polynucleotide chain is DNA polymerase. This enzyme is essential for DNA replication. Mammalian cells contain three classes of DNA polymerases designated as α , β , and γ (69). HSV-induced DNA polymerases differ from these three host cell enzymes with respect to molecular weight, elution profile on ion-exchange columns, primer template preferences and effect of monovalent and divalent cations (69-73). The unique features of HSV-induced DNA polymerases include their requirement for high salt concentration for maximal activity (74) and sensitivity to low phosphonoacetate concentrations (75). The virus-induced DNA polymerase enzymes are essential for the replication of HSV (76). The viral DNA polymerase is considered to be the primary target of the antiviral action of several selective antiviral drugs (61).

Herpes simplex encephalitis (HSE) is a rare clinical manifestation of HSV. However, it is considered to be the most common sporadic encephalitis in North America (77). Whitley *et al* have reviewed the epidemiological aspects of HSE (78). In a series of 113 biopsy-proven cases examined, HSE occurred in all age groups, in both sexes and was non-seasonal. HSE in adults is usually a focal infection and over 95% of the adult HSE are caused by HSV-1 (79, 80). Neonatal HSE is usually caused by HSV-2 and may be disseminated or localized (81). Untreated HSE is reported to be associated with a high mortality rate (70%) and severe morbidity (82).

The pathogenesis of HSE is not yet clearly understood. In neonatal HSE, the virus is most often transmitted from an infected maternal genital tract during delivery. Other less frequent routes including transplacental transmission also exist (83). Adult HSE may be caused by a primary infection or by reactivation of a latent infection (84). Restriction endonuclease analysis of viral DNA has been used to investigate the possible existence of neurovirulent strains of HSV-1 (85, 86). HSV-1 isolates used in these studies appeared to be different at the molecular level and showed no common denominator suggestive of neurovirulence (86, 87). In view of the small proportion of the DNA examined in these studies, results should not be

considered as conclusive evidence for nonexistence of neurovirulent strains of HSV. Potential routes responsible for viral spread from the site of latency have been investigated (88-92). The most common site of latency for HSV-1 is believed to be the trigeminal ganglia. Davis and Johnson have postulated that viral spread occurs from the trigeminal ganglia to the brain through tentorial nerves, which innervate the fascia near the temporal and frontal lobes (88). A more direct route involving the spread of the virus from the olfactory bulb has been proposed by other investigators (90-92). The olfactory spread theory has been supported by demonstrated presence of HSV in the olfactory bulb and degeneration in the olfactory tract in some HSE patients (90-92). It is also possible that brain itself could have been the site of latency (90). The detection of HSV-1 genome in human brain tissue supports this postulate (93, 94).

In adults, HSE causes localized tissue necrosis of brain usually in the frontal and temporal regions (95, 96). However, rare patients with infection of parietal lobe, occipital lobe and brain stem have also been reported (97-99). Pathological changes, evident from light and electron microscopy studies include lymphocyte infiltration, neuronal and glial cell loss, and eosinophilic intracellular inclusion bodies usually containing viral particles (82, 100, 101).

Clinical presentations of HSE are non-specific. Whitley *et al* have reviewed the clinical symptoms of 110 cases of biopsy-proven HSE (78). Alteration of consciousness, fever, headache, seizures all were common, but not uniform, among patients with HSE. Such clinical features could also be observed with nearly equal frequency among the biopsy-negative patients initially suspected of HSE. From these studies Whitley *et al* have concluded that there is no unique group of symptoms that distinguishes patients with HSE from those having other illness affecting the CNS.

Non-invasive methods investigated for the diagnosis of HSE include electroencephalography (EEG) (102, 103), X-ray transmission computed tomography (CT) (104, 105), and radionuclide brain imaging using [$^{99}\text{Tc}^{\text{m}}$]-sodium pertechnetate or chelates (106, 107). Whitley *et al* assessed the diagnostic value of these tests in a number of

biopsy-positive and biopsy-negative patients, all initially suspected of having HSE (78). A comparison of the sensitivities and specificities of the various diagnostic tests evaluated for HSE (Table 3) indicated that EEG was the most sensitive of these tests, but suffered from unacceptably high false positive results. Radionuclide and CT imaging showed higher specificity, but had unacceptably low sensitivity. Two immunological methods have been investigated as diagnostic tests for HSE. A ratio of serum to cerebrospinal fluid (CSF) concentrations of HSV antibodies lower than 20 has been proposed as indicative of HSE (108). Another method involving detection of HSV antigens in CSF has also been proposed (109). The low sensitivities of these methods particularly early in disease make them unreliable tests for definitive diagnosis of HSE.

A definitive diagnosis of HSE is currently achieved by brain biopsy and then identification of the virus by *in vitro* culture techniques (110, 111). The presence of the virus in the biopsy tissue may be demonstrated more rapidly by electron microscopy or immunofluorescence (79, 112). Brain biopsy as a diagnostic test has a sensitivity of 95% (79). The invasive nature of this procedure has been the major objection to its use (113). In a consecutive series of 50 brain biopsy studies, Kaufman *et al* have noted a total morbidity and mortality rate of 13% (110), whereas Bazra *et al* estimated these risks to be in the range of 0.5 to 2% (114). In view of the risks involved in brain biopsy, Caplan has argued in favour of blind therapy using ara-A in patients with clinical picture and non-invasive tests suggestive of HSE (115). This view is likely to gain increasing support with the availability of less toxic antiviral agents such as acycloguanosine (ACG) for the treatment of HSE. Whitley *et al* have pointed out the special benefit of brain biopsy in that, as well as confirming the diagnosis in the HSE positive cases, it may also provide alternate diagnosis for other treatable diseases in a significant number of HSE-negative patients (116). The present controversy associated with the diagnosis of HSE clearly illustrates the urgent need for the development of a specific and sensitive non-invasive test for HSE.

Table 3. Assessment of Different 'Non-Invasive' Diagnostic Tests for HSE

Diagnostic Test	Sensitivity (%)	Specificity (%)
Electroencephalography	81	41
Radionuclide Brain Imaging	50	86
Computed Tomography	59	78
Serum to CSF Antibody Ratio	50	81
HSV Antigen in CSF	64	86

Ara-A is the only drug currently licensed for the treatment of HSE (82, 116). Treatment with ara-A is estimated to decrease the mortality rate of HSE from 70% to 40% (116). The level of consciousness at the time of initiation of therapy and the age of the patient are the major factors influencing the therapeutic outcome. Prognosis is usually much better in patients below 30 years of age at all levels of consciousness. Ara-A therapy is most successful favouring complete recovery in patients within this age group, provided they were only lethargic at the beginning of therapy. Older patients, who are comatose at the time of treatment initiation are unlikely to benefit from ara-A. The toxic effects reported with use of this drug include nausea, vomiting, diarrhea, bone marrow suppression, tremor and confusion (116, 117). Due to its poor water solubility, the intravenous administration of ara-A requires a large fluid load. This poses a problem in HSE patients with cerebral edema. The use of ara-AMP, a prodrug of ara-A, has been proposed to overcome this problem (118). However, the National Institute of Allergy and Infectious Diseases (NIAID) collaborative clinical trials indicated that the patients who received ara-AMP did not benefit from therapy (119). It has been pointed out that this may be due to unfavourable factors related to the patient such as age and level of consciousness at the time of therapy initiation. A selective and specific drug acycloguanosine (ACG) is currently being investigated as a therapeutic agent for HSE. A recent multicenter study from Sweden has compared the therapeutic efficacy of ACG versus ara-A in 53 confirmed cases of HSE (120). They reported a significantly lower mortality rate for ACG treated patients (19%) as compared to ara-A treated patients (50%). Six months after the acute illness, 56% of ACG treated patients returned to normal life as compared to 13% of ara-A treated patients. These results suggest the superiority of ACG for the treatment of HSE relative to ara-A. More recent antiherpes drugs such as (*E*)-5-(2-bromovinyl)-2'-deoxyuridine (BVdU), 1-(2-deoxy-2-fluoro- β -D-arabinofuranosyl)-5-iodocytosine (FIAC), and 9-[(1,3-dihydroxy-2-propoxy)methyl]guanine (DHPG) await clinical evaluation as therapeutic agents for HSE.

C. Nucleoside Analogs as Selective anti-HSV Drugs

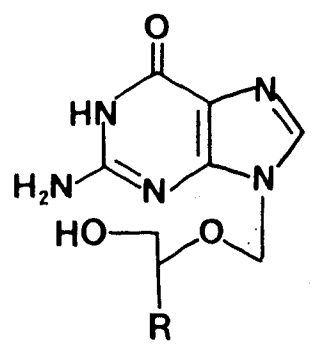
Three nucleoside analogs that have been used as therapeutic agents for herpes simplex infections during the past two decades are 5-iodo-2'-deoxyuridine (IdU), 5-trifluoromethyl-2'-deoxyuridine (trifluorothymidine, TFT) and 9- β -D-arabinofuranosyl adenine (adenine arabinoside, ara-A). These compounds are often referred to as first generation antiherpes drugs. In recent years several new analogs have been developed, which are superior in selectivity and/or potency to the first generation drugs. There are two major factors that have contributed to the development of these second generation nucleoside analogs. First, recent advances in nucleoside chemistry has increased the possibility for molecular modification of nucleosides, resulting in synthesis of numerous chemical analogs of naturally occurring nucleosides. Second, elucidation of the biochemical steps involved in HSV replication has revealed certain virus-specific enzymes which are potential targets for the design of antiviral drugs. The selective antiviral action of the nucleoside analogs has been reviewed recently. (61, 121, 122). The present discussion is focussed on the biochemical aspects of the selective antiherpes activity of the second generation nucleoside analogs and their metabolic degradation *in vivo*.

The most important selective nucleoside analogs which are active against HSV may be grouped into three categories :

1. acycloguanosine nucleosides,
2. (*E*)-5-(2-halovinyl)-2'-deoxyuridines and their analogs, and
3. 1-(2-deoxy-2-fluoro- β -D-arabinofuranosyl)pyrimidine analogs.

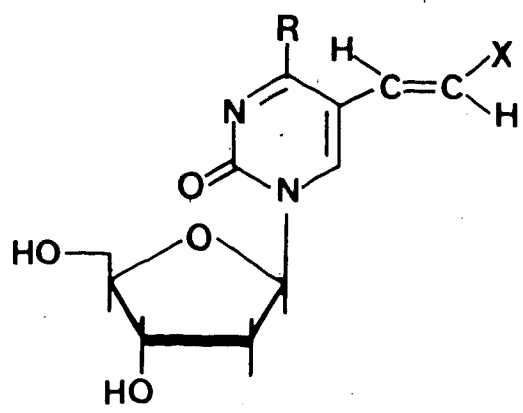
The chemical structures of these compounds are shown in Fig 2. These compounds have all been reported to be highly potent and selective in their action against HSV. The relative potencies of these compounds are listed in Table 4. While acycloguanosine nucleosides and 1-(2-deoxy-2-fluoro- β -D-arabinofuranosyl)pyrimidines are equally effective against HSV-1 and HSV-2 replication, (*E*)-5-(2-halovinyl)-2'-deoxyuridine analogs exhibit a 100-1000 fold greater potency against HSV-1 relative to HSV-2. The greatest selectivity index (TD_{50}/ID_{50})

Acycloguanosine Nucleosides



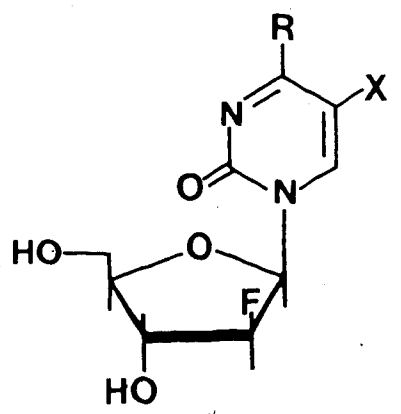
R	Compound
H	ACG
CH ₂ OH	DHPG

(E)-5-(2-Halovinyl)-2'-deoxyuridines and their Analogs



R	X	Compound
OH	Br	BVdU
OH	I	IVdU
NH ₂	Br	BVdC

1-(2-Deoxy-2-fluoro-β-D-arabinofuranosyl)pyrimidine Nucleosides



R	X	Compound
NH ₂	I	FIAC
OH	I	FIAU
OH	CH ₃	FMAU

Fig. 2 Some Second Generation Nucleoside Analogs with Antitherpes Activity.

Table 4. *In Vitro* Anti-HSV Activities of Some Second Generation Nucleoside Analogs

Compound	ID ₅₀ ¹ (μM)		TD ₅₀ ² (μM)	References
	HSV-1	HSV-2		
ACV	0.1	0.1	15-300	123-129,129,133
DHPG	0.2	0.3	150	125-129
BVdU	0.003	1	200	128, 130-133
IVdU	0.012	2	200	128,130
BVdC	0.2	30	200	134
FIAC	0.01	0.01	10	128,131,135
FIAU	0.03	0.06	3	136
FMAU	0.01	0.01	1	136

¹ Concentration required to inhibit virus replication by 50%

² Concentration required to inhibit host cell growth or metabolism by 50%

was noted for (*E*)-5-(2-bromovinyl)-2'-deoxyuridine (BVdU) in its inhibitory effects against HSV-1. 9-(2-Hydroxyethoxymethyl)guanine (acycloguanosine, ACG, acyclovir) has been evaluated extensively in the clinic. BVdU and 1-(2-fluoro-2-deoxy- β -D-arabinofuranosyl)-5-iodocytosine (fluoriodoarabinosylcytosine, FIAC) have been subjected to phase I clinical trials. A large number of placebo-controlled double-blind clinical studies have demonstrated the clinical efficacy of ACG for the treatment of a variety of HSV-1 and HSV-2 infections (137). ACG is effective for the topical treatment of herpes keratitis, and primary genital herpes (138, 139). ACG has been used successfully by the oral route for the treatment of primary and recurrent genital herpes (140), and intravenously for the treatment of mucocutaneous HSV infections in immunocompromised patients (141-144) and herpes simplex encephalitis (120). BVdU has been shown to be effective clinically for the topical treatment of HSV-1 herpes keratitis (145) and for the oral treatment of HSV-1 mucocutaneous infections (146). Clinical trials involving FIAC have been directed mainly at the systemic treatment of VZV infections in immunocompromised patients (147). The toxic effects (nausea and myelosuppression) reported in this study suggest a narrow safety margin for FIAC.

Nucleosides are subject to a number of metabolic alterations in biological systems. Their preferential transformation by HSV-encoded enzymes provides the basis for their selective antiviral activity. They are also subject to several degradative enzymatic changes *in vivo*. Such biotransformations may limit their antiviral activity *in vivo*. An understanding of the different viral and host enzymes interacting with antiviral drugs would be of great value in the design of nucleoside analogs for use as therapeutic or diagnostic agents for HSV infections.

Some unique features of deoxythymidine kinase (TK) enzymes encoded by HSV-1 and HSV-2 have already been discussed in section B. These enzymes have a much broader substrate specificity than the human cytosolic TK. The inhibition constants (K_i) for several nucleoside analogs for TKs of various origins are compared in Table 5. The nucleosides referred to all have greater affinity for HSV-1 and HSV-2 encoded TKs than host cytosolic enzymes. Therefore

Table 5. Inhibition Constants (K_i) of Some Antiviral Nucleosides for Deoxythymidine Kinases of Various Origins

Compound	Mean K_i (μM)			
	Cytosolic	Human Mitochondrial	HSV-1	HSV-2
BVdU	>150	0.83	0.24	4.24
IVdU	>150	1.08	0.27	5.71
FIAC	>100	1.09	6.59	-
FIAU	26	100	0.68	1.54
FMAU	>100	>100	2.99	44.37

these compounds could serve as preferential substrates for the viral TKs and are selectively phosphorylated to their 5'-monophosphates in HSV-infected cells (127, 148-152). Table 5 suggests that mitochondrial TK have a high affinity for these nucleosides and therefore may phosphorylate them. However, such phosphorylation mediated by mitochondrial TK would be minimal, as this enzyme does not play an important role in generating nucleotides for nuclear DNA synthesis. Therefore, in the uninfected cells phosphorylation of the above nucleosides occurs only to a very limited level. The TK-mediated phosphorylation of nucleosides is very crucial to their selective inhibitory activity on HSV replication. Mutations of the viral genome within the TK locus often results in viral strains which are resistant to one or more nucleoside analogs (153-155). Such mutants may show a reduction or total loss in their ability to synthesise TK or express a TK with altered substrate specificity (156-160). HSV mutants which have completely lost their ability to synthesise TK (TK⁻ strains) are usually resistant to all nucleoside analogs shown in Fig. 2. The mutant strains with altered substrate specificity show resistance to some nucleosides while being sensitive to others (160).

It is the 5'-triphosphate derivative of the nucleosides that exerts the antiviral action. Therefore the nucleoside-5'-monophosphates formed in HSV-infected cells must undergo further phosphorylation to the 5'-diphosphates and subsequently to the 5'-triphosphates before they inhibit HSV replication. The TK encoded by HSV-1 has deoxythymidylate kinase activity and therefore phosphorylates some but not all nucleoside-5' monophosphates to the 5'-diphosphates (161, 162). (*E*)-5-(2-Hydroxyl)-2'-deoxyuridine-5'-monophosphates (BVdU-MP, IVdU-MP) have been shown to be converted to the corresponding 5'-diphosphates by HSV-1 encoded TK (151, 161, 163). HSV-2-encoded TK has little or no deoxythymidylate kinase activity and therefore cannot phosphorylate BVdU-MP and IVdU-MP. This may explain in part the 100-1000 fold lower activity of BVdU and IVdU against HSV-2 as compared to HSV-1. Mutations of the TK gene resulting in loss of deoxythymidylate kinase activity of this multifunctional enzyme gives HSV strains which are resistant to BVdU (164). ACG-5'-monophosphate (ACG-MP) does not serve as a substrate

for TK induced by HSV. Instead ACG-MP is phosphorylated by host cell-encoded guanosine monophosphate (GMP) kinase (165). Conversion of the nucleoside diphosphates to the corresponding triphosphates is effected by one or more of the non-specific host cell kinase enzymes (166).

The most important target enzyme for the antiviral action of the nucleosides is the virus-encoded DNA polymerase. The 5'-triphosphates of the nucleosides may interact with DNA polymerases at two levels. First, they act as inhibitors of viral DNA polymerase enzymes. For example, the triphosphates of ACG, BVdU, FIAC (ACG-TP, BVdU-TP, FIAC-TP) compete with the structurally similar natural substrates dGTP, dTTP and dCTP respectively, for the corresponding sites of DNA polymerase enzymes (167-170). Table 6 compares the K_i values for ACG-TP, BVdU-TP and FIAC-TP for HSV-1 and cellular DNA polymerases. These triphosphate analogs have a greater affinity for the HSV-1-encoded DNA polymerases relative to human DNA polymerases and therefore can act as selective competitive inhibitors of the former. ACG-TP has been recently reported to be a suicide inhibitor of herpes simplex virus DNA polymerase (171). In general the inhibitory effects of these compounds on HSV-1 and HSV-2 DNA polymerases are nearly equal (172). The selective inhibitory effects of the nucleoside-5'-triphosphates on HSV-encoded DNA polymerases would partly explain their selective antiviral activity. In addition, the nucleoside triphosphates can also serve as substrates for DNA polymerases and thus be incorporated into DNA. ACG-TP, BVdU-TP, IVdU-TP and FIAC-TP all have been reported to be substrates for DNA polymerases and incorporated into DNA (167, 170-174). ACG-TP and FIAC-TP are better substrates for viral than cellular DNA polymerases (167, 170). BVdU-TP and IVdU-TP are very good substrates for both viral and cellular DNA polymerases (172-174). Since initial phosphorylation of the above nucleosides is limited to HSV-infected cells, the eventual incorporation into DNA will also be confined to DNA of such infected cells. BVdU, even in infected cells, when used in low concentrations is incorporated only into viral DNA (175). The incorporation of ACG into DNA causes chain termination, since ACG does not have a 3'-OH group for further chain elongation

Table 6. Inhibition Constants (K_i) of Some Antiviral Nucleoside Triphosphates for DNA Polymerases of Various Origins

Nucleoside Triphosphate	HSV-1	K_i (μM)	
		Human (α)	Human (β)
ACG-TP	0.03	0.15	11.9
BVdU-TP	0.25	3.6	16.4
FIAC-TP	0.26	2.7	7.9

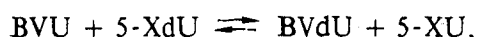
(176). This results in accumulation of short DNA fragments in the infected cells. ACG-MP incorporated into DNA is not excised by the 3',5' exonuclease activity associated with HSV-encoded DNA polymerases (169). The incorporation of BVdU into viral DNA proceeds via an internucleotide linkage. The DNA thus formed has been shown to be more labile, which is evident from the dose-dependent increase in single strand breaks (175). Besides, the substitution of dT in DNA by BVdU impairs the template activity of DNA for transcription (177). FIAC and FMAU may be incorporated by the internucleotide linkage or at the 3' terminals of the DNA (61). Thus, the abnormal DNA formed by incorporation of the antiviral nucleoside is one important factor contributing to the inhibitory effect of these drugs on HSV replication.

The incorporation of any of the above nucleoside analogs into the host cell DNA would result in toxic side effects such as teratogenesis, carcinogenesis, induction of oncogenic viruses, and chromosomal damage. Such toxic effects have been reported for the first generation antiviral drug IdU (178). Since selective antiherpes drugs such as ACG and BVdU are not incorporated into host DNA to any significant degree, these drugs would be expected to be free from such toxic effects. Toxicity studies for ACG and BVdU indicates they are free from carcinogenic and teratogenic effects (61, 137). In contrast to IdU, ACG and BVdU do not induce the release of oncorna particles (179). They do not cause chromosomal damage except at very high concentrations (137, 180). In view of the higher safety margin observed for the second generation nucleoside analogs it is not surprising that new compounds such as ACG are replacing the more toxic first generation drugs in clinical use.

Mutations of the DNA polymerase gene of HSV would result in strains expressing altered DNA polymerase enzymes (153-155, 181). Such HSV mutants may be resistant to one or more antiviral nucleosides. Mutations in different regions of the DNA polymerase locus would result in induction of resistance to different nucleosides. ACG resistance is located within map units 40.2 - 41.8, whereas BVdU resistance is located within map units 41.0 - 42.8 (153, 181). Since the regions of the enzyme conferring resistance to different compounds vary,

resistance to one of them need not necessarily mean cross-resistance to other analogs (155).

The nucleoside analogs discussed are also subject to degradative changes *in vivo*. A major catabolic pathway for the 5-substituted analogs of deoxythymidine involves phosphorolytic cleavage of the N-glycosidic bond (182). In mammals two enzymes are known to catalyze this cleavage, namely deoxythymidine phosphorylase and uridine phosphorylase (182, 183). Thymidine phosphorylase is specific for 2'-deoxypyrimidines and is the main enzyme responsible for degradation of deoxythymidine in man (182). Blood platelets, liver and spleen are very rich sources of this enzyme (184,185). The 5-substituted deoxythymidine analogs are very good substrates for this enzyme (186). Thus, BVdU is rapidly metabolised *in vivo* to the corresponding base (*E*)-5-(2-bromovinyl)uracil (BVU) and 2-deoxyribose-1-phosphate (187). Unlike BVdU, BVU possesses very slow elimination characteristics and could be detected in blood over a period of 24 hours after the administration of BVdU. This rapid *in vivo* metabolism of BVdU limits its bioavailability and therefore the therapeutic efficacy. Two approaches to counteract the phosphorolysis of BVdU have been investigated in animal models. 6-Aminothymine, an inhibitor of deoxythymidine phosphorylase, has been shown to increase the biological half-life of BVdU significantly (188). However, this requires the use of large amounts of inhibitor and is unlikely to gain clinical acceptance. An alternate approach involves the regeneration of BVdU by reversal of phosphorolysis (187, 188). This may be achieved by the administration of a deoxyribosyl donor such as deoxythymidine or 5-substituted deoxythymidine analogs (5-XdU, X=CH₃, F, Cl, I). The general reaction is as follows:



where 5-XU is the 5-substituted uracil. This suggests that other 2'-deoxyuridine analogs may be used *in vivo* to potentiate the therapeutic activity of BVdU.

The 5'-monophosphates of pyrimidine nucleosides may interact with deoxythymidylate synthetase (TS). This enzyme is responsible for the conversion of deoxyuridine-5'-monophosphate to deoxythymidine-5'-monophosphate (189). BVdU-MP is a

good substrate for TS (190). The *in vitro* studies on BVdU-MP have suggested TS-mediated conversion of the inert 5-bromovinyl group to a reactive allylic bromide group. If such a chemically reactive form of BVdU-MP is formed *in vivo*, it may interact with a number of nucleophiles present in the cells. Thus, the possibility of generating an alkylating agent derived from BVdU-MP cannot be excluded. The nature of intracellular metabolites produced by the action of TS on BVdU-MP and its implication to antiviral action is not yet clearly understood. The 5'-monophosphates of 5-iodo- and 5-bromopyrimidine nucleosides are known to undergo TS-mediated dehalogenations (191). Such a deiodination has been reported for FIAU-MP (192). However, TS does not deiodinate FIAC-MP (192).

Deoxycytidine analogs such as BVdC and FIAC and their 5'-monophosphates are subject to deamination by deoxycytidine deaminase and deoxycytidine monophosphate deaminase (193, 194). This results in formation of the corresponding deoxyuridine derivatives. Although the metabolic products arising from deamination of the above nucleosides are still active as antiviral agents, this transformation is considered to be undesirable. Deoxycytidine analogs offer certain advantages over the deoxyuridine compounds since they are not susceptible to phosphorolytic cleavage and their 5'-monophosphates are not substrates or inhibitors of TS. Deamination may be blocked by the administration of tetrahydrouridine or 2'-deoxytetrahydrouridine, which are potent inhibitors of the deaminase enzymes (193, 194). The use of these deaminase inhibitors in conjunction with antiviral drugs such as BVdC and FIAC is yet to be investigated.

Unlike the pyrimidine nucleosides discussed above ACG does not undergo extensive metabolic degradations *in vivo* (195). The only major metabolite is 9-carboxymethoxymethyl guanine, which accounts for up to 14% of the administered dose in humans. This biotransformation is mediated by alcohol dehydrogenase (195).

The previous discussion describing the biochemical aspects of nucleosides suggest certain general requirements for their selective antiviral activity. To exert a selective and potent inhibitory effect on HSV, the nucleoside analog should be able to selectively interact with viral

TK, viral and/or cellular deoxythymidylate kinase, and viral DNA polymerases, while avoiding enzymes such as cellular TKs, cellular DNA polymerases, nucleoside phosphorylases, dC(dCMP) deaminases and TS.

II. MATERIALS AND METHODS

A. General

Chemicals and solvents

All chemicals were of reagent grade quality. 2'-Deoxyuridine (dU), N-iodosuccinimide (NIS), and chloramine-T were purchased from Sigma Chemical Company, St. Louis, Missouri, USA. 5-(Hydroxymethyl)uracil was obtained from Aldrich Chemical Company, Inc., Milwaukee, Wisconsin, USA. N-Bromosuccinimide (NBS) was purchased from Fisher Scientific Company, Fair Lawn, New Jersey, USA. [⁷¹Br]-Sodium bromide (97.8% enriched ⁷¹Br) was obtained from Oakridge National Laboratories, Oakridge, USA. All solvents used for high-pressure liquid chromatography (HPLC) were of HPLC grade and were purchased from Fisher Scientific Company. Solvents used for chemical and radiochemical syntheses were dried by routine methods, fractionally distilled and stored over molecular sieves.

Basal Medium Eagle's (BME), Minimum Essential Medium (MEM) and foetal calf serum were purchased from Flow Laboratories, Virginia, USA. All bottles of serum were heat inactivated at 56° C for 30 min and maintained at 4° C until use. Trypsin (1:250) was purchased from Difco Laboratories, Detroit, Michigan, USA. Penicillin was obtained from Ayerst Laboratories, Montreal, Canada. Streptomycin was obtained from Glaxo Laboratories, Toronto, Canada. Modified radioimmune precipitation assay (RIPA) buffer was prepared by making an aqueous solution of 0.15 M sodium chloride, 1% sodium deoxycholate, 1% Triton X-100, 1% sodium dodecyl sulphate and 0.01 M Tris HCl-buffer. All tissue culture flasks and plates were purchased from Beckton-Dickson, Oxnard, California, USA.

Radioisotopes

All radioactive iodide samples (¹³¹I, ¹²⁵I and ¹²³I) were of radioiodination grade. ¹³¹I and ¹²⁵I samples were supplied as a 'no-carrier-added' (NCA) solution of sodium iodide by

Edmonton Radiopharmacy Centre, Edmonton, Canada. ^{123}I samples obtained from Edmonton Radiopharmacy Centre were supplied as an NCA solution of sodium iodide containing ammonium hydroxide by Atomic Energy Commission Ltd., Vancouver, Canada.

^{123}Br -Bromide samples required for radiobrominations were prepared from ^{123}Br -NaBr by the following method. Amberlite CG-120 (Na^+) was converted to Amberlite CG-120 (NH_4^+) by treating with excess NH_4Cl aqueous solution and washing with deionised water several times.

^{123}Br -NaBr (10 mg) in deionised water (0.5 mL) was added to a column (1 cm id X 50 cm length) containing Amberlite CG-120 (NH_4^+) and eluted with deionised water. The eluant was evaporated *in vacuo* and the residue ^{123}Br - NH_4Br was collected (5 mg, 52.5% yield).

^{123}Br - NH_4Br was prepared from the above sample of ^{123}Br - NH_4Br by the $^{123}\text{Br}(n, \gamma)^{123}\text{Br}$ nuclear reaction at the University of Alberta SLOWPOKE Reactor Facility at a neutron flux of $1 \times 10^{12} \text{ n cm}^{-2} \text{ s}^{-1}$. A typical yield was 2.3 MBq mg^{-1} of ^{123}Br - NH_4Br for a 4 h irradiation.

The theoretical yield calculated was 2.6 MBq mg^{-1} (Appendix).

Instrumental analysis

Melting points (mp) were determined on a Buchi capillary apparatus and are uncorrected. Proton magnetic resonance spectra (^1H NMR) were recorded on a Bruker WH-200 (200 MHz) or a Bruker AM-300 (300 MHz) NMR spectrometer using deuterated dimethyl sulfoxide (DMSO-d_6) or deuterated methanol ($\text{CH}_3\text{OH-d}_4$) as solvent and tetramethylsilane as an internal standard. Ultraviolet spectra (UV) were recorded on a Unicam SP 800 spectrometer using methanol as the solvent. High resolution mass spectra (hrms) for exact mass measurement were obtained on an AEI MS-50 mass spectrometer. HPLC purifications and analysis were performed on a Tracor system (Tracor 950 Chromatographic Pump, Tracor 970 A Variable Wavelength Detector) or Waters system (Model 860 Automated Gradient Controller, Model 510 and M-45 Solvent Pumps, Model U6K Injector and Model 480 LC Ultraviolet Detector).

Chromatography

Thin layer chromatography (TLC) separations were carried out on Whatman MK 6F microslides (Whatman Inc., New Jersey, USA) using one of the following solvents:

1. chloroform : methanol (85:15 by volume)
2. chloroform : methanol (95:5 by volume)
3. ethyl acetate : acetic acid : methanol (7:1:1 by volume)
4. n-propanol : water : ethyl acetate (1:2:4 by volume)

Thin layer radiochromatography (TLRC) was performed on a Berthold LB 2832 Automatic TLC Linear Analyzer equipped with a Berthold LB 281 Proportional Counter and a Canberra Series 40 Multichannel Analyzer. Column chromatographic separations, unless otherwise specified, were performed using silica gel 60 (70-230 mesh) using a glass column (2 cm id X 40 cm length). Preparative HPLC separations were carried out using a Whatman Partisil-10 CCS/C₁₈ reverse phase M-9 preparative column (9.4 mm id X 25 cm length) using methanol : water (40 : 60 by volume) as eluant at a flow rate of 2 mL min⁻¹. Analytical HPLC were done using reverse phase C₁₈ radial pak cartridge (8 mm id X 12 cm length, 10 μ particle size), which were obtained from Waters Associates, Mississauga, Ontario, Canada. Unless otherwise stated the mobile phase and flow rates were the same as those used for preparative HPLC. An ultraviolet absorption (at 298 nm or 296 nm) detection system was used for detection of non-radioactive eluants. An ultraviolet absorption (at 298 nm or 296 nm) detection system and a γ-ray detection system were used in conjunction for the detection of radioactive eluants.

Radioactivity measurements

Radioactivities for γ-emitting radionuclide samples with high total activity (37 KBq or more) were estimated using a Picker Dose Calibrator. Samples with low total activity ¹²⁵I were counted on a Beckman 8000 gamma counter by the double photopeak method (program # 9). Samples with low total activity of ¹³¹I were counted on a Beckman 8000 (program # 6) or a Tracor 2200 (window : 300 to 420 Kev), or a Tracor 2200 gamma counter. Low activity ¹²⁵Br

samples and all ^{14}C -labeled samples were counted on a Beckman LS 9000 liquid scintillation counter (program # 10 and 3 respectively) using Aquasol II (New England Nuclear) as the fluor.

B. Chemical Synthesis

5-Chloromercuri-2'-deoxyuridine

Mercuric acetate (4.18 g, 1.31 mmol) in water (12 mL) was added to a solution of 2'-deoxyuridine (2.84 g, 1.24 mmol) in water (18 mL). To this an additional quantity of water (10 mL) was added and the mixture was stirred for 2.5 h at 50° C. This resulted in formation of a thick white suspension. The reaction mixture was cooled to 40° C and to this, a solution of sodium chloride (1.8 g, 3 mmol) in water (6 mL) was added. The reaction mixture was cooled to room temperature and stirred for another 2 h. The fine white precipitate was filtered, washed in succession with 0.1 N aqueous sodium chloride solution (24 mL), water (16 mL), ethanol (8 mL) and diethyl ether (12 mL). The air dried precipitate was stored in a vacuum dessicator over phosphorous pentoxide overnight. The dried product (4.85 g, 84.2% yield) was used for subsequent reactions without further purification; mp 210-212° C (dec) [Lit (196) 210.5-211° C (dec)].

(E)-5-(2-Carbethoxyvinyl)-2'-deoxyuridine

5-Chloromercuri-2'-deoxyuridine (3.47 g, 5 mmol), ethyl acrylate (8.9 mL, 82 mmol) and a 0.1 M methanolic solution of Li_2PdCl_4 (79 mL, 7.9 mmol) were stirred under nitrogen for 10 h. The mixture was filtered, the precipitate collected, warmed in methanol (120 mL), and refiltered. The combined filtrate was treated with hydrogen sulfide gas until precipitation was complete. The solution was filtered and the solvent was removed *in vacuo*. The residue was dissolved in water (10 mL) and left overnight at 0-4° C for crystallization. The product was collected and dried *in vacuo* to give the title product (1.25 g, 46% yield); R_f 0.5

(solvent 1), mp 186-188° C.

¹H NMR (DMSO-d₆) δ : 1.23 (3H, t, J=6 Hz, CH₂ CH₃), 2.17 (2H, m, C₂'-H₂), 3.62 (2H, m, C₃'-H₂), 4.15 (2H, q, J=6 Hz, CH₂ CH₃), 3.80 (1H, m, C₃'-H), 4.26 (1H, m, C₄'-H), 6.14 ((1H, dd, J=6 Hz, C₁'-H), 6.85 (1H, d, J=15 Hz, vinylic C₍₁₎-H), 7.37 ((1H, d, J=15 Hz, vinylic C₍₂₎-H), 8.43 (1H, s, C₆-H), 11.6 (1H, s, N₃-H).

(E)-5-(2-Carboxyvinyl)-2'-deoxyuridine

A mixture of (*E*)-5-(2-carbomethoxyvinyl)-2'-deoxyuridine (1.5 g, 4.6 mmol) and 0.5 N aqueous potassium hydroxide (4 mL) were stirred at room temperature for 1 h. The reaction mixture was neutralized with Dowex 50X 8-200-[H⁺] ion exchange resin and then the ion exchange resin was removed by filtration. The filtrate was evaporated to dryness *in vacuo*. The residue was crystallized from aqueous ethanol to yield the title compound (1.01 g, 73.7% yield); Rf 0.47 (solvent 3), mp 220-230° C.

¹H NMR (CH₃OH-d₄) δ : 2.15 (2H, m, C₂'-H₂), 3.68 (2H, m, C₃'-H₂), 3.75 (1H, m, C₄'-H), 4.40 (1H, m, C₃'-H), 6.18 (1H, dd, J=6 Hz, C₁'-H), 6.7 (1H, d, J=15 Hz, vinylic C₍₁₎-H), 6.95 (1H, d, J=15 Hz, vinylic C₍₂₎-H), 8.25 (1H, s, C₆-H).

(E)-5-(2-Iodovinyl)-2'-deoxyuridine

(a) N-Iodosuccinimide (NIS) method

(*E*)-5-(2-Carboxyvinyl)-2'-deoxyuridine (40 mg, 13 μmol) was dissolved in dry dimethyl formamide (DMF) (2.5 mL). To this, potassium acetate (30 mg, 34 μmol) and N-iodosuccinimide (34 mg, 15 μmol) were added and the mixture was stirred at room temperature for 24 h. The solvent was evaporated *in vacuo* and the residue was purified by column chromatography [solvent ; chloroform : methanol (85:15 by volume)] to give the title compound which failed to crystallize (15 mg, 30.4% yield); Rf 0.42 (solvent 1).

¹H NMR (CH₃OH-d₄) δ : 2.15 (2H, m, C₂'-H₂), 3.62 (2H, m, C₃'-H₂), 3.81 (1H, m, C₄'-H), 4.28 (1H, m, C₃'-H), 6.16 (1H, dd, J=6 Hz, C₁'-H), 7.15 (1H, d, J=15 Hz,

vinyllic C₍₁₎-H), 7.25 (1H, d, J = 15 Hz, vinyllic C₍₂₎-H), 8.10 (1H, s, C₄-H)

UV (CH₃OH) : λ_{\max} 252 nm and 298 nm, λ_{\min} 275 nm. The ¹H NMR and UV data were in agreement to those reported in the literature (197).

(b) Chloramine-T method

(E)-5-(2-Carboxyvinyl)-2'-deoxyuridine (10 mg, 30 μ mol) was dissolved in dry dimethyl formamide (DMF) (1 mL). To this, solutions of potassium acetate (5 mg, 60 μ mol) in ethanol (100 μ L), sodium iodide (5 mg, 30 μ mol) in ethanol (100 μ L) and chloramine-T (10 mg, 44 μ mol) were added and the mixture was stirred at room temperature for 1 h. The reaction product was purified as described under method (a) to give the title compound (3 mg, 26.3% yield). The product was shown to be identical to the product obtained by the NIS method with respect to R_f value, UV and ¹H NMR characteristics. It also co-chromatographed (analytical HPLC : UV detection at 298 nm, retention time 12.8 min, preparative HPLC : retention time 21.3 min) with the above product obtained under method (a).

(E)-5-(2-Bromovinyl)-2'-deoxyuridine

(a) N-Bromosuccinimide (NBS) method

(E)-5-(2-Carboxyvinyl)-2'-deoxyuridine (75 mg, 25 μ mol) was dissolved in water (4 mL) by heating with potassium acetate (50 mg, 5 μ mol). While still hot, N-bromosuccinimide (45 mg, 25 μ mol) was added in small portions to the clear mixture. The mixture was stirred at room temperature for 2 h at which time the reaction was complete as indicated by TLC. The solution was then left overnight at 0-4° C for crystallization of the product. The crystals were collected (25 mg) and the mother liquor was evaporated to dryness *in vacuo*. The residue was fractionated by column chromatography [solvent ; chloroform : methanol (90:10 by volume)] to give an additional quantity of the title product (10 mg, 42% total yield); R_f 0.45 (solvent 1), mp 164-165° C.

^1H NMR ($\text{CH}_3\text{OH}-d_4$) : 2.28 (2H, m, C_2' - H_2), 3.78 (2H, m, C_3' - H_2), 3.93 (1H, m, C_4' -H), 4.40 (1H, m, C_3' -H), 6.25 (1H, dd, $J=6$ Hz, C_1' -H), 6.80 (1H, d, $J=15$ Hz, vinylic $\text{C}_{(1)}$ -H), 7.38 (1H, d, $J=15$ Hz, vinylic $\text{C}_{(2)}$ -H), 8.14 (1H, s, C_6 -H).

UV (CH_3OH) : λ_{max} 252 nm and 296 nm, λ_{min} 271 nm. The UV and ^1H NMR data were in agreement with those reported in the literature (197).

(b) Chloramine-T method

(*E*)-5-(2-Carboxyvinyl)-2'-deoxyuridine (10 mg, 34 μmol) was dissolved in dry dimethyl formamide (DMF) (1 mL). To this a solution of potassium acetate (5 mg, 60 μmol) in ethanol (100 μL), sodium bromide (3.5 mg, 34 μmol) in ethanol (100 μL) and chloramine-T (10 mg, 44 μmol) were added and the mixture stirred at room temperature for 15 min. The reaction product was purified by preparative HPLC (uv detection at 296 nm, retention time : 18.6 min) to give the title compound (2 mg, 18% yield). This product was identical to the product obtained by NBS method with respect to *Rf* value, UV and ^1H NMR characteristics and co-chromatography (preparative HPLC).

(*E*)-5-(2-Carboxyvinyl)-2'-deoxyuridine-3',5'-diacetate

(*E*)-5-(2-Carboxyvinyl)-2'-deoxyuridine (100 mg, 336 μmol) in pyridine (1 mL) was stirred with acetic anhydride (1 mL) at room temperature overnight. The solvent was evaporated *in vacuo*. The residue was crystallized from ethanol (95%) to give the title product (71 mg, 55.4% yield); *Rf* 0.72 (solvent 3), mp 190-195° C (dec).

^1H NMR ($\text{CH}_3\text{OH}-d_4$) δ : 2.15 (6H, s, C_3' - and C_5' -O-CO- CH_3), 2.45 (2H, m, C_2' - H_2), 4.35 (2H, m, C_3' - H_2), 4.45 (1H, m, C_4' -H), 5.30 (1H, m, C_3' -H), 6.25 (1H, dd, $J=6$ Hz, C_1' -H), 7.20 (1H, d, $J=15$ Hz, vinylic $\text{C}_{(1)}$ -H), 7.40 (1H, d, $J=15$ Hz, vinylic $\text{C}_{(2)}$ -H), 7.80 (1H, s, C_6 -H).

Exact mass calculated for $\text{C}_{15}\text{H}_{19}\text{N}_2\text{O}_7$, ($[\text{M} - \text{CO}_2]^+$) : 338.11258, measured (hrms) : 338.1121 (intensity=0.41%).

(E)-5-(2-Iodovinyl)-2'-deoxyuridine-3',5'-diacetate

Potassium acetate (5 mg, 60 μ mol) and N-iodosuccinimide (6 mg, 27 μ mol) were added to a solution of (E)-5-(2-carboxyvinyl)-2'-deoxyuridine-3',5'-diacetate (10 mg, 28 μ mol) in DMF (7 mL). The reaction was allowed to proceed at 25° C with stirring for 20 h at which time TLC indicated the reaction was complete. The solvent was removed *in vacuo* and the residue was purified by column chromatography [solvent; chloroform : acetone (90:10 by volume)] to give the title product as a syrup (5 mg, 41% yield); R_f 0.79 (solvent 2).

¹H NMR (CH₃OH-d₄) δ : 2.15 (6H, s, C₃'- and C₅'-O-CO-CH₃), 2.45 (2H, m, C₂'-H₂), 4.35 (2H, m, C₃'-H₂), 4.45 (1H, m, C₄'-H) 5.30 (1H, m, C₃'-H), 6.25 (1H, dd, J=6 Hz, C₁'-H), 7.20 (1H, d, J=15 Hz, vinylic C₍₁₎-H), 7.40 (1H, d, J=15 Hz, vinylic C₍₂₎-H), 7.80 (1H, s, C₆-H).

Exact mass calculated for C₁₅H₁₇N₂O₇I (M⁺) : 464.00394 ; measured (hrms) : 464.0081 (intensity = 2.27%).

5-Formyl uracil

Silver nitrate (15 mg) and potassium persulfate (2.0 g) were added to a suspension of 5-(hydroxymethyl)uracil (500 mg, 3.5 mmol) in water (30 mL). The reaction mixture was stirred at 30° C for 10 min. Upon cooling the title product crystallized (400 mg, 80% yield); R_f 0.67 (solvent 4), mp 295-300° C [Lit (198) 300-303° C].

(E)-5-(2-Carboxyvinyl)uracil

Malonic acid (15 mg, 144 μ mol) and piperidine (1 drop) were added to a suspension of 5-formyl uracil (20 mg, 143 μ mol) in dry pyridine (1 mL). The mixture was heated in an oil bath at 65° C for 4 h. The solvent was removed and the residue was crystallized from aqueous ethanol (50%) to give the title product (6 mg, 23% yield); R_f 0.46 (solvent 4), mp 281-283° C (dec).

(E)-5-(2-Iodovinyl)uracil

Potassium acetate (20 mg, 232 μmol) in ethanol (100 μL), sodium iodide (22 mg, 147 μmol) in ethanol (100 μL) and chloramine-T (33 mg, 147 μmol) were added to a solution of (E)-5-(2-carboxyvinyl)uracil (20 mg, 110 μmol) in dry DMF (2 mL). The reaction mixture was stirred at room temperature for 40 min. The solvent was evaporated *in vacuo*. The residue was purified by preparative HPLC to give chromatographically pure title product which did not crystallize (3 mg, 10% yield). R_f 0.34 (solvent 4).

$^1\text{H NMR}$ ($\text{CH}_3\text{OH}-d_4$) : 7.12 (1H, d, $J=15$ Hz, vinylic $\text{C}_{(1)}$ -H), 7.22 (1H, d, $J=15$ Hz, vinylic $\text{C}_{(2)}$ -H), 7.56 (1H, s, C_6 -H). The $^1\text{H NMR}$ data were in agreement with those previously reported (197).

C. Radiochemical Synthesis**[^{131}I , ^{125}I , ^{123}I]- (E)-5-(2-Iodovinyl)-2'-deoxyuridine****(a) Chloramine-T method**

(i) High specific activity synthesis : A solution of sodium iodide (50 μg , 0.33 μmol) in ethanol (100 μL) and potassium acetate (500 μg) in ethanol (50 μL) were added to a 1 mL reaction vial and the solvent was removed under a stream of nitrogen. [^{131}I , ^{125}I]-Iodide (118.4 MBq) in ethanol (500 μL) was then added and the volume was then reduced to about 20 μL . (E)-5-(2-Carboxyvinyl)-2'-deoxyuridine (1 mg, 3.3 μmol) in dry DMF (100 μL) was added to the reaction vial and the reaction mixture was then stirred for 5 min using a magnetic stirrer. The reaction was initiated by addition of chloramine-T (200 μg) in dry DMF (20 μL) and stirring was continued at room temperature for 1 h. The solvent was removed under a stream of nitrogen and the residue purified by preparative HPLC. The radioactive fraction that corresponded to an authentic sample with a retention time of 20 minutes afforded IVdU (88 μg , 69% chemical yield, 80 MBq, 67.2% radiochemical yield, specific activity 344 GBq mmol^{-1}).

^{125}I -IVdU was synthesised by the procedure described above except that the reaction time was reduced to 30 min. The chemical yield was 57.0% and the radiochemical yield after purification was 40.7%.

(ii) "No-carrier added" synthesis : ^{131}I -IVdU was synthesised as described above in (i) without the addition of cold sodium iodide using Na^{131}I (37 MBq) which has not been isotopically diluted. The reaction was terminated after 30 min. The product was purified by HPLC to give ^{131}I -IVdU (24 MBq, 65% yield).

(a) Halogen-iodine exchange method

A solution of IVdU (70 μg , 0.18 μmol , ^{131}I -Iodide (3.7 MBq) and cuprous chloride (2 μg , 20 nmol) in dry DMF (20 μL) were heated at 70-80° C in a reaction vial. The incorporation of radioactivity into IVdU was monitored by TLRC. The maximum incorporation of radioactivity into IVdU was achieved after 20 h at which time the solvent was removed. The residue was purified by preparative HPLC to yield ^{131}I -IVdU (38 μg , 54.3% chemical recovery; 1.67 MBq, 45.1% radiochemical yield; specific activity 16.7 GBq mmol^{-1}).

^{131}I -(E)-5-(2-Iodovinyl)-2'-deoxyuridine-3',5'-diacetate

^{131}I -IVdU-3',5'-diacetate was synthesized by the chloramine-T method as described for the high specific activity synthesis by reaction of (E)-5-(2-carboxyvinyl)-2'-deoxyuridine-3',5'-diacetate (500 μg , 1.4 μmol) with ^{131}I -sodium iodide (5 μg , 33 nmol, 14.8 MBq) and chloramine-T (100 μg) in the presence of potassium acetate (250 μg) in DMF (50 μL) for 1 h. The product obtained after purification by column chromatography using a small glass column (0.5 cm id X 10 cm length) [solvent ; chloroform : acetone (90:10 by volume)] co-chromatographed with an authentic sample of (E)-5-(2-iodovinyl)-2'-deoxyuridine-3',5'-diacetate on TLRC (7.4 MBq, 50% radiochemical yield, specific activity 54.5 GBq mmol^{-1}).

[¹²⁵Br]-(*E*)-5-(2-Bromovinyl)-2'-deoxyuridine (BVdU)**(a) Chloramine-T method**

A solution of (*E*)-5-(2-carboxyvinyl)-2'-deoxyuridine (2 mg, 6.1 μmol), potassium acetate (1 mg), [¹²⁵Br]-ammonium bromide (300 μg , 3.1 μmol , 0.72 MBq) and chloramine-T (2 mg) in dry DMF (200 μL) and ethanol (20 μL) were stirred at room temperature using a magnetic stirrer. The reaction was complete within 10 min as indicated by TLRC. The solvent was evaporated under a slow stream of nitrogen. The residue was purified by preparative HPLC as described previously. The radioactive fraction corresponding to an authentic sample with a retention time of 18.6 min afforded BVdU (727 μg , 72% chemical yield, 0.5 MBq, 69.8% radiochemical yield; specific activity 227 MBq mmol^{-1}).

(b) Direct neutron activation

A sample of BVdU (1 mg) (containing natural abundance bromine) was irradiated in a double plastic vial at a neutron flux of $10^{12} \text{ n cm}^{-2} \text{ s}^{-1}$ for 4 h. The sample was allowed to stand for 24 h (to allow the decay of ⁷⁶Br, ⁷⁷Br^m and ⁷⁸Br^m) prior to purification by preparative HPLC as described previously. The radioactive fraction having a retention time of 18.6 min showed identical TLRC, HPLC and UV spectral characteristics to that of an authentic sample of BVdU. The specific activity of the product calculated to the end of irradiation was 32 MBq mmol^{-1} . Radiolytic decomposition was estimated to be less than 3%. The radioactivity associated with BVdU was 30% of the overall activity produced.

D. Quantitative Uptake Studies of Radiolabeled Nucleosides in HSV-1-Infected Cells *In Vitro***Cells**

Two 2-5 day old rabbits were sacrificed by cervical dislocation. The kidneys were removed, washed with phosphate buffered saline (PBS) and cut into small pieces. The pieces

were incubated at 37° C in PBS (20 mL) containing Trypsin 1:250 (0.25%). The supernatants were collected from three 20 min sequential incubations and added to Basal Medium Eagle's (BME) or Minimum Essential Medium (MEM) containing foetal calf serum. After a cell count the tissue culture flasks were seeded at a concentration of 5×10^6 cells per 25 cm² flask. Cells were maintained in 10 mL of BME or MEM supplemented with 10% foetal calf serum, penicillin-G (100 IU mL^{-1}), and streptomycin sulphate ($100 \mu\text{g mL}^{-1}$), 2 mM glutamine and sodium bicarbonate (2 g L^{-1}). When monolayers became confluent, cells were split twice at a ratio of 1:3.

Viruses

HSV-1 (strain JLJ) isolated from a patient with HSV encephalitis was used as the HSV-1 (TK⁺) infecting agent. HSV-1 (strain 2006 which is TK deficient) was used as the HSV-1 (TK⁻) infecting agent. All viral titrations were performed by Drs. D. R. Tovell or M. J. Gill (Faculty of Medicine, University of Alberta, Edmonton, Canada).

Radiolabeled nucleosides

[¹³¹I]-IVdU samples (specific activity $43.3 \text{ GBq mmol}^{-1}$, $370 \text{ GBq mmol}^{-1}$ and 80 GBq mmol^{-1}) were prepared as described in section C.

[5-¹³¹I]-1-(2-deoxy-2-fluoro- β -D-ribofuranosyl)-5-iodouracil (specific activity $20.4 \text{ GBq mmol}^{-1}$) and [2-¹⁴C]-1-(2-deoxy-2-fluoro- β -D-ribofuranosyl)-5-fluorouracil (specific activity $1.86 \text{ GBq mmol}^{-1}$) were synthesised by Mr. T. Iwashina (Faculty of Pharmacy, University of Alberta, Edmonton, Canada).

[2-¹⁴C]-1-(2-deoxy-2-fluoro- β -D-ribofuranosyl)-5-chlorouracil (specific activity $1.86 \text{ GBq mmol}^{-1}$) was synthesised by Dr. J. R. Mercer (Faculty of Pharmacy, University of Alberta, Edmonton, Canada). [5-¹³¹I]-1-(2-deoxy-2-fluoro- β -D-arabinofuranosyl)-5-iodouracil (specific activity $111 \text{ GBq mmol}^{-1}$) was synthesised by Dr. H. K. Misra (Faculty of Pharmacy, University of Alberta, Edmonton, Canada).

Quantitation of cellular uptake of radiolabeled nucleosides by primary rabbit kidney (PRK) cells

The rabbit kidney cells were grown to confluency in Falcon 25 cm² flasks or 60 mm Petri dishes. The medium was removed and the cell monolayer was infected with a known infecting dose (plaque forming units per ml, PFU/mL) either HSV-1 (TK⁺), HSV-1 (TK⁻) or mock infection in 0.2 mL of medium. Unless otherwise stated, HSV-1 (TK⁺) infections were performed in triplicate and HSV-1 (TK⁻) and mock infections were performed in duplicate. After the infection, the flasks were incubated at 37° C for 1 h, at which time 2 mL of medium was added to each flask. After 7 h of post-infection incubation a known quantity of the radiolabeled nucleoside was added to each flask. Unless otherwise stated the flasks were incubated for a further 4 h. The early cytopathic effect was confirmed microscopically before determining the radioactivity in the cells. The supernatant was decanted, and the cells were washed twice with 1 mL PBS. The supernatant along with the washings were counted for radioactivity. Modified RIPA buffer (1 mL) was added to dissolve the cells (199). The flask was left for 5 min and the fluid was removed. The flask was further washed twice with 1 mL of modified RIPA buffer. The solubilized cells and the washings were counted for radioactivity in a gamma counter or a liquid scintillation counter.

E. Tissue Distribution of [¹³¹I]-IVdU in a Herpes Simplex Encephalitis Animal Model

Animal model

The herpes encephalitis animal model was developed by Drs. M. J. Gill, D. R. Tovell and D. L. Tyrrell (Faculty of Medicine, University of Alberta, Edmonton, Canada). Rabbits (Dutch) were infected with intracerebral injection of 10⁶ PFU of HSV-1 (JLJ). After 4 days the infected rabbits showing symptoms of HSE including convulsions were used for the tissue distribution studies or diagnostic imaging using [¹²⁵I or ¹²³I]-IVdU. Brain samples of HSV-1-infected rabbits were obtained and the radioactivity was compared with the virus titer.

Quantitative tissue distribution of [¹²⁵I]-IVdU

Rabbits (infected and uninfected controls) were given a bolus i.v injection of 0.74 MBq of [¹²⁵I]-IVdU. The animals were sacrificed at 1 or 6 h after the injection. Blood samples were collected by cardiac puncture just before sacrificing the animals. Organ samples (brain, liver, kidney, spleen, lung and muscle) were collected, weighed and the radioactivity quantitated by gamma counting.

F. Pharmacokinetics and Metabolism of [¹³¹I]-IVdU in Dogs

Quantitative radio high-pressure liquid chromatography (r-HPLC)

The radioactive components of the plasma were separated, identified and quantitated by the following method. The plasma samples were mixed with an equivalent volume of methanol and chilled in ice (0-4° C) for 5 min. The supernatant was subsequently evaporated at room temperature under a stream of nitrogen and the residue dissolved in aqueous methanol (30% by volume). Two reference compounds [(*E*)-5-(2-iodovinyl)-2'-deoxyuridine and (*E*)-5-(2-iodovinyl)uracil] were added and the methanolic solution was filtered through a Millex®-HV₄ filter (Waters Scientific, LTD., 3688, Nashua Drive, Mississauga, Ont. L4V 1M3, Canada) and injected onto the r-HPLC system (Waters Scientific, LTD., column: Waters radial pak C₁₈, 1.8 mm cartridge). The mobile phase was either A: a mixture of aqueous 0.01 M KH₂PO₄ (polar eluent) and methanol (non-polar eluent) B: a mixture of paired ion chromatography (PIC) solution [(aqueous 0.01 M KH₂PO₄ containing 1 vial of low UV PIC A reagent® (Waters Scientific, LTD.) in a 2L volume] and methanol (9:1 by volume). The plasma components were eluted by gradient elution with mobile phase A, increasing from 30% to 70% of the non-polar eluant over 15 min (Waters curve profile 7), followed by an additional elution for 5 min at 70% non-polar eluant. The identities of the radioactive components were confirmed by co-elution with authentic reference compounds, as evidenced by the simultaneous detection of radioactivity (by NaI-Tl γ-ray detector) and UV absorbance (at

298 nm). The fractions corresponding to the radioactive peaks were quantitated by gamma counting (Tracor Gamma 2200). A typical radiochromatogram (Fig.14) showed four radioactive peaks: A, B, C, and D. Peaks C and D were identified as [^{131}I]-(*E*)-5-(2-iodovinyl)uracil (IVU) and [^{131}I]-IVdU respectively. The identification of peak A was achieved by paired ion chromatography. The radioactive fraction A, on rechromatography with mobile phase B, co-eluted with the reference sample of inorganic iodide (UV absorption at 214 nm) with a retention time of 6.5 min.

Metabolism of [^{131}I]-IVdU in blood *in vitro*.

Heparinised blood (5 mL) obtained from a dog was incubated at 37° C with ^{131}I -IVdU (1.85 MBq in 100 μL of saline; specific activity: 2035 GBq mmol^{-1}). Blood samples (250 μL each) were periodically withdrawn into precooled Eppendorf® tubes, cooled for 30 sec and centrifuged at 20,000 rpm for 2 min. The supernatant was removed and analysed by quantitative r-HPLC as described above.

Metabolism of [^{131}I]-IVdU in blood *in vivo*.

The *in vivo* metabolism was studied using both low (1665 MBq mmol^{-1}) and high specific activity (37 TBq mmol^{-1}) samples of [^{131}I]-IVdU. Dogs were anaesthetised by i.v administration of sodium pentobarbital (25 mg/kg body wt) and the femoral vein was cannulated for blood sampling. [^{131}I]-IVdU (2.5 MBq/kg body wt) in saline was injected via the radial vein and the blood samples were periodically (30 sec, 1, 2, 3, 5, 7, 9, 11, 15, 20, 30, 45 min, 1, 2, 3.5, 4, 6, 8, and 24 h) collected through the femoral canula into precooled tubes and the plasma was separated from cells by centrifugation as described previously. An aliquot of the plasma sample was counted to estimate total radioactivity. Another portion (1 mL) was processed immediately and analysed by r-HPLC as described above. Alternatively some samples (1 mL) at selected time points (3, 11, 30 min and 3.5 h) were dialysed in PBS and the radioactivity remaining in the dialysis bag was estimated by gamma counting.

Urine samples were collected at 2, 4.5 and 8 h after the injection of [^{131}I]-IVdU, using a catheter. The urinary bladder was rinsed with saline to ensure efficient removal of urinary metabolites. Aliquots of each urine and wash samples were counted for radioactivity. Other aliquots of the urine sample were filtered through a Millex®-HV₄ filter and analysed by quantitative r-HPLC.

G. Diagnostic Imaging

Planar imaging

Rabbits (2 infected and 2 uninfected) were anaesthetised by i.v injection of sodium pentobarbital injection (25 mg/Kg body wt). [^{131}I]-IVdU (37 MBq) was administered as an intravenous bolus injection. Diagnostic imaging in the planar mode (static images) was performed at 30 min, 45min, 1 h, and 6 h after injection of [^{131}I]-IVdU using a Searle gamma camera (Pho/Gamma III) interfaced with an ADAC (CAM III) computer. For each static image 200,000 counts were collected.

SPECT

Rabbits (1 infected and 2 uninfected) were anaesthetised as described above. Right common carotid artery was exposed by dissection. [^{131}I]-IVdU (37 MBq) in saline (0.2 mL) was administered carefully as an intracarotid bolus injection. Intracarotid injection was carried out by Dr. D. L. Tyrrell (Faculty of Medicine, University of Alberta, Edmonton, Canada). Diagnostic brain imaging in the tomographic mode was started 20 minutes after the injection using a GE-400 AT gamma camera interfaced with a DEC-11/70 computer (Department of Nuclear Medicine, Cross Cancer Institute, University of Alberta, Edmonton, Canada). The radioactive counts were acquired at different angular orientations in 64 frames, with each frame collecting 50,000 counts. The time required for the acquisition of the data was about 30 min.

III. RESULTS AND DISCUSSION

A. The Problem and the Approach

The objective of this study was to develop a radionuclide brain imaging agent for the diagnosis of HSE. The metabolic transformations of the antiviral nucleosides in HSV-infected cells discussed in chapter I offer a new approach to the development of specific biochemical probes for the non-invasive diagnosis of HSE. The nucleoside phosphates selectively formed in the HSV-infected cells would be expected to have a very low permeability across the plasma membrane. Therefore, these nucleosides may be metabolically trapped in HSV-infected cells. Since such metabolic transformations are limited to the infected cells, the uninfected cells will be free of any selective accumulation of these nucleoside analogs (Fig. 3). Therefore an anti-HSV nucleoside analog labeled with a suitable gamma emitting isotope may be used as a specific probe to non-invasively differentiate a normal from HSV-infected brain with the aid of brain imaging techniques. While this study was in progress, Siatto *et al* have reported the successful application of the selective metabolic trapping of radiolabeled nucleosides for quantitative autoradiographic mapping of HSE in a rat model (200-202), supporting the *in vivo* feasibility of such an approach.

Several antiviral nucleosides qualify as potential candidates for the development of radiopharmaceuticals for the diagnosis of HSE. We have chosen (*E*)-5-(2-iodovinyl)-2'-deoxyuridine (IVdU) and (*E*)-5-(2-bromovinyl)-2'-deoxyuridine (BVdU) in our investigations for the following reasons. IVdU and BVdU are among the most selective and potent compounds effective against HSV-1, which is the most common causative agent of adult HSE. Since IVdU and BVdU already contain halogens, labeling these molecules with radiohalogens does not alter their chemical or biological properties. IVdU labeled with ¹³¹I may be used for two-dimensional (planar) conventional brain imaging using equipment currently available to many general hospitals. Alternatively, the incorporation of ¹²³I into IVdU would permit its use in tomographic brain imaging using a SPECT system. BVdU offers the

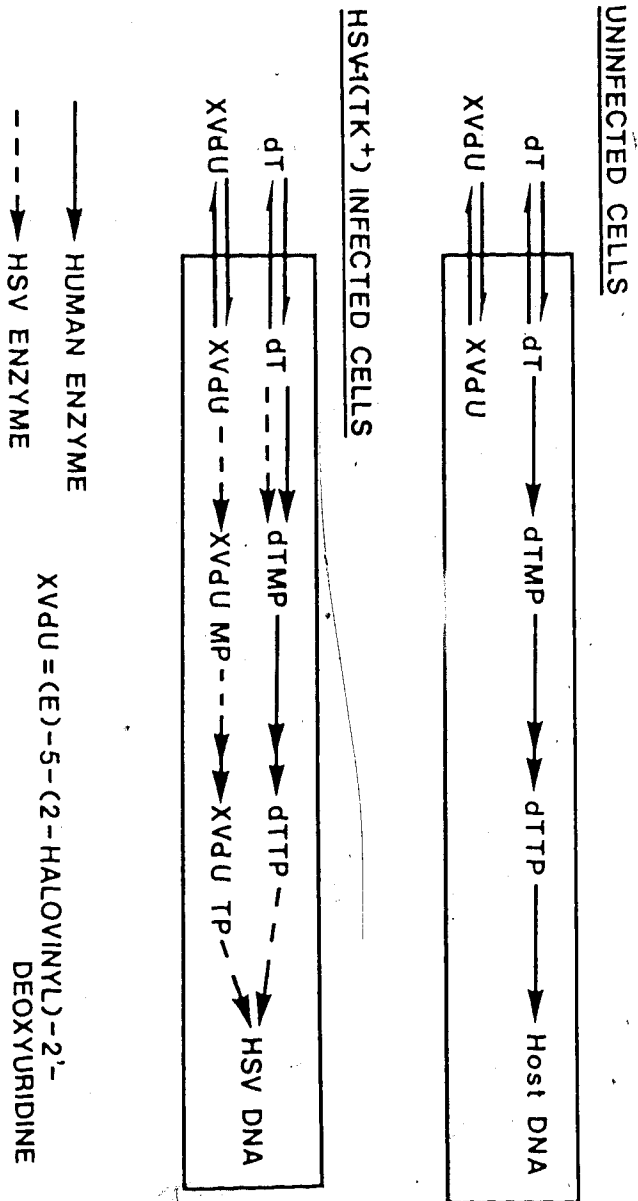


Fig. 3 Selective Metabolic Trapping of (E)-5-(2-Halovinyl)-2'-deoxyuridines in Herpes Simplex Virus-Infected Cells.

possibility of introduction of ^{75}Br , a positron emitting radionuclide, and therefore the development of a diagnostic test for HSE, using PET.

B. Chemical Synthesis

The major objectives of the non-radioactive syntheses were twofold :

1. To prepare authentic samples of nucleoside analogs as reference compounds for radiochemical syntheses and metabolic studies.
2. To explore alternate synthetic routes suitable for radiochemical syntheses and to show that the products thus formed are identical to those obtained from previously reported methods.

The syntheses of (*E*)-5-(2-halovinyl)-2'-deoxyuridines (Fig. 4) have been reported (197). The general synthetic route employed for the syntheses of iodo and bromo derivatives is shown in Fig. 5. 5-Chloromercuri-2'-deoxyuridine (2) was synthesised from commercially available 2'-deoxyuridine in 84.2% yield by the reaction of 2'-deoxyuridine with mercuric acetate followed by sodium chloride (196). Introduction of the 5-alkenyl group onto 2'-deoxyuridine was achieved by coupling ethyl acrylate with an organopalladium intermediate generated *in situ* from 5-chloromercuri-2'-deoxyuridine (2) (203). The use of organometallic intermediates for the syntheses of nucleoside analogs has been reviewed by Bergstrom (204). The reaction of ethyl acrylate with C_5 -organopalladium derivatives of 2'-deoxyuridine is stereospecific. The reaction mechanism is likely to be similar to that proposed for the Heck reaction for the arylation of olefins (Fig. 6) (203-206). 5-Chloromercuri-2'-deoxyuridine reacted with dilithium palladium tetrachloride to form a bond between C_5 of the pyrimidine ring and Pd (2a). This is followed by formation of a π complex between ethyl acrylate and Pd to afford an intermediate 2b. The insertion of the π -bonded olefin into the C_5 -Pd bond would then give 2c which on *cis* elimination of Pd-H leads to the formation of a π complex 2d. This π complex then undergoes dissociation to give Pd(0) and the nucleoside 3. Compound 3 was readily hydrolysed to the corresponding carboxylic acid (4) by 0.5 N aqueous potassium

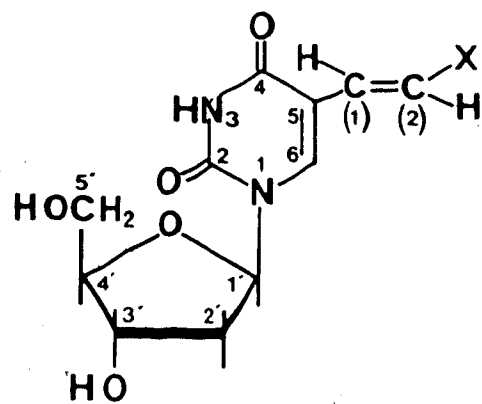


Fig. 4 Chemical Structure for (*E*)-5-(2-Halovinyl)-2'-deoxyuridines.

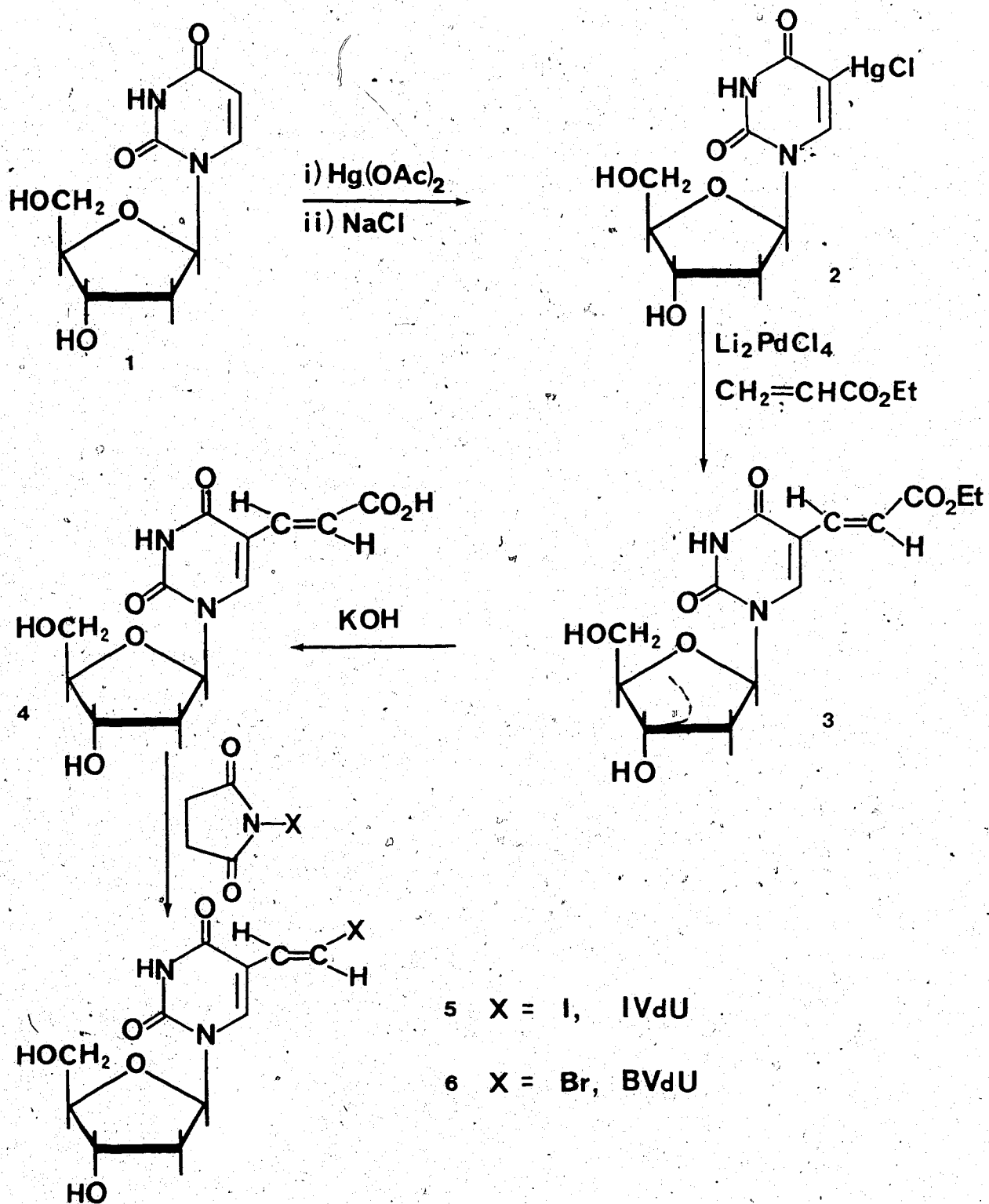


Fig. 5 General Synthetic Route for the Synthesis of IVdU and BVdU.

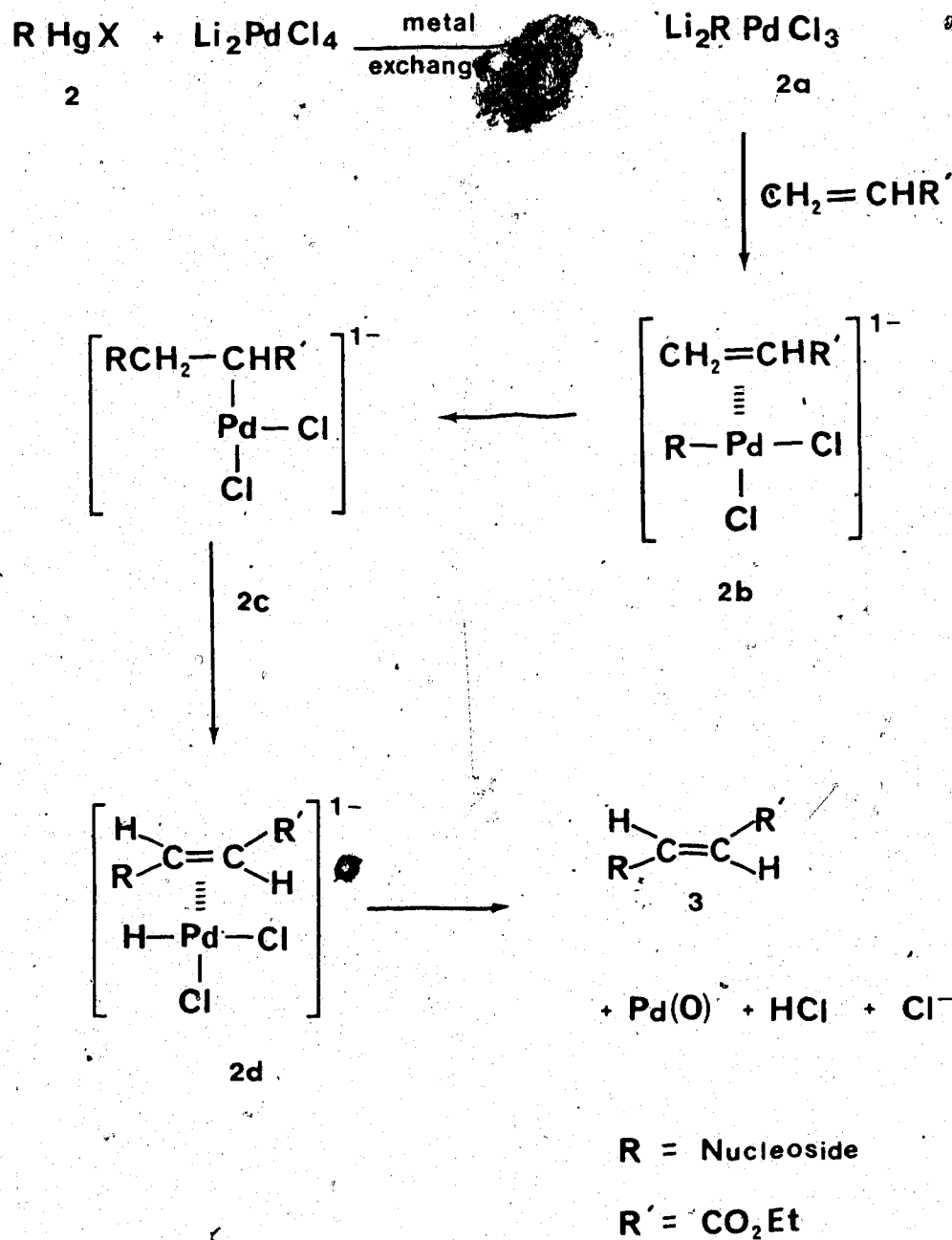


Fig. 6 Reaction Mechanism for Coupling of Dilithium Palladium Tetrachloride with 5-Chloromercuri Nucleosides.

hydroxide (73.7% yield) (197). The carboxylic acid **4** was the key intermediate in several subsequent chemical and radiochemical syntheses. The final step involved the reaction of **4** with N-iodo- or N-bromosuccinimide (NIS or NBS) to give (*E*)-5-(2-iodovinyl)-2'-deoxyuridine (IVdU, **5**, 30.4% yield) or (*E*)-5-(2-bromovinyl)-2'-deoxyuridine (BVdU, **6**, 42% yield). The NBS reaction was performed in aqueous medium, whereas the NIS reaction required dry DMF due to the instability of NIS in water. The halogenation reactions were stereospecific since little or no *Z* isomer was produced. The identities of products were established by *R_f* values (TLC and HPLC), UV and ¹H NMR spectral data. These data were in agreement with those reported in the literature (197). The vicinal coupling constant (*J*) of 15 Hz for the vinylic protons confirmed that compounds **5** and **6** were *E* isomers. The *Z* isomer of BVdU has been reported to have a *J* value of 8 Hz for the vinylic protons (207). The NIS and NBS reactions are not suitable for radiohalogenations employing short-lived isotopes such as ¹²⁵I, ⁷⁵Br and ⁸²Br, since these require the radiochemical synthesis of radiohalogenated NIS and NIS as the first step. Therefore, alternate methods using chloramine-T, amenable to a radiochemical synthesis were developed (Fig. 7). IVdU and BVdU obtained in these reactions were identical to the corresponding products formed by the NIS or NBS reaction with respect to *R_f* value, UV and ¹H NMR spectral characteristics and HPLC retention time. The chemical yields obtained by the chloramine-T method (26.3% for IVdU, 18% for BVdU) were lower than those obtained by the NIS and NBS methods.

(*E*)-5-(2-Iodovinyl)-2'-deoxyuridine-3',5'-diacetate was required as a reference compound for the radiochemical synthesis of [¹³¹I]-(*E*)-5-(2-iodovinyl)-2'-deoxyuridine-3',5'-diacetate. The synthetic route employed is shown in Fig. 8. Acetylation of (*E*)-5-(2-carboxyvinyl)-2'-deoxyuridine (**4**) using acetic anhydride in pyridine gave the corresponding diacetyl compound **7** (55.4% yield), which on iodination by the NIS method gave (*E*)-5-(2-iodovinyl)-2'-deoxyuridine-3',5'-diacetate (**8**) (41% yield). The ¹H NMR confirmed the presence of the two acetyl groups in this molecule. The vicinal coupling constants (*J*) of 15 Hz for the vinylic protons confirmed that it is an *E*

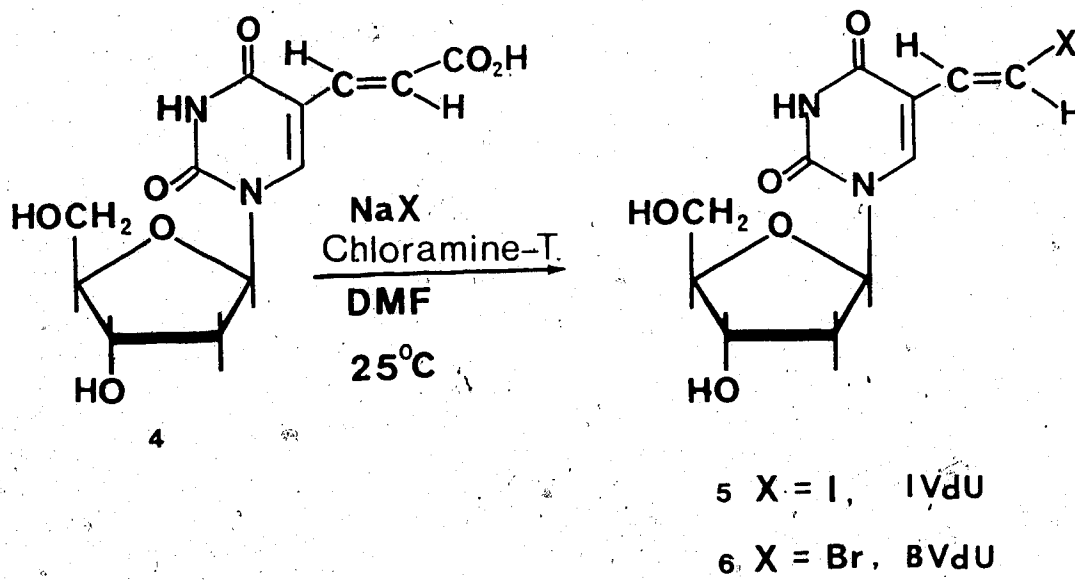


Fig. 7 Synthesis of IVdU and BVdU Using the Chloramine-T Method.

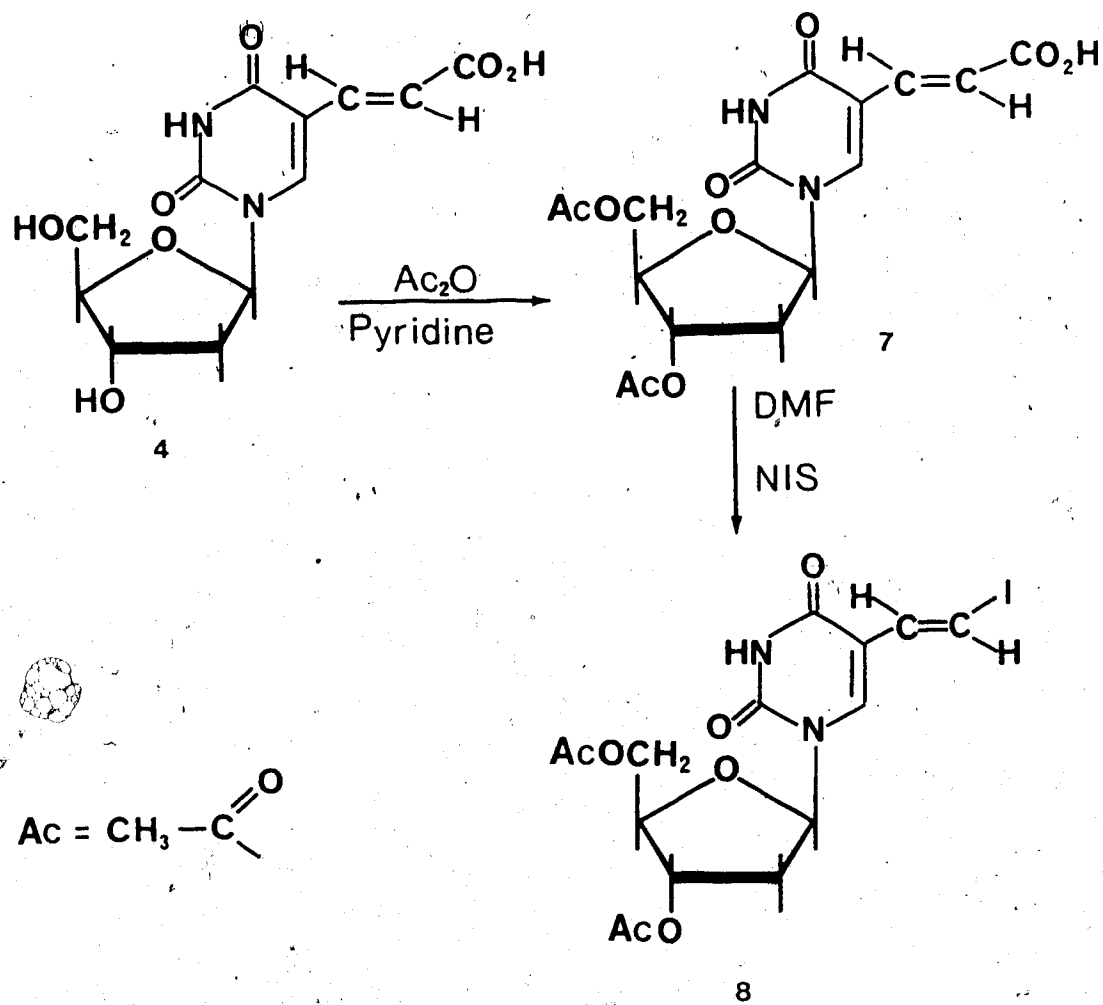


Fig. 8 Synthesis of IVdU-3',5'-diacetate.

isomer. The high resolution mass spectra showed a molecular ion (M^+) at 464.0081 which corresponded to the molecular formula $C_{13}H_{17}N_2O_7I$ (calculated mass : 464.00394)

(*E*)-5-(2-Iodovinyl)uracil was required as one of the reference compounds for metabolic studies of [^{131}I]-IVdU. It was synthesised by a 3 step procedure from commercially available 5-(hydroxymethyl)uracil (Fig. 9). Oxidation of 5-(hydroxymethyl)uracil (9) with potassium persulfate and silver nitrate at 30° C gave 5-formyluracil (10) (80% yield), which on condensation with malonic acid in the presence of piperidine gave (*E*)-5-(2-carboxyvinyl)uracil (11) (23% yield). (*E*)-5-(2-Iodovinyl)uracil (12) was obtained by iodination of compound 11 using chloramine-T and sodium iodide (10% yield)

C. Radiochemical Syntheses

The major objective of the radiochemical syntheses was to develop radiochemical routes suitable for the high specific activity syntheses of radiohalogenated IVdU and BVdU labeled with short-lived isotopes such as ^{125}I , ^{77}Br and ^{75}Br . Specific activity is an important factor to be considered in the design of a radiopharmaceutical aimed at a relatively small number of molecular targets (208). A low specific activity sample may quickly saturate the small number of molecular sites and any selective uptake may be left unnoticed due to the small ratio of radiolabeled to unlabeled molecules in the target. The specific activity of radiolabeled IVdU or BVdU used in this study is likely to be a critical factor, since the ratio of the HSV-infected cells to uninfected cells in an infected region of the brain of an HSE patient is likely to be very small.

The techniques for radioiodination and radiobromination of small molecules have been reviewed (209-211). Radioiodination reactions very often require *in situ* generation of an electrophilic species of iodine. Mild oxidising agents such as chloramine-T (212, 213), iodogen (214-216), and lactoperoxidase (213, 217, 218) are commonly used to oxidise radioactive iodide. The electrophilic species is believed to be I^+ . A simpler method for radioiodination of small molecules is the halogen-halogen exchange of a radioactive iodine isotope for a

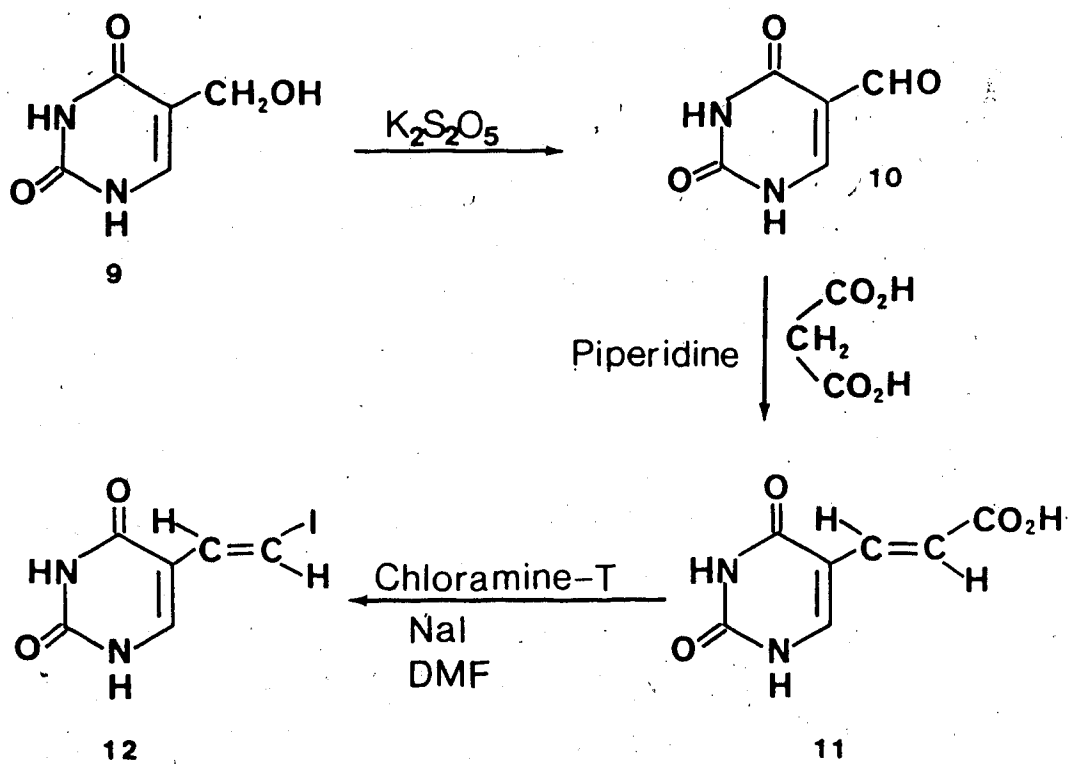


Fig. 9 Synthesis of (E)-5-(2-iodovinyl)uracil.

non-radioactive iodine atom (219, 220). This can often be achieved by simply heating the compound with radioactive iodide in a suitable solvent. Copper (I) salts have been reported to catalyze this isotope exchange (221, 222). The major limitation of this method is that it is not useful for the preparation of 'high specific activity' or 'no-carrier-added' ('NCA') syntheses. Electrophilic radiobromination reactions involve generation of an electrophilic species of bromine from bromide using a mild oxidising agent. Chloramine-T and N-chlorosuccinimide have been used for the *in situ* generation of an electrophilic species of bromine (probably BrCl) from bromide. (223-225).

The synthetic routes developed for the preparation of radiohalogenated IVdU and BVdU are shown in Fig. 10. These include

1. radioiodination and radiobromination using chloramine-T (routes C and D)
2. halogen isotope exchange reaction for radioiodination (route E) and
3. direct neutron activation of unlabeled BVdU (route F).

The radiochemical yields of radioiodinated IVdU (5a) using a variety of reaction conditions is summarised in Table 7. The Chloramine-T reaction used for the 'high specific activity' synthesis of [^{131}I or ^{125}I]-IVdU was complete in less than 1 h and gave 67.2% chemical yield and 69% radiochemical yield. A NCA reaction using ^{131}I , terminated at 30 min, gave [^{131}I]-IVdU without any substantial reduction in radiochemical yield (65%). This method was shown to be suitable for the synthesis of [^{125}I]-IVdU for the imaging studies using single photon emission computed tomography (SPECT). The lower radiochemical yield (40.7%) obtained for the ^{125}I synthesis is due to the short half-life of the isotope (13.26 h). The radiochemical yield corrected for decay is 57% and corresponds closely with that for ^{131}I synthesis. [^{131}I]-(*E*)-5-(2-Iodovinyl)-2'-deoxyuridine-3',5'-diacetate was also synthesised by chloramine-T method. The radiochemical yield was 50%.

The cuprous ion catalysed halogen isotope exchange reaction (route E) required heating for a prolonged time (20 h). The low chemical recovery (54.3%) and radiochemical yield (45.1%) may have been due to thermal decomposition. The stereospecificity of the iodine

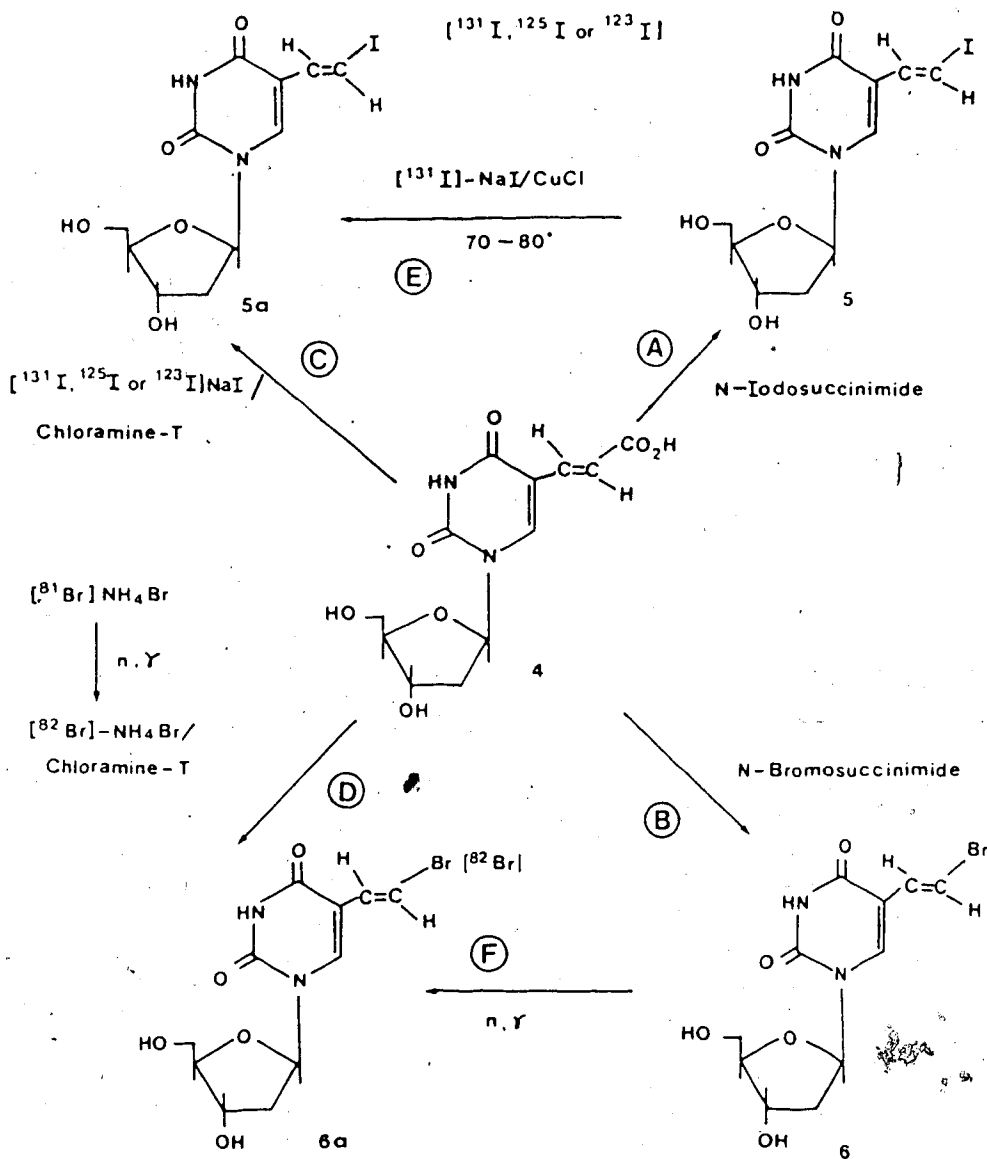


Fig. 10 Synthesis of Radiohalogenated IVdU and BVdU.

Table 7. Radiochemical Synthesis of IVDU

Method	Isotope	Specific Activity (GBq mmol ⁻¹)	Temperature (°C)	Time ¹	Radiochemical Yield ² (%)	Chemical Yield Isolated
Chloramine-T	¹²⁵ I, ¹²⁴ I	343.5	25	1 h	67.2	69.0
Chloramine-T	¹²⁵ I	370	25	30 min	40.7	57.0
Chloramine-T	¹²⁵ I	"NCA"	25	30 min	65.0	-
Halogen Isotope Exchange	¹²⁵ I	16.7	70-80	20 h	45.1	54.3

¹ Does not include the time required for purification.

² Radiochemical yields are those obtained at the end of purification.

exchange is consistent with previous studies involving halogen exchange reactions for other vinyl iodides (226). The exchange reaction is believed to proceed via generation of a small quantity of Cu^{131}I , which undergoes ligand exchange with the unlabeled IVdU (5). There is less radiation hazard using this technique since it does not generate a volatile radioiodine species. This exchange reaction is limited to the preparation of low and medium specific activity products.

^{82}Br was used as a model isotope of radiobromine in these studies since it is easily prepared at the University of Alberta SLOWPOKE Reactor Facility. $[^{81}\text{Br}]\text{-NH}_4\text{Br}$, required for the preparation of $[^{82}\text{Br}]\text{-NH}_4\text{Br}$ was obtained from $[^{81}\text{Br}]\text{-NaBr}$ by ion exchange using Amberlite CG 120 $[\text{NH}_4^+]$ resin. Neutron activation of $[^{81}\text{Br}]\text{-NH}_4\text{Br}$ using the $^{81}\text{Br}(n, \gamma)^{82}\text{Br}$ nuclear reaction at a flux of $10^{12} \text{ n cm}^{-2} \text{ s}^{-1}$ for 4 h gave $[^{82}\text{Br}]\text{-NH}_4\text{Br}$ with a specific activity of 2.3 MBq mg^{-1} . The theoretical yield calculated was 2.6 MBq mg^{-1} (Appendix). It would be possible to increase the specific activity to 6 MBq mg^{-1} with a subsequent 16 h irradiation at a neutron flux of $0.5 \times 10^{12} \text{ n cm}^{-2} \text{ s}^{-1}$. The SLOWPOKE reactor conditions do not allow irradiations at a higher neutron flux during this second period of 16 h irradiation.

The chemical and radiochemical yields of $[^{82}\text{Br}]\text{-BVdU}$ obtained by chloramine-T method and by direct neutron activation are shown in Table 8. The reaction of (*E*)-5-(2-carboxyvinyl)-2'-deoxyuridine (4) with $[^{82}\text{Br}]\text{-NH}_4\text{Br}$ in the presence of chloramine-T gave $[^{82}\text{Br}]\text{-BVdU}$ (6a) (69.8% radiochemical yield; specific activity $227 \text{ MBq mmol}^{-1}$). The short reaction time (10 min) makes this a suitable method for the incorporation of the positron emitter ^{82}Br (half-life 95.5 min) into BVdU. The direct neutron activation for the preparation of $[^{82}\text{Br}]\text{-BVdU}$ was carried out using BVdU which contained natural abundance bromine (^{79}Br and ^{81}Br). A 24 h cool-off time was required to allow decay of ^{80}Br , $^{80}\text{Br}^{\text{m}}$ and $^{82}\text{Br}^{\text{m}}$ (half-lives of 17.6 min, 4.3 h and 6.05 min respectively) before the irradiated sample was purified. Although radiolytic decomposition was minimal (<3%), only 30% of the overall activity produced was associated with $[^{82}\text{Br}]\text{-BVdU}$. This is due to the Szilard-Chalmers cleavage reaction which frequently occurs during neutron activation of organic halides (227).

Table 8. Preparation of [¹²⁵I]Br-BVDU

Method	Specific Activity (MBq mmol ⁻¹)	Temperature (°C)	Time ¹	Radio-chemical Yield ² (%)	Chemical Yield Isolated (%)
Chloramine-T	227	25	<10 min	69.8	72.0
Direct Neutron Activation	31.82		4 h	30.0	97.0

¹ Does not include the time required for purification

² Radiochemical yields are those obtained at the end of purification.

The neutron capture by bromine nucleus is followed by emission of a γ -ray, which gives recoil energy to the radioactive nucleus. This recoil energy may cause cleavage of the bond between C and radioactive Br. Because of this, the specific activity achieved from an organic bromide by direct neutron activation is much lower than the calculated theoretical yield. The radioactive inorganic bromine formed by Szilard-Chalmers cleavage would be of high specific activity. Therefore, Szilard-Chalmers cleavage of organic bromides could be used for the generation of high specific activity samples of inorganic bromine, which if separated from the organic compounds, could be used for high specific activity radiobrominations. A recent study at the University of Alberta SLOWPOKE Reactor Facility has shown that the inorganic bromine generated by the Szilard-Chalmers cleavage of an organic bromide attained a specific activity of about 500 times greater than that attained for an inorganic bromine sample by direct irradiation under the same irradiation conditions (228). The specific activity of [^{76}Br]-BVdU calculated to the end of irradiation was 32 MBq mmol $^{-1}$. The theoretical specific activity attainable for [^{76}Br]-BVdU by neutron irradiation of BVdU containing natural abundance bromine at a flux of 1×10^{12} n cm $^{-2}$ s $^{-1}$ for 4 h is 130 MBq mmol $^{-1}$ (Appendix). The direct irradiation method is not the method of choice for the preparation of [^{76}Br]-BVdU, since most *in vivo* studies require a much higher specific activity product.

D. Quantitative Uptake Studies of ^{131}I -Labeled (E)-5-(2-Iodovinyl)-2'-deoxyuridine in Herpes Simplex Virus-Infected Cells *In Vitro*

The biochemical rationale for the development of radiolabeled nucleoside analogs as potential diagnostic agents for the diagnosis of herpes simplex encephalitis (HSE) is based on their selective trapping in HSV-infected cells. The metabolic trapping of the radiolabeled nucleoside [^{131}I]-IVdU was evaluated by quantitating its uptake in HSV-1 (TK $^{-}$)-infected PRK cells *in vitro*. In biological evaluations IVdU was preferred over BVdU, since radioisotopes of iodine are more commonly used in clinical nuclear medicine than radioisotopes of bromine. The uptake of [^{131}I]-IVdU was studied with respect to three variables :

1. duration of exposure of cells to radiolabeled drug
2. concentration of radiolabeled drug and
3. the infecting dose of virus.

HSV-1 (TK⁻) and mock-infected PRK cells were used as controls. The mean and range values of the cellular uptake of IVdU under various conditions are shown in Fig. 11, 12 and 13.

Time-response curve for cellular uptake of [¹³¹I]-IVdU

Confluent PRK cells in Falcon 25-cm² flasks were either infected with 6 X 10⁶ PFU of HSV-1 (TK⁺) or mock infected. After 7 h of incubation, 0.629 KBq of [¹³¹I]-IVdU was added to each flask to give a final concentration of 2.76 ng ml⁻¹. Quantitation of both the intracellular and extracellular radiolabeled IVdU were determined at 20 s, 30 min, 1 h, 2h, 4 h, and 9 h respectively. Four HSV-1-infected flasks and three mock-infected flasks were used for the quantitation of intracellular and extracellular radioactivity at each time point.

The response for the cellular uptake of IVdU relative to time is shown in Fig. 11. The amount of radiolabeled IVdU in mock-infected cells remained low throughout the period of the study, whereas uptake of IVdU in HSV-infected cells increased with increasing time of exposure to the drug. The concentration of radiolabeled IVdU in the supernatant of HSV-1 (TK⁺)-infected cells decreased with time, while that of the mock-infected cells remained high throughout the period of the experiment. The uptake of [¹³¹I]-IVdU by the HSV-1 (TK⁺)-cells up to 9 h corresponded to 36% of the total activity present. This study demonstrates the selective time dependent uptake of ¹³¹I-IVdU by HSV-1-infected cells. A 5-10 fold higher concentration of the isotope could be detected in HSV-infected cells relative to uninfected cells as early as 1 h after the administration of IVdU. This suggests that uptake was rapid enough to permit the development of a radionuclide brain image even using a nucleoside with a relatively fast excretion or metabolism.

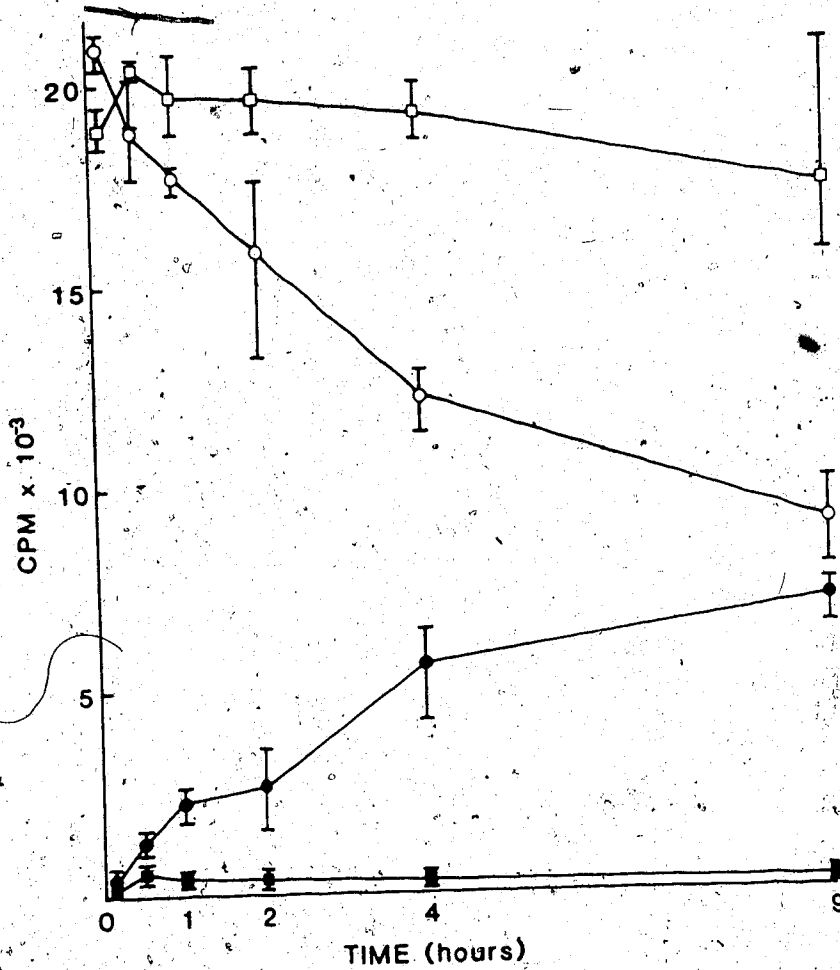


Fig. 11 Time-Response Curve for [¹²⁵I]-1VdU Uptake in HSV-1 (TK⁻) ($n=3$) and Mock-Infected ($n=2$) PRK cells. ● Intracellular Counts in HSV-1 (TK⁻)-Infected cells
○ Extracellular Counts in Medium Overlay of HSV-1 (TK⁻)-Infected cells ■ Intracellular Counts in Mock-Infected cells □ Extracellular Counts in Medium Overlay of Mock-Infected cells (Mean and Range).

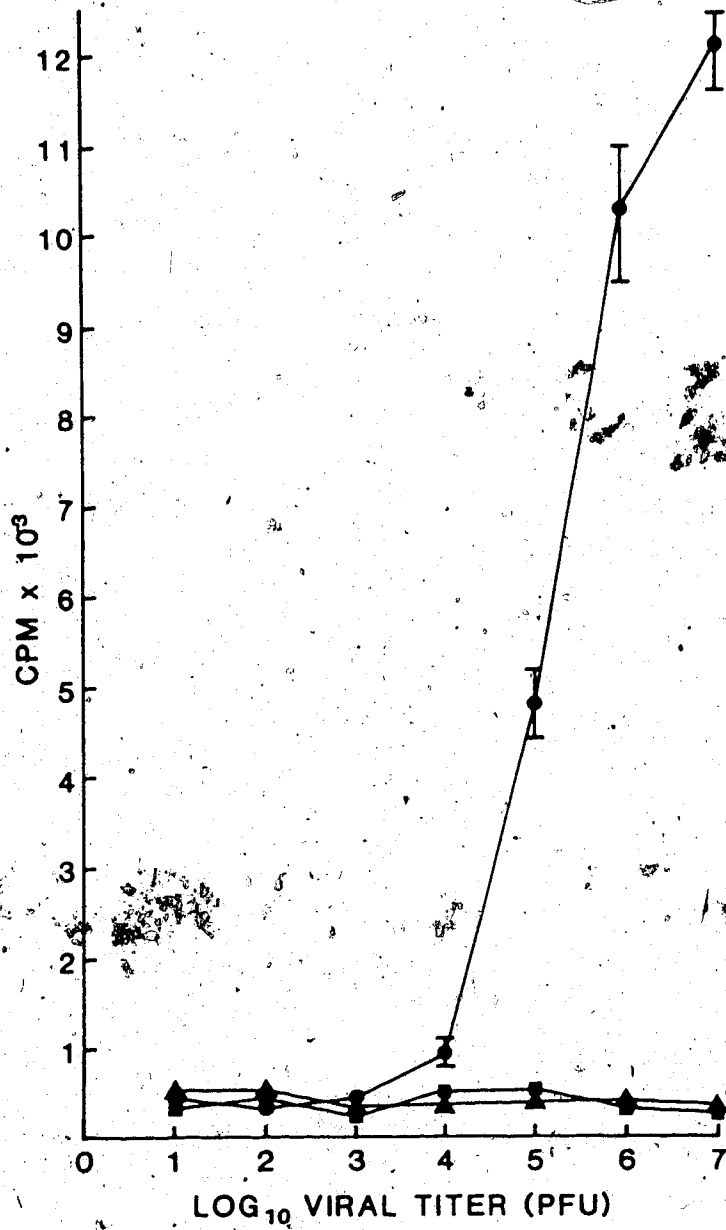


Fig. 12 Effect of Increasing the Titer of the Infecting Dose on the Uptake of [¹³¹I]-IVdU in HSV-1 (TK⁻) (n=3) (●), HSV-1 (TK⁻) (n=2) (▲), Mock-Infected Cells (n=3) (■) (Mean and Range).

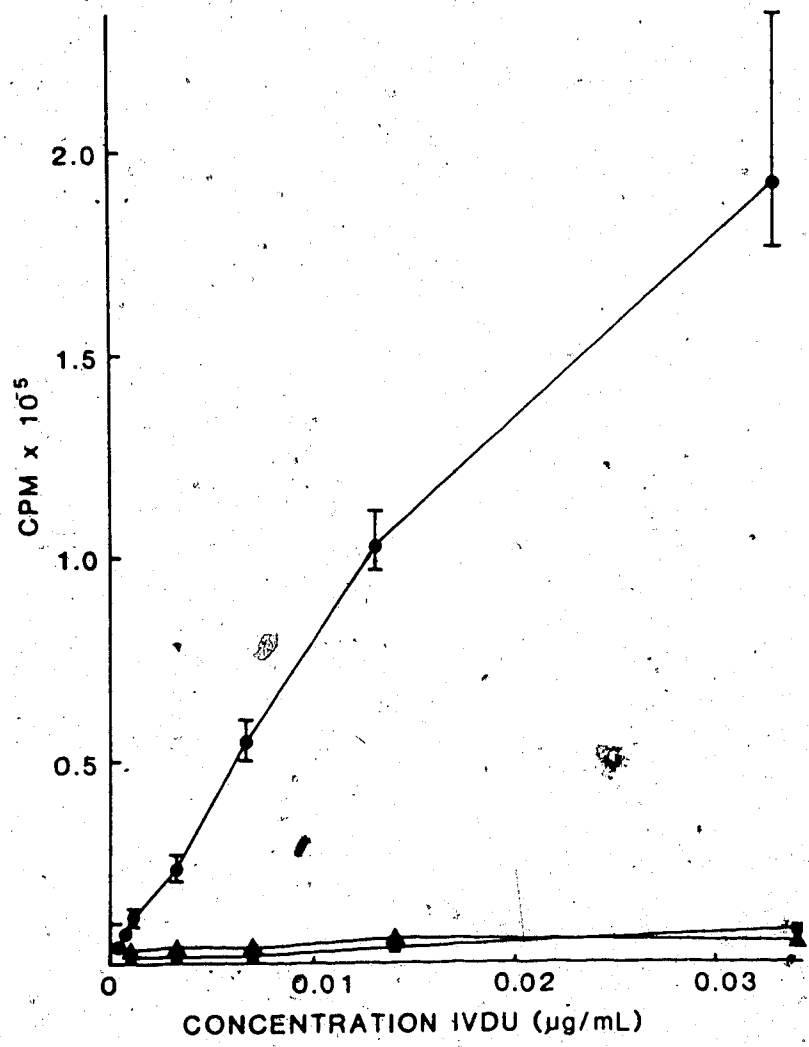


Fig. 13 Effect of Increasing Concentrations of [¹²⁵I]-IVdU on its Uptake in HSV-1 (TK⁻) (n=3) (●), HSV-1 (TK⁻) (n=2) (▲), Mock-Infected Cells (n=2) (■) (Mean and Range).

Effect of increasing infecting dose of virus on [¹³¹I]-IVdU uptake

Serial dilutions of stock HSV-1 (TK⁺) and HSV-1 (TK⁻) were made to give an infecting dose range of 10¹ to 10⁷ PFU per flask. Three flasks were infected with HSV-1 (TK⁺), two flasks were infected with HSV-1 (TK⁻), and two flasks were mock infected. After 7 h 0.836 KBq of [¹³¹I]-IVdU was added to each flask to give a final concentration of 0.858 ng·ml⁻¹. The cells were removed for the quantitation of the radioactivity after 4 h of incubation. The results are shown in Fig. 12. The quantity of [¹³¹I]-IVdU taken up by HSV-1 (TK⁺)-infected cells increased with increasing titer of infecting virus. HSV-1 (TK⁻)-infected cells showed insignificant uptake even at high doses of infecting virus. The inclusion of HSV-1 (TK⁻) controls in this study demonstrates that the selective uptake observed was mediated by HSV-encoded TK.

Since this experiment was completed in less than 14 h, it was assumed that the time was inadequate for a second phase of viral infection to occur. As shown in Fig. 12, an infecting dose of 10⁴ PFU for a 25-cm² flask containing 5 x 10⁵ cells is required before significant uptake can be detected. On this basis, in an animal model, at least 1 in 50 cells at any time would have to be infected before selective concentration of ¹³¹I-labeled IVdU could conceivably be detected by radionuclide brain imaging. The titer of HSV measured in brain biopsy specimens from HSE patients is not well documented. Nahmias *et al* have reported that in 11 out of 18 brain biopsies, the virus concentration was less than 10⁴ 50% tissue culture infective dose per g brain (79). A number of factors could affect the titer of virus from brain biopsy. The most important factor is probably the proximity of the biopsy to the most active site of infection. Since there is extensive histological destruction of HSV-infected brain tissue, it is likely that the titer of virus at the site of infection will be adequate to allow selective sequestration of the radiolabeled nucleoside.

Dose-response curve for [¹³¹I]-IVdU uptake

Known dilutions of ¹³¹I-labeled IVdU (specific activity 80 GBq mmol⁻¹) were made and added to the flasks 7 h after infection with either 6 X 10⁶ PFU of HSV-1 (TK⁺), HSV-1 (TK⁻), or mock infection. Concentrations were selected to cover a broad range around the dose known to cause a 50% reduction of PFU (ID₅₀). The ID₅₀ of IVdU for the JLJ strain used in these experiments was 8 ng per mL. The cells were incubated with [¹³¹I]-IVdU for 4 h. The uptake of ¹³¹I-labeled IVdU increased proportionately to the amount of the labeled drug in the media (Fig. 13). This relationship was observed only in HSV-1 (TK⁺)-infected cells and occurred even at concentrations greater than the ID₅₀. [¹³¹I]-IVdU was intracellularly trapped even when the nucleoside concentration was sufficient to inhibit virus replication. This suggests that medium specific activity compounds may be satisfactorily used for a radionuclide imaging and that the selective uptake of a nucleoside analog into HSV-infected cells may not be inhibited by the presence of an antiviral drug. A recent study on the effect of ara-AMP and acycloguanosine (ACG) on the *in vitro* uptake of [¹³¹I]-IVdU in HSV-1-infected cells have shown that the uptake was virtually not affected by the presence of inhibitory concentrations of ara-AMP and ACG for a period of 24 h (229). This suggests that a diagnostic imaging of HSE using a radiolabeled nucleoside may prove to be successful even during the initial period of therapy by an antiviral nucleoside.

The results of these *in vitro* studies validate the concept of metabolic trapping of radiolabeled nucleoside in HSV-infected tissues as a basis for the development of a radiopharmaceutical for the non-invasive diagnosis of HSE.

E. Tissue Distribution of [¹²⁵I]-IVdU in a Herpes Simplex Encephalitis Animal Model

The main objective of the preliminary tissue distribution study was to compare the uptake of [¹²⁵I]-IVdU in HSV-1-infected brain with that in uninfected brain to determine the feasibility of IVdU as a radiopharmaceutical for the *in vivo* detection of HSE. Eight rabbits (4 infected and 4 uninfected) were injected with an i.v dose of [¹²⁵I]-IVdU. A group of tissues

including blood, brain, liver, kidney, spleen, lung, and muscle were collected at 1 h and 6 h after injection and counted for radioactivity. The brain samples of the infected rabbits were assayed for the viral titer to confirm the presence of HSV infection. A viral titer of about 1×10^5 per g brain could be detected. Tissue distribution expressed as % injected dose per g tissue at 1 h and at 6 h are shown in Table 9 and Table 10 respectively. Tissue distribution expressed as a tissue to blood ratio at 1 h and 6 h are shown in Table 11 and 12.

None of the organs examined demonstrated high uptake of radioactivity. The uptake of radioactivity by brain was found to be relatively low at both time points studied. This may be due to a relatively low permeability of the nucleoside across the BBB. IVdU has a log P value of 0.60, whereas the optimal log P range for good permeability across BBB is 0.9 to 2.5. The mean uptake of the radiotracer in the infected brain was 5.4 to 6.4 times higher than in uninfected brain after injection. The difference was smaller (1.5 to 1.9 times greater in the infected brain compared to the uninfected) 6 h after injection. The reasons for this are not clear. One plausible explanation is that radioactive IVdU, selectively trapped in infected cells may undergo metabolic degradation to radioactive compound(s) having good permeability across plasma membrane, resulting in decreased intracellular radioactivity. The differences in the brain uptake between infected and uninfected animals was highest at 1 h. However, these data need to be viewed with caution since this study does not exclude the possibility that the higher uptake noted in infected brain tissue may in part be due to non-selective accumulation caused by increased BBB permeability in infected animals. The only organs other than brain which showed a pronounced difference in uptake of radioactivity between the infected and uninfected animals were liver and spleen for the organs examined. The reason for this is not clearly understood. Since these rabbits did not have antibodies to HSV, there is a possibility of infection of organs other than brain. However, this could not be confirmed, since organs other than brain were not assayed for the viral titer.

The radioactivity in blood remained higher than that in the target organ brain at 1 and 6 h. A comparison of the blood activity at 1 h and at 6 h (Table 9 and 10) indicated that

Table 9. Tissue distribution of ^{125}I -IVdU (Expressed as % Injected Dose per Gram Tissue) in a Rabbit Model 1 Hour After i.v Injection of 0.74 MBq of ^{125}I -IVdU (mean of two animals with range)

Tissue	Uninfected Rabbit	Infected Rabbit
Blood	0.1756 ± 0.0130	0.2045 ± 0.0017
Brain	0.0155 † ± 0.0039	0.0989 † ± 0.0089
Liver	0.1132 ± 0.0169	0.2511 ± 0.0105
Kidney	0.2512 ± 0.0080	0.3261 ± 0.1069
Spleen	0.0787 ± 0.0065	0.1667 ± 0.0257
Lung	0.1185 ± 0.0086	0.0764 ¹
Muscle	0.0565 ± 0.0047	0.0676 ± 0.0413

† $p < 0.025$

¹ Data from a single animal

Table 10. Tissue distribution of ^{125}I -IVdU (Expressed as % Injected Dose per Gram Tissue) in a Rabbit Model 6 Hours After i.v. Injection of 0.74 MBq of ^{125}I -IVdU (mean of two animals with range)

Tissue	Uninfected Rabbit	Infected Rabbit
Blood	0.1332 ± 0.0057	0.0958 ± 0.0058
Brain	0.0057 † ± 0.0005	0.0075 † ± 0.0015
Liver	0.0673 ± 0.0033	0.0420 ± 0.0031
Kidney	0.1236 ± 0.0068	0.0972 ± 0.0183
Spleen	0.0427 ¹	0.0392 ± 0.0033
Lung	0.0823 ¹	0.0589 ¹
Muscle	0.0177 ± 0.0019	0.0184 ± 0.0057

† $p < 0.40$

¹ Data from a single animal

Table 11. Tissue distribution of ^{125}I -IVdU (Expressed as Tissue to Blood Ratio) in a Rabbit Model 1 Hour After i.v Injection of 0.74 MBq of ^{125}I -IVdU (mean of two animals with range)

Tissue	Uninfected Rabbit	Infected Rabbit
Blood	1.0000	1.0000
Brain	0.0906 † ±0.0291	0.4881 † ±0.0477
Liver	0.6553 ±0.1448	1.2386 ±0.0621
Kidney	1.4415 ±0.1518	1.6035 ±0.5140
Spleen	0.4532 ±0.0701	0.8228 ±0.1336
Lung	0.6750 ±0.0006	0.3796 ¹
Muscle	0.3254 ±0.0510	0.3347 ±0.1062

† p < 0.025

¹ Data from a single animal

Table 12. Tissue distribution of ^{125}I -IVdU (Expressed as Tissue to Blood Ratio) in Rabbit Model 6 Hours After i.v Injection of 0.74 MBq of ^{125}I -IVdU (mean of two animals with range)

Tissue	Uninfected Rabbit	Infected Rabbit
Blood	1.0000	1.0000
Brain	0.0426 † ±0.0020	0.0798 † ±0.0209
Liver	0.5053 ±0.0032	0.4369 ±0.0054
Kidney	0.9272 ±0.0114	0.9700 ±0.1325
Spleen	0.3346 ¹	0.4089 ±0.0092
Lung	0.6456 ¹	0.5793 ¹
Muscle	0.1316 ±0.0084	0.1892 ±0.0417

† $p < 0.40$

¹ Data from a single animal

clearance of radioactivity from blood during this period was slow. Intact nucleosides usually have fast blood clearance characteristics due to their high water solubility. Lee *et al* have recently reported the tissue distribution of [2-¹⁴C]-5-ethyl-2'-deoxyuridine in tumor bearing mice (230). The biological half-life of [2-¹⁴C]-5-ethyl-2'-deoxyuridine in blood in the second phase of a bifunctional clearance curve was estimated to be 33 min. The slow blood clearance of radioactivity for [¹²⁵I]-IVdU in this preliminary study may be largely due to radioactive metabolites of [¹²⁵I]-IVdU. The high background radioactivity may present a major problem for diagnostic imaging, since it would obscure any selective uptake in the brain of the infected animal.

Saito *et al* have reported the use of quantitative autoradiography for the *in vivo* evaluation of the feasibility of radiolabeled nucleosides as non-invasive diagnostic agents for HSE (200-202). They have reported regional distribution of [2-¹⁴C]-1-(2-deoxy-2-fluoro- β -D-arabinofuranosyl)-5-methyluracil in the infected brain of an HSE rat model using this technique. The HSV-infected regions of the brain (presence of the virus confirmed by detection of viral antigens) showed 13 times higher uptake of radioactivity relative to the uninfected regions. Quantitative autoradiography offers an advantage over tissue distribution studies using scintillation counting in that it is able to demonstrate the high uptake by a small number of cells. In tissue distribution studies using scintillation counting, high uptake in a small area may be left unnoticed, since it may be masked by the background activity associated with the surrounding cells. Our tissue distribution studies succeeded in showing 5.4 to 6.4 times higher radioactivity in the infected brain as compared to the uninfected brain 1 h after injection. However, quantitative autoradiography could have demonstrated even a higher difference in regional uptake of radioactivity.

Our preliminary tissue distribution studies on [¹²⁵I]-IVdU indicated that there is a need for a clear understanding of pharmacokinetic and metabolic aspects of radioiodinated IVdU *in vivo*. Therefore the next phase of investigation was directed towards an evaluation of the *in vivo* kinetics of IVdU and its metabolites in a dog model.

F. Pharmacokinetics and Metabolism of [¹³¹I]-(E)-5-(2-Iodovinyl)-2'-deoxyuridine in Dogs

The pharmacokinetics and metabolism of a radiopharmaceutical may significantly influence its diagnostic value. Rapid excretion and/or metabolism to inactive compounds are usually undesirable since it would result in decreased bioavailability of the compound for accumulation into target tissue. In addition, radioactive metabolites having a long biological half-life may contribute to high background activity and increase the radiation dose.

The metabolic degradation of deoxythymidine and its 5-substituted analogs via phosphorolytic cleavage of the nucleoside bond by pyrimidine phosphorylases (182) have already been discussed in chapter I. The base formed as result of a phosphorolysis may be further catabolised by a reductive pathway (231). The first step is the reduction of the C₅-C₆ double bond of the ring to give dihydropyrimidines, followed by the oxidative cleavage of the N₃-C₄ bond to give β-uriedo acids, from which β-aminoacids, carbon dioxide and ammonia are formed. The 5'-monophosphates of the pyrimidine nucleosides which have halogens or halogen containing substituents at the 5 position are subject to thymidylate synthetase-catalysed dehalogenation (191) as indicated previously. The present investigation involved identification and quantitation of the major radioactive metabolites of [¹³¹I]-IVdU in *in vitro* and *in vivo* biological systems.

Metabolism of [¹³¹I]-IVdU in blood *in vitro*

[¹³¹I]-IVdU was incubated with heparinised whole blood and the radioactive components present in methanolic extracts of plasma were analysed by quantitative r-HPLC. Control experiments indicated that HPLC samples ready for injection contained greater than 90% of the original activity of the plasma sample prior to extraction with methanol. A typical radiochromatogram (Fig. 14) showed four radioactive peaks : A, B, C and D. Peaks C and D were identified as [¹³¹I]-(E)-5-(2-iodovinyl)uracil (IVU) and [¹³¹I]-IVdU respectively. Peak A was suspected to be radioactive iodide. However, the identity could not be confirmed initially since it eluted very close to the solvent front using the solvent system employed.

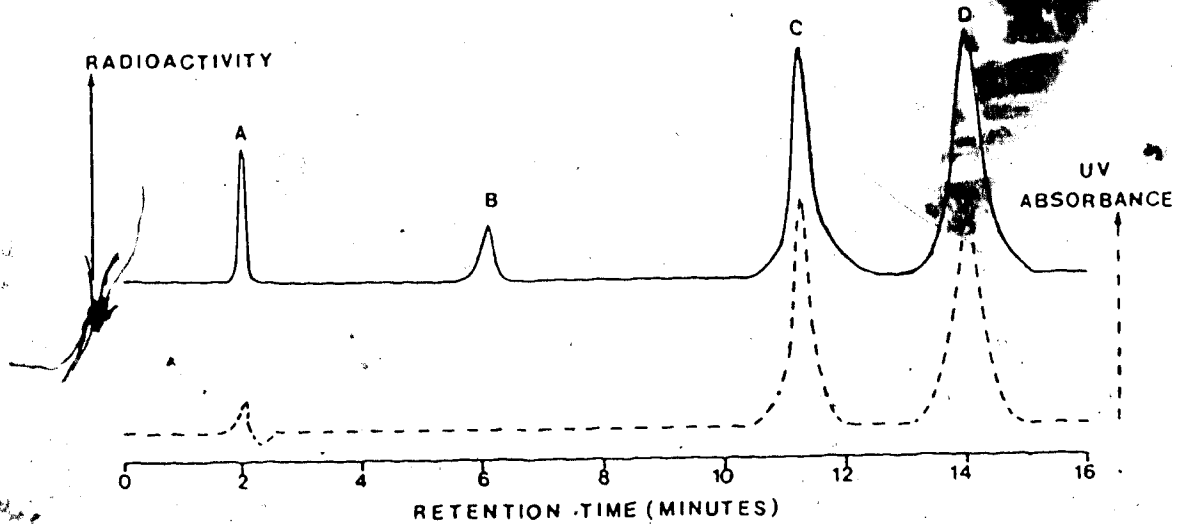


Fig. 14 A Typical Radio High-Pressure Liquid Chromatogram of Plasma Sample Containing $[^{131}\text{I}]$ -IVdU and its Metabolites. Peaks A, C, and D are $[^{131}\text{I}]$ -I⁻, $[^{131}\text{I}]$ -IVU, and $[^{131}\text{I}]$ -IVdU respectively. Peak B has not been identified.

the other radioactive compounds in plasma. The identity of peak A was subsequently established by rechromatography on r-HPLC using paired ion chromatography (PIC) separation conditions (232). The mobile phase used in PIC may contain a quaternary ammonium compound having hydrophobic groups so that it increases the retention of the anion being analysed on a reverse phase column by formation of an ion pair. Peak A co-chromatographed with a non-radioactive sample of iodide under PIC separation conditions. A peak B, not identified to date, did not correspond to any of the reference compounds used in the experiment.

The kinetics of [^{131}I]-IVdU, [^{131}I]-IVU and [^{131}I]-iodide in blood *in vitro* are shown in Fig. 15. The rapid disappearance of [^{131}I]-IVdU corresponded to an increase in the amount of [^{131}I]-IVU formed (Fig. 15). After a 2 hour incubation, 73% of the radioactivity was associated with [^{131}I]-IVU. Radioactive iodide represented less than 10% of the total radioactivity over a 24 hour period.

The major catabolic pathway for IVdU in blood appears to be phosphorylase to the corresponding base IVU. Blood platelets are rich in the enzyme deoxythymidine phosphorylase (184) which would be primarily responsible for the observed rapid *in vitro* conversion of IVdU to IVU. These results may be compared with the recently reported data describing the phosphorylase activity of intact blood platelets on several 5-substituted deoxythymidine analogs including BVdU (186). BVdU on incubation with human blood platelets was metabolised (95% in 2 h) to the corresponding base (*E*)-5-(2-bromovinyl)uracil (BVU). This *in vitro* study on BVdU did not include evaluation of possible debromination. The formation of radioactive iodide from ([^{131}I]-IVdU or [^{131}I]-IVU) remained low (<10% of the radioactivity in the plasma) over a period of 24 hours. This observation is consistent with the relatively high chemical stability expected for the vinyl iodides.



National Library
of Canada

Bibliothèque nationale
du Canada

Canadian Theses Service

Services des thèses canadiennes

Ottawa, Canada
K1A 0N4

CANADIAN THESES

THÈSES CANADIENNES

NOTICE

The quality of this microfiche is heavily dependent upon the quality of the original thesis submitted for microfilming. Every effort has been made to ensure the highest quality of reproduction possible.

If pages are missing, contact the university which granted the degree.

Some pages may have indistinct print especially if the original pages were typed with a poor typewriter ribbon or if the university sent us an inferior photocopy.

Previously copyrighted materials (journal articles, published tests, etc.) are not filmed.

Reproduction in full or in part of this film is governed by the Canadian Copyright Act, R.S.C. 1970, c. C-30. Please read the authorization forms which accompany this thesis.

**THIS DISSERTATION
HAS BEEN MICROFILMED
EXACTLY AS RECEIVED**

AVIS

La qualité de cette microfiche dépend grandement de la qualité de la thèse soumise au microfilmage. Nous avons tout fait pour assurer une qualité supérieure de reproduction.

S'il manque des pages, veuillez communiquer avec l'université qui a conféré le grade.

La qualité d'impression de certaines pages peut laisser à désirer, surtout si les pages originales ont été dactylographiées à l'aide d'un ruban usé ou si l'université nous a fait parvenir une photocopie de qualité inférieure.

Les documents qui font déjà l'objet d'un droit d'auteur (articles de revue, examens publiés, etc.) ne sont pas microfilmés.

La reproduction, même partielle, de ce microfilm est soumise à la Loi canadienne sur le droit d'auteur, SRC 1970, c. C-30. Veuillez prendre connaissance des formules d'autorisation qui accompagnent cette thèse.

**LA THÈSE A ÉTÉ
MICROFILMÉE TELLE QUE
NOUS L'AVONS REÇUE**



National Library of Canada

Bibliothèque nationale du Canada

Ottawa, Canada
K1A 0N4

TC -

0-315-22935-7

CANADIAN THESES ON MICROFICHE SERVICE - SERVICE DES THÈSES CANADIENNES SUR MICROFICHE

PERMISION TO MICROFILM - AUTORISATION DE MICROFILMER

• Please print or type - Écrire en lettres moulées ou dactylographier

AUTHOR - AUTEUR

Full Name of Author - Nom complet de l'auteur

Muhammad Hussien Alvic Saad

Date of Birth - Date de naissance

27.12.1959

Canadian Citizen - Citoyen canadien

Yes / Oui

No / Non

Country of Birth - Lieu de naissance

Sierra Leone
West Africa

Permanent Address - Résidence fixe

9-70 Basic Medical Sciences
Bldg, Dept of pharmacology
U of A, Edmonton, Alta

THESIS - THÈSE

Title of Thesis - Titre de la thèse

Studies on the modulation of airway reactivity in the guinea pig

Degree for which thesis was presented
Grade pour lequel cette thèse fut présentée

PhD

Year this degree conferred
Année d'obtention de ce grade

1985

University - Université

Alberta

Name of Supervisor - Nom du directeur de thèse

J. F. Burka

AUTHORIZATION - AUTORISATION

Permission is hereby granted to the NATIONAL LIBRARY OF CANADA to microfilm this thesis and to lend or sell copies of the film.

L'autorisation est, par la présente, accordée à la BIBLIOTHÈQUE NATIONALE DU CANADA de microfilmer cette thèse et de prêter ou de vendre des exemplaires du film.

The author reserves other publication rights, and neither the thesis nor extensive extracts from it may be printed or otherwise reproduced without the author's written permission.

L'auteur se réserve les autres droits de publication; ni la thèse ni de longs extraits de celle-ci ne doivent être imprimés ou autrement reproduits sans l'autorisation écrite de l'auteur.

THE UNIVERSITY OF ALBERTA

STUDIES ON THE MODULATION OF
AIRWAY REACTIVITY IN THE GUINEA PIG

By

©

Maan Saad

A THESIS

SUBMITTED TO THE FACULTY OF GRADUATE STUDIES AND RESEARCH
IN PARTIAL FULFILMENT OF THE REQUIREMENTS FOR THE DEGREE OF
Doctor of Philosophy

Pharmacology

Edmonton, Alberta

Fall 1985

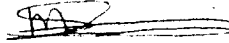
THE UNIVERSITY OF ALBERTA

RELEASE FORM

NAME OF AUTHOR Maan H.A. Saad
TITLE OF THESIS Studies on the Modulation of airway
reactivity in the guinea pig
DEGREE FOR WHICH THESIS WAS Doctor of Philosophy
PRESENTED
YEAR THIS DEGREE GRANTED Fall 1985

Permission is hereby granted to THE UNIVERSITY OF ALBERTA LIBRARY to reproduce single copies of this thesis and to lend or sell such copies for private, scholarly or scientific research purposes only.

The author reserves other publication rights, and neither the thesis nor extensive extracts from it may be printed or otherwise reproduced without the author's written permission.

(SIGNED) 

PERMANENT ADDRESS:

10 Ferngate Drive

Withington, Manchester

England

M20 9AX

DATED:

July 18 1985

THE UNIVERSITY OF ALBERTA
FACULTY OF GRADUATE STUDIES AND RESEARCH

The undersigned certify that they have read, and recommend to the Faculty of Graduate Studies and Research, for acceptance, a thesis entitled 'Studies on the modulation of airway reactivity in the guinea pig' submitted by Maan H.A. Saad in partial fulfilment of the requirements for the degree of Doctor of Philosophy in Pharmacology.

John B. Buxton
.....

Supervisor

D. A. B. ...
.....
H. B. ...
.....
Ernest Long
.....

Gene Lewis
.....

External Examiner

June 10, 1985
Date

ABSTRACT

The effects of immunological sensitization to ovalbumin (OA) were investigated in isolated guinea-pig airway tissues. It was found that the responses and sensitivity of normal and sensitized tracheal spirals and lung parenchymal strips to bronchoconstrictors including leukotrienes (LTs) C₄ and D₄, and bronchodilators, including isoproterenol and vasoactive intestinal peptide (VIP), were similar in both groups of animals. Indomethacin-pretreatment enhanced the responses of trachea to high concentrations of bronchoconstrictors and reduced responses of lung parenchymal strips to bronchodilators.

The bronchodilators stimulated adenylate cyclase activity of normal and sensitized lung parenchyma to similar extents.

It was concluded that immunological sensitization to OA does not induce airway hyperreactivity to bronchoconstrictors or airway hyporeactivity to bronchodilators in guinea-pig airways in vitro. Apparent airway-hyperreactivity of the trachea to bronchoconstrictors may result from removal of the negative modulatory influence of PGE₂ upon treatment of tissues with indomethacin. The reduction in bronchodilator efficacy in lung parenchyma upon indomethacin-pretreatment is unexplained and was not paralleled by a reduction in adenylate cyclase activity. Thus, there is a lack of correlation between bronchodilation and adenylate cyclase activation of lung strips.

It was further demonstrated that calcium ionophore A23187- and AA-induced contractions of airway tissues were similar in both normal

and sensitized tissues. Furthermore, it was found that airway-tissue contraction induced by OA and A23187 was reduced by mepacrine and nordihydroguaiaretic acid (NDGA) pretreatment. These agents inhibit phospholipase A₂ and lipoxygenase-enzyme activity, respectively. The effects of all these stimuli were enhanced by indomethacin-pretreatment of trachea. The effects were similar on both normal and sensitized tissues.

It was concluded that OA and A23187 stimulate AA metabolism via the lipoxygenase pathway. The mediators responsible for OA-A23187-, and AA-induced contractions were isolated and purified by high performance-liquid chromatography and subjected to bioassay and ultraviolet spectrometry studies. The evidence indicated that these mediators included LTC₄ and LTD₄.

Contractions to AA were reduced in calcium-free media and further reduced by EDTA and lanthanum ions. Re-addition of calcium reversed the inhibition. Nitrendipine prevented this reversal. Nitrendipine and verapamil inhibited AA-induced contractions but did not affect LTD₄-induced contractions. Hence it was concluded that extracellular calcium is more important for metabolism of AA to LTs than for smooth muscle contraction induced by the newly synthesized LTs.

Finally, the effects of LTD₄ on the adenylate cyclase activity of lung membranes were investigated. Current evidence indicated that LTD₄ inhibited adenylate cyclase. The effects of LTD₄ were investigated on guinea-pig lung and rat cerebellar adenylate cyclase.

GTP γ S-induced inhibition can be used as an index of the inhibitory potential of hormones in various cyclase systems. It was found that GTP γ S inhibition of lung cyclase was small relative to inhibition measured in the cerebellar cyclase system. Moreover, LTD₄-induced inhibition of lung cyclase activity was small and erratic. LTD₄ did inhibit the lung and cerebellar enzyme to a marked degree on some occasions. However, the reproducibility of the data was a major problem in these experiments.

ACKNOWLEDGEMENTS

I wish to express my sincere thanks to Dr. J.F. Burka, my supervisor and friend, for his invaluable guidance and support throughout the course of my tenure as a graduate student at the University of Alberta.

I also gratefully acknowledge the council, criticism, and encouragement that I received from the other members of my supervisory committee, viz, Drs. H.P. Baer, D.F. Biggs, and K. Wong. I would especially like to further thank Dr. H.P. Baer for allowing me to perform the cyclase assays in his laboratory, and for his numerous helpful suggestions regarding my work.

I extend my sincere thanks to all my colleagues and friends, too numerous to mention by name, for their moral and technical support. Special thanks are due to Mr. Gus Duchon for drafting some of the figures in this thesis, and to Mrs. Cecilia Kwong and Mrs. Linda Chambers for uncomplainingly typing and retyping successive drafts of the manuscript.

Finally, I wish to thank the Alberta Heritage Foundation for Medical Research for the generous financial support during the course of my studies at the University of Alberta.

Table of Contents

Chapter	Page
1. INTRODUCTION	1
1.1 ASTHMA AND AIRWAY HYPERREACTIVITY	2
1.2 MECHANISMS OF ASTHMA	3
1.2.1 Humoral and immunological mechanisms in asthma .	3
1.2.1.1 Biochemical events preceding mediator release	4
1.2.1.2 Chemical mediators in asthma	6
1.2.1.3 Prostaglandins and the airways	6
1.2.1.3.1 Prostaglandin biosynthesis	6
1.2.1.3.2 Effects of PGs on the airways	12
1.2.1.4 Pharmacology of the leukotrienes	13
1.2.1.4.1 Leukotriene biosynthesis	15
1.2.1.4.2 Inhibition of lipoxygenase product synthesis and effects	17
1.2.1.4.3 Biological sources of lipoxygenase products	18
1.2.1.4.4 Effects of leukotrienes on the airways	21

	Page	
1.2.1.4.5	Effects of leukotrienes on the central nervous system	23
1.2.1.4.6	Leukotriene receptors	24
1.2.1.4.7	Possible intracellular mechanism of action of LTD ₄	27
1.2.2	Autonomic control of the airways	28
1.2.2.1	Parasympathetic and sympathetic nervous system	28
1.2.2.2	Non-adrenergic non-cholinergic (NANC) inhibitory innervation	30
1.2.3	Basic regulatory processes in the airways	31
1.2.3.1	Adenylate cyclase	32
1.2.3.1.1	Characteristics of adenylate cyclase inhibition	34
1.2.3.2	Cyclic AMP and the airways	35
1.2.3.3	Calcium and the airways	37
1.2.3.3.1	Sources of utilizable calcium in the airways	38
1.2.3.3.2	Calcium channels in smooth muscle	38
1.2.3.3.3	Excitation-contraction coupling in smooth muscle	40
1.2.3.3.4	Calcium antagonists in asthma	40

	Page
1.3 STUDIES ON MODELS OF ASTHMA: MECHANISMS OF AIRWAY HYPERREACTIVITY	42
1.3.1 Sensitization-dependent changes in pharmacologic receptors	43
1.3.2 Sensitization-dependent changes in cyclic AMP and PGs	46
1.3.3 Sensitization-dependent changes in the role of lipoxygenase metabolites	48
2. RESEARCH OBJECTIVES	50
3. MATERIALS AND METHODS	54
3.1 MATERIALS	55
3.2 METHODS	56
3.2.1 Sensitization of animals and preparation of tissues	56
3.2.2 Concentration-response curves to broncho- constrictors and bronchodilators: Effects of cyclooxygenase and lipoxygenase inhibitors on responses to agonists	59
3.2.3 Responses to antigen, ionophore, A23187 and AA. Effect of AA metabolism inhibitors and calcium modulatory treatments	62

	Page
3.2.4 Extraction, initial purification, reverse-phase high performance liquid chromatography, ultraviolet spectrometry and bioassay of leukotrienes released from airway tissues	65
3.2.5 Adenylate cyclase assay procedure	69
3.2.5.1 Preparation of membranes	69
3.2.5.2 Adenylate cyclase assay procedure	70
4. RESULTS	73
4.1 RESPONSES OF NORMAL AND SENSITIZED AIRWAY TISSUES TO BRONCHOCONSTRICTORS AND BRONCHODILATORS	74
4.1.1 Contractile responses to bronchoconstrictors	74
4.1.2 Sensitivity of tracheal and parenchymal strips to bronchoconstrictors	77
4.1.3 Effects of cyclooxygenase and lipoxygenase inhibitors on the responsiveness and sensitivity of airways to bronchoconstrictors	79
4.1.4 Relaxant responses to bronchodilators	89
4.1.5 Effects of indomethacin-pretreatment on drug-induced relaxations	89
4.1.6 Effects of bronchodilators on adenylate cyclase activity in control and indomethacin-pretreated lung membranes	93

	Page
4.1.6.1 Effect of indomethacin-pretreatment on adenylate cyclase activation	98
4.2 ANTIGEN-, A23187-, AND AA-INDUCED CONTRACTIONS OF NORMAL AND SENSITIZED AIRWAY TISSUES	98
4.2.1 Effects of indomethacin, NDGA, or mepacrine	98
4.2.2 High performance liquid chromatography	111
4.2.3 Bioassay of released LTs	115
4.2.4 Nature of the mediators released from airway tissue after stimulation with AA, A23187 or OA	119
4.3 ROLE OF CALCIUM IN ARACHIDONIC ACID-INDUCED CONTRACTION OF GUINEA PIG AIRWAYS	119
4.3.1 Effects of calcium and TMB-8	119
4.3.2 Effects of nitrendipine and verapamil	121
4.3.3 Effects of lanthanum and EDTA. Reversal by calcium readdition	122
4.3.4 Concentration-response curves to LTC ₄	126
4.4 EFFECTS OF LTD ₄ ON LUNG CEREBELLAR ADENYLATE CYCLASE ACTIVITY	128
4.4.1 Initial studies	128
4.4.2 Effects of LTD ₄ on lung adenylate cyclase	141
4.4.3 Effects of GTPγS on guinea-pig lung and rat cerebellar adenylate cyclase	154

	Page
4.4.4 Effects of GABA and LTD ₄ on cerebellar adenylate cyclase activity	164
5. DISCUSSION	175
5.1 Effects of bronchoconstrictors and bronchodilators . . .	176
5.2 AA metabolism in guinea-pig airways. Role of calcium	188
5.3 Effects of LTD ₄ on lung and cerebellar adenyate cyclase	197
6. BIBLIOGRAPHY	206

List of Tables

Table	Page
1 Mediators in asthma	7
2 Representative sources of lipoxygenase products	19
3 Neurohumoral influences acting on airway smooth muscle (ASM)	29
4 Experimental protocol for the investigation of the effects of mepacrine and NDGA on the contractile effects of A23187, ovalbumin, and AA	63
5 Experimental protocol for Ca ²⁺ studies	64
6 Percentage recovery of [³ H]-LTC ₄ utilizing C ₁₈ -SEP-PAKs	67
7 Increases in force after the addition of bronchoconstrictors	76
8 Sensitivity of normal and sensitized-airway tissues to bronchoconstrictors	78
9 Effect of inhibitors on tone and percentage change from preincubation tone	80
10 Effect of inhibitors on sensitivity of tracheal spirals to histamine and carbachol	88
11 Sensitivity of airway tissues from normal and sensitized animals to relaxant agents in vitro	91

	Page
12 Maximum control relaxations of airway tissues from normal and sensitized guinea pigs after addition of bronchodilators	92
13 Sensitivity of normal and sensitized airway tissues to bronchodilators	95
14 Adenylate cyclase activity of control and indomethacin-pretreated lung membranes	101
15 Release of LTs from guinea-pig airway tissue in the first hour	118
16 Effects of GTP on lung adenylate cyclase in the presence or absence of adenosine deaminase	136
17 Basal adenylate cyclase activities	140
18 GTP γ S inhibition of adenylate cyclase activity	156
19 Percentage inhibition of rat cerebellar cyclase basal activity in the presence of Mg ²⁺ and Mn ²⁺	170

List of Figures

Figure	Page
1 Arachidonic acid metabolism	11
2 Arachidonic acid metabolism by 5-lipoxygenase	16
3 Length-tension relationships of isolated guinea pig airways	58
4 Elution pattern of LTC ₄	68
5 Concentration-response curves to bronchoconstrictors in tracheal spirals and parenchymal strips from normal and ovalbumin-sensitized guinea pigs	75
6 Effects of indomethacin, phenidone and NDGA on responses of normal and sensitized trachea to histamine and carbachol	81
7 Effects of indomethacin, phenidone, and NDGA on responses of normal and sensitized trachea to LTC ₄ and LTD ₄	83
8 Effects of indomethacin on responses of normal and sensitized trachea to U-44069	84
9 Effects of indomethacin, phenidone, and NDGA on responses of normal and sensitized parenchyma to histamine, carbachol and U-44069	85
10 Effects of indomethacin, phenidone, and NDGA on responses of normal and sensitized parenchyma to LTC ₄ and LTD ₄	87
11 Relaxant responses to isoproterenol, PGE ₂ , VIP, and forskolin in normal and sensitized airway tissues	90

	Page
13 Effects of indomethacin on the relaxant responses of normal and sensitized parenchymal strips	96
14 Hormonal specificity of the responses of guinea-pig lung parenchymal adenylate cyclase	97
15 Activation of normal and sensitized lung adenylate cyclase by isoproterenol, pGE ₂ , and VIP	99
16 Effects of indomethacin-pretreatment on lung adenylate cyclase activation induced by forskolin	100
17 Concentration-response curves to A23187 on normal and sensitized lung tracheal strips	102
18 Concentration-response curves to A23187 on normal and sensitized lung parenchymal strips	103
19 Responses of sensitized airway tissues to ovalbumin	105
20 Contractile responses of normal and sensitized trachea to A23187 and ovalbumin	106
21 The responses of normal and sensitized trachea to AA: effects of mepacrine pretreatment	107
22 The responses of normal and sensitized parenchymal strips to AA: effects of mepacrine	108
23 The responses of indomethacin-treated tracheal spirals to AA, A23187, or OA in the presence of mepacrine	109
24 The responses of indomethacin-treated parenchymal strips to AA, A23187, or OA in the presence of mepacrine	110

	Page
25 Effects of NDGA on the tracheal response to AA, A23187, or ovalbumin	112
26 Effects of NDGA on the lung parenchymal response to AA, A23187, or ovalbumin	113
27 Typical HPLC chromatograms of released LTs	114
28 Ultraviolet spectra of synthetic and natural LTC ₄	116
29 Typical bioassay tracings of natural LTC ₄	117
30 The effects of calcium and TMB-8 on AA-induced contractions of airway tissues	120
31 Effects of nitrendipine and verapamil on AA-induced contractions of trachea and parenchyma	123
32 Effects of lanthanum chloride and EDTA on AA-induced contractions of trachea	124
33 Effects of lanthanum chloride and EDTA on AA-induced contractions of parenchyma	125
34 Contractions of trachea and parenchyma to LTC ₄	127
35 Time-course of lung adenylate cyclase activation at 20°C	129
36 Protein-linearity of lung adenylate cyclase assays	130
37 Activation of lung adenylate cyclase at 30°C	131
38 Stimulation of lung adenylate cyclase at 37°C in the presence of two different Mg ²⁺ concentrations	132
39 Stimulation of lung adenylate cyclase at 20°C by forskolin and isoproterenol	133

	Page
40 Stimulation of lung adenylate cyclase by GTP in the absence and presence of LTD ₄	135
41 The effects of adenosine deaminase on the responses of rat-cerebellar adenylate cyclase to GTP	137
42 The effects of adenosine deaminase on the responses of rat cerebellar cyclase to GTP and adenosine	138
43 Lack of effect of LTD ₄ on forskolin or isoproterenol-stimulated lung adenylate cyclase activity	142
44 Effect of LTD ₄ on forskolin-stimulated lung adenylate cyclase	143
45 Effect of LTD ₄ on lung adenylate cyclase in the absence or presence of NaCl	144
46 Effect of GTP on LTD ₄ -induced inhibition of lung adenylate cyclase	145
47 Effect of LTD ₄ on lung adenylate cyclase activity at 37°C	147
48 Effect of LTD ₄ on lung adenylate cyclase activity in the presence of Mg ²⁺ or Mn ²⁺	148
49 Effect of LTD ₄ on lung adenylate cyclase activity in the absence or presence of NaCl	149
50 Binding of [³ H]-LTC ₄ to guinea pig lung membranes at 20°C	151
51 Inhibition of lung adenylate cyclase activity by Ca ²⁺	152
52 Inhibition of cerebellar adenylate cyclase activity by Ca ²⁺	153

	Page
53 Inhibition and stimulation of lung adenylate cyclase activity by GTP γ S at 20°C	155
54 Effects of GTP γ S on forskolin-stimulated lung adenylate cyclase at 37°C	158
55 Effects of GTP γ S on lung and cerebellar cyclase activities at 37°C	159
56 Time course of GTP γ S inhibition of cerebellar cyclase activity	160
57 Effect of GTP γ S on cerebellar adenylate cyclase activity at 20°C	162
58 Effect of protease inhibitors on lung adenylate cyclase activity	163
59 Effects of GTP γ S on cerebellar adenylate cyclase activity in the presence of GABA or LTD ₄	165
60 Effects of LTD ₄ and GABA on cerebellar adenylate cyclase activity at 20°C	166
61 Inhibition of cerebellar adenylate cyclase activity by GABA at 20°C	168
62 Inhibition of cerebellar adenylate cyclase activity by GABA and GTP γ S under various conditions	169
63 Percentage inhibition of cerebellar adenylate cyclase activity by GABA, LTD ₄ and LTC ₄ at 20°C	172
64 Effects of LTD ₄ on cerebellar adenylate cyclase in the presence of GTP	173

ABBREVIATIONS

AA:	Arachidonic acid (5,8,11,14, eicosatetraenoic acid)
AD:	Adenosine deaminase
ASM:	Airway smooth muscle
ATP:	Adenosine Triphosphate
BSA:	Bovine serum albumin
Cyclic AMP:	Cyclic adenosine 3',5',monophosphate ✓
DTT:	Dithiothreitol (Cleland's reagent)
EDTA:	Ethylenediaminetetracetic acid
GABA:	γ -aminobutyric acid
Gpp(NH)p:	Guanyl-5'-(β , γ ,imino)triphosphate
GTP:	Guanosine triphosphate
GTP γ S:	Guanosine-5'-(3-O-thio)triphosphate
HETE:	Hydroxyeicosatetraenoic acid
HPETE:	Hydroperoxyeicosatetraenoic acid
HPLC:	High performance liquid chromatography
IgE and IgG:	Immunoglobulins E and G, respectively
INA:	Isoproterenol
KHS:	Krebs Hensleit solution
LT:	Leukotriene
NANC:	Non-adrenergic non-cholinergic innervation
NDGA:	Nordihydroguaiaretic acid
OA:	ovalbumin

PG: Prostaglandin
PLA₂: Phospholipase A₂
RBL-1: Rat basophilic leukaemia cells
TXA₂: Thromboxane A₂
VIP: Vasoactive intestinal polypeptide

INTRODUCTION

1.1 ASTHMA AND AIRWAY HYPERREACTIVITY: INTRODUCTION

Bronchial asthma is a complex disease characterized by reversible obstruction of both conducting (large) and distensible (small) airways. The main components of airway obstruction in asthma include airway smooth muscle constriction, smooth muscle hypertrophy and hyperreactivity, mucosal inflammation, goblet cell and mucus gland hypertrophy, mucus hypersecretion and plug formation, and a decreased rate of mucus clearance (Leff, 1982; Wanner, 1983). Pulmonary function tests of asthmatic patients indicates increases in resistance to airflow due to constriction of the larger airways, decreases in compliance due to decreases in distensibility of the smaller airways and increases in residual volume of the lung due to trapping of air in alveolae. Post mortem examinations of patients who died of asthma consistently show that edema and infiltration of inflammatory cells in the bronchial mucosa have occurred (Hogg, 1983) suggesting the development of inflammation.

The etiology of asthma is complex. Factors implicated in its development and pathogenesis include atopy (Cross, 1981), viral and bacterial respiratory tract infections (Welliver, 1983), psychological influences (Herrera & Fialkor, 1981), environmental influences (Hendrick et al. 1981), and a genetic predisposition towards airway hyperreactivity to nonspecific and pharmacological agents. Patients with asthma can be broadly divided into extrinsic and intrinsic groups. In the former group, there is a known causative external

agent (Garland, 1984), as opposed to the latter group, where an external stimulus is not apparent.

1.2 MECHANISMS OF ASTHMA

Asthma is a syndrome that arises as a consequence of immunological, humoral, autonomic and cellular biochemical regulatory mechanisms that operate within the airways. Dysfunctions in these regulatory influences may contribute to the hyperreactivity of airways inherent in asthma.

1.2.1. Humoral and Immunological Mechanisms in Asthma:

Allergic asthma is initiated in susceptible individuals by prior sensitization of components of the immune system with a foreign substance (i.e. allergen) which is usually a protein moiety (Foreman & Lichtenstein, 1980). Subsequent development of specific antigen hypersensitivity then paves the way for the immediate (type 1) hypersensitivity reaction which results in anaphylactic release of mediators when antigen bivalently crosslinks antibodies bound to the effector cells of the immune system (e.g. mast cells, basophils, macrophages (Ishizaka, 1982). Subsequent release of mediators in the vicinity of the airway smooth muscle and other effector cells initiates bronchoconstriction, edema, and mucus accumulation (Austen & Orange, 1975; Eyre & Burka, 1978; Leff, 1982; Lagunoff, 1983).

The mediators primarily involved in airway obstruction include

histamine, prostaglandins (PGs) $F_2\alpha$ and D_2 and leukotrienes (LTs) C_4 , D_4 and E_4 . The pharmacology of PGs and LTs in the airways is reviewed in sections 1.2.1.3 and 1.2.1.4. Histamine can act directly to contract airway smooth muscle via H_1 receptors or indirectly via irritant receptors in the airways to induce vagally-mediated reflex bronchoconstriction (Gold et al. 1972; Leff, 1982; Biggs, 1984). Histamine can also increase the release of acetylcholine from cholinergic nerve terminals in the airways (Theoharides et al. 1982).

1.2.1.1. Biochemical events preceding mediator release:

The Ishizakas in 1967 showed that the reaginic antibody in human asthma is immunoglobulin E (IgE). This is similar to the situation in rat, mouse, dog, and monkey. In the guinea pig, the reaginic antibody appears to be of the IgG_1 class (Mongar, 1965; Andersson, 1980). However, the guinea pig can be made to produce IgE in addition to IgG_1 (Andersson, 1980). Bryant et al. (1973, 1975) showed that IgG can play a role in human asthma, but that this involves a subgroup of IgG called IgG_4 which has homocytotropic properties. IgE has the capacity to sensitize tissues from normal individuals passively. Details of the structure of IgE have been reviewed (Tada, 1975; Ishizaka, 1976; Metzger, 1979; Foreman & Lichtenstein, 1980; Ishizaka, 1982).

Activation of mast cell mediator release can occur when antigen bivalently crosslinks two IgE molecules via their antigen binding regions (Fab). Other stimuli that can activate mast cells to induce

mediator release include compound 48/80, polymyxin B, dextran, mellitin, formyl-met-leu-phe, C5a and C3a anaphylatoxins, phosphatidic acid, and degranulating peptide from cobra venom. The calcium ionophore A23187 is a useful nonspecific tool in mediator release experiments.

A variety of biochemical processes appear to be important in mast cell activation. These include phospholipid methylation, phosphatidylinositol (PI) turnover, adenylate cyclase activation and Ca^{2+} entry into the cell. The first three processes appear to be vital for the last process to occur (Metzger, 1979, Hirata & Axelrod, 1980; Ishizaka et al. 1980; Ishizaka et al. 1984).

Histamine secretion by activated mast cells parallels Ca^{2+} uptake (Foreman et al. 1977; Foreman, 1980; Ishizaka et al. 1983). The rise in ionized calcium inside the mast cell induced by various secretagogues serves to activate phospholipase (PL) A_2 (Billah et al. 1980; Lapetina et al. 1981; Wightman et al. 1982) which splits off arachidonic acid (AA) from phosphatidylcholine. Free AA is metabolized by cyclooxygenase and the calcium-dependent lipoxygenase (Jakschik & Lee, 1980) to produce PGs and LTs, respectively. Moreover, calcium is required in the exocytotic release of preformed mediators from the mast cell. The effects of calcium are probably exerted via calmodulin (Cheung, 1980; Steinhardt & Alderton, 1982).

1.2.1.2 Chemical mediators of asthma:

The mast cell is central to the currently held views of the pathogenesis of allergic asthma (Austen & Orange, 1975; Lagunoff, 1983). Upon stimulation, mast cells release a plethora of mediators (summarized in Table 1).

1.2.1.3 Prostaglandins and the airways:

PGs are local modulators of cellular responses. The role of PGs in homeostasis and body functions has received intense attention. The literature has been well reviewed (Moncada & Vane, 1979; Stenson & Parker, 1980; McGiff, 1981; Moncada, 1981, Goetzl, 1981; Spannhake et al. 1981; O'Flaherty, 1982; Burka, 1983).

1.2.1.3.1 Prostaglandin biosynthesis:

PGs and thromboxanes (TXs) are derived via cyclooxygenase metabolism of AA (Fig. 1). The bulk of AA in cells is esterified in the 2-acyl position of glycerophospholipids of the cell membrane (see Irvine, 1982). PGs are not stored to any great extent in a tissue. An increase in their levels represents de novo synthesis. It is generally agreed that the first rate limiting step in PG synthesis is the release of bound AA into a free form. This is accomplished by a calcium dependent PLA₂ (see section 1.2.1.1).

Activation of PLA₂ can be induced by mechanical or electrical stimulation (Turker & Zengil, 1976), and by challenge of airway tissue

TABLE 1. Mediators in Asthma

Mediator	Status in tissue	Main Biologic Activity	Comments	Selected References
Histamine	Preformed	Constricts airway smooth muscle, activates irritant receptors leading to vagal reflex contraction of the airways, increases vascular permeability, induces hypotension	Released with heparin, released very rapidly after mast cell activation in the early stages of the immediate-hypersensitivity reaction.	Dale & Laidlaw, (1910). Kazimierczak & Diamant, (1978). Austen & Orange (1975). Theoharides et al. (1982). Biggs, (1984).
5-Hydroxy-tryptamine	Preformed	As histamine	Rodent mast cells	Theoharides et al. (1982).
LTC ₄ , LTD ₄ , LTE ₄	Newly synthesized from AA via the lipoxigenase pathway	Potent bronchoconstrictors, increase mucus secretion, decrease mucus clearance, stimulate PG synthesis, increase vascular permeability, vasoconstrictors and contractile on a variety of smooth muscles.	Peptidolipid leukotrienes. 1000-10,000 times more potent as bronchoconstrictors than histamine. More potent on small airways than large airways. Shown to be released from human asthmatic lung after antigen challenge.	Kellaway & Trethewie, (1940). Brocklehurst, (1968). Lewis et al. (1980). Morris et al. (1980). Goetzl (1981). Peters et al. (1981). Samuelsson, (1982). O'Flaherty, (1982).

TABLE 1. (Cont'd) Mediators in Asthma

Mediator	Status in tissue	Main Biologic Activity	Comments	Selected References
LTB ₄ (5,12-di-HETE)	Newly synthesized from AA via the lipoxigenase pathway	Bronchoconstrictor on small airways, induces TXA ₂ synthesis. Chemokinesis and chemotaxis of leucocytes.	Most potent chemokinetic and chemotactic agent for neutrophils and eosinophils.	Borgeat & Samuelsson (1979) Ford-Hutchinson et al. (1980). Sirois et al. (1982). Bray, (1983).
5-HETE		Bronchoconstrictor, stimulates histamine release from mast cells	Modulator of histamine release	Peters et al. (1981).
PGD ₂ , PGF ₂ α TXA ₂	Newly synthesized from AA via the cyclooxygenase pathway.	Bronchoconstrictors, vasoconstrictors, stimulate irritant receptors, immunomodulators.	PGD ₂ is the major PG released from human lung mast cells.	Goetzl, (1981). Spannhake et al (1981). O'Flaherty, (1982).
PGE ₂ PGI ₂	cyclooxygenase products.	Bronchodilator and bronchoconstrictors depending on dose, vasodilators. Inhibit mediator release via cyclic AMP synthesis.	Important modulators of airway responses to bronchoconstrictors.	Goetzl, (1981). Spannhake, (1981).

TABLE 1. (Cont'd) Mediators in Asthma

Mediator	Status in tissue	Main Biologic Activity	Comments	Selected References
Platelet-activating factor (PAF)	Newly synthesized phospholipid	Bronchoconstrictor on small airways, hypotensive, induces platelet aggregation and release of platelet 5HT. Increases vascular permeability.	Bronchoconstrictor effect partially due to TXA ₂ synthesis. Released from mast cells after immunological activation.	Benveniste (1974). Stimler et al. (1983). Hamasaki et al. (1984).
Vasoactive intestinal polypeptide (VIP)	Preformed peptide	Bronchodilator, inhibits mediator release, stimulates adenylate cyclase in lung.	Released from mast cells, main candidate neurotransmitter for the inhibitory innervation of the airways (non-cholinergic-non-adrenergic)	Cutz et al. (1978).
Adenosine	Preformed nucleoside	Bronchoconstrictor in asthmatics. Inhibits or stimulates mediator release depending on concentration.	Release from mast cells demonstrated. Theophylline may exert its anti-asthmatic effect by antagonism of adenosine at R _a receptors.	Sydbom and Fredholm (1982). Cushley et al. (1983). Cushley et al. (1984). Holgate et al. (1984). Marquardt et al. (1984). Hughes et al. (1984).

with histamine, acetylcholine, KCl (Orehek et al. 1975; Grodzinska et al. 1975), A23187, and antigen in sensitized tissues (Burka et al. 1981) (See Burka, 1983 for a review).

PLA₂ can be inhibited by drugs such as the anti-inflammatory glucocorticoids which induce the synthesis of a protein known as macrocortin which then causes PLA₂ inhibition (Blackwell et al. 1980; Hirata et al. 1980). Mepacrine also inhibits PLA₂ activity in airway tissue (Blackwell et al. 1978).

Following release from membrane pools, AA is rapidly enzymatically metabolized to various oxygenated products via the cyclooxygenase and/or the lipoxygenase pathways. The products of cyclooxygenation of AA include PG endoperoxides, PGE₂, PGD₂, PGF₂α, PGI₂ and its breakdown product 6-keto PGF₁α, and TXA₂ and its breakdown product TXB₂ (Fig. 1). PG synthesis has been demonstrated in guinea pig, human, and dog airways. The principal PG in guinea pig and dog trachea is PGE₂ (Orehek et al. 1975; Yamaguchi et al. 1976; Burka et al. 1981). The principal cyclooxygenase metabolites in lung tissue are TXA₂, PGD₂, and PGI₂ (Schulman et al. 1981). The majority of PGD₂ is probably produced by lung mast cells upon immunological activation (Peters et al. 1983), whereas the other metabolites may be produced indirectly by the action of other anaphylactic mediators upon other cells in the lung.

Selective inhibition of the cyclooxygenase enzyme can be brought about by aspirin (Vane, 1971), which irreversibly inhibits the enzyme

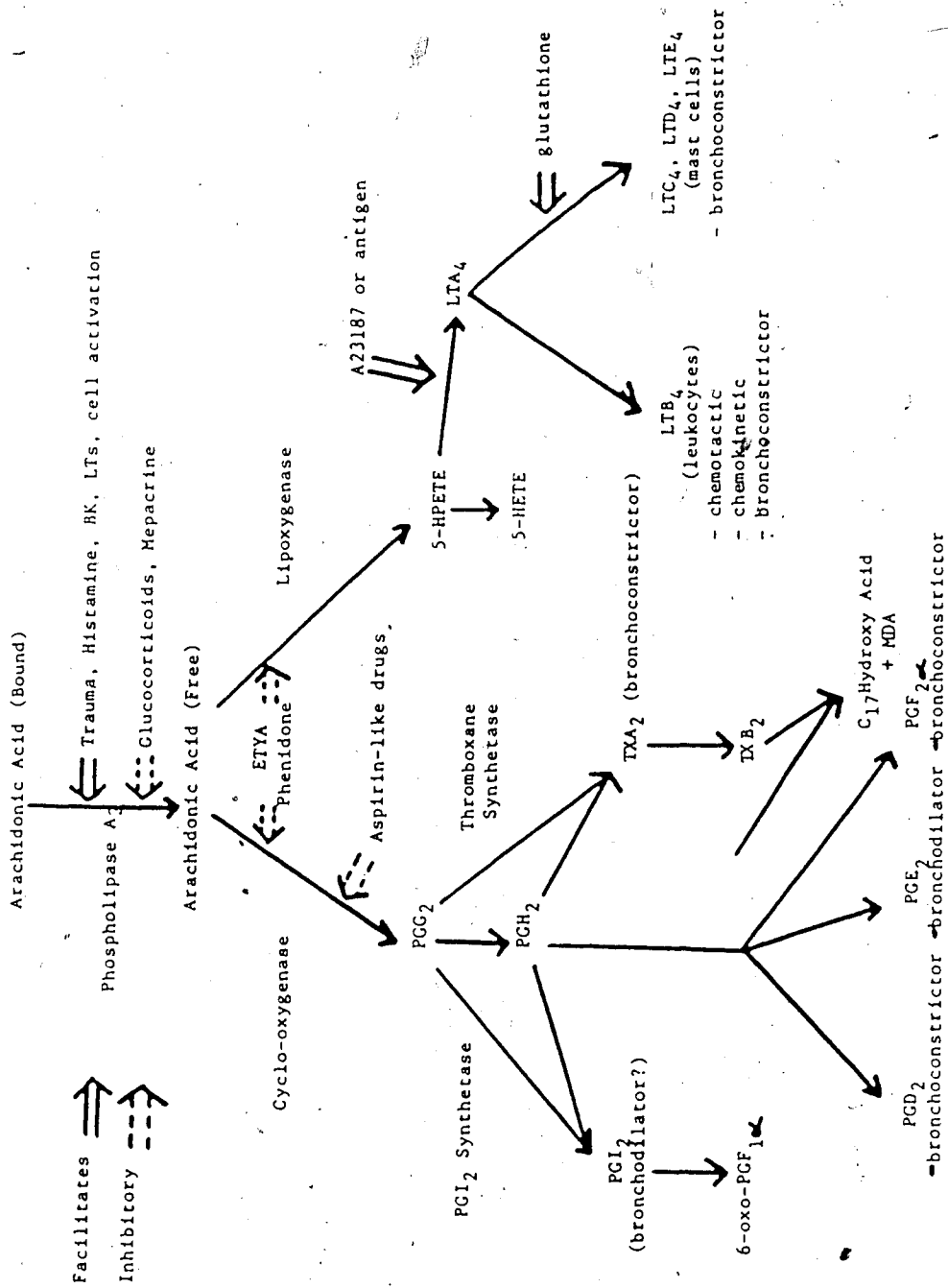


Figure 1: ARACHIDONIC ACID METABOLISM

and indomethacin, which reversibly inhibits the enzyme in guinea pig airways (Burka & Paterson, 1980) and other tissues. One possible consequence of cyclooxygenase-enzyme inhibition is diversion of AA metabolism into the lipoyxygenase pathway with increases in the amount of products formed via this pathway (Engineer et al. 1978; Adcock & Garland, 1980; Burka & Paterson, 1980). Another consequence of inhibition of PG synthesis is the removal of any modulatory effects. This is described below.

1.2.1.3.2 Effects of PGs on the airways:

In 1974, Farmer et al. showed that indomethacin treatment reduced tone in guinea-pig trachea. Inhibition of PG synthesis by aspirin in guinea-pig trachea decreases the responses to low concentrations of bronchoconstrictor agents, but enhances responses to higher concentrations of bronchoconstrictors (Orehek et al. 1975; Grodzinska et al. 1975). PGE_2 levels were reduced concomitant with the above effects. PGE_2 is a weak bronchodilator in the airways and inhibition of its synthesis would lead to removal of its negative modulatory influence on the airways. Furthermore, the guinea-pig trachea can produce PGE_2 in greater amounts than $PGF_{2\alpha}$, 6-Keto $PGF_{1\alpha}$, or TXB_2 (Burka et al. 1981; Brink et al. 1981). These products may serve to regulate tone in guinea-pig trachea. PGs also have direct contractile and relaxant effects in the airways. Ghelani et al. (1980) and Chand & De Roth (1979) showed that $PGF_{2\alpha}$ contracts human and guinea-pig lung

parenchymal preparations. Furthermore, PGD_2 and TXA_2 can contract, and PGE_2 and PGI_2 can relax, human airways in vitro (Hutas et al. 1981) and in vivo (Walters et al. 1982; Hardy et al. 1985). Gardiner & Collier (1980) suggested the existence of contractile, relaxant, and irritant (cough reflex) receptors for PGs based on the rank order of potency of a range of PGs and analogues in mediating the above effects.

Schneider & Drazen (1980) used the 9α , 11α , (U-44069), and the 11α , 9α -epoxymethanoendoperoxide analogues to demonstrate contractile effects on guinea-pig lung and trachea. These analogues exceeded the ability of $\text{PGF}_2\alpha$, PGD_2 , and histamine to constrict lung parenchymal strips, but did not exceed the ability of histamine to contract tracheal spirals. The effects of U-44069 are similar to those of TXA_2 and it has been used in place of TXA_2 as a potent constrictor of many smooth muscles including airways (Wasserman, 1976) and is more potent on smaller airways. Furthermore, it also aggregates platelets (Menzel et al. 1976).

1.2.1.4 Pharmacology of the leukotrienes

In 1938, Feldberg & Kellaway stimulated lung tissue with cobra venom and caused the release of a substance that produced characteristic slow contractions of guinea-pig intestine. Subsequent work by Kellaway & Trethewie (1940) showed that a similar factor was released from guinea-pig lung undergoing anaphylaxis and they named it "slow

reacting substance." During the 1950s, Brocklehurst coined the term slow reacting substance of anaphylaxis (SRS-A). Subsequent work (reviewed by Bach, 1982) by many groups of researchers throughout the world on the structure, origin, and functions of SRS-A in physiological and pathological states has led to the present state of knowledge on this important group of AA metabolites.

The major highlights of knowledge on SRS-A were the facts that SRS-A constituted a mixture of LTC₄, LTD₄, and LTE₄, that these were products of AA metabolism by the lipoxygenase pathway, and that these potent mediators play an important role in the pathogenesis of inflammatory and allergic states such as asthma. Many reviews have been published on various aspects of LT research. These include reviews on LT chemistry and nomenclature (Samuelsson, 1981; Corey, 1982; Hammarstrom, 1983), biological sources and release of LTs (Burka, 1981; Bach, 1982; Taylor & Morris, 1983). Biological actions of LTs and modulation of these effects (Sirois & Borgeat, 1980; Hedqvist et al. 1980; Borgeat & Sirois, 1981; Burka, 1981; Goetzl, 1981; Lewis & Austen, 1981; O'Flaherty, 1982; Bray, 1983; Piper, 1983). The above references also detail the role of LTs in asthma and other disease states.

1.2.1.4.1 Leukotriene biosynthesis:

Lipoxygenase enzymes are widely distributed in the plant and animal kingdom. AA can be oxidized by 5-, 8-, 9-, 11-, and 15-

lipoxygenases (see Burka, 1981 for review) forming 5-HPETE, 8-HPETE, 9-HPETE, 11-HPETE, and 15-HPETE, which after reduction, form the corresponding HETE, respectively. The most widely studied is 5-lipoxygenase which is found in mast cells, basophils, macrophages, and lung tissue of various species.

The production of the more polar leukotrienes occurs when 5-HPETE loses water to form an unstable epoxide, 5(6)-oxido-7,9,11,14-eicosatetraenoic acid (LTA_4) (Fig. 2). After enzymatic hydrolysis of LTA_4 , polar compounds such as 5,12-dihETE (LTB_4) and its geometric isomers (Borgeat & Samuelsson, 1979a,b,c,d; reviewed by Sirois & Borgeat, 1980; Bray, 1983) are produced in eosinophils, neutrophils and mast cells. LTB_4 is a potent chemotactic and chemokinetic agent. The smooth muscle contracting LTC_4 , LTD_4 , and LTE_4 are also produced from LTA_4 in mast cells, macrophages, basophils and lung tissue. 5-hydroxy-6-S-glutathionyl-7,9-trans-11,14-cis-eicosatetraenoic acid (LTC_4) (Hammarstrom et al. 1979; Murphy et al. 1979) is formed after reaction of glutathione with LTA_4 , catalyzed by glutathione-S-transferase. LTC_4 is further metabolized by the enzyme γ -glutamyl-transpeptidase to 5-hydroxy-6-S-cysteinylglycyl-7,9-trans-11, 14-cis-eicosatetraenoic acid (LTD_4) (Anderson et al. 1982; Morris et al. 1982). Another cysteine-containing LT, 5-hydroxy-6-S-cysteinyl-7, 9-trans-11,14-cis-eicosatetraenoic acid (LTE_4), is formed from LTD_4 by the actions of aminopeptidases inhibited by L-cysteine and other thiols (Sok et al. 1980). The structure of LTC_4 was first determined

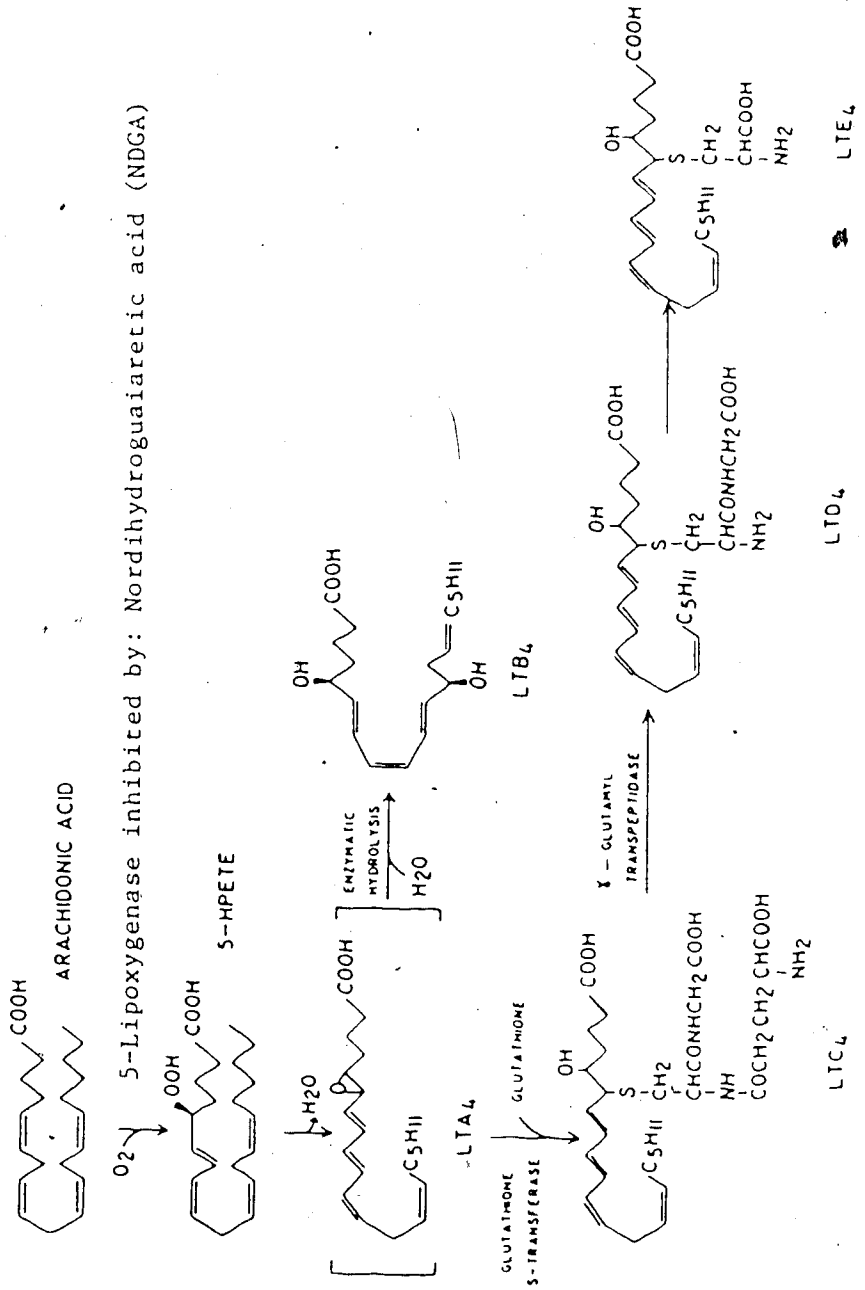


Fig. 2. Arachidonic acid metabolism by 5-lipoxygenase.

from mass spectrometry of biologically produced material from rat basophilic leukaemia (RBL) cells challenged with A23187 (Morris et al. 1980a). Further work indicated that LTs from guinea-pig lung had identical structures (Morris et al. 1980b).

The 5-lipoxygenase enzyme is calcium dependent (Jakschik & Lee, 1980; Furukawa et al. 1984). The enzyme from RBL cells has been purified using ATP linked to sepharose (Furukawa et al. 1984). These authors demonstrated that ATP stimulated enzyme activity in the presence of calcium. The 5-lipoxygenase, γ -glutamyl transpeptidase, and aminopeptidase of RBL cells were isolated by Kuo et al. (1984) who showed that the lipoxygenase enzyme is present in a soluble fraction of RBL cell homogenates whereas the latter two enzymes were membrane bound particulate enzymes. This confirmed earlier work by Jakschik et al. (1982) and Morris et al. (1982) who also studied the presence of these enzymes in guinea-pig lung and ileum.

1.2.1.4.2 Inhibition of lipoxygenase product synthesis and effects:

The pharmacological manipulation of 5-lipoxygenation of AA and subsequent enzymatic steps has received intense attention. Compounds that selectively inhibit 5-lipoxygenase have been developed and used to determine the involvement of 5-lipoxygenase metabolites in various tissue responses (Falkenhein et al. 1980)..

The compounds, 1-phenyl-3-pyrazolidone (phenidone) (Blackwell & Flower, 1978), nordihydroguaiaretic acid (NDGA) (Morris et al. 1979),

and U-60,257 (piriprost) (Bach et al. 1982) have been shown to inhibit 5-lipoxygenase activity in various tissues and cells including guinea-pig lung and mast cells. As a consequence of inhibition of enzyme activity, these compounds reduce the production of SRS-A and other lipoxygenase products. Phenidone also inhibits the cyclooxygenase enzyme.

U-60,257 has been reported (Bach et al. 1982) to inhibit glutathione S-transferase activity in addition to 5-lipoxygenase. Furthermore, this compound may also antagonize LTs at their receptor sites; an action similar to that of the selective SRS-A antagonist FPL55712 (Augstein et al. 1973).

Finally, L-serine-borate complex has been shown to be an effective inhibitor of γ -glutamyl transpeptidase (Tate & Meister, 1978), hence reducing the formation of LTD₄ from LTC₄.

1.2.1.4.3 Biological sources of lipoxygenase products:

A variety of cells and tissues have been shown to produce lipoxygenase products after stimulation with antigen, A23187, AA, or other stimulants. Representative sources are summarized in Table 2. In this regards, it is noteworthy that such techniques as reverse-phase high performance liquid chromatography (RP-HPLC) (Morris et al. 1978; Borgeat & Samuelsson, 1979a,b,c; Blackwell et al. 1980), ultraviolet spectrometry (Morris et al. 1978), bioassay on guinea-pig ileum and lung parenchymal strips, mass spectrometry (Morris et al. 1980a),

and radioimmunoassay (RIA) (Levine et al. 1981), have contributed to the identification of these metabolites in various systems.

The Schultz-Dale reaction that occurs in various smooth muscle preparations (reviewed by Chand & Eyre, 1978) upon the addition of minute amounts of antigen, is due to the release of pharmacological mediators of the immediate (type I) hypersensitivity reaction. Immunologically produced lipoxygenase products from airway smooth muscle have been observed since 1940. However, the chemical nature of the mediator released from guinea-pig trachea was not fully characterized.

Many lines of evidence support the contention that the mediators released from this tissue are derived via the lipoxygenase pathway. Adams & Lichtenstein (1979), Mitchell & Denborough (1979), and Burka & Paterson (1980; 1981) demonstrated that antigen-induced contractions of guinea-pig tracheal spirals were enhanced by indomethacin pretreatment, and that antihistamines reduced the early phase (0-10 minutes) of the contractile response. By contrast, lipoxygenase inhibitors and the selective SRS-A antagonist FPL55712, reduced the late phase (15-60 minutes) of the contractile response. These observations agreed with the hypothesis that histamine and SRS-A contribute to the early and late phase of antigen-induced contractions, respectively. Furthermore, indomethacin-pretreatment enhances contractions by removing the modulatory influence of relaxant PGs on the trachea (Orehek et al. 1975) and possibly cause the diversion of AA into the lipoxygenase

pathway, hence producing more lipoxygenase metabolites, leading to an enhanced response (Burka & Paterson, 1980; Adcock & Garland, 1980). Finally, Yen & Kreutner (1980), Mitchell & Denborough (1980), and Burka & Paterson (1980) showed that AA relaxed guinea-pig trachea and contracted lung parenchymal strips. However, after indomethacin pretreatment, AA-induced relaxations of the trachea were converted to contractions with a concomitant reduction in PGE₂ synthesis (Burka & Paterson, 1980), and contractions of parenchymal strips were reduced with a concomitant reduction in TXA₂ synthesis (Mitchell & Denborough, 1980). Furthermore, lipoxygenase inhibitors and FPL55712 reduced the AA-induced contractions of trachea after indomethacin-pretreatment. Hence, the possibility that LTs may be synthesized in guinea-pig trachea after antigen, A23187, and AA challenge. This possibility and the role of calcium in the above processes was investigated in this thesis.

1.2.1.4. Effects of leukotrienes on the airways:

LTC₄, LTD₄, and LTE₄ are 100-1,000 times more potent than histamine in contracting airway smooth muscle from man, guinea pig, and monkey. Furthermore, the LTs are more potent on the small terminal airways, e.g., bronchioles, than the large conducting airways e.g., trachea. LT effects, in vitro, develop slowly and are long lasting despite exhaustive washing of airway tissues. (Hedqvist et al. 1980; Drazen et al. 1980; Hanna et al. 1981; Sirois et al. 1981;

Piper & Samhoun, 1981). Also, LTB_4 contracts guinea-pig lung parenchymal strips and to a lesser extent guinea-pig tracheal spirals (Sirois et al. 1981). LTB_4 does not contract guinea-pig ileum, whereas LTs C_4 , D_4 and E_4 do; LTD_4 is the most potent.

Administration of LTC_4 , LTD_4 , and LTE_4 to guinea pigs in vivo results in a long lasting increase in airway resistance and a decrease in lung compliance. The latter persisted after the former returned to normal baseline levels (Drazen, 1980; Drazen et al. 1982). In addition to the above effects, LTC_4 and LTD_4 induce vasoconstriction and increased vasopermeability, respectively (Drazen et al. 1980; Drazen et al. 1982).

In vitro human bronchial smooth muscle contracts to both LTC_4 and LTD_4 (Jones et al. 1982). This effect is not blocked after atropine, mepyramine, or indomethacin-pretreatment. However, responses to both LTs are reduced by FPL55712. Human asthmatic lung strips also contract to LTs, but there is no hyperreactivity to LTs when compared to control lungs (Schellenberg & Foster, 1984). These findings are supported by those of Griffin et al. (1983), who showed that asthmatics are not hyperreactive to the bronchoconstrictor effects of LTD_4 .

LTC_4 -, LTD_4 -, and LTB_4 -induced contractions of guinea-pig lung parenchymal strips are reduced by indomethacin-pretreatment (Piper & Samhoun, 1981 and 1982; Creese et al. 1981; Sirois et al. 1982). The effects of LTB_4 on the same tissue are reduced by inhibition of

cyclooxygenase or by inhibition of PLA₂ with mepacrine (Sirois et al. 1982). The reduction of LT-induced contractions of lung parenchyma by cyclooxygenase blockade, occurs with a concomitant decrease in TXA₂ synthesis. Also, others have reported the synthesis of the bronchodilator PGI₂ after LT-induced contractions of guinea-pig lung strips (Creese et al. 1981; Omini et al. 1981). Hence, on the guinea-pig lung parenchyma, LT effects are mediated partly via the synthesis of cyclooxygenase products, such as the bronchoconstrictor TXA₂. However, in human isolated bronchial and lung parenchymal strips, LTB₄-, LTC₄-, and LTD₄-induced contractions were not affected by cyclooxygenase inhibition (Samhoun & Piper, 1984).

1.2.1.4.5 Effects of leukotrienes on the central nervous system:

The effects of the LTs on CNS function have not been widely studied. However, the following studies suggest a possible role for lipoxygenase metabolites in the CNS.

Palmer et al. (1980) and (1981) showed that pressure-injection of LTC₄ and LTD₄ onto rat cerebellar Purkinje fibers caused a prolonged excitatory action; i.e., increase in firing rate, which could be antagonized by FPL55712. LTB₄ had no effect in the above system. Recently, LTs have been shown to be synthesized in various areas of rat brain including cerebellum (Lindgren et al. 1984). Finally, LTC₄ in low concentrations has been shown to stimulate luteinizing hormone release from rat pituitary cells in culture (Hulting et al. 1985).

1.2.1.4.6 Leukotriene receptors:

The greater potency of LTD₄ relative to LTC₄ in contracting guinea-pig lung parenchymal strips and tracheal spirals, and the greater antagonistic effect of FPL55712 on LTD₄-induced contractions suggests that LTC₄ and LTD₄ probably act at different receptor sites (Drazen et al. 1980; Krell et al. 1981; Snyder & Krell, 1984). Moreover, Fleisch et al. (1982) showed that FPL55712 was more potent in antagonizing LTD₄-induced contractions of ileum than those induced on isolated airways of guinea pig. This suggests that LTD₄ receptors may be different in various smooth muscles.

The fact that LTC₄ can be converted to LTD₄ which can be further converted to LTE₄ by enzymes present in airway smooth muscle and in guinea-pig ileum (Morris et al. 1982) (see Fig. 2) complicates the study of receptor subtyping in these tissues. However, by the judicious use of inhibitors of γ -glutamyl transpeptidase (inhibitor: serine borate complex) and aminopeptidase (inhibitor: cysteine) the relatively undistorted effects of LTC₄ and LTD₄ can be assessed. Snyder et al. (1984) demonstrated that under conditions where LTC₄ and LTD₄ remain unmetabolized their potency increased since conversion to LTE₄ was prevented. Furthermore, the slight antagonistic effects of FPL55712 on guinea-pig trachea against LTC₄ were abolished in the presence of serine borate complex (Snyder & Krell, 1984). These findings suggest that LTC₄ acts at a different receptor site from LTD₄.

Radioligand binding studies of the LTs has confirmed the previous pharmacological evidence. LT-binding sites equated with receptors based on their high affinity, pharmacological specificity, tissue specificity, saturability, reversibility, and stereoselectivity have been demonstrated for LTC₄ and LTD₄ in membranes of guinea-pig lung (Pong & DeHaven, 1983; Bruns et al. 1983; Mong et al. 1984 a,b; Cheng & Townley, 1984 a,b,c). Receptor sites for LTE₄ appear to be identical to those for LTD₄ (Cheng & Townley, 1984c). Specific LTC₄-binding sites have been shown in rat lung (Pong et al. 1983), a smooth muscle cell line derived from hamster vas deferens (Krilis et al. 1983; Clark et al. 1984), human fetal lung (Lewis et al. 1984), guinea-pig ileum (Krilis et al. 1984; Nicosia et al. 1984), guinea-pig uterus (Levinson, 1984), and guinea-pig brain (Cheng et al. 1985).

The order of potency for inhibition of [³H]LTD₄ binding in guinea-pig lung is LTD₄ > LTE₄ > LTC₄ >> FPL55712 (Pong & DeHaven, 1983; Cheng et al. 1985). In the same tissue, the dissociation constant (K_d) for LTD₄ binding at saturation and at 20°C ranges from 0.5 nM to 10 nM in various studies. The number of binding sites at saturated equilibrium (B_{max}) range from 384 to 2100 fmol/mg protein. Some tissues do not exhibit specific LTD₄ binding sites and LTD₄ can compete with [³H]LTC₄ in binding to the LTC₄ receptors with an inhibitory constant (K_i) supportive of the presence of two receptor sites for the LTs. Furthermore, FPL55712 can inhibit LTD₄ binding with K_i values similar to K_b values obtained in

pharmacological studies (Pong & DeHaven, 1983). FPL55712 does not inhibit LTC₄ binding effectively.

LTC₄ may be metabolized to LTD₄ during the binding assay and may give rise to curvilinear Scatchard plots and erroneous competition data. The inclusion of serine borate complex (45 mM) in the assay minimizes possible degradation of the radioligand and changes the order of potency for inhibition of [³H]LTC₄ binding in guinea-pig lung from LTC₄ = LTD₄ > LTE₄ to LTC₄ >> LTD₄ >> LTE₄ and for inhibition of [³H]LTD₄ binding from LTC₄ = LTD₄ > LTE₄ to LTD₄ > LTE₄ = LTC₄ (Cheng & Townley, 1984b).

LTC₄ binding is not regulated by guanine nucleotides or monovalent cations but is divalent cation sensitive (Pong et al. 1983 and others). LTD₄ binding is reduced by monovalent cations especially Na⁺. A 50% reduction in the B_{max} by Na⁺ (50 mM) was observed by Mong et al. 1985. Na⁺ does not affect the K_D. Mg²⁺, Mn²⁺, and Ca²⁺ at 5-10 mM increase the B_{max} of LTC₄ and LTD₄ receptors in various tissues to 175-200% of control levels without affecting the K_D (Pong & DeHaven, 1983, Bruns et al. 1983; Mong et al. 1985). Addition of GTP increases the rate of dissociation of bound LTD₄ (Pong & DeHaven, 1983). Furthermore, guanine nucleotides reduce the level of assayable high affinity LTD₄ binding sites in lung (Pong & DeHaven, 1983; Bruns et al. 1983; Mong et al. 1985). Guanine nucleotides (the nonhydrolyzable analogs, GTPγS and GppNHp, being most potent) reduce the B_{max} but do not affect the K_D of the residual binding, possibly they

shift LTD₄ receptors into a lower affinity and less easily assayable form (Mong et al. 1985).

1.2.1.4.7 Possible intracellular mechanism of action of LTD₄:

The inhibition of LTD₄ binding to its receptors by Na⁺ and guanine nucleotides indicates that the receptor may be linked to adenylate cyclase in an inhibitory manner. This is because similar guanine nucleotide and Na⁺-dependent regulation of other receptors that inhibit adenylate cyclase has been observed. These receptors include muscarinic receptors in mouse brain, rat brain and ileum (Sokolovsky et al. 1980; Ehlert et al. 1980; Olianias et al. 1982), adenosine R₁ receptors in brain and fat cells (Cooper et al. 1980; Gavish et al. 1982; Ukena et al. 1984), opiate receptors in brain and ileum (Koski et al. 1982), α₂-adrenergic receptors in platelets (Tsai et al. 1979; Hoffman et al. 1980; Motulsky et al. 1983), and GABA receptors in rat cerebellum (Hill & Bowery, 1981; Wojick & Neff, 1983).

The effects of guanine nucleotides are transmitted to the receptor via the GTP regulatory proteins of adenylate cyclase (Rodbell, 1980; Jakobs et al. 1981). These hormones have all been shown to inhibit adenylate cyclase (for reviews see Jakobs et al. 1981; Cooper, 1982; Jakobs et al. 1984) and section 1.2.3.1.1.

By analogy with the above hormone-receptor systems, it seems likely that LTD₄ may interact with its receptor in a similar fashion.

Further support for this hypothesis was the observation that LT-induced contractions of guinea-pig tracheal smooth muscle occurred along with a reduction in cyclic AMP levels. FPL 55712 blocked the contractile response, and the reduction in cyclic AMP (Hedman & Anderson, 1982). Since LTs exert effects on airway smooth muscle and on rat cerebellum, these tissues were studied in this thesis with regards a possible inhibitory action of LTD₄ on adenylate cyclase.

1.2.2. Autonomic control of the airways

Autonomic nervous activity modulates a variety of body functions. The airways are no exception. Reviews on the relative contributions of sympathetic, parasympathetic, and other inhibitory pathways to airway smooth muscle (ASM) include those by Richardson (1979) and Nadel & Barnes (1984). Table 3 briefly summarizes the various pathways exerting influences on ASM.

1.2.2.1 Parasympathetic and sympathetic nervous system:

Radioligand binding studies and autoradiographic localization studies demonstrate the presence of muscarinic receptors, (Murlas et al., 1982; Barnes et al. 1983), β , and α receptors (Barnes et al. 1982; Nadel & Barnes, 1984) in the airways of various species. The β_2 receptor subtype predominates over the β_1 receptor in the airways (β_2 : β_1 , 85:15) (Nadel & Barnes, 1984).

The effects of muscarinic and α - and β -adrenergic receptor

stimulation on airway functions are shown in Table 3. The effects of β -adrenoceptor stimulation may be related to increases in intracellular levels of cyclic AMP (Sullivan & Parker, 1976; Lefkowitz et al. 1983).

1.2.2.2 Non-adrenergic non-cholinergic (NANC) inhibitory innervation:

NANC inhibitory innervation has been documented in a variety of smooth muscles (Burnstock, 1972). The neurotransmitter may be vasoactive intestinal peptide (VIP) (Richardson, 1981; Diamond & Richardson, 1982; Said, 1982). Other possible candidate neurotransmitters include purines (Burnstock, 1972), substance P, enkephalins, prostaglandins, and a host of others (See Richardson, 1981; Diamond & Richardson, 1982).

NANC innervation has been demonstrated to exert substantial influence in human (Richardson & Beland, 1976) and in guinea-pig airways (Yip et al. 1981; Grundstrom et al. 1981). In fact, it has been estimated that 60% of nerve-induced inhibition in man and guinea pig is due to NANC activation (Richardson, 1981; Richardson & Beland, 1976; Diamond & Richardson, 1982).

In the guinea pig, two lines of evidence implicate VIP as being the NANC transmitter. First, antisera to VIP reduced the relaxation obtained after stimulation of the NANC innervation, and secondly, by using radioimmunoassay, it was demonstrated that relaxation can be correlated to the levels of immunoreactive VIP released (Matsuzaki et

al. 1980). Furthermore, VIP containing neurones have been immunocytochemically localized in close vicinity to airway smooth muscle in dog, man, and guinea pig (Uddman et al. 1978; Dey & Said, 1980; Richardson, 1981).

VIP can prevent the bronchoconstriction induced by histamine, kinins and $\text{PGF}_2\alpha$ (Said et al. 1974). VIP receptors have been demonstrated on rat lung and activate adenylate cyclase linked to these receptors (Robberecht et al. 1981). VIP also increases cyclic AMP levels in guinea-pig trachea (Fransden et al. 1978), and inhibits antigen-induced mediator release from guinea-pig lung (Undem et al. 1983). Finally, VIP has been shown to inhibit mucus secretion by human airways in vitro (Coles et al. 1981).

The protective effects of VIP (bronchodilation, inhibition of mediator release, and inhibition of mucus secretion) on the airways serve to highlight the fact that an abnormality in NANC innervation may lead to asthmatic hyperreactivity. A substantial amount of evidence is still needed to establish VIP as the prime neurotransmitter in the NANC innervation of the airways.

1.2.3 Basic regulatory processes in the airways:

In this section, consideration is given to regulatory processes exerted upon airway smooth muscle and secretory cells in the lung by cyclic AMP and calcium. The pathogenesis of asthmatic hyperreactivity (1.3) may find correlates in changes or dysfunctions in the regulatory

roles of these secondary messenger of cellular function.

1.2.3.1 Adenylate cyclase:

Adenylate cyclase is a membrane bound enzyme universally distributed in animal cells. The enzyme catalyzes the conversion of ATP into cyclic AMP and pyrophosphate.

Various stimulatory and inhibitory hormones regulate adenylate cyclase activity in a variety of cell types (Cooper, 1982 for review). These hormones hence control the intracellular levels of cyclic AMP in the cell and thus affect the transfer of information, ultimately leading to the characteristic cellular response to the particular hormone.

The components of this information transmission system consist of the hormone receptor (R) which acts as the recognition transduction element, the guanine nucleotide binding proteins, N_s and N_i which mediate the effects of R occupation by stimulatory and inhibitory hormones, respectively, onto the catalytic subunit (C) of the enzyme (Rodbell, 1980). Activation of C involves the exchange of inactive GDP for active GTP at N_s or N_i . This exchange is probably initiated by hormone binding to R. N_s and N_i are probably two separate proteins (Hildebrandt et al. 1983). C utilizes a complex formed between Mn^{2+} or Mg^{2+} and ATP to produce cyclic AMP.

Various models of the interaction of cyclase components in stimulation and inhibition of the enzyme induced by hormones, have

been developed (for review see Muller, 1985). The "exchange-collision-coupling model" of Levitski (1982) and the "disaggregation-coupling" model of Rodbell (1980) seem to account for experimentally observed interactions between R, Ns, Ni and C. In Levitski's model and other models, GTP, at a concentration range of 0.01 - 0.1 μ M for stimulation and at a concentration range of 0.2 - 6.0 μ M for inhibition, is essential for stimulatory and inhibitory hormone effects on adenylate cyclase.

In both the above models, high affinity binding of a hormone to its receptor is converted to a low affinity interaction upon the binding of guanine nucleotides to Ns or Ni. Furthermore, Rodbell's model implies reciprocal effects, i.e. hormone binding facilitates the interaction of guanine nucleotides with Ns or Ni.

Studies of adenylate cyclase were greatly clarified following the discovery of forskolin (see Seamon et al. 1981). This diterpene increases cyclic AMP synthesis in all cyclase systems studied to date (reviewed by Seamon & Daly, 1981b). Forskolin does not utilize guanine nucleotides in its rapid and massive (i.e. relative to hormonal stimulants) stimulation of the enzyme (Seamon & Daly, 1981a). Furthermore, forskolin enhances the ability of stimulatory hormones to activate the enzyme. This implies an interaction of forskolin with the processes of Ns activation of C. Forskolin has been shown to bind to rat brain membranes (Seamon et al. 1984). Analogs of forskolin which do not activate adenylate cyclase did not compete for the

binding site. It is now currently accepted that forskolin activates C directly, although interactions with Ns cannot be ruled out.

1.2.3.1.1 Characteristics of adenylate cyclase inhibition:

Non-hydrolysable analogs of GTP can inhibit the basal and the forskolin-stimulated enzyme (Seamon & Daly, 1982). In fact, this effect is exploited to determine the presence of Ni in a given cell. Although Ns has been shown to exist (functionally and physically) in a variety of cells, the situation with Ni is not as clear.

The reduction in cyclic AMP levels in cells may act as a signal to promote various other cellular activatory processes including phospholipid metabolism, release of AA from membrane pools and its subsequent peroxidation into active metabolites, and Ca^{2+} entry which activates the latter processes, prior to the tissue-specific biological response (Michell & Kirk, 1980; Jakobs & Schultz, 1980; Jakobs et al. 1984; Berridge & Irvine, 1984; Baron et al. 1984).

Common features shared by hormone-induced and GTP analog-induced inhibition of cyclase include a greater effect at low temperatures ($20^{\circ}C$ vs $37^{\circ}C$), at low Mg^{2+} concentrations in the assay (around 1-2 mM), a higher GTP requirement than for enzyme-stimulating receptors (does not apply to GTP analogs), and sensitivity to proteases (proteases abolish cyclase inhibition). Furthermore, Mn^{2+} concentrations over 1 mM have been shown to reduce adenylate cyclase inhibition. A high Na^{+} concentration (100 mM) has been shown to optimize inhibition.

induced by certain receptors e.g. the α_2 receptor in the fat cell system (Aktories et al. 1979; Aktories et al. 1981; reviewed by Jakobs et al. 1981).

Inhibitory hormones generally reduce basal adenylate cyclase activity by about 30-80%. In the presence of a stimulatory hormone or compound; e.g., forskolin, the degree of inhibition is generally greater than observed if the enzyme is in the basal state.

1.2.3.2, Cyclic AMP and the airways:

In the airways, cyclic AMP may be involved in smooth muscle contractility, mediator release, and mucus secretion. In this section some of the evidence for cyclic AMP involvement in airway smooth muscle contractility is discussed. The area has been reviewed (Baer, 1974; Andersson & Nilsson, 1977; Diamond, 1978; Hardman, 1981).

Since the original studies of Sutherland & Rall (1960), the second messenger role of cyclic AMP in cellular function has received intense attention. Hormones activating smooth muscle relaxant receptors such as the β -adrenoceptor, adenosine receptor, various relaxant PG receptors, and other hormonal receptors have been studied in airway, intestinal, vascular and uterine smooth muscle. Cyclic AMP levels in tissues can be increased or decreased by activation of the membrane bound enzyme, adenylate cyclase, or by inhibition or stimulation of cyclic nucleotide phosphodiesterase.

It has been suggested, as a general working hypothesis, by

Sutherland (1974) that β -adrenoceptor effects are mediated by increases in cellular levels of cyclic AMP. It has been theorized that decreases in cyclic AMP levels, or increases in cyclic guanosine monophosphate (cyclic GMP), will promote contraction of smooth muscle (see Baer, 1974; Diamond, 1978 and others). This simplified scheme has not found convincing evidence and the roles of cyclic AMP and cyclic GMP in smooth muscle relaxation are still controversial.

The above hypothesis is based on the fact that cyclic AMP and some of its analogues can induce smooth muscle relaxation. Secondly, adrenergically induced smooth muscle relaxation can sometimes be correlated with tissue levels of cyclic AMP. Both effects are abolished by β -adrenoceptor antagonists. Thirdly, inhibitors of cyclic AMP phosphodiesterases can induce relaxation, increase cyclic AMP levels, and potentiate effects induced by other relaxant agents. These observations are derived from studies on vascular, uterine, airway and intestinal smooth muscle.

Various authors have shown that airway smooth muscle relaxes in response to β -adrenoceptor stimulation concomitant with increases in tissue levels of cyclic AMP. These two effects generally exhibit similar concentration-response and time-response relationships and are similarly blocked by propranolol (Murad, 1974; Ohkubo et al. 1976; Katsuki & Murad, 1977; Rinard et al. 1983; Lau & Lum, 1983). Furthermore, theophylline and other phosphodiesterase inhibitors can potentiate relaxation and cyclic AMP increases following stimulation

with β agonists (Lohmann et al. 1977; Polson et al. 1982)

Other hormones studied in airway smooth muscle include PGI₂ (Macdermot & Barnes, 1980), and VIP (Robberecht et al. 1981). Both substances increase cyclic AMP levels by stimulation of adenylate cyclase in guinea-pig and rat lung, respectively. Recent studies utilizing forskolin have demonstrated that this diterpene is a potent inhibitor of mediator release from the airways. Burka (1983 a,b) has demonstrated that forskolin inhibits antigen- and calcium ionophore-induced contractions of guinea-pig airways and is a potent bronchodilator in vitro. Kreutner et al. (1984) have also shown that forskolin is a bronchodilator when administered by aerosol. It prevents and reverses allergic bronchoconstriction in guinea pigs. The initial observations of Assem & Schild (1969) that epinephrine can inhibit antigen-induced histamine release from human lung and the recent work with forskolin further demonstrate a role for cyclic AMP in mediator release (Sullivan & Parker, 1976; Tung & Lichtenstein, 1981; Alms & Bloom, 1982) and smooth muscle contractility (Scheid et al. 1978). In fact, current bronchodilator therapy in asthma probably depends on these two mechanisms of action.

1.2.3.3 Calcium and the airways:

The important roles of Ca²⁺ in the airways has been well documented (for reviews see Middleton, 1980 and 1984; Rasmussen & Barrett, 1984). Unfortunately, there are very few studies of the

molecular basis of contraction of airway smooth muscle and its Ca^{2+} regulation per se. It is only with the advent of calcium entry blockers in the therapy of asthma (Goodman, 1981; Fanta & Drazen, 1983; Triggle, 1983; Barnes, 1983) that more attention has been paid to Ca^{2+} regulation of airway smooth muscle contractility.

1.2.3.3.1 Sources of utilizable calcium in the airways:

Creese & Denborough (1981) showed that contractile responses of guinea-pig trachea to KCl, histamine, acetylcholine, and $\text{PGF}_2\alpha$ were reduced, but not abolished, in a Ca^{2+} -free medium. These authors concluded that there were two sources of Ca^{2+} in the trachea: an extracellular source probably in equilibration with the medium and an internal source of utilizable Ca^{2+} . Furthermore, responses to high concentrations of bronchoconstrictors were less dependent on extracellular Ca^{2+} . Similar results were obtained by Farley & Miles (1978) using dog tracheal smooth muscle. Burka (1984) showed that calcium-ionophore-A23187-induced contractions of guinea-pig trachea were totally dependent on extracellular Ca^{2+} , but that antigen-induced contractions were partially dependent on intracellular calcium.

1.2.3.3.2. Calcium channels in smooth muscle:

During periodic stimulation of smooth muscle by Ca^{2+} mobilizing agents, intracellular Ca^{2+} concentrations may increase up to a 1000 times those in the relaxed state (Middleton, 1984). This rise occurs

via entry of Ca^{2+} into the cell through specific conductance channels, or via mobilization of intracellular bound Ca^{2+} from sarcoplasmic or endoplasmic reticulum, mitochondria, or other Ca^{2+} sequestering organelles (Webb & Bhalla, 1976). Mechanisms also exist to return Ca^{2+} concentrations to resting levels (Rasmussen & Barrett, 1984).

Ca^{2+} movement across the membrane occurs through specific channels activated in response to depolarization (i.e. voltage-dependent channels) or in response to receptor occupation by a contractile agonist (i.e. receptor-operated channel) (see Triggle, 1983). A group of drugs known collectively as Ca^{2+} channel blockers, including verapamil, D600, nifedipine, nitrendipine, and diltiazem have a high affinity for Ca^{2+} channels in a variety of cells including airway smooth muscle cells. These compounds can selectively inhibit the activation of Ca^{2+} channels especially the voltage-dependent channels and inhibit Ca^{2+} -mediated effects (Triggle, 1981, Goodman, 1981; Triggle, 1983; Barnes, 1983).

An intracellular Ca^{2+} antagonist, 8-(diethylamino)octyl-3,4,5-trimethoxybenzoate hydrochloride (TMB-8) (Chiou & Malagodi, 1975) stabilizes intracellular Ca^{2+} ions to binding sites and inhibits contractions of skeletal and smooth muscle.

1.2.3.3.3 Excitation-contraction coupling in smooth muscle:

A rise in intracellular Ca^{2+} concentrations activates the calcium binding protein, calmodulin (Cheung, 1980; Bröstrom & Wolff, 1981).

The Ca^{2+} -calmodulin complex interacts with inactive myosin light chain kinase, which becomes activated and subsequently phosphorylates myosin to myosin- PO_4 , which in the presence of the contractile protein, actin, activates the myosin ATPase. Subsequent cleavage of ATP yields energy which is utilized in muscle shortening according to the sliding filament theory (See Stull & Sanford, 1981; Middleton, 1984; Rasmussen and Barrett, 1984).

Sparrow et al. (1984) recently demonstrated that calmodulin increased sensitivity to Ca^{2+} in skinned muscle fibers from guinea-pig trachealis. Furthermore, a cyclic AMP-dependent protein kinase inhibited tension development induced by the Ca^{2+} -calmodulin complex after β_2 -adrenergic stimulation. An earlier study by Hogaboom et al. (1982) using tracheal smooth muscle demonstrated cyclic AMP- and cyclic GMP-dependent phosphorylation of 2 membrane proteins ultimately involved in transport of Ca^{2+} into microsomes via phosphorylation of a Ca^{2+} -transport ATPase.

1.2.3.3.4 Calcium antagonists and asthma:

Calcium entry blockers have demonstrable therapeutic use in certain types of asthma (Goodman, 1981; Barnes, 1983; Fanta & Drazen, 1983; Middleton, 1984). Patel (1981a) showed that nifedipine prevented exercise-induced asthma in a group of fifteen asthmatics. Other authors have demonstrated similar effects of nifedipine, verapamil, and cinnarizine against exercise-induced and cold

air-induced bronchoconstriction in asthmatics (see Middleton, 1984). Furthermore, Patel (1981b) showed that verapamil given by inhalation did not alter histamine- and methacholine-induced bronchoconstriction in asthmatics. Similar results were obtained by McIntyre et al. (1983). They concluded that calcium antagonists inhibit mediator release and not the smooth muscle bronchoconstriction effected by asthmatic mediators. This conclusion was partly supported by the findings of Henderson et al. (1983) who showed that in vitro contraction of sensitized guinea-pig trachea and human bronchial muscle induced by acetylcholine, histamine, and specific antigen were either unaffected by nifedipine (100 μ M) or reduced by about 50% in human bronchial muscle. Moreover, these authors showed that nifedipine-pretreatment inhibited antigen-induced bronchoconstriction in asthmatics challenged with grass pollen. These findings contradict those of So et al. (1982) who showed that inhaled verapamil and nifedipine did not alter antigen-induced bronchoconstriction in eight asthmatics, and Patel et al. (1983) who also showed that inhaled verapamil did not affect allergen-induced bronchoconstriction in human asthmatics.

Weiss et al. (1982) showed that in vitro verapamil inhibited antigen-induced contractions of guinea-pig tracheal spirals. However, antigen-induced histamine release was unaffected. Fanta et al. (1982) also showed that nifedipine reversed existing tone in guinea-pig tracheal spirals and inhibited constriction induced by histamine and

carbachol in tracheal and parenchymal preparations in vitro.

The above representative studies leave no doubt that calcium-entry blockers are effective in preventing or reversing asthmatic bronchoconstriction. However, there is controversy surrounding their mechanisms of action. They may work by inhibition of mediator release, by inhibition of smooth muscle contraction, or both.

1.3 STUDIES ON MODELS OF ASTHMA: MECHANISMS OF AIRWAY HYPERREACTIVITY

Unfortunately, most animal models of human diseases are not "true" models of the human situation. This is basically the situation with animal models of human bronchial asthma. Models have included dog, guinea pig, monkey, sheep, and rats, and airway tissues and cells derived from these models, and from human sources. Although a huge amount of data has accumulated from studies, as yet there is no concrete theory to describe the origin and pathogenesis of human asthmatic hyperreactivity. However, a lot of knowledge has been gained on processes of anaphylactic mediator release, and the effects of mediators that may likely translate into the pathologic induction of hyperreactivity. In this section various studies of animal models and their human counterpart will be reviewed in order to demonstrate the variety of hypotheses that have been originated to account for airway hyperreactivity.

1.3.1 Sensitization-dependent changes in pharmacologic receptors:

Szentivanyi (1968) first proposed that β -receptors are hypoactive in the airways of asthmatics. Hence, the relaxant influence these receptors mediate is lost and bronchoconstrictor tone overrides the fine balance of airway caliber leading to an enhanced bronchoconstrictor response to various stimulants. These observations were supported by the fact that propranolol induces bronchoconstriction in asthmatics, but not in normal individuals (Richardson & Sterling, 1969). Szentivanyi's theory has gained a lot of support especially since it has been reported that a variety of β -mediated effects such as vasodilation, hyperglycemia, platelet aggregation, increases in urinary cAMP, and increases in blood lactate were decreased in asthmatics (Sly, 1981).

An extension of the β -hyporesponsiveness theory of asthma is the premise that excitatory α -adrenoceptor and muscarinic receptor function is increased in asthmatic individuals. This was based partly on the fact that α -adrenergic antagonists and atropine can prevent exercise- and histamine-induced bronchoconstriction in asthmatics (Bianco et al. 1974; Kerr et al. 1970). Furthermore, Kaliner et al. (1982) have shown that allergic subjects, including asthmatics, have muscarinic-receptor, α -adrenoceptor hyperresponsiveness, and β -adrenoceptor hyporesponsiveness (Shelhamer et al. 1983).

In opposition to the hypoactive beta-adrenoceptor theory of asthma, it must be noted that most asthmatic subjects have a history

of treatment with β -adrenergic agonists, and the observed β -hyporesponsiveness may be a manifestation of receptor desensitization and/or down regulation of receptors (Lefkowitz et al. 1983). Furthermore, the stress of asthma may cause metabolic changes leading to the observed effects, i.e., receptor hyporesponsiveness is a consequence rather than a cause of asthma.

Radioligand binding studies have demonstrated significantly lower β -receptor density in mononuclear leukocytes of asthmatics not taking any medication, whereas in asthmatics on medication, including β -agonists, there was a significantly reduced β -adrenoceptor binding density in mixed leukocytes, mononuclear cells and in polymorphonuclear leukocytes (Sano et al. 1983). Studies by Makino et al. (1983) have demonstrated diminished cyclic AMP responses of asthmatic lymphocytes after stimulation with β -agonists. Furthermore, there was a significant correlation between β -hyporesponsiveness and muscarinic-hyperresponsiveness determined by measurement of the respiratory threshold to acetylcholine. However, another study (Meurs et al. 1982) found no difference between asthmatic and normal lymphocytes in terms of β -adrenoceptor binding density and the cyclic AMP response to β -agonists.

Animal studies have produced conflicting evidence. Barnes et al. (1980) showed that in the ovalbumin-sensitized and challenged guinea-pig model of asthma there was a decreased pulmonary β -receptor density and an increased α -receptor density. Furthermore, the

magnitude of adenylate cyclase activation by isoproterenol in lungs from these animals was less than that of control animals. The animal model used by Barnes et al. (1980) exhibited symptoms of asthma; i.e., coughing, wheezing, and hyperreactivity to bronchoconstrictors. Therefore, Cheng & Townley (1982) investigated the effects of bronchoconstriction on β -adrenoceptor density and showed that only in animals that were exposed to bronchoconstrictors like histamine was a reduced binding density observed. Therefore, they concluded that β -adrenoceptor hypoactivity can result as a consequence of the stress induced by bronchoconstriction.

Studies comparing naturally ascaris-sensitive beagle dogs and normal beagle dogs demonstrated that α -adrenoceptor-mediated bronchoconstriction only occurred in the allergic dogs (Malo & Wasserman, 1983). Furthermore, this effect was potentiated by propranolol/indomethacin pretreatment. Hence, it appears that α -adrenoceptor-induced bronchospasm only plays a role in allergic dogs and not in the unsensitized controls. Finally, Bongrani et al. (1983) showed that β -adrenoceptor blockade potentiated bronchospasm induced by acetylcholine, histamine, or LTC₄.

The above representative studies demonstrate the diversity of results obtained from investigations of β -adrenoceptor function in asthma. There is clearly a need to investigate the role of other relaxant receptors, e.g., the VIP receptor, in the airways. Furthermore, it is apparent that a variety of factors, including prior

administration of β -agonists and stresses of bronchoconstriction, can contribute to the lack of uniformity of the conclusions reached.

1.3.2 Sensitization-dependent changes in cyclic AMP and PGs:

Various studies have suggested alterations in cyclic AMP levels after immunological sensitization. Sydbom et al. (1979) showed that the basal levels of cyclic AMP in rat mast cells was significantly reduced by sensitization, and that anaphylactic histamine release was increased. Cyclic GMP levels were unchanged by sensitization and the cyclic AMP/cyclic GMP ratio was decreased. However, Mathe et al. (1978) demonstrated earlier a decreased cyclic AMP response in sensitized guinea-pig lung in response to histamine stimulation. Hence, it is not known if the decreased cyclic AMP levels in rat mast cells is due to increased histamine release or if decreased cyclic AMP levels causes greater amounts of histamine to be released.

Rimard et al. (1979) showed that in dogs sensitive to ascaris, the isoproterenol-induced relaxation of trachealis muscle was less than in control animals. Furthermore, sensitized-dog trachealis had lower basal cyclic AMP levels than control trachealis and lower isoproterenol stimulated increases in cyclic AMP. These dogs had not been previously exposed to a β -agonist. Hence these authors ruled out desensitization of the β -receptor.

Sensitization increases the release of bronchoconstrictor PGs from the lung. Mathe et al. (1977) showed that ovalbumin sensitization

of guinea pigs caused significantly more $\text{PGF}_2\alpha$ in addition to histamine to be spontaneously released from the lung relative to control animals. Yen et al. (1978) obtained similar results. Rothberg & Hitchcock (1982) showed that microsomal fractions prepared from ovalbumin-sensitized guinea-pig lung synthesized more bronchoconstrictor TXA_2 and PGD_2 upon AA-induced stimulation than control microsomes. Boots et al. (1978) obtained similar results using perfused guinea-pig lungs. From these studies, it appears that immunological sensitization increases the production of bronchoconstrictor PGs in the airways.

Fish et al. (1981) showed that indomethacin-pretreatment of allergic asthmatic and allergic nonasthmatic (i.e. patients with allergic rhinitis) subjects, increased the sensitivity of the latter group to antigen-induced decreases in pulmonary function. Furthermore, sensitivity to methacholine was not changed by indomethacin. The authors concluded that PGs may be regulating mediator release in non-asthmatic subjects in a different fashion from asthmatics.

Walters et al. (1981) studied the effects of $\text{PGF}_2\alpha$ -pretreatment on the pulmonary responses to histamine in normal subjects and showed that the sensitivity to histamine increased without a change in reactivity when the data was compared to placebo-pretreatment. However, opposite results were obtained by Fish et al. (1984) in asthmatic subjects. $\text{PGF}_2\alpha$ -pretreatment decreased the response of human asthmatic airways to histamine. Also, experiments by Walters (1983) showed that immunization of normal humans against influenza

virus increased the sensitivity and decreased reactivity of the airways to histamine. Indomethacin-pretreatment abolished the increased sensitivity but increased reactivity, implying a role of PGs released in the inflammatory response to influenza virus in the induction of airway hyperresponsiveness.

1.3.3 Sensitization-dependent changes in the role of lipoxygenase metabolites:

Lipoxygenase products have been implicated in the pathogenesis of asthmatic hyperreactivity.

Increased synthesis of lipoxygenase products has been shown to occur as a consequence of immunological sensitization. This has been demonstrated in guinea-pig lung fragments (Piper & Seale, 1979) and in platelets from normal and asthmatic individuals (Yen & Morris, 1982). Furthermore, lipoxygenase products have been shown to increase release of histamine from human basophils (Peters et al. 1981).

The influence of prior exposure of airway tissue to lipoxygenase products on subsequent responses to bronchoconstrictors has also been studied. Generally, lipoxygenase products sensitize airway smooth muscle to the bronchoconstrictor effects of histamine and other contractile agonists. Copas et al. (1982) showed that 5-HETE contracted human isolated bronchial muscle and guinea-pig lung strips. 5-HETE at subthreshold doses also potentiated histamine-induced contractions of human airway muscle. LTD₄ and LTE₄ enhanced contractions of guinea-

pig tracheal spirals to histamine and acetylcholine (Creese & Bach, 1983; Lee et al. 1984). These effects are antagonized by FPL55712.

2. RESEARCH OBJECTIVES

2. RESEARCH OBJECTIVES

This thesis consists of three separate but related studies. Studies one and two utilize the actively-sensitized (ovalbumin as the antigen) guinea-pig model of asthma. The hypothesis explored in the first study was that immunological sensitization alters the responsiveness and sensitivity of airway tissues to bronchoconstrictors and bronchodilators. By analogy with human allergic bronchial asthma, immunological sensitivity to an antigen may result in bronchoconstrictor hyperreactivity and/or bronchodilator hypoactivity. These may arise as a consequence of altered AA metabolism (Yen & Morris, 1982), changes in receptor concentration (Szentivanyi, 1968; Kaliner et al. 1982), and/or changes in cellular regulatory processes of the airways (Mathe et al. 1978; Rinard et al. 1979).

In order to investigate such possible changes, the reactivity of sensitized airway tissue to bronchoconstrictors and bronchodilators was compared to appropriate unsensitized controls. Contractile responses and sensitivity of normal and sensitized isolated tracheal spirals (large airways) and lung parenchymal strips (small airways) to histamine, carbachol, LTC₄, LTD₄ and U-44069 were determined. These agents being chosen by virtue of their involvement in human asthma. Furthermore, the relaxant responses of normal and sensitized airway tissues to isoproterenol, PGE₂, forskolin and vasoactive intestinal polypeptide (VIP) were investigated. In conjunction with the relaxant effects of these bronchodilators, the responses of adenylate cyclase

in membranes prepared from normal and sensitized lung parenchyma were measured. This was done so as to obtain a direct index of receptor occupation and activation by these agents and to determine whether immunological sensitization alters tissue relaxation and/or cyclic AMP production. Again, this hypothesis was based on literature reports of changes in the effect of bronchodilator receptors and the adenylate cyclase complex in asthma. The compounds used in this study were chosen by virtue of the probable importance of the β - and VIP-receptor in asthma. Forskolin was used to obtain a non-receptor-mediated measurement of adenylate cyclase activation and PGE₂ because of the important modulatory function of this PG in the airways (Spannhake et al. 1981).

Since AA metabolites are synthesized and are active in airway tissues, the effects of inhibitors of the cyclooxygenase enzyme; i.e., indomethacin, the lipoxygenase enzyme; i.e., NDGA, and an inhibitor of both enzymes, i.e., phenidone, were investigated on the contractile responses of normal and sensitized tissues. The effects of indomethacin were also investigated on bronchodilator-induced relaxation of normal and sensitized airway tissues and on adenylate cyclase activation in normal and sensitized lung parenchymal membranes.

Various studies have suggested that AA metabolism is altered in allergic states. The use of inhibitors of AA metabolism in the above study served to define such a defect. This phenomenon was investigated more directly by comparing A23187- induced

contractions of normal and sensitized airway tissues. Furthermore, the nature of lipoxygenase metabolite(s) released from the airways upon antigen, A23187, and AA challenge was investigated using reverse-phase high performance liquid chromatography techniques supplemented with UV spectrometry and bioassay techniques.

The nature of calcium regulation in the synthesis of the metabolite(s) mediating AA-induced contractions of the airways was also examined. This was done so as to determine whether calcium modulatory drugs preferentially antagonize mediator synthesis as opposed to smooth muscle contraction initiated by released mediators (See evidence presented in Section 1.2.3.3.4.). The third and final study in this thesis was to investigate the effects of LTD₄ on the guinea-pig lung and rat-cerebellar adenylate cyclase systems. The hypothesis that LTD₄ interacts with a receptor negatively linked to adenylate cyclase was tested (See evidence presented in Section 1.2.1.4.7). In this study adenylate cyclase was prepared from the above tissues and tested under conditions which were optimal for demonstration of inhibition of the enzyme.

3. MATERIALS AND METHODS

3. MATERIALS AND METHODS

3.1 Materials:

Histamine dihydrochloride, carbamylcholine chloride, nordihydroguaiaretic acid (NDGA), 1-phenyl-3-pyrazolidone (phenidone), adenosine, adenosine deaminase, vasoactive intestinal peptide (VIP), γ -amino butyric acid (GABA), arachidonic acid (AA), prostaglandin E₂ (PGE₂), and ovalbumin (OA, grade II for sensitization and grade V for challenge) were obtained from Sigma (St. Louis, MO). 8-(diethylamino)-octylo-3,4,5-trimethoxybenzoate hydrochloride (TMB-8) was from Aldrich Chemical Company (Milwaukee, WI). Forskolin, calcium ionophore A23187, GTP (trilithium salt), GTP γ S, creatine kinase, dithiothreitol, creatine phosphate (potassium salt), AMP, cyclic AMP and ATP were from Calbiochem-Behring (San Diego, CA). [α -³²P]-ATP (25 Ci/mole) was obtained from ICN chemicals (Irvine, CA).

LTC₄, LTD₄ and indomethacin were gifts from Drs. J. Rokach and Wm. D. Dorian, Merck Frosst Laboratories (Pointe Claire - Dorval, P.Q.). U-44069 was a gift from Dr. M. K. Bach, the Upjohn Company (Kalamazoo, MI).

All drugs were dissolved in water, except U-44069 (10⁻³ M) which was dissolved in 95% ethanol, indomethacin (10 mg ml⁻¹) in 1 M Tris buffer (pH 8.4) or ethanol, NDGA (100 mM) in water containing 1.5% NaOH to make a salt, A23187 (1 mg ml⁻¹) in ethanol, PGE₂ (10⁻² M) in ethanol, forskolin (10⁻² M) in DMSO, isoproterenol in water containing 100 μ M ascorbic acid and AA (10 mg ml⁻¹) in 1 M Tris buffer (pH 8.4).

and stored in the dark at -70°C until used. LT stock solutions (0.2 mg ml^{-1}) were checked for purity by HPLC and the concentration adjusted to 10^{-4} M , and divided into aliquots and stored at -70°C until the day of use. Diluted solutions were stored at 4°C and used for a maximum of 1 week and then discarded.

The effect of vehicle was always tested on the responses being measured and it was ensured that none of the vehicles significantly affected the response.

All drugs were diluted in deionized water or in Krebs-Henseleit solution (KHS). Furthermore, drugs used in adenylate cyclase assays were always adjusted to pH 7.5 with Tris acid or base before storage or use.

All solvents used in HPLC were of HPLC grade. All other drugs, chemicals and solvents were at least of reagent quality.

3.2 METHODS

3.2.1 Sensitization of animals and preparation of tissues:

Male English short-hair guinea pigs (200-250 g) (Connaught Laboratories, Toronto, Ontario) were actively sensitized with ovalbumin (OA) (grade II) 100 mg s.c. and 100 mg i.p. Normal animals were untreated and age and weight matched with sensitized animals in all experiments. Animals were killed by stunning and exsanguination (3-4 weeks after OA injection for sensitized animals). The trachea and lung were removed immediately and placed in KHS. The composition

(mM) of the KHS was NaCl, 118; KCl, 4.7; MgSO₄·7H₂O, 1.2; CaCl₂, 2.2; KH₂PO₄, 1.2; NaHCO₃, 24.9; D-glucose, 11.1. The trachea was cut spirally (Constantine, 1965) and divided into four equal segments so that one always acted as a control to detect changes occurring as a result of time, vehicle, or previous additions of drugs. Parenchymal strips were prepared from the distal edges of each lung lobe (Lulich et al. 1976). Each strip was approximately 3 x 3 x 30 mm. Four tissues were obtained from each animal and used as above. Tissues were placed in water-jacketed 10 ml baths, maintained at 37°C in KHS aerated with 95% O₂ and 5% CO₂. Tissues were attached by silk threads to force displacement transducers (Grass FT03C) and the responses displayed on Grass polygraphs (Model 7D). An initial load of 1 g was placed on each tissue. At the end of a 90 min equilibration period, during which the bath fluid was replaced with fresh KHS every 15 min, the resting tone was adjusted to 1 g. Initial experiments with KCl-induced contractions (Fig. 3) demonstrated that the length-tension relationships were similar for both normal (N) and sensitized (S) tissues. The optimal tension was 1.0 - 1.5 g for both trachea and parenchyma. Higher applied tension, e.g., 2 g tended to tear parenchymal strips. Tracheal spirals normally increased in tone whereas parenchymal strips tended to relax slightly under 1 g applied tension. The dry weight of each tissue was determined at the end of the experiment (after drying overnight at 60°C). The dry weight was used to normalize the force developed to the smooth muscle mass (Brink

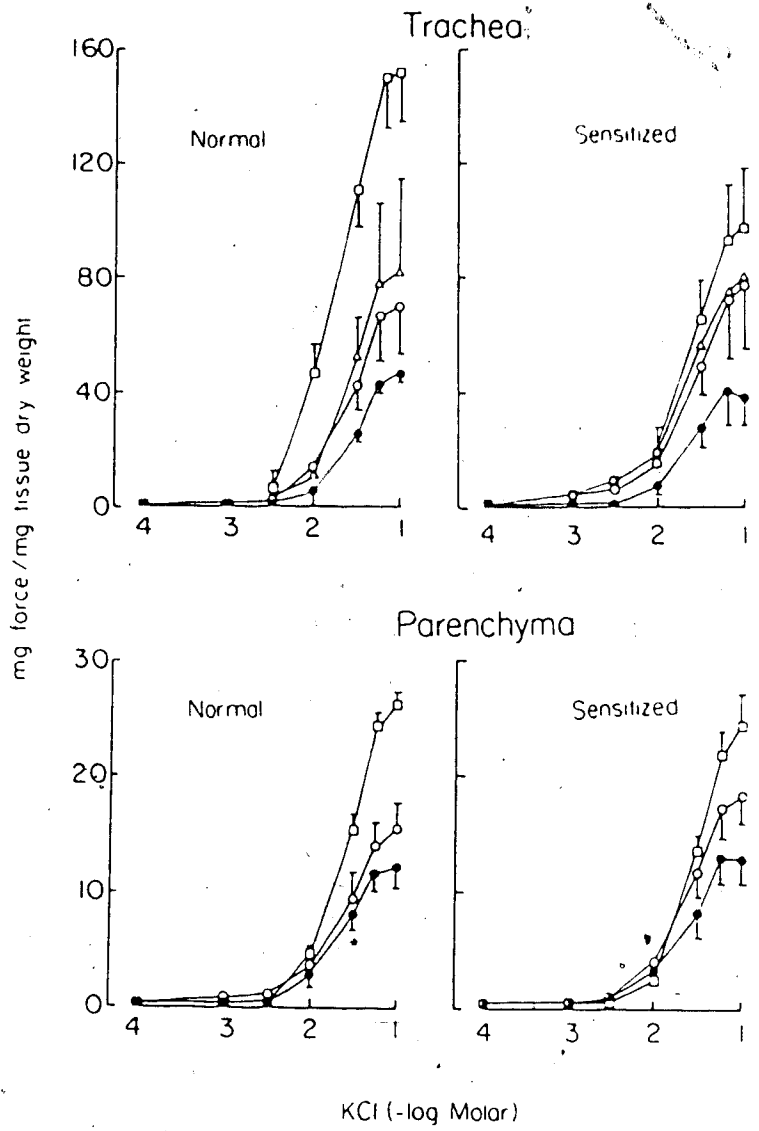


Fig. 3. Length-tension relationships of isolated guinea pig airways. Contractile responses of normal and sensitized tissues to KCl are shown. Resting tension imposed upon the tissues was 0.5 g (●), 1.0 g (○), 1.5 g (□), and 2.0 g (△). The results are the mean ± SEM (n=3).

et al. 1980). This normalization assumes that the percentage of smooth muscle in trachea and parenchyma is constant. Furthermore, the maximal response to histamine (100 μM) was determined initially and other responses expressed as a percentage of this value.

3.2.2 Concentration-response curves to bronchoconstrictors and bronchodilators: Effects of cyclooxygenase and lipoxygenase inhibitors on responses to agonists:

After the responses to histamine (100 μM) became constant, concentration-response (C-R) curves were established for histamine, carbachol, LTC_4 , LTD_4 and U-44069 on N and S tracheal spirals and parenchymal strips. Only one bronchoconstrictor was studied on tissues from any one animal. Additions of drugs were made in graded dose form given in random order with two exceptions; (i) on tracheal spirals U-44069, LTC_4 , and LTD_4 were added in cumulative fashion since the tissue responses to these agonists were very prolonged and difficult to reverse by washing (in initial experiments we did not note any differences in C-R curves achieved by graded dose or cumulative addition); (ii) on parenchymal strips the LTs were added in graded doses given in increasing concentrations. These agonists were not added randomly since the tissues desensitized completely after high concentrations. Only one C-R curve was generated using these agonists on the parenchyma.

After establishment of the initial C-R curves, the tissues were

incubated for 30 min with indomethacin (8.5 μM), NDGA (30 μM), or phenidone (185 μM). These concentrations effectively inhibit the cyclooxygenase (indomethacin, phenidone) and lipoxygenase (NDGA, phenidone) enzymes (Vane, 1971; Blackwell and Flower, 1978; Morris et al. 1979). The fourth control tissue was incubated with vehicle in the final concentration used with the test tissues. The inhibitors were kept in the bath upon reestablishment of the second C-R curves to the bronchoconstrictors. Hence, all tissues had two curves generated on them except for LTC₄ and LTD₄ on lung parenchyma where only one curve was generated on control and inhibitor treated tissues, immediately after establishment of the optimal response to histamine (100 μM).

When sensitized tissues were used, they were challenged with OA (1 $\mu\text{g/ml}$) at the end of the experiment to confirm that the sensitization procedure was effective.

The increases in force as a result of drug addition were determined from the recorded responses and normalized in two ways: (i) after dividing by the tissues dry weight and (ii) by expressing as a percentage of the maximum response to histamine determined initially for every tissue before the addition of inhibitors. The effects of inhibitors on tissue tone was expressed as percentage change from preincubation tone.

The concentration of an agonist required to increase tension by 50% of the maximum attained and by 50% of the maximum attained by

histamine were the EC_{50} and EC_{50} maximum histamine, respectively. These values were extrapolated from hand-fitted individual C-R curves. The negative logarithm of the EC_{50} is the pd_2 and is an indication of the potency of an agonist. The EC_{50} maximum histamine values were also converted into negative logarithms. Data was analyzed for statistical significance by the use of Student's t -test for paired and unpaired data as appropriate. The difference between groups was considered significant when $p < 0.05$.

The relaxant effects of isoproterenol, forskolin, PGE_2 , and VIP were determined on N and S tissues prepared as above. Tracheal spirals were pre-contracted with carbachol ($1 \mu M$) a concentration which produces 70-80% of the maximum response. Parenchymal strips were not precontracted, but mechanically adjusted to maintain 1 g baseline tension. The agents were added cumulatively until the maximum response reached a plateau at which isoproterenol ($10 \mu M$) was added to fully relax the tissue. Responses were expressed as percentage maximum response to isoproterenol ($10 \mu M$), and as mg relaxation/mg dry weight of tissue. Both forms of data expression gave similar conclusions. Hence, only the former are presented.

Two relaxant drugs were studied on tissues from one animal. One acted as a paired time control and the other to determine the effect of indomethacin ($8.5 \mu M$) on the reestablished C-R curves to the above relaxants.

All comparisons (to detect the effects of inhibitor treatment)

were made with the appropriate time and vehicle control tissue. Further analyses were as described for bronchoconstrictors.

3.2.3 Responses to antigen, ionophore A23187 and AA. Effects of AA metabolism inhibitors and calcium-modulatory treatments:

Tissues from N and S animals were prepared as described in section 3.2.1. Tissues were treated with indomethacin (8.5 μM), NDGA (100 μM) or vehicle. After treatment of tissues with the above inhibitors for 30 min, the tissues were challenged with A23187 (5.7 μM) or ovalbumin (3 $\mu\text{g/ml}$). A23187 was added to both normal and sensitized tissues. AA (66 μM) was added to some tissues 1 min before the above stimuli.

In further experiments the effects of mepacrine (210 μM), a phospholipase inhibitor, were also investigated. The protocol in these experiments is shown in Table 4.

In the above experiments, the bath fluid was collected at the end of 60 min and LTs extracted as described later in section 3.2.4.

In further experiments to investigate the effects of Ca^{2+} modulatory treatments on AA-induced contractions, the following experiments were performed on normal airway tissues only. Tissues were set up as described earlier and pretreated with indomethacin (8.5 μM) for 30 min. They were then incubated as shown in table 5 for 30 min prior to the addition of AA (66 μM). In experiments 6, 7, 8 and 9, AA-induced contractions were measured for 60 min after which

Table 4. Experimental protocol for the investigation of the effects of mepacrine and NDGA on A23187- and ovalbumin-induced contractions of indomethacin (8.5 μM)- pretreated N and S tracheal spirals and lung parenchymal strips.

Experiment	Modulatory agent (30 min incubation)	Stimulus
1	None	A23187 (5.7 μM)* or OA (3 μgm l ⁻¹)
2	None	AA (66 μM)
3	Mepacrine (210 μM)	AA (66 μM)
4	Mepacrine (210 μM)	A23187 (5.7 μM) or OA (3 μgm l ⁻¹) and AA (66 μM)
5	Mepacrine (210 μM)	A23187 (5.7 μM) or OA (3 μgm l ⁻¹)
6	NDGA (100 μM)	AA (66 μM)
7	NDGA (100 μM)	A23187 (5.7 μM) or OA (3 μgm l ⁻¹) and AA (66 μM)

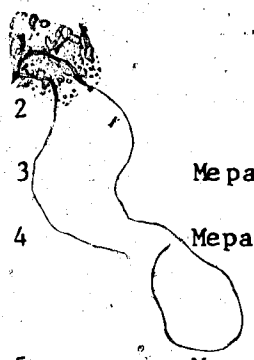


Table 5. Experimental protocol for Ca^{2+} studies. Tissues in Ca^{2+} -free KHS were washed frequently during the prechallenge period to ensure removal of extracellular Ca^{2+} .

All tissues challenged with AA (66 μM)

Experiment	Ca^{2+} concentration in bath	Treatment (30 min)
1	2.2 mM (control)	None
2	2.2 mM	Lanthanum chloride (1 mM)
3	2.2 mM	Nitrendipine (1, 10 or 100 μM)
4	2.2 mM	Verapamil (100 μM)
5	8.8 mM	None
6	Ca^{2+} -free	None
7	Ca^{2+} -free	Lanthanum chloride (1 mM)
8	Ca^{2+} -free	EDTA (300 μM)
9	Ca^{2+} -free	TMB-8 (100 μM)

Ca^{2+} (2.2 mM) was added and the contractions measured for a further 60 min.

Cumulative C-R curves to LTC_4 were also constructed on indomethacin (8.5 μM)-pretreated tissues in normal KHS (control), in Ca^{2+} -free KHS with and without lanthanum chloride (1 mM) and in normal KHS in the presence of nitrendipine (10 μM). Ca^{2+} (2.2 mM) was added to all tissues after the response to LTC_4 (0.1 μM) was obtained. Responses were expressed as a percentage of the maximum response to LTC_4 (100 μM) obtained in normal KHS.

3.2.4 Extraction, initial purification, reverse-phase high performance liquid chromatography, ultraviolet spectrometry and bioassay of leukotrienes released from airway tissues:

After 1 hour of release reaction induced by OA, A23187 or (section 3.2.3), the bath fluid was collected and kept on ice. The pH was adjusted to 3 with 1N HCL and the solution passed through a 0.22 μm filter (MILLEX-GS, Millipore). The filtered solution was then passed through a primed SEP-PAK C_{18} cartridge (Waters Associates). Priming was carried out by washing the cartridge with 5 ml methanol followed by 40 ml water. The loaded cartridge was successively washed with 5 ml water, 5 ml water/methanol (65:35 vol:vol) and 5 ml methanol. The last fraction was collected and the methanol blown off at 50°C under a nitrogen stream. Experiments with added [^3H]- LTC_4 standard indicated that this fraction contained about 80% of the

initial LTC₄ in the sample (Table 6). Furthermore, none of the drugs used interfered with the recovery of LTs.

The residue left after evaporation of methanol was suspended in a small volume (200 μ l) of distilled water and used in high performance liquid chromatography (HPLC) or bioassay procedures.

The final purification and analysis of samples was carried out by HPLC using a C₁₈ column (Radial-pak, Waters Associates). Elution was carried out using methanol/water/acetic acid (65:35:0.1, vol/vol) (pH 5.5, adjusted with ammonium hydroxide). The flow rate was 1 ml min⁻¹ and column back pressure was 1000 psi. Eluants were continuously monitored at 280 nm. Synthetic LTC₄ and LTD₄ were injected as standard. Peaks in the samples corresponding to the retention times of LTC₄ and LTD₄ were collected (Fig. 4), the pH adjusted to neutrality with 1 N NaOH, evaporated to dryness, resuspended in water and rechromatographed.

Rechromatographed samples were concentrated as above and suspended in methanol for ultraviolet spectrometry on a Carey 15 spectrophotometer. Bioassay was carried out on the atropinized (1 μ M) and mepyraminized (1 μ M) guinea-pig ileum longitudinal strip and lung parenchymal strip. Positive contractions were reversed with FPL55712 (0.17-8.7 μ M). Synthetic LTC₄ was used as a standard in the above bioassay procedures. Further experiments with an LTC₄-specific radioimmunoassay carried out by Dr. Burka confirmed the identity of the above mediators.

Table 6. Percentage recovery of [^3H]-LTC $_4$ utilizing C $_{18}$ -SEP-PAKs^a

Condition	% of initial radioactivity
KHS	2.8 \pm 0.8 ^b
Water wash	0.0 \pm 0.0
35% Methanol wash	7.7 \pm 1.1
100% Methanol wash	79.0 \pm 2.6
Cartridge	8.2 \pm 2.5

^anumber of experiments = 12

^bvalues are mean \pm SEM

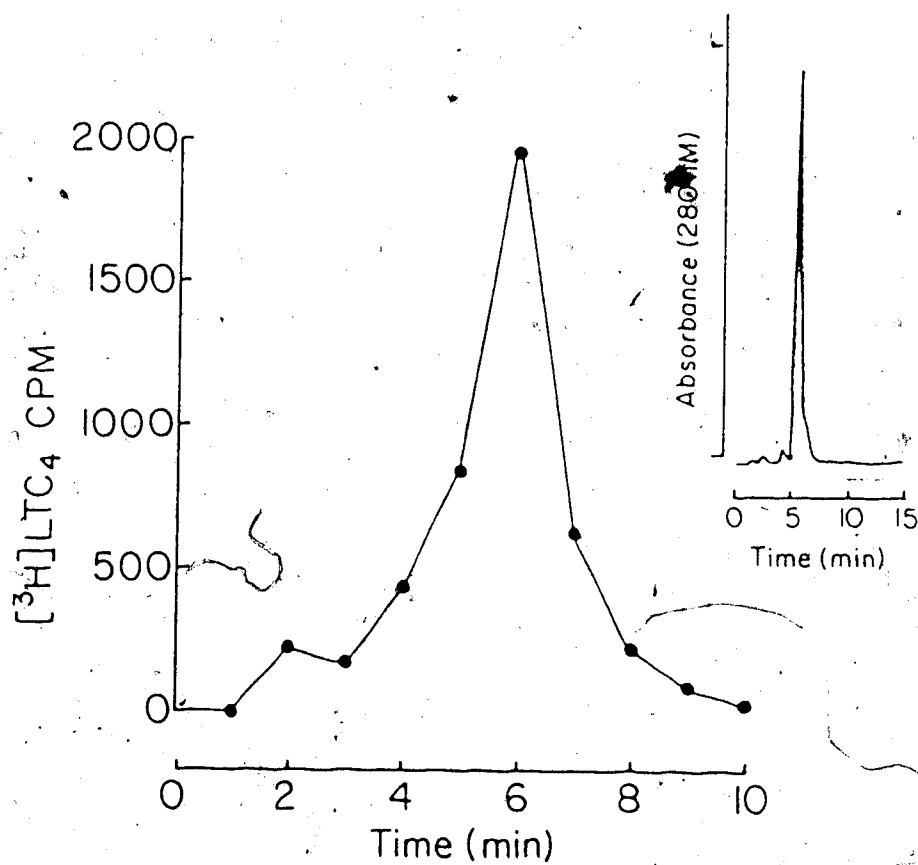
Elution pattern of LTC₄

Fig. 4. High performance liquid chromatography of LTC₄ monitored by liquid scintillation counting of [³H]-LTC₄ (main figure) and by UV absorbance at 280 nm (Inset). Elution times were similar.

3.2.5 Adenylate cyclase assay procedures:

Two studies involving measurement of adenylate cyclase activity were performed in this thesis. The first study attempted to determine whether adenylate cyclase activation induced by various bronchodilator drugs differed between N and S guinea-pig lung parenchymal tissue. Due to the inherent difficulty in obtaining hormone-sensitive adenylate cyclase from pure smooth muscle preparations (Muller, 1985), guinea-pig trachea was not studied in this thesis.

The second study of adenylate cyclase carried out in this thesis involved investigating the effects of LTD₄ on guinea-pig lung and rat cerebellar cyclases. The methods used in studies 1 and 2 differed slightly. These differences will be pointed out as appropriate.

3.2.5.1 Preparation of membranes:

Lungs from two animals were used for each membrane preparation. Whole lungs were removed from animals and perfused through the pulmonary artery with ice cold KHS until the perfusate was free of blood. The lungs were then chopped (excluding large bronchi, fat and adhering tissue) on ice. The chopped lung was then divided equally into two portions, placed in oxygenated KHS (30 ml) and incubated at 37°C for 30 minutes. One portion was treated with indomethacin (8.5 μM) and the other with vehicle for 30 min. Hence, experiments were done on a paired basis. The above incubation procedure was not followed in the second adenylate cyclase study. The lung portions

were then homogenized at 4°C in a glass homogenizer with a motor driven Teflon pestle (300 rpm) for 1 min in 10 volumes of homogenization buffer of the following composition: Tris-HCl (50 mM), dithiothreitol (1 mM) and sucrose (0.25 M) pH 7.5 at 4°C. The homogenate was filtered through glass wool and cheese cloth and centrifuged at 500 x g for 10 minutes at 4°C. The pellet made up of tissue fragments, unbroken cells and nuclei was discarded. The supernatant was subsequently centrifuged at 25,000 x g for 20 min at 4°C. The resultant pellet was resuspended in buffer identical to the homogenization buffer except not containing sucrose, and centrifuged again at 25,000 x g for 20 min at 4°C. The resultant pellet was gently resuspended in the above buffer with a hand-held teflon pestle in a glass homogenizer. Protein concentration was adjusted between 0.5-3.0 mg/ml. Protein was determined by the method of Lowry et al. (1951). Aliquots of 500 µl were frozen and stored (less than four weeks) until use under liquid nitrogen.

Essentially the same procedure was followed for preparation of rat cerebellar adenylate cyclase. Male Sprague-Dawley rats (300-500 g) were used in these experiments.

3.2.5.2 Adenylate cyclase assay procedure:

The procedure followed was that of Baer (1975). This method uses polyethyleneimine thin layer chromatography plates (Macherey-Nagel/Brinkman Instruments, Rexdale, Ontario), and development in lithium

chloride (0.25 M) to separate cyclic AMP from ATP. Assays were conducted in duplicate or triplicate in a final volume of 50 μ l. Each tube contained the following: 25 mM 4-(2-hydroxyethyl)-1-piperazine-ethane sulphonic acid (HEPES, pH 7.5) or Tris acid - Tris base (25 mM, pH 7.5), 5 mM $MgCl_2$ (for study 1, $MgCl_2$ or $MnCl_2$ at various concentrations in study 2 as indicated in results), 1 mM cyclic AMP, 10 mM creatine phosphate, 0.2 mg ml^{-1} creatine kinase, 0.1 mM [α - ^{32}P]-ATP (500,000-800,000 cpm) and 5-50 μ g membrane protein (the reaction was always shown to be linear under various conditions. See results). Drugs and other additions or changes in the conditions are shown under the appropriate results.

Incubations were carried out at 20°C and 37°C for various times (3-40 min) as indicated in results. The reaction was stopped by adding 10 μ l of a "stop" solution (pH 7.5) containing sodium salts of cyclic AMP, ATP, AMP, and EDTA, each at 25 mM. Alternatively for time course studies, 5 μ l of a 3 fold water diluted "stop" solution were spotted on water-washed thin layer plates (20 x 10 or 20 x 6.5 cm) and a 5 μ l aliquot of the adenylate cyclase reaction mixture spotted on top of this at the appropriate time.

The plates were then developed in LiCl (0.25 M). Spots were visualized under ultraviolet light and those corresponding to "ATP plus 5'-AMP" and "cyclic AMP" were cut out in small pieces and placed in scintillation vials containing 10 ml scintillation fluid (Quenchmate containing PPO (4 g/l) and POPOP (0.2 g/l)). The ratio of cpm in the

cyclic AMP and ATP + 5'AMP spots provided a measure of percent conversion of ATP to cyclic AMP. These values were calculated by a computer program after subtraction of blank values (assays carried out in the absence of enzyme determined with every experiment).

The results are reported as the mean \pm SEM of duplicate or triplicate determinations which never varied by more than 3.10%. Enzyme activity was calculated as cyclic AMP formed (pmoles/min/mg protein) or as percentage conversion values.

4. RESULTS

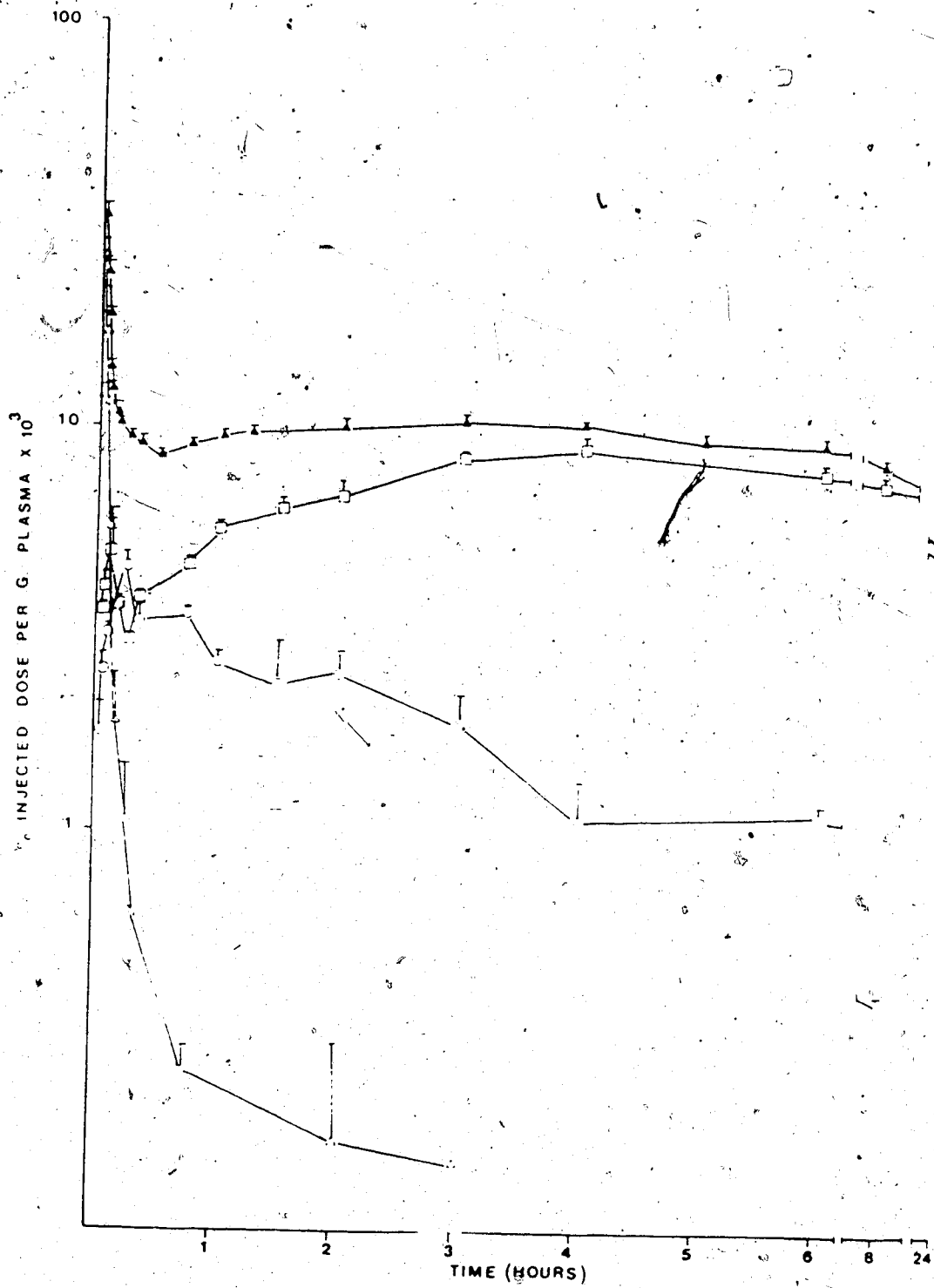


Fig. 16 Metabolites of [¹³¹I]-IVdU (specific activity, 1665 MBq /mmol) in Dogs *In Vivo* (n=2). ▲ Total Radioactivity, △ [¹³¹I]-IVdU, ○ [¹³¹I]-IVU, □ [¹³¹I]-I-. (Mean and Range)

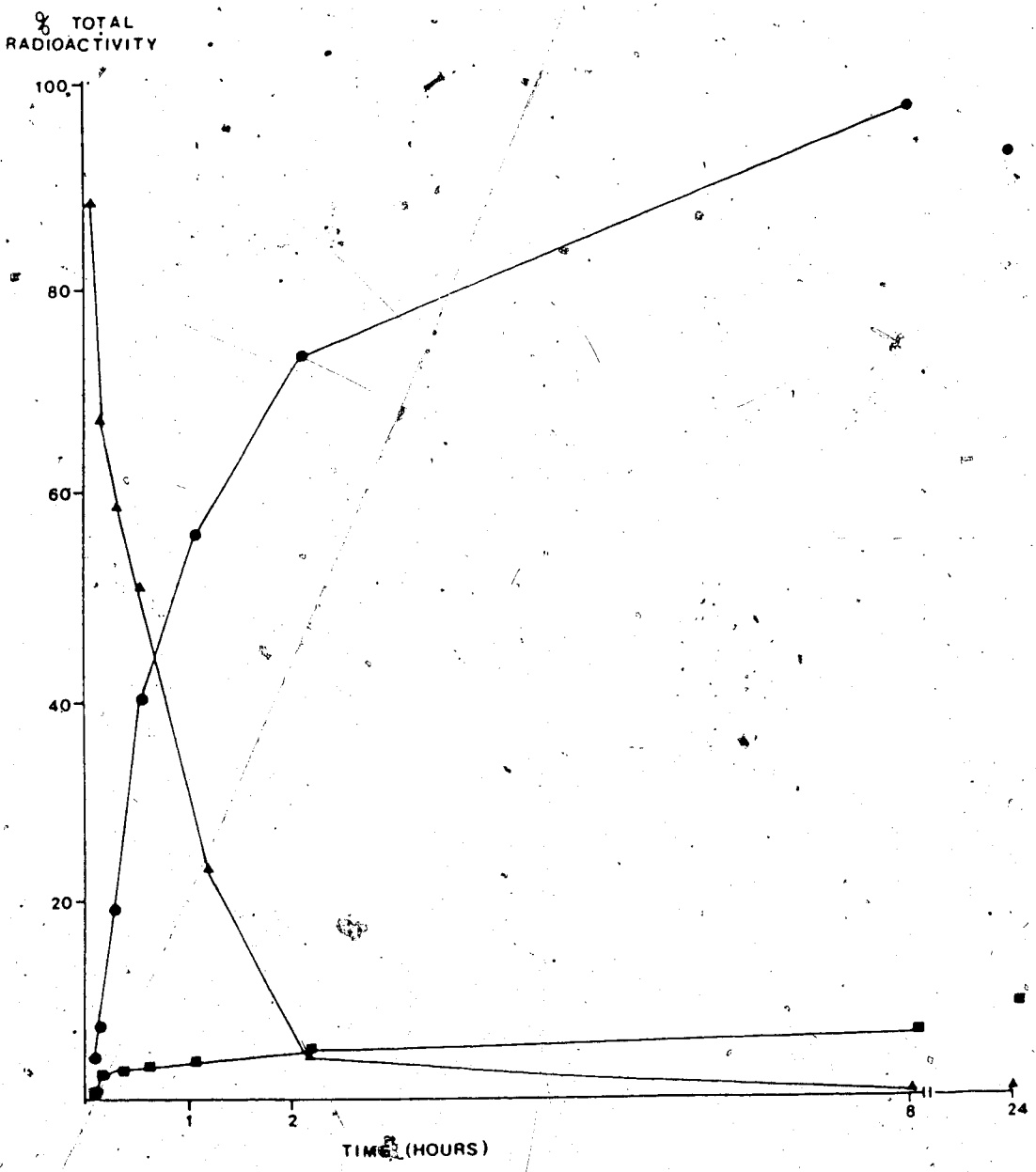


Fig. 15 Metabolites of $[^{131}\text{I}]$ -IVdU in Blood *In Vitro.* ($n=1$) \blacktriangle $[^{131}\text{I}]$ -IVdU, \bullet $[^{131}\text{I}]$ -IVU, \blacksquare $[^{131}\text{I}]$ -I

Metabolism of [¹³¹I]-IVdU in dog *in vivo*

The *in vivo* pharmacokinetics and metabolism of a radiopharmaceutical may depend on the specific activity of the drug. Therefore, the *in vivo* studies were performed using both low (1665 MBq/mmol) and high specific activity (37 TBq/mmol) [¹³¹I]-IVdU compounds.

The kinetics of the total radioactivity and its components in plasma for a 24 hour period after an i.v injection of [¹³¹I]-IVdU (low specific activity) are shown in Fig. 16. The plasma clearance curve for total radioactivity showed an initial rapid clearance of the isotope followed by a very slow clearance phase (Fig. 16). An unexpected increase in the total radioactivity in the blood could be noticed during the period of 30 min to 1.5 h. This was reproducible. This may be due to the release of radioactive metabolites of [¹³¹I]-IVdU from body compartment(s), which might have selectively accumulated [¹³¹I]-IVdU during the first phase of the curve. The clearance profile for intact [¹³¹I]-IVdU was characterised by a major rapid clearance phase. The concentration of [¹³¹I]-IVdU in plasma 1 hour after injection accounted for less than 2% of the overall radioactivity. The kinetics of the metabolites [¹³¹I]-IVU and radioactive inorganic iodide are also shown in Fig. 16. The radioactivity due to the unidentified component B rarely exceeded 10% of the total radioactivity in each plasma sample. Inorganic iodide was the major radioactive component (95%) in the plasma sample collected 24 hours after injection. Similar results were obtained from an experiment using a high specific activity sample of [¹³¹I]-IVdU (Fig. 17). The protein binding of radioactive compounds in the plasma was evaluated by equilibrium dialysis. The protein bound form of radioactivity remained less than 2% of the total activity, suggesting that [¹³¹I]-IVdU and its radioactive metabolites existed *in vivo* in unbound form.

The urine samples were collected using a catheter at 2, 4.5, and 8 h after the injection of [¹³¹I]-IVdU. The total radioactivity in urine at each time point was quantitated and an aliquot from each sample was analysed by quantitative r-HPLC. The total radioactivity recovered from urine for the three periods and the relative proportions of the radioactive components are shown in Table 13. Less than 8 % of the injected radioactive dose was excreted

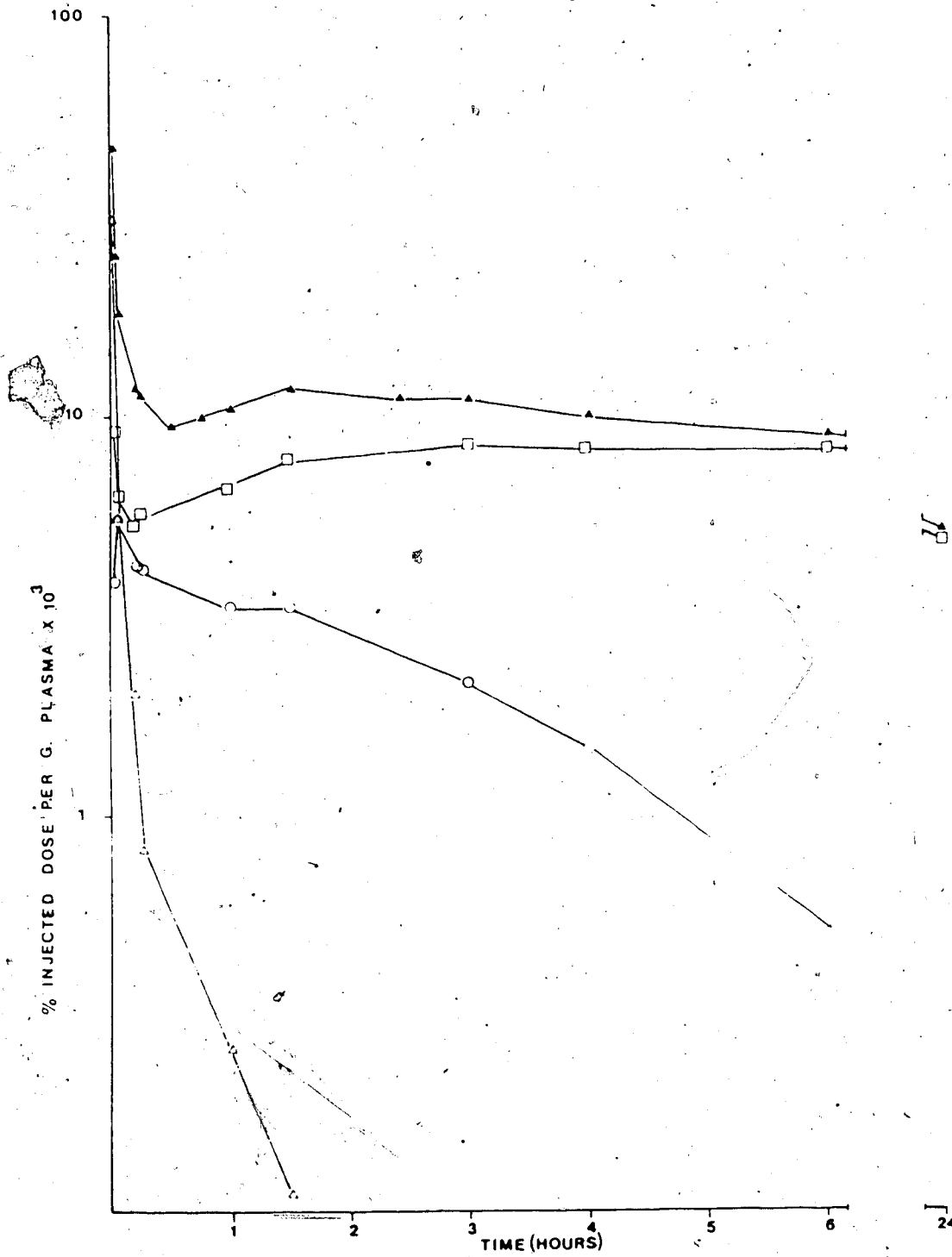


Fig. 17 Metabolites of [¹³¹I]-IVdU (specific activity, 37 TBq /mmol) in Dog *In Vivo* (n=1).

▲ Total Radioactivity, △ [¹³¹I]-IVdU, ○ [¹³¹I]-IVU, □ [¹³¹I]-I.

Table 13. Recovery of the Radioactivity from Urine at Various Times After the i. v. Injection of ^{131}I -IVDU (mean of two experiments with range)

Time Hours	Radioactivity % Inj. Dose	IVDU	Radioactive Components (% of the total activity in urine) IVU	Other
0.0 - 2.0	2.34 ±0.10	43.5 ±4.72	8.50 ±0.11	33.37 ±3.16
2.0 - 4.5	2.47 ±0.25	5.22 ±3.72	8.86 ±0.80	73.06 ±5.83
4.5 - 8.0	2.94 ±0.06	1.24 ±0.40	7.34 ±0.18	79.13 ±2.97
				12.27 ±2.52

by the kidney during an 8 hour period after intravenous injection.

A comparison of the kinetic data for low and high specific activity samples of [^{131}I]-IVdU (Fig. 16 and 17) suggests a slightly faster rate of clearance of radioactivity from the plasma (in the lower phase of the curve) for the high specific activity compound. The differences in plasma clearance kinetics are of very little importance, considering the 200,000 fold difference in the dose of IVdU administered. The rapid *in vivo* clearance of [^{131}I]-IVdU from plasma corresponds to its distribution in the body, renal excretion and biological transformations to the metabolites [^{131}I]-IVU and radioactive iodide. (Figs. 16, 17 and Table 13). The kinetic data correspond to a volume of distribution of about 2 L and a biological half-life of less than 3 minutes. The metabolites, [^{131}I]-IVU and [^{131}I]-iodide, account for most of the radioactivity in the second slow clearance phase. The total radioactivity in the plasma compartment at 1 hour corresponded to about 6.5% of the injected dose, suggesting extensive (possibly nearly uniform) distribution of these metabolites in one or more other body compartments. The increase in free iodide concentration in the plasma even after the virtual disappearance of the intact nucleoside suggests *in vivo* deiodination of the newly formed base [^{131}I]-IVU. The metabolic fate of the radioiodine introduced as [^{131}I]-IVdU *in vivo* is summarised in Fig. 18. The *in vivo* metabolic transformations of [^{131}I]-IVdU are distinctly different from the *in vitro* study since neither [^{131}I]-IVdU nor [^{131}I]-IVU undergo *in vitro* deiodination in blood. The mechanism of the deiodination is not clear. Since IVdU is not phosphorylated to its 5'-monophosphates in uninfected cells, thymidylate synthetase-catalysed dehalogenation of IVdU is unlikely. Such dehalogenations are usually limited to nucleotides (191, 192). Cytochrome P-450-catalysed oxidation of the C-H bond of the carbon atom bearing the halogen is a major route for the metabolism of alkyl halides (233). Metabolic degradations of halogenated alkenes may be mediated by epoxidation (233). It is likely that IVdU and IVU might have undergone dehalogenation by either of the above routes.

The percentage of injected radioactivity recovered from urine (8%) over a period of 8 hours was substantially lower than expected. This data may be compared with the renal

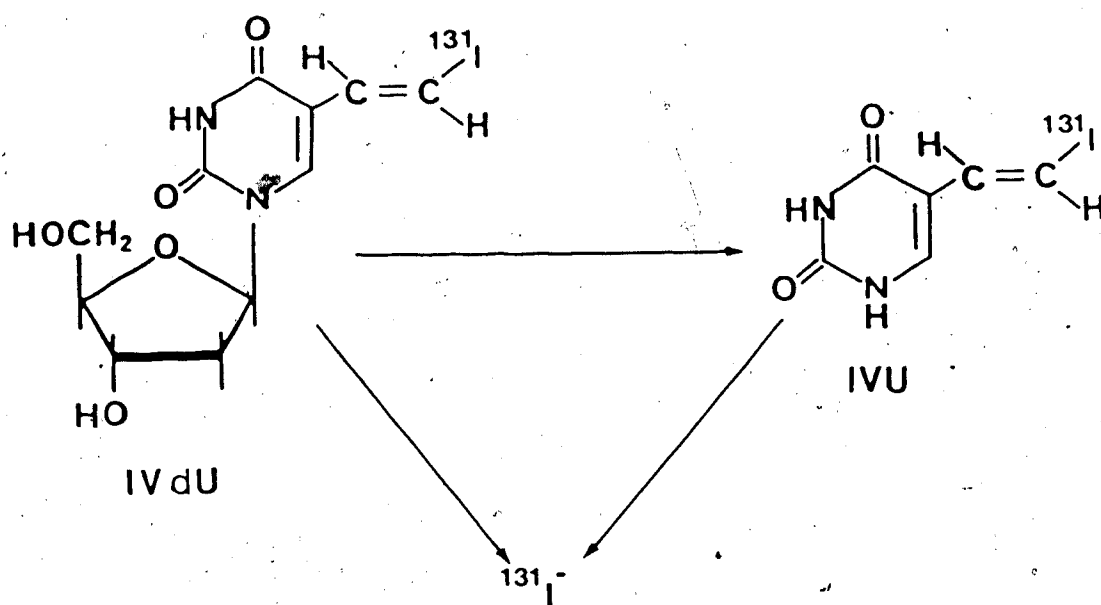


Fig. 18 Schematic Presentation of the Metabolism of [¹³¹I]-IVdU in Dogs *in vivo*.

clearance data for [^{131}I]-5-iodo-2'-deoxyuridine in mice where 77.8% of the radioactivity injected was recovered in urine over a period of 8 hours. (234). The renal excretion data for the radioactive components (Table 13) show that the intact nucleoside was the most rapidly excreted major radioactive component. The base (IVU) showed extremely slow renal excretion. Desgranges *et al* recently reported the pharmacokinetics and *in vivo* metabolism of BVdU in mice which demonstrated the persistence of high concentrations of the base (BVU) in plasma over a period of 24 hours (187). This suggests similarities in the excretion behaviour of IVU and BVU. However, the kinetics of the metabolism and excretion of IVdU are more complicated due to deiodination. The possible *in vivo* debromination of BVdU has not been investigated.

The prevention or reversal of undesired *in vivo* metabolic transformations of IVdU would be of great value with respect to its use as a diagnostic agent. Such steps would result in increased bioavailability of the active radiopharmaceutical and faster clearance of the background radioactivity from the blood prior to imaging. The chemical modification of IVdU to develop analogs which are resistant to glycosidic bond cleavage would be one approach. Rosowsky *et al* have recently reported that the 5'-pivaloate of deoxythymidine does not undergo phosphorolytic cleavage by deoxythymidine phosphorylase *in vitro* (235). Deoxythymidine 5'-pivaloate acts as a prodrug of deoxythymidine *in vivo*. Plasma levels of deoxythymidine were significantly higher (about 2.5 times 1 h after a subcutaneous injection) when deoxythymidine was given to mice as the 5'-pivaloate than when it was given as the free nucleoside (236). In view of these results, Lee *et al* have made a preliminary *in vivo* evaluation of the tracer kinetics of [^{131}I]-IVdU-3',5'-diacetate, a prodrug of [^{131}I]-IVdU, in mice (237). The tracer kinetics of [^{131}I]-IVdU-3',5'-diacetate was virtually the same as that for [^{131}I]-IVdU, presumably due to the rapid *in vivo* degradation of the ester to the free nucleoside. This is consistent with the high serum esterase activity reported for mice (238). Studies using [^{131}I]-IVdU-3',5'-diacetate were not continued beyond this point. Another approach to increasing the bioavailability of IVdU would be its regeneration from IVU using

deoxythymidine, in a manner analogous to that reported for BVdU (187). However, preliminary studies in this direction by Lee *et al* showed that tracer kinetics of [¹³¹I]-IVdU in mice was virtually unaltered by a subsequent intravenous administration of deoxythymidine (237).

The *in vivo* pharmacokinetic and metabolism studies on [¹³¹I]-IVdU suggested that its rapid *in vivo* metabolism may prove to be a limiting factor with respect to its development as a radiopharmaceutical for the diagnosis of HSE.

G. Diagnostic Imaging

The feasibility for *in vivo* use of radiolabeled IVdU as a radiopharmaceutical for HSE was also evaluated by diagnostic imaging in planar and tomographic modes. Rabbits (2 infected and 2 uninfected) were injected i.v with [¹³¹I]-IVdU (37 MBq). Planar brain imaging was performed at 30 min, 45 min, 1 h and 6 h after the injection of IVdU. Planar images from an uninfected and an infected rabbit 1 h after injection of [¹³¹I]-IVdU are shown in Fig. 19 and 20 respectively. The region of greatest activity in the whole body scintigram was urinary bladder. Uptake in the area corresponding to brain was minimal. None of the images succeeded in differentiating HSV-1-infected from normal brains. This was not surprising in view of the high blood radioactivity observed in the tissue distribution studies, which could obscure any small differences in radiotracer uptake between infected and uninfected brains.

Brain imaging in the tomographic mode (ECT) offers the potential to detect differential uptake in a relatively small region. The radioisotope of iodine most suited for SPECT is ¹²³I. The rapid and efficient methods developed for radioiodination permitted the synthesis of [¹²³I]-IVdU ready for injection (about 37 MBq) in a radiochemical yield of 40%. In view of the rapid *in vivo* metabolism of IVdU, intracarotid injection was chosen as the route of administration of the labeled drug. The injection of drug via common carotid artery would be expected to allow a major portion of the drug to pass through brain at least once before any significant metabolic degradation occurs. The optimum time point for imaging was thought to

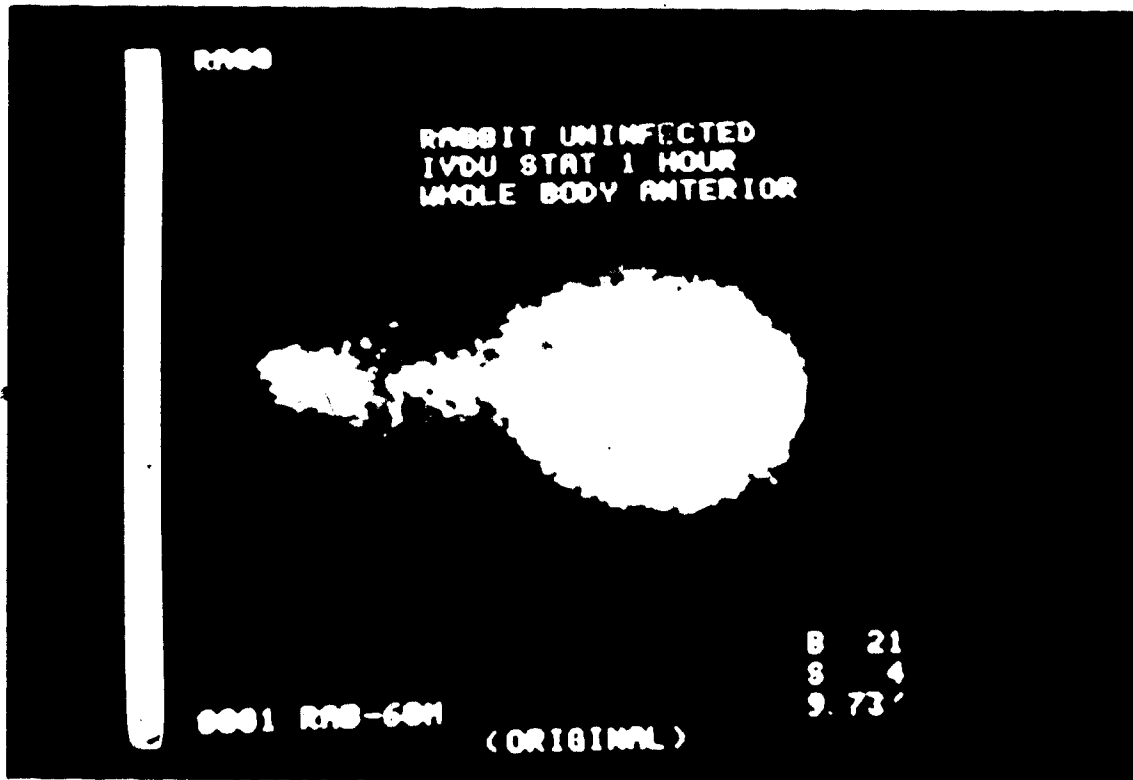


Fig. 19 Planar Whole Body Image of an Uninfected Rabbit 1 h After an Intravenous Injection of $[^{99m}\text{Tc}]\text{-IVDU}$

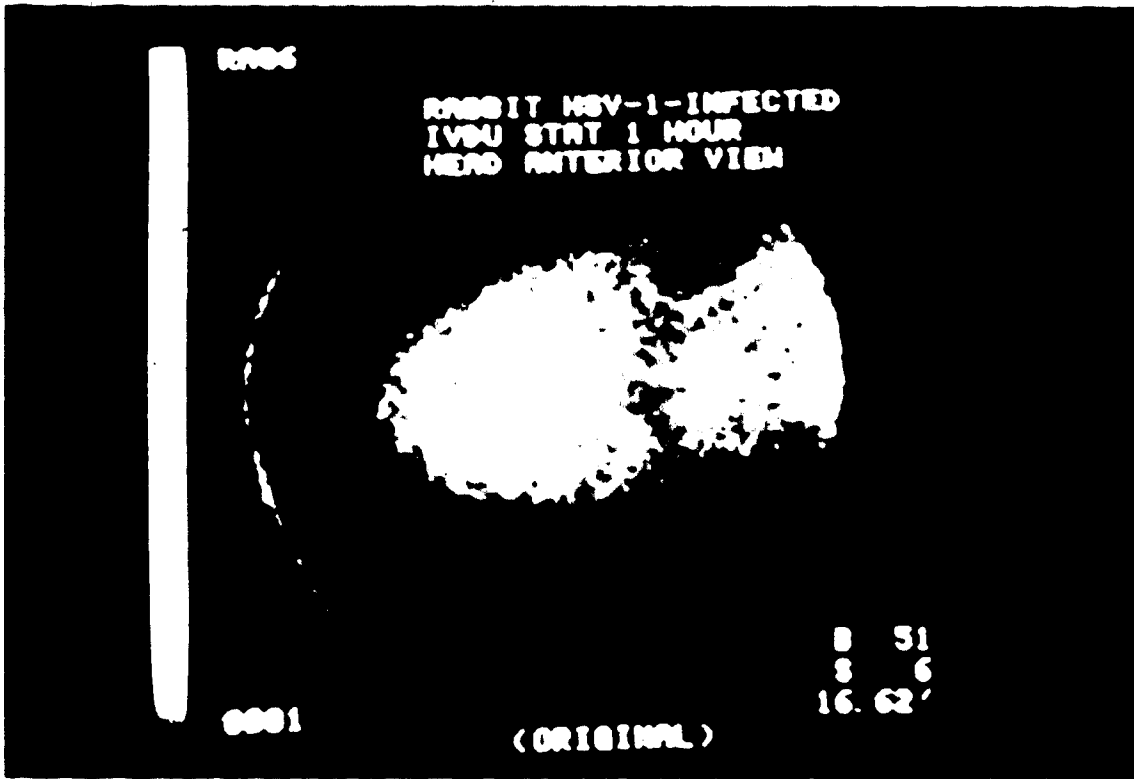


Fig. 20 Planar Image (Head) of an HSV-1-infected Rabbit 1 h After an Intravenous Injection of ¹²⁵I-IVdU

be around 30 min after the injection of [¹²⁵I]-IVdU for two reasons. First, pharmacokinetic and metabolic studies in dogs suggested that within a period of 2 h after injection of IVdU, blood radioactivity was lowest at 30 min. Second, most of the labeled IVdU was already metabolised at this point. Therefore prolonging the time of imaging beyond this time offers little or no advantage. Brain imaging in the tomographic mode (SPECT) was performed on rabbits (2 normal and 1 infected) over a period of 30 min (20 to 50 min after injection of [¹²⁵I]-IVdU). The tomographic images clearly showed a 'cold spot' in uninfected animals in the area corresponding to brain (Plate 1). Uptake in the infected rabbit brain was not significantly higher than that of controls (Plate 2). This may be due to several reasons. Two important factors deserve mention. The pharmacokinetic and metabolic studies have indicated that the *in vivo* bioavailability of IVdU is very low with a biological half-life of approximately 3 min in dogs. Any increase in bioavailability of IVdU due to intracarotid administration of the drug is limited to the 'first pass' of the drug through brain. The *in vitro* uptake studies of [¹²⁵I]-IVdU (section D) have shown that HSV-1-infected cells need to be exposed to radiolabeled nucleoside for a period of 30 min to 1 h before a significantly higher uptake could be detected in infected cells relative to uninfected cells. A second factor is the resolution of the imaging system and its relationship to the size of the animal brain. Although the resolution of SPECT is much higher than that of planar imaging, it is still limited to the order of 1 cm. This presents a problem in brain imaging studies with animals having small brains. It would be more desirable to use a non-human primate such as monkey as the animal model for HSE, since they have brains of larger size.

The tissue distribution, pharmacokinetic and metabolic and brain imaging studies indicate radioiodinated IVdU is not the nucleoside of choice as a radiopharmaceutical for non-invasive diagnosis of HSE. The major limiting factor of this nucleoside appears to be its rapid *in vivo* metabolism. In view of this, the next phase of the investigation was directed towards evaluation of a series of nucleoside analogs with structural features likely to be more resistant to *in vivo* metabolism.

Plate 1. SPECT Images of an Uninfected Rabbit 30 min After an Intracarotid Injection of
[¹²⁵I]-IVdU

NR RABBIT 4. UNINFECTED. BRAIN. D. 13-02-85

NRRA

A
X
I
A
L



NR RABBIT 4. UNINFECTED. BRAIN. D. 13-02-85

NRRA

S
A
M
P
L
E
S



NR RABBIT 4. UNINFECTED. BRAIN. D. 13-02-85

NRRA

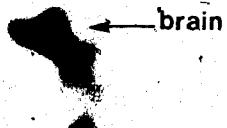


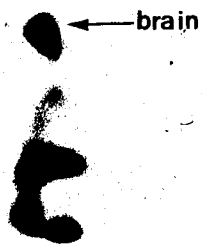
Plate 2. SPECT Images of a HSV-1-Infected Rabbit 30 min after an Intracarotid Injection of [¹²⁵I]-IVdU.

NR RABBIT INF. INFECTED. BRAIN. D. 06-03-05

NRRA

NR RABBIT INF. INFECTED. BRAIN. D. 06-03-05

NRRA



NRRA

NR RABBIT INF. INFECTED. BRAIN. D. 06-03-05

NRRA

H. Quantitative Uptake Studies of Radiolabeled Nucleosides in Herpes Simplex Virus-Infected Cells *In Vitro*

The biochemical aspects of selective antiviral activity for nucleoside analogs has already been discussed in Chapter I. A nucleoside requires the following biochemical characteristics for selective anti-HSV activity:

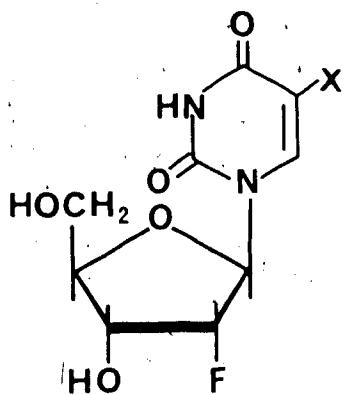
1. Selective phosphorylation by HSV-encoded TKs to its 5'-monophosphate.
2. Conversion of the nucleoside-5'-monophosphate thus produced to the 5'-diphosphate and then to the 5'-triphosphate by cellular and/or viral kinases.
3. Selective inhibition of HSV-encoded DNA polymerases by the nucleoside-5'-triphosphate.

From these three requirements, only the first characteristic (selective phosphorylation to 5'-monophosphate) is essential for selective metabolic trapping of the nucleoside in HSV-infected cells. Therefore it is plausible that certain nucleosides, which are not potent antiviral agents, may still undergo selective metabolic trapping in HSV-infected cells. This fact is illustrated clearly by the biochemical transformation of BVdU in HSV-2-infected cells *in vivo* (151). BVdU exhibits a 100-1000 times lower activity against HSV-2, relative to HSV-1. However, BVdU is metabolically transformed to BVdU-MP in HSV-1- and HSV-2-infected cells with equal or nearly equal efficiency. The low potency of BVdU against HSV-2 is due to the failure of HSV-2-encoded TK to further phosphorylate BVdU-MP to BVdU-DP as discussed in Chapter I. Thus, antiviral activity is not essential for metabolic trapping of nucleosides in HSV-infected cells. Therefore evaluation of nucleoside analogs as potential radiopharmaceuticals for HSE diagnosis need not be limited to compounds having a potent inhibitory effect on HSV-replication.

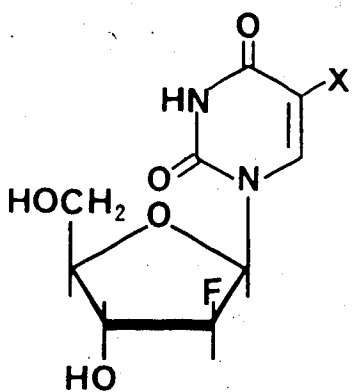
The *in vivo* stability of nucleosides is an important factor to be considered in the choice of a radiopharmaceutical for HSE diagnosis. Nucleoside analogs possessing structural features which provide resistance to glycosidic bond cleavage by phosphorylase enzymes offer a distinct advantage in this regard. Deoxythymidine phosphorylase has a high substrate specificity with respect to the 2'-deoxy position (185). Therefore any structural modification at the 2'-position

of a 2'-deoxypyrimidine nucleoside renders it a poor substrate for deoxythymidine phosphorylase. 1-(2-Deoxy-2-fluoro- β -D-arabinofuranosyl)cytosine, 1-(2-deoxy-2-fluoro- β -D-arabinofuranosyl)-5-fluorouracil and 1-(2-deoxy-2-fluoro- β -D-arabinofuranosyl)-5-methyluracil have been shown to have little or no affinity for the enzymes thymidine phosphorylase and uridine phosphorylase (185). Introduction of a 2'-fluoro substituent (with ribo or arabino configuration) into 2'-deoxyuridine derivatives appears to be a good approach to make them resistant to glycosidic bond cleavage. On this basis, a series of 5-halogenated derivatives of 1-(2-deoxy-2-fluoro- β -D-ribofuranosyl)uracils and 1-(2-deoxy-2-fluoro- β -D-arabinofuranosyl)uracils were selected for preliminary evaluation as potential non-invasive probes for HSE.

The chemical structures for 1-(2-deoxy-2-fluoro- β -D-ribofuranosyl)-5-iodouracil (FIRU, 13), 1-(2-deoxy-2-fluoro- β -D-ribofuranosyl)-5-bromouracil (FBRU, 14), 1-(2-deoxy-2-fluoro- β -D-ribofuranosyl)-5-chlorouracil (FCRU, 15), 1-(2-deoxy-2-fluoro- β -D-ribofuranosyl)-5-fluorouracil (FFRU, 16), 1-(2-deoxy-2-fluoro- β -D-arabinofuranosyl)-5-iodouracil (FIAU, 17), 1-(2-deoxy-2-fluoro- β -D-arabinofuranosyl)-5-bromouracil (FBAU, 18), 1-(2-deoxy-2-fluoro- β -D-arabinofuranosyl)-5-chlorouracil (FCAU, 19) and 1-(2-deoxy-2-fluoro- β -D-arabinofuranosyl)-5-fluorouracil (FFAU, 20) are shown in Fig. 21. Compounds 13 to 16 were recently synthesised by Dr. J. R Mercer at the Faculty of Pharmacy, University of Alberta (239). [5-¹³¹I]-FIRU, [5-¹²⁵Br]-FBRU, [2-¹⁴C]-FCRU and [2-¹⁴C]-FFRU were evaluated as potential diagnostic agents in oncology (239). [2-¹⁴C]-FCRU and [2-¹⁴C]-FFRU showed selective accumulation in tumor tissue with a tumor to blood ratio of 4.2 and 10.3 at 4 h after injection respectively. Renal excretion studies for [5-¹³¹I]-FIRU, [5-¹²⁵Br]-FBRU, [2-¹⁴C]-FCRU and [2-¹⁴C]-FFRU in mice indicated that the unmetabolised nucleoside was the major radioactive component present in urine up to 8 h after injection for all four compounds. These results indicated that ribofuranosyl nucleosides 13 to 16 possess high



X	Compound
I	FIRU 13
Br	FBRU 14
Cl	FCRU 15
F	FFRU 16



X	Compound
I	FIAU 17
Br	FBAU 18
Cl	FCAU 19
F	FFAU 20

Fig. 21 Chemical Structures for 1-(2-deoxy-2-fluoro- β -D-ribofuranosyl)-5-halouracils and 1-(2-deoxy-2-fluoro- β -D-arabinofuranosyl)-5-halouracils

in vivo stability (239). The antiviral activity of compounds 13 to 16 has not been reported whereas compounds 17 to 20 have been reported to exhibit pronounced inhibitory activity against HSV-1 (Table 14) (135,240). The biochemical aspects of their (compounds 17 to 20) antiviral activity have already been discussed in Chapter I. Metabolic studies of the related compounds 1-(2-deoxy-2-fluoro- β -D-arabinofuranosyl)-5-iodocytosine (FIAC) and 1-(2-deoxy-2-fluoro- β -D-arabinofuranosyl)-5-methyluracil (FMAU) have demonstrated resistance to *in vivo* phosphorolytic cleavage (241).

The presence of a halogen atom at the 5-position of the nucleosides 13 to 20 offers the possibility for radiohalogenation. Thus, FFRU and FFAU, if found useful as *in vivo* biochemical probes for HSE, could be labeled with ^{18}F to develop a PET scan for HSE. A radiochemical synthesis of [5- ^{18}F]-FFRU has been developed by Dr. J. R. Mercer (239). It is quite likely that this method would also be suitable for the synthesis of [5- ^{18}F]-FFAU. FBRU and FBAU, if labeled with ^{75}Br may also hold promise as PET radiopharmaceuticals. Radioiodination reactions suitable for incorporation of ^{123}I into FIRU and FIAU have been developed by Drs. J. R. Mercer (239) and H. K. Misra (242) at the Faculty of Pharmacy, University of Alberta, which offer the possibility for developing SPECT imaging for HSE. At the present time, chlorine isotopes are not used in clinical nuclear medicine. However compounds 15 and 19 may be useful in developing structure activity relationships for the selective uptake of nucleoside analogs by HSV-infected cells.

The selective uptake of compounds 13, 15, 16 and 17 has been evaluated in HSV-1-infected cells *in vitro*. Confluent PRK cells in 60 mm-Petri dishes were infected with 6×10^6 PFU of HSV-1 (TK⁺), HSV-1 (TK⁻) or were mock infected. After a 7 h incubation, a known quantity of radiolabeled nucleoside ([5- ^{131}I]-FIRU, specific activity 20.4 GBq mmol⁻¹, total activity 1.33 KBq ; [2- ^{14}C]-FCRU, specific activity 1.86 GBq mmol⁻¹, total activity 1.17 KBq ; [2- ^{14}C]-FFRU, specific activity 1.86 GBq mmol⁻¹, total activity 1.17 KBq ; [5- ^{131}I]-FIAU, specific activity 111 GBq mmol⁻¹, total activity 1.33 KBq) was added to each Petri dish. The final volume of the media contained in each dish was 2 mL. The Petri dishes

Table 14. *In Vitro* Anti-HSV Activity of Some 5-Halogenated
1-(2-deoxy-2-fluoro- β -D-arabinofuranosyl)uracils (135, 240)

Compound	Anti-HSV-1 Activity ID ₉₀ (μ M) ¹	Cytotoxicity TD ₅₀ (μ M) ²
FIAU 17	0.04	0.7
FBAU 18	0.08	0.7
FCAU 19	0.2	1.0
FFAU 20	0.02	0.07

¹ Concentration required to inhibit HSV-1 replication by 90%

² Concentration required for 50% inhibition of growth in Vero cells.

were incubated at 37° C until the cells were removed for radioactive counting. Intracellular and extracellular radioactivities were quantitated at 30 min, 1, 2, 4, 6, 10, and 24 h respectively after addition of the radiolabeled nucleoside. Five HSV-1 (TK⁺)-infected, four HSV-1 (TK⁻)-infected, and four mock-infected dishes were quantitated for the intracellular radioactivity.

The cellular uptake responses for [5-¹³¹I]-FIRU, [2-¹⁴C]-FCRU, [2-¹⁴C]-FFRU and [5-¹³¹I]-FIAU are shown in Figs 22, 23, 24 and 25 respectively. The uptake is presented as a % of the total activity added (mean and range for each time point is shown). The uptake of radiolabeled nucleoside in HSV-1 (TK⁺)-infected cells for all four nucleosides increased with increasing time of exposure of cells to the drug for a period of 24 h. Uptake in HSV-1 (TK⁻)-infected and mock-infected cells remained low (usually less than 2%) at all times for all four radiolabeled nucleosides evaluated. These results suggest that uptake by HSV-1 (TK⁺)-infected cells was selective and mediated by HSV-1-encoded TK. The percent uptake of [5-¹³¹I]-FIRU, [2-¹⁴C]-FCRU, [2-¹⁴C]-FFRU and [5-¹³¹I]-FIAU in HSV-1 (TK⁺)-infected cells for a 4 and 24 h incubation of cells with the nucleoside is shown in Table 15. The nucleoside which demonstrated the highest uptake at the 4 h (27.1%) and 24 h (58.5%) incubation periods was [¹³¹I]-FIAU. The rapid and selective uptake of [¹³¹I]-FIAU in HSV-1 (TK⁺)-infected cells is consistent with the potent anti-HSV activity (ID₅₀ 0.1 μM for HSV-1, Table 4) and high affinity of HSV-1-encoded TK (K_i 0.68 μM) reported for FIAU (59). [2-¹⁴C]-FFRU showed the lowest percent uptake both at 4 h (7.8%) and 24 h (17.7%).

The uptake studies of radiolabeled nucleosides in HSV-infected cells *in vitro* is intended to be first of several screening tests designed to identify a nucleoside analog having optimal biological characteristics suitable as a radiopharmaceutical for HSE diagnosis. Subsequent screening tests proposed include *in vitro* metabolism by blood platelets, *in vivo* pharmacokinetic and metabolism studies, tissue distribution and quantitative autoradiographic studies in HSV-1-infected animal models and tomographic brain imaging in a non-human primate model such as the monkey. The final stage of these investigations is expected to be the clinical

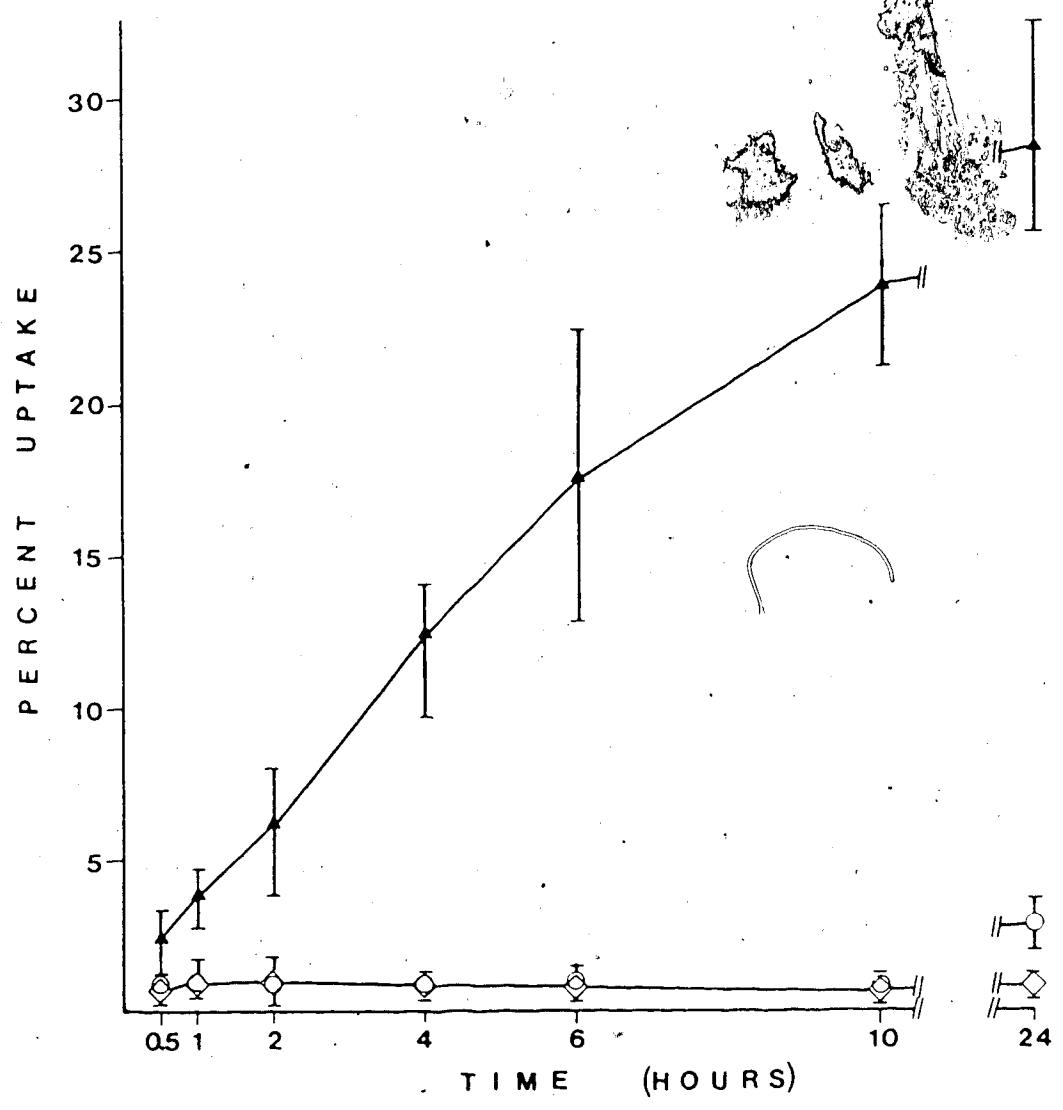


Fig. 22 *In Vitro* Uptake of [5-¹³¹I]-FIRU in HSV-1 (TK⁺) (n=5) (▲), HSV-1 (TK⁻) (n=4) (○), and Mock-Infected Cells (n=4) (◇) (Mean and Range)

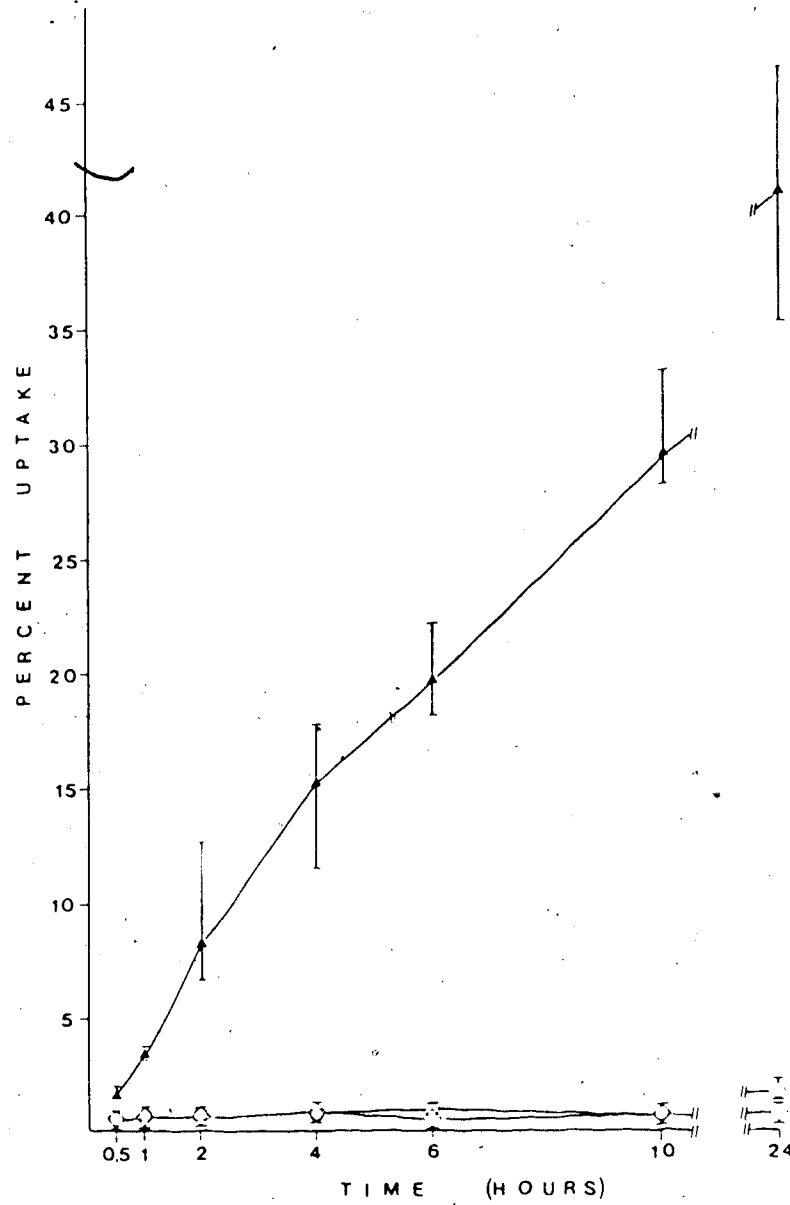


Fig. 23 *In Vitro* Uptake of $[2\text{-}^{14}\text{C}]$ -FCRU in HSV-1 (TK⁻) ($n=5$) (\blacktriangle), HSV-1 (TK⁺) ($n=4$) (\circ), and Mock-Infected Cells ($n=4$) (\square) (Mean and Range)

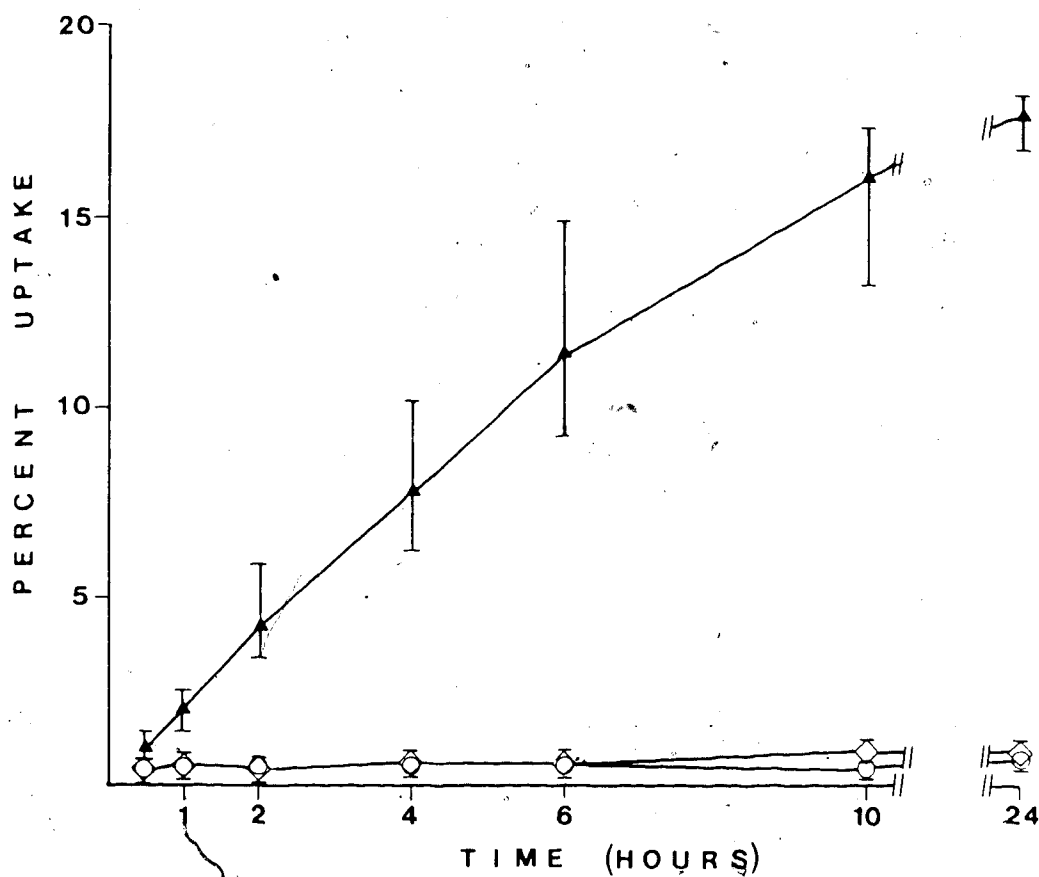


Fig. 24 *In Vitro* Uptake of [2-¹⁴C]-FFRU in HSV-1 (TK⁻) ($n=5$) (\blacktriangle), HSV-1 (TK⁻) ($n=4$) (\circ), and Mock-Infected Cells ($n=4$) (\square) (Mean and Range)

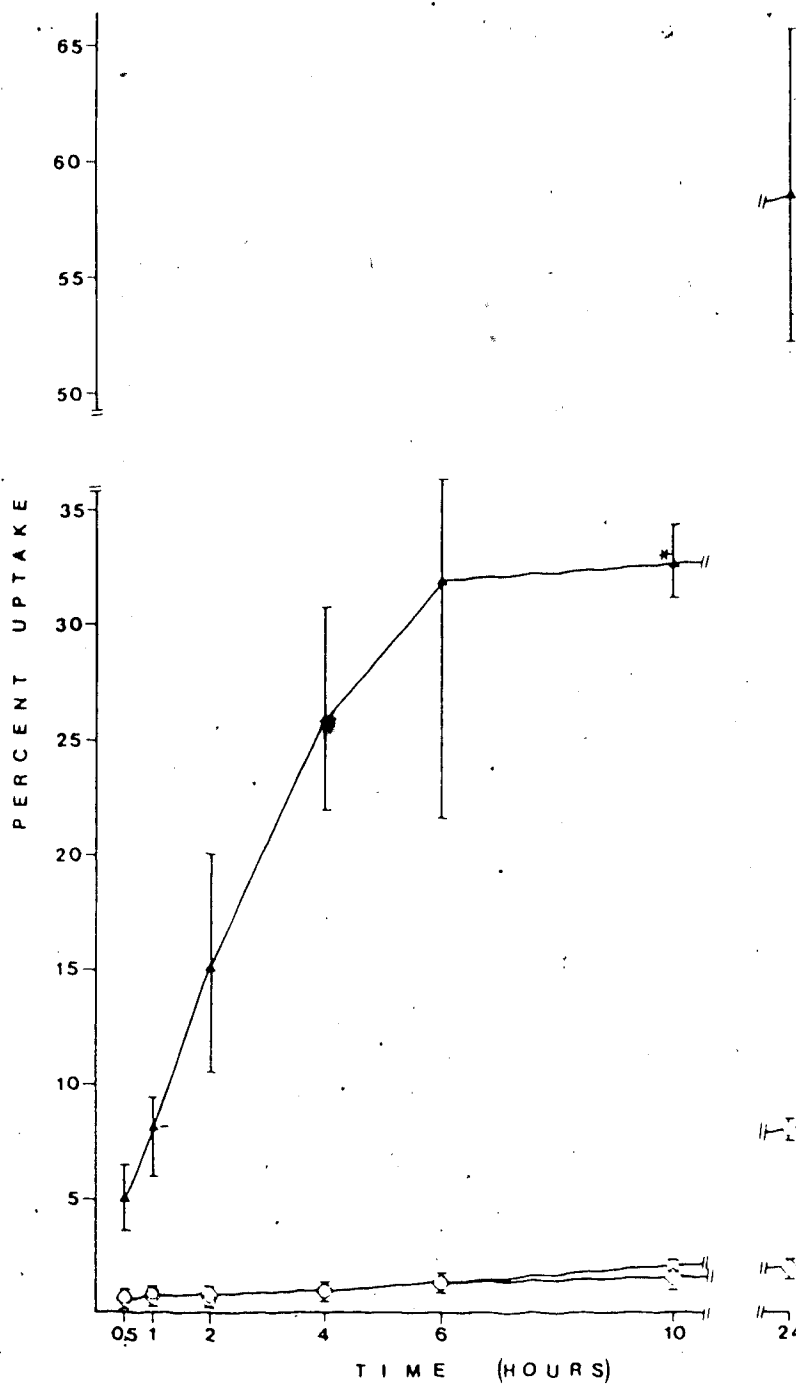


Fig. 25. *In Vitro* Uptake of [5-¹³¹I]-FIAU in HSV-1 (TK⁺) ($n=5$) (\blacktriangle), HSV-1 (TK⁻) ($n=4$) (\circ), and Mock-Infected Cells ($n=4$) (\square) (Mean and Range)

* $n = 2$

Table 15. Percent Uptake of Radiolabeled Nucleoside Analogs in HSV-1 (TK⁻)-Infected cells at 4 h and 24 h (Mean and Range, *n*=5)

Compound	Percent Uptake	
	4 h	24 h
[5- ¹³¹ I]-FIRU 13	12.5 (9.8-14.5)	28.5 (25.6-32.5)
[2- ¹⁴ C]-FCRU 15	15.3 (11.4-17.9)	41.0 (25.3-46.3)
[2- ¹⁴ C]-FFRU 16	7.8 (6.2-10.2)	17.7 (16.7-18.1)
[5- ¹³¹ I]-FIAU 17	27.1 (22.1-31.0)	58.5 (52.1-66.1)

evaluation of the nucleoside(s), showing most favourable characteristics in these screening tests, in HSE patients using tomographic brain imaging. .

IV. SUMMARY AND CONCLUSIONS

The aim of this study was to develop radiohalogenated nucleoside analogs as non-invasive diagnostic agents for HSE. Investigations in this direction included chemical and radiochemical syntheses of nucleosides, *in vitro* uptake studies of radiolabeled nucleosides in HSV-infected cells, and *in vivo* evaluation of a radiolabeled nucleoside involving tissue distribution, pharmacokinetic, metabolic and diagnostic imaging studies in animal models.

The objectives of the chemical syntheses were to prepare nucleoside analogs as reference compounds for radiochemical and metabolism studies and to explore synthetic routes suitable for radiochemical syntheses. IVdU and BVdU were synthesised from (*E*)-5-(2-carboxyvinyl)-2'-deoxyuridine using the N-halosuccinimide method in 30.4 and 42% yield respectively. Alternatively, IVdU and BVdU were also prepared by the chloramine-T method (26.3 and 18% respectively), a procedure suitable for radiochemical syntheses. The products obtained using the chloramine-T method were shown to be identical to the corresponding compound obtained employing the N-halosuccinimide method.

IVdU-3',5'-diacetate was prepared from

(*E*)-5-(2-carboxyvinyl)-2'-deoxyuridine-3',5'-diacetate using the N-iodosuccinimide method in 41.0% yield. (*E*)-5-(2-iodovinyl)uracil (IVU) was prepared from

(*E*)-5-(2-carboxyvinyl)uracil employing the chloramine-T method in 10.0% chemical yield.

The identity of all compounds described above was established by spectroscopic analysis (¹H NMR, UV and MS).

The two reactions investigated for the synthesis of radioiodinated IVdU were the chloramine-T and halogen isotope exchange method. [¹³¹I, ¹²⁵I, and ¹²³I]-IVdU were synthesised by the chloramine-T method (30 min to 1 h reaction time, 40.7 to 67.2% radiochemical yield, 57 to 69.0% chemical yield). The synthesis of [¹³¹I]-IVdU using the halogen isotope exchange method required a longer reaction time (20 h) and gave lower yields (45.1% radiochemical yield and 54.3% chemical yield). The halogen isotope exchange method is limited to the preparation of low and medium specific activity compounds and is not suitable

for ^{123}I synthesis. [^{131}I]-IVdU-2',5'-diacetate was synthesised by the chloramine-T method in 50% radiochemical yield. [^{82}Br]-BVdU was synthesised by the chloramine-T method (10 min reaction time, 69.8% radiochemical yield, 72% chemical yield). The chloramine-T method employed for radiobromination is suitable for the synthesis of [^{75}Br]-BVdU. [^{82}Br]-BVdU was also prepared by direct neutron activation of BVdU containing natural abundance bromine (^{79}Br and ^{81}Br) (30.0% radiochemical yield and 97.0% chemical recovery, specific activity 31.82 MBq mmol $^{-1}$). The direct neutron activation of BVdU is limited to the low specific activity synthesis of [^{82}Br]-BVdU.

Quantitative uptake studies of [^{131}I]-IVdU in HSV-infected cells *in-vitro* demonstrated selective trapping of [^{131}I]-IVdU in HSV-1 (TK $^{+}$)-infected cells. The uptake was dependent on the duration of exposure of cells to [^{131}I]-IVdU, the infecting dose of the virus, and the concentration of [^{131}I]-IVdU in the medium. The observation that the exposure of cells to [^{131}I]-IVdU for 30 min to 1 h was sufficient to differentiate the HSV-1 (TK $^{+}$)-infected cells from HSV-1 (TK $^{-}$)- and mock-infected cells suggested that a nucleoside analog having a relatively fast excretion or metabolism may be used as a radiopharmaceutical for the diagnosis of HSE. The effect of the virus infecting dose on the uptake of [^{131}I]-IVdU suggested that at least 1 in 50 cells need to be infected with HSV-1 before an infected brain could be differentiated from a normal brain by using a radiolabeled nucleoside. The effect of increasing concentrations of [^{131}I]-IVdU on its uptake suggested that a medium specific activity sample of radiolabeled nucleoside may be satisfactorily used as a radiopharmaceutical for HSE diagnosis.

Tissue distribution studies for [^{123}I]-IVdU in a rabbit model showed 5.4 to 6.4 times higher uptake in HSV-1-infected brain relative to uninfected brain 1 h after i.v. injection of the drug. However, radioactivity in blood was 2 to 10 times higher than that in brain at 1 h. This presents a problem in diagnostic imaging since the high blood activity may obscure any selective uptake in the infected brain.

Pharmacokinetic and metabolic studies for [^{131}I]-IVdU in dogs have shown a very rapid metabolic degradation of [^{131}I]-IVdU. The major catabolic pathway of [^{131}I]-IVdU in blood *in*

in vitro was phosphorolysis of the nucleoside to the corresponding base [^{131}I]-IVU (73% of the total radioactivity in blood at 2 h). The major radioactive components resulting from *in vivo* metabolism of [^{131}I]-IVdU were [^{131}I]-IVU and [^{131}I]-iodide. Both [^{131}I]-IVdU and [^{131}I]-IVU appeared to undergo deiodination *in vivo*. The biological half-life of [^{131}I]-IVdU was less than 3 min. [^{131}I]-IVdU-3',5'-diacetate, in preliminary *in vivo* evaluation, did not demonstrate any advantage over [^{131}I]-IVdU with respect to pharmacokinetic characteristics. The renal excretion of the radioactivity was extremely slow (8% of the total radioactivity was recovered in urine over a period of 8 h). The rapid *in vivo* metabolism of [^{131}I]-IVdU into radioactive components having slow excretion characteristics suggested that radioiodinated IVdU is unlikely to be useful as a brain imaging agent for the diagnosis of HSE.

A series of radiolabeled 1-(2-deoxy-2-fluoro- β -D-ribofuranosyl)-5-halouracils and 1-(2-deoxy-2-fluoro- β -D-arabinofuranosyl)-5-halouracils (halogen = I, Br, Cl, F) have been proposed as potential candidates for preliminary evaluation as radiopharmaceuticals for HSE. Quantitative *in vitro* uptake studies for [$^5\text{-}^{131}\text{I}$]-1-(2-deoxy-2-fluoro- β -D-ribofuranosyl)-5-iodouracil (FIRU), [$^2\text{-}^{14}\text{C}$]-1-(2-deoxy-2-fluoro- β -D-ribofuranosyl)-5-chlorouracil (FCRU), [$^2\text{-}^{14}\text{C}$]-1-(2-deoxy-2-fluoro- β -D-ribofuranosyl)-5-fluorouracil (FFRU), and [$^5\text{-}^{131}\text{I}$]-1-(2-deoxy-2-fluoro- β -D-arabinofuranosyl)-5-iodouracil (FIAU) have demonstrated selective uptake of all four compounds in HSV-1 (TK⁺)-infected cells. The highest uptake was shown by [$^5\text{-}^{131}\text{I}$]-FIAU (27.1% at 4 h and 58.5% at 24 h).

Based on these investigations a general outline may be drawn for the evaluation of radiolabeled nucleoside analogs as non-invasive diagnostic agents for HSE.

1. *In vitro* uptake studies in HSV-infected cells.
2. *In vitro* evaluation of phosphorolysis using whole blood or blood platelets.
3. *In vivo* pharmacokinetic and metabolic studies.
4. Tissue distribution quantitative autoradiographic studies in a HSE animal model such as rabbits or rats.

5. Diagnostic imaging in the tomographic mode in an HSE animal model having a large brain
(eg: monkey)

These screening procedures would be expected to identify the nucleoside(s) having favourable biological characteristics suitable for a radiopharmaceutical for the diagnosis of HSE.

REFERENCES

1. Moore, G. E. 1948. Use of radioactive diiodofluorescein in the diagnosis and localization of brain tumors. *Science* 107:569-571.
2. Cassen, B., L. Curtis, and C. Reed. 1950. A sensitive directional gamma ray detector. *Nucleonics* 6:78-81
3. Cassen, B., L. Curtis, C. Reed, and R. Libby. 1951. Instrumentation for ¹³¹I use in medical studies. *Nucleonics* 9:46-50.
4. Newell, R. R., W. Saunders, and E. Miller. 1952. Multichannel collimators for gamma ray scanning with scintillation counters. *Nucleonics* 10:36-40.
5. Anger, H. O. 1958. Scintillation camera. *Rev. Scient. Instrum.* 29:27-33.
6. Harper, P. V., R. Beck, D. Charleston, and K. A. Lathrop. 1964. Optimization of a scanning method using Tc-99m. *Nucleonics* 22:50-54.
7. Kuhl, D. E., and R. Q. Edwards. 1963. Image separation radioisotope scanning. *Radiology* 80:653-662.
8. Hounsfield, G. N. 1973. Computerized transverse axial scanning (tomography). Part 1. Description of system. *Brit. J. Radiol.* 46:1016-1022.
9. Ambrose, J. 1973. Computerized transverse axial scanning (tomography): Part 2. Clinical application. *Brit. J. Radiol.* 46:1023-1047
10. Ter-Pergossian, M. M. 1977. Basic principles of computed axial tomography. *Sem. Nucl. Med.* 7:109-127.
11. Hendee, W. R. 1983. The physical principles of computed tomography, p 1-192. Little, Brown and Company, Toronto.
12. Phelps, M. E. 1977. What is the purpose of emission computed tomography in nuclear medicine. *J. Nucl. Med.* 18:399-401.
13. Shaw Dunn, J., and G. M. Wyburn. 1972. The anatomy of the blood brain barrier : a review. *Scot. Med. J.* 17:21-36.
14. Phelps, M. E. 1981. Positron computed tomography studies of cerebral glucose metabolism in man : theory and application in nuclear medicine. *Sem. Nucl. Med.* 11:32-49.
15. Bidder, T. G. 1968. Hexose translocation across blood-brain interface : configurational aspects. *J. Neurochem.* 15:867-874.
16. Oldendorf, W. H. 1971. Brain uptake of radiolabeled aminoacids, amines, and hexoses after arterial injection. *Am. J. Physiol.* 221:1629-1638.
17. Garnett, E. S., G. Firnau, F. C. Nahmias, S. Sood, and L. Belbeck. 1980. Blood-brain barrier transport and cerebral utilization of dopa in living monkeys. *Am. J. Physiol.*

238:R318-R327.

18. Garnett, E. S., G. Firnau, and F. C. Nahmias. 1983. Dopamine visualised in the basal ganglia of the living man. *Nature* 305:137-138.
19. Levin, V. A., 1980. Relationship of octanol/water partition coefficient and molecular weight to rat brain capillary permeability. *J. Med. Chem.* 23:682-684.
20. Dischino, D., M. J. Welch, M. R. Kilbourn, and M. E. Raichle. 1983. Relationship between lipophilicity and brain extraction of ^{11}C -labeled radiopharmaceuticals. *J. Nucl. Med.* 24:1030-1038.
21. Phelps, M. E., S. C. Huang, E. J. Hoffman, C. Selin, L. Sokoloff, and D. E. Kuhl. 1979. Tomographic measurement of local cerebral glucose metabolic rate in humans with [^{18}F]-2-fluoro-2-deoxy-D-glucose : validation of method. *Ann. Neurol.* 6:371-388.
22. Gallagher, B. M., J. S. Fowler, N. I. Gutterson, R. R. MacGregor, C.-N. Wang, and A. P. Wolf. 1978. Metabolic trapping as a principle of radiopharmaceutical design : some factors responsible for the biodistribution of [^{18}F]-2-deoxy-2-fluoro-D-glucose. *J. Nucl. Med.* 19:1154-1161.
23. Bessell, E. M., A. B. Foster, and J. H. Westwood. 1972. The use of deoxyfluoro-D-glucopyranoses in a study of yeast hexokinase specificity. *Biochem. J.* 128:199-204.
24. Bessell, E. M., and P. Thomas. 1973. The effect of substitution of C-2 of D-glucose-6-phosphate on the rate of dehydrogenation by glucose phosphate dehydrogenase (from yeast and from rat liver). *Biochem. J.* 131:83-89.
25. Bessell, E. M., and P. Thomas. 1973. The deoxyfluoro-D-glucopyranose-6-phosphates and their effect on yeast glucose phosphate isomerase. *Biochem. J.* 131:77-82.
26. Hers, H. G., and C. De Duve. 1950. Le systeme phosphatasique : repartition de l'activite glucose-6-phosphatasique dan les tissus. *Bull. Soc. Chem. Biol.* 32:20-29.
27. Raggi, F., D. S. Kronfeld, and M. Kleiber. 1960. Glucose-6-phosphatase activity in various sheep tissues. *Proc. Soc. Exp. Biol. Med.* 105:485-486.
28. Sokoloff, L. 1981. Localization of functional activity in the central nervous system by measurement of glucose utilization with radioactive deoxyglucose. *J. Cereb. Blood Flow Metabol.* 1:7-36.
29. Alavi, A., M. Reivich, J. H. Greenberg, and A. P. Wolf: 1982. Positron emission tomography of the brain, p. 134-187. In P. J. Ell, and B. L. Holman (ed.), *Computed Emission Tomography*. Oxford University Press, New York.
30. Comar, D., E. Zarifan, M. Verhas, F. Soussaline, M. Maziere, G. Berger, H. Loo, H. Cuche, C. Kellersohn, and P. Deniker. 1979. Brain distribution and kinetics of ^{11}C -chlorpromazine in schizophrenics : positron emission tomography studies. *Psychiat. Res.* 1:23-29.
31. Comar, D., M. Mazierie, J. M. Godot, G. Berger, F. Soussaline, C. H. Menini, G. Artel, and G. Naguet. 1979. Visualization of ^{11}C -flunitrazepam displacement in the brain of the live baboon. *Nature* 280:329-331.

32. Rosen, B. R., and T. J. Brady. 1983. Principles of nuclear magnetic resonance for medical application. *Sem. Nucl. Med.* 13:308-318.
33. Buonanno, F. S., J. P. Kristler, L. D. De Witt, K. R. Davis, R. De Lapaz, P. F. J. New, C. T. Burt, and T. J. Brady. 1983. Nuclear magnetic imaging in central nervous system diseases. *Sem. Nucl. Med.* 13:329-338.
34. Fenner, F. 1976. The classification and nomenclature of viruses. Summary of results of meetings of the international committee on taxonomy of viruses in Madrid, September 1975. *Virology* 71:371-378.
35. Roizman, B. 1965. An enquiry into the mechanism of recurrent herpes infections of man. *Perspect. Virol.* 4:283-301.
36. Baringer, J. R. 1975. Herpes virus infections of nervous tissue in animals and man. *Progr. Med. Virol.* 20:1-26.
37. Stevens, J. G. 1975. Latent herpes simplex virus and nervous system. *Curr. Top. Microbiol. Immunol.* 70:31-50
38. Klein, R. J. 1976. Pathogenetic mechanisms of recurrent herpes simplex virus infections. *Arch. Virol.* 51:1-13.
39. Klein, R. J. 1982. The pathogenesis of acute, latent and recurrent herpes simplex virus infections. *Arch. Virol.* 72:143-168.
40. Cook, M. J., and J. G. Stevens. 1973. Pathogenesis of herpetic neuritis and ganglionitis in mice : evidence of intra-axonal transport of infection. *Infect. Immun.* 7:272-288.
41. Kristensson, K., B. Ghetti, and H. M. Wisnieski. 1974. Study on the propagation of herpes simplex virus (type 2) into the brain after intraocular injection. *Brain Res.* 69:189-201.
42. Kristensson, K., A. Vahlne, L. A. Persson, and E. Lycke. 1978. Neural spread of herpes simplex virus type 1 and 2 in mice after corneal or subcutaneous (footpad) inoculation. *J. Neurol. Sci.* 35:331-340.
43. Cook, M. L., and J. G. Stevens. 1976. Latent herpetic infections following experimental viremia. *J. Gen. Virol.* 31:75-80.
44. Field, H. J., and T. J. Hill. 1974. The pathogenesis of pseudorabies in mice following peripheral inoculation. *J. Gen. Virol.* 23:145-157.
45. Ritchie, D. A., and M. C. Timburry. 1980. Herpes viruses and latency : possible relevance of the structure of the viral genome. *FEMS Microbiol. Letters* 9:67-72.
46. Wheeler, C. E. 1975. Pathogenesis of recurrent herpes simplex infections. *J. Invest. Dermatol.* 64:341-346.
47. Hill, T. J., and W. A. Blyth. 1976. An alternate theory of herpes simplex recurrence and a possible role of prostaglandins. *Lancet* i:397-398.
48. Blyth, W. A., T. J. Hill, H. J. Field, and D. A. Harbour. 1976. Reactivation of herpes simplex infection by ultraviolet light and possible involvement of prostaglandins. *J. Gen.*

Viol. 33:547-550.

49. Harbour, D. A., W. A. Blyth, and T. J. Hill. 1978. Prostaglandins enhance spread of herpes simplex virus in cell cultures. *J. Gen. Virol.* 41:87-95.
50. Kit, S., W.-C. Leung, G. N. Jorgensen, D. Trakula, and D. R. Dubbs. 1975. Viral-induced thymidine kinase isoenzymes. *Progr. Med. Virol.* 21:13-34.
51. Kit, S., W.-C. Leung, and D. Trakula. 1974. Properties of thymidine kinase enzymes isolated from mitochondrial and cytosolic fractions of normal, bromodeoxyuridine-resistant, and virus-infected cells, p. 103-145. In M. A. Mehlman, and R. W. Hanson (ed.), *Control Processes in Neoplasia*. Academic Press Inc., New York.
52. Kit, S., W.-C. Leung, G. N. Jørgensen, and D. R. Dubbs. 1974. Distinctive properties of thymidine kinase isoenzymes induced by human and avian herpesviruses. *Int. J. Cancer* 14:598-610.
53. Cheng, Y.-C. 1976. Deoxythymidine kinase induced by HeLa TK⁻ cells by herpes simplex virus type 1 and type 2. Substrate specificity and kinetic behaviour. *Biochim. Biophys. Acta* 452:370-381.
54. Lee, L.-S., and Y.-C. Cheng. 1976. Human deoxythymidine kinase I. Purification and general properties of the cytoplasmic and mitochondrial isoenzymes derived from blast cells of acute myelocytic leukemia. *J. Biol. Chem.* 251:2600-2604.
55. Cheng, Y. C., and M. Ostrander. 1976. Deoxythymidine kinase induced in HeLa TK⁻ cells by herpes simplex virus type I and type II. Purification and characterization. *J. Biol. Chem.* 251:2605-2610.
56. Lee, L.-S., and Y.-C. Cheng. 1976. Human deoxythymidine kinase II : substrate specificity and kinetic behaviour of the cytoplasmic and mitochondrial isoenzymes derived from blast cells of acute myelocytic leukemia. *Biochemistry* 15:3686-3690.
57. Thouless, M. E., and P. Wildy. 1975. Deoxypyrimidine kinases of herpes simplex virus type 1 and 2 : comparison of serological and structural properties. *J. Gen. Virol.* 26:159-170.
58. Orgino, T., R. Shiman, and F. Rapp. 1973. Deoxythymidine kinase from rabbit cells infected with herpes simplex type 1 or type 2. *Intervirology* 1:80-95.
59. Cheng, Y.-C., G. Dutschman, J. J. Fox, K. A. Watanabe, and H. Machida. 1981. Differential activity of potential antiviral nucleoside analogs on herpes simplex virus-induced and human cellular thymidine kinases. *Antimicrob. Agents Chemother.* 20:420-423.
60. Cheng, Y.-C., G. Dutschamn, E. De Clercq, A. S. Jones, S. G. Rahim, G. Verhelst, and R. T. Walker. 1981. Differential affinities of 5-(2-halogenovinyl)-2'-deoxyuridines for deoxythymidine kinases of various origins. *Mol. Pharmacol.* 14:2159-2169.
61. De Clercq, E. 1984. Biochemical aspects of selective antiherpes activity of nucleoside analogues. *Biochem. Pharmacol.* 33:2159-2169.
62. Murphree, S., E. C. Moore, and P. T. Beall. 1968. Regulation by nucleotide of the activity of partially purified ribonucleotide reductase from rat embryos. *Cancer Res.*

- 28:860-863.
63. Skoog, L., and B. Nordenkjold. 1971. Effects of hydroxyurea and 1- β -D-arabinofuranosyl cytosine in deoxyribonucleotide pools in mouse embryo cells. *Eur. J. Biochem.* **19**:81-89.
 64. Averett, D. R., C. Lubbers, G. B. Elion, and T. Spector. 1983. Ribonucleotide reductase induced by herpes simplex type 1 virus. Characterization of a distinct enzyme. *J. Biol. Chem.* **258**:9831-9838.
 65. Bachetti, S., M. J. Eveleigh, B. Muirhead, C. S. Sartori, and H. Huszar. 1984. Immunological characterization of herpes simplex virus type 1 and 2 polypeptide(s) involved in viral ribonucleotide reductase activity. *J. Virol.* **49**:591-593.
 66. Field, H. J., and P. Wildy. 1978. The pathogenicity of thymidine kinase-deficient mutants of herpes simplex virus in mice. *J. Hyg.* **81**:267-274.
 67. Tenser, R. B., R. L. Miller, and F. Rapp. 1979. Trigeminal ganglion infection by thymidine kinase-negative mutants of herpes simplex virus. *Science* **205**:915-917.
 68. Tenser, R. B., S. Ressel, and M. E. Dunstan. 1981. Herpes simplex virus thymidine kinase expression in trigeminal ganglion infection: correlation of enzyme activity with ganglion virus titer and evidence of *in vivo* complementation. *Virology* **112**:328-341.
 69. Weissbach, A. 1977. Eucaryotic DNA polymerases. *Ann. Rev. Biochem.* **46**:25-47.
 70. Sarangadharan, M. G., M. Robert-Guroff, and R. C. Gallo. 1978. DNA polymerases of normal and neoplastic mammalian cells. *Biochim. Biophys. Acta* **516**:419-487.
 71. Weissbach, A., S.-C. L. Hong, J. Aucker, and R. Muller. 1973. Characterization of herpes simplex virus-induced deoxyribonucleic acid polymerase. *J. Biol. Chem.* **248**:620-627.
 72. Ostrander, M., and Y.-C. Cheng. 1980. Properties of herpes simplex virus type 1 and type 2 DNA polymerases. *Biochim. Biophys. Acta.* **609**:232-245.
 73. Powell, K. L., and D. J. M. Purifoy. 1977. Non-structural proteins of herpes simplex virus I. Purification of the induced DNA polymerase. *J. Virol.* **24**:618-626.
 74. Kier, H. M., J. Hay, J. M. Morrison, and J. H. Subaksharpe. 1966. Altered properties of deoxyribonucleic acid nucleotidyl transferase after infection of mammalian cells with herpes simplex virus. *Nature* **210**:369-371.
 75. Mao, J. C.-H., E. E. Robinshaw, and L. R. Overby. 1975. Inhibition of DNA polymerase from herpes simplex virus-infected Wi-38 cells by phosphonoacetic acid. *J. virol.* **15**:1281-1283.
 76. Aron, G. M., D. J. M. Purifoy, and P. A. Schaffer. 1975. DNA synthesis and DNA polymerase activity of herpes simplex virus type 1-temperature sensitive mutants. *J. Virol.* **16**:498-507.
 77. Meyer, Jr. H. M., R. T. Johnson, I. P. Crawford, H. E. Dascomb, and N. G. Rogers. 1960. Central nervous system syndromes of "viral" aetiology - a study of 713 cases. *Am. J. Med.* **29**:334-347.
 78. Whitley, R. J., S.-J. Soong, C. Linneman, C. Liu, G. Pazin, C. A. Alford, and the

- National Institute of Allergy and Infectious Diseases (NIAID) Collaborative antiviral study group.** 1982. Herpes simplex encephalitis : clinical assesment. *J. Am. Med. Assoc.* 15:317-320.
79. **Nahmias, A. J., R. J. Whitley, A. N. Vinstine, Y. Takei, C. A. Alford, and NIAID Collaborative study group.** 1982. Herpes simplex virus encephalitis : laboratory evaluation and their diagnostic significance. *J. Infect. Dis.* 145:829-836.
 80. **Oommen, K. J., P. C. Johnson, and C. J. Ray.** 1982. Herpes simplex' type 2 virus encephalitis presenting as psychosis. *Am. J. Med.* 73:445-448.
 81. **Whitley, R. J., A. J. Nahmias, S.-J. Soong, G. G. Galasso, C. L. Fleming, and C. A. Alford.** 1980. Vidarabine therapy of neonatal herpes simplex virus infection. *Pediatrics* 66:495-501.
 82. **Whitley, R. J., S.-J. Soong, R. Dolin, G. J. Galasso, L. T. Chien, C. A. Alford, and the Collaborative study group.** 1977. Adenine arabinoside therapy of biopsy-proved herpes simplex encephalitis. *N. Engl. J. Med.* 297:289-294.
 83. **Florman, A. L., A. A. Gershon, P. P. Blacsett, and A. J. Nahmias.** 1973. Intrauterine infection with herpes simplex virus. *J. Am. Med. Assoc.* 225:129-132.
 84. **Whitley, R. J., A. D. Lakeman, A. Nahmias, and B. Roizman.** 1982. DNA restriction-enzyme analysis of herpes simplex virus isolates obtained from patients with encephalitis. *N. Engl. J. Med.* 307:1060-1062.
 85. **Buchman, T. G., T. Simpson, C. Nosal, B. Roizman, and A. J. Nahmias.** 1980. The structure of herpes simplex virus DNA and its application to molecular epidemiology. *Ann. N. Y. Acad. Sci.* 354:279-290.
 86. **Hammer, S. M., T. G. Buchman, L. J. D'Angelo, A. W. Karchmer, B. Roizman, and H. S. Hirsch.** 1980. Temporal cluster of herpes simplex encephalitis : investigation by restriction endonuclease cleavage of viral DNA. *J. Infect. Dis.* 141:436-440.
 87. **Pereira, L., E. Cassai, R. W. Honess, B. Roizman, M. Terni, and A. Nahmias.** 1976. Variability in the structural polypeptides of herpes simplex virus type 1 strains : potential application in molecular epidemiology. *Infect. Immun.* 13:211-220.
 88. **Davis, J. E., and R. T. Johnson.** 1978. An explanation for the localization of herpes simplex encephalitis. *Ann. Neurol.* 5:2-5.
 89. **Warren, K. G., S. M. Brown, Z. Wroblewska, D. Gilden, H. Koprowski, and J. Subak-Sharpe.** 1978. Isolation of latent herpes simplex virus form superior cervical and vagus ganglions of human beings. *N. Engl. J. Med.* 298:1068-1069.
 90. **Eseri, M. M.** 1982. Herpes simplex encephalitis. An immunohistological study of the distribution of viral antigen within the brain: *J. Neurol. Sci.* 54:209-226.
 91. **Twomey, J. A., C. M. Barker, G. Robinson, and D. A. Howell.** 1979. Olfactory mucosa in herpes simplex encephalitis. *J. Neurol. Neurosurg. Psychiatr.* 42:983-987.
 92. **Dinn, J. J.** 1980. Transolfactory spread of virus in herpes simplex encephalitis. *Brit. Med. J.* 281:1392.

93. Sequiera, L. W., J. C. Lennings, L. H. Carrasco, M. A. Lord, A. Curry, and R. N. P. Sutton. 1979. Detection of herpes simplex virus genome in brain tissue. *Lancet* ii:609-612.
94. Fraser, N. W., W. C. Lawrence, Z. Wroblewska, D. H. Gilden, and H. Kroprowski. 1981. Herpes simplex virus type 1 DNA in human brain tissue. *Proc. Natl. Acad. Sci. USA*. 78:6461-6465.
95. Baringer, J. R. 1974. Human herpes simplex virus infections. *Adv. Neurol.* 6:41-51.
96. Drachman, D. A., and R. D. Adams. 1962. Herpes simplex acute inclusion-body encephalitis. *Arch. Neurol.* 7:45-63.
97. Bergey, G. K., P. K. Coyle, A. Krumholz, and E. Niedermeyer. 1982. Herpes simplex encephalitis with occipital localization. *Arch. Neurol.* 39:312-313.
98. Tucker, B. A., R. C. Dockett, R. J. Whitley, and W. E. Dismukes. 1978. Herpes simplex viral encephalitis: an atypical presentation. *South. Med. J.* 71:1431-1433.
99. Dayan, A. D., W. Gooddy, M. J. G. Harrison, and P. Rudge. 1972. Brain stem encephalitis caused by herpesvirus hominis. *Brit. Med. J.* 4:405-406.
100. Chore, S. M., and J. D. Cherry. 1967. Ultrastructure of Cowdry type A inclusions. I. In herpes simplex encephalitis. *Neurology* 17:575-586.
101. Vanderhaeghen, J. J., O. Prier, and Y. Bossaert. 1966. Acute necrotizing encephalitis. Observation of herpes-like particle by electron microscopy. *Path. Europ.* 1:29-49.
102. Upton, A., and J. Gumpert. 1970. Electroencephalography in diagnosis of herpes simplex encephalitis. *Lancet* i:650-652.
103. Illis, L. S., and F. M. Taylor. 1972. The electroencephalogram in herpes simplex encephalitis. *Lancet* i:718-721.
104. Davis, J. M., K. R. Davis, G. M. Kleinman, H. S. Kirchner, and J. M. Taveras. 1978. Computed tomography of herpes simplex encephalitis with clinico-pathological correlation. *Radiology* 129:409-417.
105. Greenberg, S. B., L. Taber, E. Septimus, S. Kohl, J. Puck, and N. Byran. 1981. Computerized tomography in brain biopsy-proven herpes simplex encephalitis. Early normal results. *Arch. Neurol.* 38:58-59.
106. Karlin, C. A., R. G. Robinson, D. R. Hinthorn, and C. Liu. 1978. Radionuclide imaging in encephalitis. *Radiology* 126:181-184.
107. Kim, E. E., F. H. Deland, and J. Montebello. 1979. Sensitivity of radionuclide brain-scan and computed tomography in early detection of viral meningoencephalitis. *Radiology* 132:425-429.
108. Levine, D. P., C. B. Lauter, and A. M. Lerner. 1978. Simultaneous serum and CSF antibodies in herpes simplex virus encephalitis. *J. Am. Med. Assoc.* 240:356-360.
109. Coleman, R. M., P. D. Bailey, R. J. Whitley, H. Keyserling, and A. J. Nahmias. 1983. ELISA for the detection of herpes simplex virus antigens in the cerebrospinal fluid of patients with encephalitis. *J. Virol. Methods* 7:117-125.

110. Kaufman, H. H., and L. N. Catalano. 1979. Diagnostic brain biopsy : a series of 50 cases and a review. *Neurosurgery* 4:129-136.
111. Morawetz, R. B., R. J. Whitley, and D. M. Murphy. 1983. Experience with brain biopsy for suspected herpes encephalitis. A review of forty consecutive cases. *Neurosurgery* 12:654-657.
112. Adam, J. H., and G. E. D. Urquhart. 1977. Early diagnosis of herpes encephalitis. *N. Engl. J. Med.* 297:1288.
113. York, G. K. 1980. Herpes simplex encephalitis : biopsy or treatment? *Ann. Int. Med.* 93:506.
114. Barza, B., and S. G. Pauker. 1980. The decision to biopsy, treat or wait in suspected herpes encephalitis. *Ann. Int. Med.* 92:641-649.
115. Caplan, L. R. 1980. Brain biopsy in herpes simplex encephalitis. *N. Engl. J. Med.* 303:700.
116. Whitley, R. J., S.-J. Soong, M. S. Hirsch, A. W. Karchmer, R. Dolin., G. Galasso, J. K. Dunnick, C. A. Alford, and NIAID Collaborative Antiviral study group. 1981. Herpes simplex encephalitis : vidarabine therapy and diagnostic problems. *N. Engl. J. Med.* 304:313-318.
117. Nadel, A. M. 1981. Vidarabine therapy for herpes simplex encephalitis. The development of unusual tremor during treatment. *Arch. Neurol.* 38:384-385.
118. Kern, E. R., J. T. Richards, J. G. Overall, and L. A. Glasgow. 1981. Alteration of mortality and pathogenesis of three experimental herpesvirus hominis infections of mice with adenine arabinoside-5'-monophosphate, adenine arabinoside and phosphonoacetic acid. *Antimicrob. Agents Chemother.* 13:53-60.
119. Whitley, R. J. 1984. Treatment of herpesvirus infections. *N. Engl. J. Med.* 310:654.
120. Skoldenberg, B., M. Frosgren, K. Alestig, T. Bergstrom, L. Burman, E. Dahlqvist, A. Forkman, A. Fryden, K. Lovgren, K. Norlin, A. Norrby, E. Olding-Stenkvist, G. Steirnstedt, I. Uhnöo, and K. De Vahl. 1984. Acyclovir versus vidarabine in herpes simplex encephalitis. Randomised multicentre study in consecutive Swedish patients. *Lancet* ii:707-711.
121. De Clercq, E. 1983. Pyrimidine nucleoside analogs as antiviral agents, p. 203-231. In E. De Clercq and R. T. Walker (ed.), *Targets for the design of antiviral agents*. Plenum Press., New York.
122. Drach, J. C. 1983. Purine nucleoside analogs as antiviral agents, p. 231-258. In E. De Clercq and R. T. Walker (ed.), *Targets for the design of antiviral agents*. Plenum Press., New York.
123. Schaeffer, H. J., L. Beauchamp, P. de Miranda, G. B. Ejlertson, D. J. Bauer, and P. Collins. 1978. 9-(2-Hydroxyethoxymethyl)guanine activity against viruses of the herpes group. *Nature* 272:583-585.
124. Crumpacker, C. S., L. E. Schnipper, J. A. Zaia, and M. J. Levin. 1979. Growth inhibition of acycloguanosine of herpes viruses isolated from human infections. *Antimicrob. Agents Chemother.* 15:642-645.

125. Smee, D. S., J. C. Martin, J. P. H. Verheyden, and T. R. Mathews. 1983. Anti-herpes virus activity of acyclic nucleoside 9-(1,3-dihydroxy-2-propoxymethyl)guanine. *Antimicrob. Agents Chemother.* 23:676-682.
126. Cheng, Y.-C., E.-S. Huang, J.-C. Lin, E.-C. Mar, J. S. Pagano, G. E. Dutschman, and S. P. Grill. 1983. Unique spectrum of activity of 9-[(1,3-dihydroxy-2-propoxy)methyl]guanine against herpesviruses *in vitro* and its mode of action against herpes simplex virus type 1. *Proc. Natl. Acad. Sci. USA* 80:2767-2770.
127. Field, A. K., M. E. Davies, C. De Witt, H. C. Perry, R. Liou, J. Germershausen, J. D. Karkas, W. T. Ashton, D. B. R. Johnston, and R. L. Tolman. 1983. 9-{2-Hydroxy-1-(hydroxymethyl)ethoxymethyl}guanine : a selective inhibitor of herpes group virus replication. *Proc. Natl. Acad. Sci. USA* 80:4139-4143.
128. De Clercq, E., J. Descamps, G. Verhelst, R. T. Walker, A. S. Jones, P. F. Torrence, and D. Shugar. 1980. Comparative efficacy of antiherpes drugs against different strains of herpes simplex virus. *J. Infect. Dis.* 141:563-574.
129. Smith, K. O., K. S. Galloway, W. I. Kennell, K. K. Ogilvie, and B. K. Radatus. 1982. A new nucleoside analog, 9-[[2-hydroxy-1-(hydroxymethyl)ethoxy]methyl]guanine, highly active *in vitro* against herpes simplex virus type 1 and 2. *Antimicrob. Agents Chemother.* 22:55-61.
130. De Clercq, E., J. Descamps, P. De Somer, and R. T. Walker. 1979. (E)-5-(2-Bromovinyl)-2'-deoxyuridine : a potent and selective anti-herpes agent. *Proc. Natl. Acad. Sci. USA* 76:2947-2951.
131. De Clercq, E. 1982. Comparative efficacy of antiherpes drugs in different cell lines. *Antimicrob. Agents Chemother.* 21:661-663.
132. Reefschlager, J., P. Wutzler, K.-D. Thiel, D. Barwolff, P. Langen, M. Sprossig, and H. A. Rosenthal. 1982. Efficacy of (E)-5-(2-bromovinyl)-2'-deoxyuridine against different herpes simplex virus strains in cell culture and experimental herpes encephalitis in mice. *Antiviral Res.* 2:255-265.
133. Wingrad, J. R., A. D. Hess, R. K. Stuart, R. Sarl, and W. H. Burns. 1983. Effect of several antiviral agents on human lymphocyte function and marrow progenitor cell proliferation. *Antimicrob. Agents Chemother.* 23:593-597.
134. De Clercq, E., J. Balzarini, J. Descamps, G.-F. Huang, P. F. Torrence, D. E. Bergstrom, A. S. Jones, P. Serafinowski, G. Verhelst, and R. T. Walker. 1982. Antiviral, antimetabolic, and cytotoxic activities of 5-substituted 2'-deoxycytidine. *Mol. Pharmacol.* 21:217-223.
135. Lopez, C., K. A. Watanabe, and J. J. Fox. 1980. 2'-Fluoro-5-iodo-aracytosine, a potent and selective anti-herpesvirus agent. *Antimicrob. Agents Chemother.* 17:803-806.
136. Watanabe, K. A., T.-L. Su, R. S. Klein, C. K. Chu, A. Matsuba, and M. W. Chun. 1983. Nucleosides 123. Synthesis of antiviral nucleosides : 5-substituted 1-(2-deoxy-2-halogeno- β -D-arabinofuranosyl)cytosine and -uracils: Some structure-activity relationships. *J. Med. Chem.* 26:152-156.
137. Richards, D. M., A. A. Carmine, R. N. Brogden, R. C. Heel, T. M. Speight, and G. S. Avery. 1983. Acyclovir. A review of its pharmacodynamic properties and therapeutic

- efficacy. *Drugs* 26:378-438.
138. Jones, B. R., D. J. Coster, P. N. Fison, G. M. Thompson, L. M. Cobo, and M. G. Falcon. 1979. Efficacy of acycloguanosine (Wellcome 248U) against herpes-simplex corneal ulcers. *Lancet* i:243-244.
 139. Corey, L., A. J. Nahmias, M. E. Guinan, J. K. Benedetti, C. W. Critchlow, and K. K. Holmes. 1982. A trial of topical acyclovir in genital herpes simplex virus infections. *N. Engl. J. Med.* 306:1313-1319.
 140. Nielsen, A. E., T. Aesen, A. M. Halsos, B. R. Kinge, E. A. L. Tjøtta, K. Wikstrom, and A. P. Fiddian. 1982. Efficacy of oral acyclovir in the treatment of initial and recurrent genital herpes. *Lancet* ii:571-573.
 141. Bryson, Y. J., M. Dillon, M. Lovett, G. Acuna, S. Taylor, J. D. Cherry, B. L. Johnson, E. Wiessmeir, W. Growdon, T. Creagh-Kirk, and R. Keeney. 1983. Treatment of first episodes of genital herpes simplex virus infections with oral acyclovir. *N. Engl. J. Med.* 308:916-921.
 142. Mitchell, C. D., B. Bean, S. R. Gentry, K. E. Groth, J. R. Boen, and H. H. Balfour Jr. 1981. Acyclovir therapy for mucocutaneous herpes simplex infections in immunocompromised patients. *Lancet* i:1389-1392.
 143. Chou, S., J. G. Gallagher, and T. C. Merigan. 1981. Controlled clinical trial of intravenous acyclovir in transplant patients with mucocutaneous herpes simplex infections. *Lancet* i:1392-1394.
 144. Wade, J. C., B. Newton, C. McLaren, N. Flournoy, R. E. Keeney, and J. D. Meyers. 1982. Intravenous acyclovir to treat mucocutaneous herpes simplex virus infection after marrow transplantation. *Ann. Int. Med.* 96:265-269.
 145. Maudgal, P. C., L. Missotten, E. De Clercq, J. Descamps, and E. de Meuter. 1981. Efficacy of (E)-5-(2-bromovinyl)-2'-deoxyuridine in the topical treatment of herpes simplex keratitis. *Albrecht von Graefes Arch. Klin. Ophthalmol.* 216:261-268.
 146. De Clercq, E. 1983. The chemotherapy of herpesvirus infections with reference to bromovinyldeoxyuridine and other antiviral compounds, p. 295-315. In C. H. Stuart-Harris and J. Oxford (ed.), *Problems of antiviral therapy*. Academic Press. New York.
 147. Young, C. W., R. Schneider, B. Leyland-Jones, D. Armstrong, C. T. C. Tan, C. Lopez, K. A. Watanabe, J. J. Fox, and F. S. Phillips. 1983. Phase I evaluation of 2'-fluoro-5-iodo-1- β -D-arabinofuranosyl cytosine in immunosuppressed patients with herpesvirus infections. *Cancer Res.* 43:5006-5009.
 148. Elion, G. B., P. A. Furman, J. A. Fyfe, P. de Miranda, L. Beauchamp, and H. J. Schaeffer. 1977. Selectivity of action of an antiherpetic agent, 9-(2-hydroxyethoxymethyl)guanine. *Proc. Natl. Acad. Sci. USA* 74:5716-5720.
 149. Furman, P. A., P. de Miranda, M. H. St. Clair, and G. B. Elion. 1981. Metabolism of acyclovir in virus-infected and uninfected cells. *Antimicrob. Agents Chemother.* 20:518-524.
 150. Descamps, J., and E. De Clercq. 1981. Specific phosphorylation of (E)-5-(2-iodovinyl)-2'-deoxyuridine by herpes simplex virus-infected cells. *J. Biol. Chem.*

256:5973-5976.

151. Ayisi, N. K., E. De Clercq, R. A. Wall, H. Hughes, and S. L. Sacks. 1984. Metabolic fate of (*E*)-5-(2-bromovinyl)-2'-deoxyuridine in herpes simplex virus- and mock-infected cells. *Antimicrob. Agents Chemother.* 26:762-765.
152. Kreis, W., L. Damin, J. Colcino, and C. Lopez. 1982. *In vitro* metabolism of 1- β -D-arabinofuranosylcytosine and 1- β -2'-fluoro-arabino-5-iodocytosine in normal and herpes simplex type 1 virus-infected cells. *Biochem. Pharmacol.* 31:767-773.
153. Crumpacker, C. S., P. Chartrand, J. H. Subak-Sharpe, and N. M. Wilkie. 1980. Resistance of herpes simplex virus to acycloguanosine - genetic and physical analysis. *Virology* 105:171-184.
154. Coen, C. M., and P. A. Schaffer. 1980. Two distinct loci confer resistance to acycloguanosine in herpes simplex virus type 1. *Proc. Natl. Acad. Sci. USA* 77:2265-2269.
155. Schnipper, L. E., and C. S. Crumpacker. 1980. Resistance of herpes simplex virus to acycloguanosine : role of viral thymidine kinase and DNA polymerase loci. *Proc. Natl. Acad. Sci. USA* 77:2270-2273.
156. Field, H. J., A. McMillan, and G. Darby. 1981. The sensitivity of acyclovir-resistant mutants of herpes simplex virus to other antiviral drugs. *J. Infect. Dis.* 143:281-285.
157. Darby, G., and H. J. Field. 1981. Altered substrate specificity of herpes simplex virus thymidine kinase confers acyclovir resistance. *Nature* 289:81-83.
158. Larder, B. A., and G. Darby. 1982. Properties of a novel thymidine kinase induced by an acyclovir-resistant herpes-simplex virus type 1 mutant. *J. Virol.* 42:649-658.
159. Larder, B. A., Y.-C. Cheng, and G. Darby. 1983. Characterization of abnormal thymidine kinases induced by drug-resistant strains of herpes simplex virus type 1. *J. Gen. Virol.* 64:523-532.
160. Field, H. J., and J. Neden. 1982. Isolation of bromovinyldeoxyuridine-resistant strains of herpes simplex virus and successful chemotherapy of mice treated with one such strain using acyclovir. *Antiviral Res.* 2:243-254.
161. Chen, M. S., and W. H. Prusoff. 1978. Association of thymidylate kinase activity with pyrimidine deoxyribonucleoside kinase induced by herpes simplex virus. *J. Biol. Chem.* 253:1325-1327.
162. Chen, M. S., W. P. Summers, J. Walker, W. C. Summers, and W. H. Prusoff. 1979. Characterization of pyrimidine deoxyribonucleoside kinase (thymidine kinase) and thymidylate kinase as a multifunctional enzyme in cells transformed by herpes simplex virus type 1 and in cells infected with mutant strains of herpes simplex virus. *J. Virol.* 30:942-945.
163. Fyfe, J. A. 1982. Differential phosphorylation of (*E*)-5-(2-bromovinyl)-2'-deoxyuridine monophosphate by thymidylate kinases from herpes simplex virus type 1 and 2 and varicella zoster virus. *Mol. Pharmacol.* 21:432-437.
164. Fyfe, J. A., S. A. McKee, and P. M. Keller. 1983. Altered thymidine-thymidylate kinases from strains of herpes simplex virus with modified drug sensitivities to acyclovir and

- (*E*)-5-(2-bromovinyl)-2'-deoxyuridine. *Mol. Pharmacol.* 24:316-323.
165. Miller, W. H., and R. L. Miller. 1980. Phosphorylation of acyclovir (acycloguanosine) monophosphate by GMP kinase. *J. Biol. Chem.* 255:7204-7207.
166. Miller, W. H., and R. L. Miller. 1982. Phosphorylation of acyclovir diphosphate by cellular enzymes. *Biochem. Pharmacol.* 31:3879-3884.
167. Furman, P. A., M. H. St. Clair, J. A. Fyfe, J. L. Rideout, P. M. Keller, and G. B. Elion. 1979. Inhibition of herpes simplex virus-induced DNA polymerase activity and viral DNA replication by 9-(2-hydroxyethoxymethyl)guanine and its triphosphate. *J. Virol.* 32:72-77.
168. Allaudeen, H. S., J. W. Kozarich, J. R. Berlino, and E. De Clercq. 1981. On the mechanism of selective inhibition of herpes virus replication by (*E*)-5-(2-bromovinyl)-2'-deoxyuridine. *Proc. Natl. Acad. Sci. USA* 78:2698-2702.
169. Derse, D., Y.-C. Cheng, P. A. Furman, M. H. St. Clair, and G. B. Elion. 1981. Inhibition of purified human and herpes simplex virus-induced DNA polymerase by 9-(2-hydroxyethoxymethyl)guanine triphosphate. Effects on primer-template function. *J. Biol. Chem.* 256:11447-11451.
170. Allaudeen, H. S., J. Descamps, R. K. Sehgal, and J. J. Fox. 1982. Selective inhibition of DNA replication in herpes simplex virus-infected cells by 1-(2'-deoxy-2'-fluoro- β -D-arabinofuranosyl)-5-iodocytosine. *J. Biol. Chem.* 257:11879-11882.
171. Furman, P. A., M. H. St. Clair, and P. Spector. 1984. Acyclovir triphosphate is a suicide inactivator of herpes simplex virus DNA polymerase. *J. Biol. Chem.* 259:9575-9579.
172. Ruth, J. L., and Y.-C. Cheng. 1981. Nucleoside analogs with clinical potential in antiviral chemotherapy. The effect of several thymidine and 2'-deoxyuridine analog 5'-triphosphates on purified human (α , β) and herpes simplex virus (types 1, 2) DNA polymerases. *Mol. Pharmacol.* 20:415-422.
173. Sagi, J., A. Szabolcs, A. Szemzo, and L. Otvos. 1981. (*E*)-5-(2-bromovinyl)-2'-deoxyuridine 5'-triphosphate as a DNA polymerase substrate. *Nucleic Acids Res.* 9:6985-6994.
174. Allaudeen, H. S., M. S. Chen, J. J. Lee, E. De Clercq, and W. H. Prusoff. 1982. Incorporation of (*E*)-5-(2-halovinyl)-2'-deoxyuridines into deoxyribonucleic acids of herpes simplex virus type 1-infected cells. *J. Biol. Chem.* 257:603-606.
175. Mancini, W. R., E. De Clercq, and W. H. Prusoff. 1983. The relationship between incorporation of (*E*)-5-(2-bromovinyl)-2'-deoxyuridine into herpes simplex virus type 1 DNA with virus infectivity and DNA integrity. *J. Biol. Chem.* 258:792-795.
176. Furman, P. A., P. V. McGuirt, P. M. Keller, J. A. Fyfe, and G. B. Elion. 1980. Inhibition by acyclovir of cell growth and DNA synthesis of cells biochemically transformed with herpesvirus genetic information. *Virology* 102:420-430.
177. Sagi, J., A. Czuppon, M. Katzar, A. Szabolcs, A. Szemzo, and L. Otvos. 1982. Modified polynucleotides. VI. Properties of synthetic DNA containing the antiherpetic agent (*E*)-5-(2-bromovinyl)-2'-deoxyuridine. *Nucleic Acids Res.* 10:6051-6066.

178. Goz, B. 1978. The effects of incorporation of 5-halogenated deoxyuridine into the DNA of eukaryotic cells. *Ann. Rev. Pharmacol.* 29:249-272.
179. De Clercq, E., H. Heremans, J. Descamps, G. Verhelst, M. De Ley, and A. Billiau. 1981. Effects of (*E*)-5-(2-bromovinyl)-2'-deoxyuridine and other selective antiherpes compounds on the induction of retrovirus particles in mouse BALB/3T3 cells. *Mol. Pharmacol.* 19:122-129.
180. Cassiman, J. J., E. De Clercq, A. S. Jones, R. T. Walker, and H. Van Den Berghe. 1981. Sister chromatid exchange induced by antiherpes drugs. *Brit. Med. J.* 283:817-818.
181. Crumpacker, C. S., L. E. Schnipper, P. N. Kowalsky, and D. M. Shannon. 1982. Resistance of herpes simplex virus to adenine arabinoside and (*E*)-5-(2-bromovinyl)-2'-deoxyuridine : a physical analysis. *J. Infect. Dis.* 146:167-172.
182. Zimmerman, M., and J. Siedenbergl. 1964. Deoxyribosyl transfer I. Thymidine phosphorylase and nucleoside 2-deoxyribosyl transferase in normal and malignant tissues. *J. Biol. Chem.* 239:2618-2621.
183. Krenitsky, T. A., M. Barklay, and J. A. Jacquez. 1964. Specificity of mouse uridine phosphorylase. *J. Biol. Chem.* 239:805-812.
184. Desgranges, C., G. Razaka, M. Rabaud, and H. Bricaud. 1981. Catabolism of thymidine in human blood platelets. Purification and properties of thymidine phosphorylase. *Biochim. Biophys. Acta* 654:211-218.
185. Niedzwicki, J. G., M. H. El Kouni, S. Hsi Chu, and S. Cha. 1983. Structure-activity relationship of ligands of the pyrimidine nucleoside phosphorylase. *Biochem. Pharmacol.* 32:399-415.
186. Desgranges, C., G. Razaka, M. Rabaud, H. Bricaud, J. [redacted]rini, and E. De Clercq. 1983. Phosphorolysis of (*E*)-5-(2-bromovinyl)-2'-deoxyuridine (BVDU) and other 5-substituted 2'-deoxyuridines by purified human thymidine phosphorylase and intact blood platelets. *Biochem. Pharmacol.* 32:3583-3590.
187. Desgranges, C., G. Razaka, F. Drouillet, H. Bricaud, P. Herdewijn, and E. De Clercq. 1984. Regeneration of the antiviral drug (*E*)-5-(2-bromovinyl)-2'-deoxyuridine. *Nucleic Acids Res.* 12:2081-2090.
188. Desgranges, C., G. Razaka, H. Bricaud, and E. De Clercq. 1985. Inhibition and reversal of the degradation of the antiviral drug (*E*)-5-(2-bromovinyl)-2'-deoxyuridine *in vivo*. *Biochem. Pharmacol.* 34:405-406.
189. Friedkin, M. 1973. Thymidylate synthetase. *Adv. Enzymol.* 38:235-292.
190. Barr, P. J., N. J. Oppenheimer, and D. V. Santi. 1983. Thymidylate synthetase catalysed conversions of (*E*)-5-(2-bromovinyl)-2'-deoxyuridylate. *J. Biol. Chem.* 258:13627-13631.
191. Garret, C., Y. Wataya, and D. V. Santi. 1979. Thymidylate synthetase. Catalysis of dehalogenation of 5-bromo- and 5-iodo-2'-deoxyuridylate. *Biochemistry* 18:2798-2804.
192. Chou, T.-C., A. Fienberg, A. J. Grant, P. Vidal, U. Reichman, K. A. Watanabe, J. J. Fox, and F. S. Philips. 1981. Pharmacological disposition and metabolic fate of 2'-fluoro-5-iodo-1- β -D-arabinofuranosylcytosine in mice and rats. *Cancer Res.*

41:3336-3342.

193. North, T. W., and C. K. Mathews. 1983. Tetrahydrouridine specifically facilitates deoxycytidine incorporation into herpes simplex virus DNA. *J. Virol.* 37:987-993.
194. Fox, L., M. J. Dobersen, and S. Greer. 1983. Incorporation of 5-substituted analogs of deoxycytidine into DNA of herpes simplex-infected or transformed cells without deamination to thymidine analogs. *Antimicrob. Agents Chemother.* 23:465-476.
195. de Miranda, P., S. S. Good, H. C. Krasny, J. D. Connor, O. L. Laskin, and P. S. Lietman. 1982. Metabolic fate of radioactive acyclovir in humans. Acyclovir symposium. *Am. J. Med.* 73:215-220.
196. Bergstrom, D. E., and J. L. Ruth. 1977. Preparation of C-5 mercurated pyrimidine nucleosides. *J. Carbohydr. Nucleosides Nucleotides* 4:257-269.
197. Jones, A. S., G. Verhelst, and R. T. Walker. 1979. The synthesis of the potent anti-herpes virus agent (*E*)-5-(2-bromovinyl)-2'-deoxyuridine and related compounds. *Tetrahedron Lett.* 45:4415-4418.
198. Brossmer, R., und D. Ziegler. 1966. Zur darstellung heterocyclischer aldehyde (1,2). *Tetrahedron Lett.* 43:5253-5256.
199. Lamb, R. A., P. R. Etkind, and P. W. Choppin. 1978. Evidence for a ninth influenza viral polypeptide. *Virology* 91:60-78.
200. Saito, Y., R. W. Price, D. A. Rottenberg, J. J. Fox, T. L. Su, K. A. Watanabe, and F. S. Philips. 1982. Quantitative autoradiographic mapping of herpes simplex virus encephalitis with a radiolabeled antiviral drug. *Science* 217:1151-1153.
201. Price, R. W., Y. Saito, and J. J. Fox. 1983. Prospects for the use of radiolabelled antiviral drugs in the diagnosis of herpes simplex encephalitis. *Biochem. Pharmacol.* 32:2455-2461.
202. Saito, Y., R. Rubenstein, R. W. Price, J. J. Fox, and K. A. Watanabe. 1983. Diagnostic imaging of herpes simplex encephalitis using a radiolabeled antiviral drug: autoradiographic assessment in an animal model. *Ann. Neurol.* 15:548-558.
203. Bergstrom, D. E., and M. K. Ogawa. 1978. C-5 Substituted pyrimidine nucleosides. 2. Synthesis via olefin coupling to organopalladium intermediates derived from uridine and 2'-deoxyuridine. *J. Am. Chem. Soc.* 100:8106-8112.
204. Bergstrom, D. E. 1982. Organometallic intermediates in the synthesis of nucleoside analogs. *Nucleosides Nucleotides* 3:1-34
205. Heck, R. F. 1968. Arylation, methylation, and carboxyalkylation of olefins by group VIII metal derivatives. *J. Am. Chem. Soc.* 90:5518-5526.
206. Heck, R. F. 1969. The mechanism of arylation and carboxymethylation of olefins with organopalladium compounds. *J. Am. Chem. Soc.* 91:6707-6714.
207. Jones, A. S., S. G. Rahim, and R. T. Walker. 1981. Synthesis and antiviral properties of (*Z*)-5-(2-bromovinyl)-2'-deoxyuridine. *J. Med. Chem.* 24:759-760.
208. Frost, J. J. 1982. Pharmacokinetic aspects of the in vivo, noninvasive study of

- neuroreceptors in man. p. 25-39. *In* W. C. Eckleman (ed.), Receptor binding radiotracers, vol II. CRC press Inc., Florida.
209. Seevers, R. H., and R. E. Counsell. 1982. Radioiodination techniques for small organic molecules. *Chem. Rev.* **82**:575-590.
210. Dewanjee, M. K., and S. A. Rao. 1983. Principles of radioiodination and iodine-labeled tracers in biomedical investigations, p. 1-94. *In* G. V. S. Rayadu (ed.), Radiotracers for Medical Applications. CRC Press, Inc., Florida.
211. Stocklin, G. 1978. Bromine-77 and iodine 123 radiopharmaceuticals. *Int. J. Appl. Radiat. Isot.* **28**:131-147.
212. Hunter, W. M., and F. C. Greenwood. 1962. Preparation of iodine-131 labelled human growth hormone of high specific activity. *Nature* **194**:495-496.
213. Hadi, U. A. M., D. Malcom-Lawes, and G. Oldham. 1978. The labelling of small molecules with radioiodine. *Int. J. Appl. Radiat. Isot.* **29**:621-623.
214. Salacinski, P. R. P., J. E. C. Sykes, V. V. Clement-Jones, and P. J. Lowry. 1981. Iodination of proteins, glycoproteins, and peptides using a solid-phase oxidising agent 1,3,4,6-tetrachloro-3 α ,6 α -diphenyl glycoluril (iodogen). *Anal. Biochem.* **117**:136-146.
215. Bakker, C. N. M., F. M. Kaspersen, A. Van Langevelde, and E. J. K. Pauwels. 1981. The synthesis of ¹³¹I-iodo-2-thiouracil with iodo-gen. *Int. J. Appl. Radiat. Isot.* **31**:513-515.
216. Bakker, C. N. M., and F. M. Kaspersen. 1981. The electrophilic iodination with ¹³¹I of N₁-substituted uracils using chloramine-T as oxidant. *Int. J. Appl. Radiat. Isot.* **32**:176-178.
217. Marchalonis, J. J. 1968. An enzymatic method for the trace iodination of immunoglobulins and other proteins. *Biochem. J.* **113**:299-305.
218. Bakker C. N. M., and F. M. Kaspersen. 1979. Iodination reactions with lactoperoxidase immobilized on phenoxyacetyl cellulose. *Int. J. Appl. Radiat. Isot.* **30**:320.
219. Bovington, C. H., D. F. Maundrell, and B. Dacre. 1971. Aromatic nucleophilic exchange reactions. Part 1. Heterogeneous catalysis. *J. Chem. Soc. B.* 767-770.
220. Spevacek, V. 1973. Exchange of halogen bonded on aromatic core. Heterogeneous catalysis - I. Reaction mechanism of iodine exchange in o-iodobenzoic acid. *Tetrahedron* **29**:2285-2291.
221. Stanko, V. I., and N. G. Iroshnikova. 1979. Kinetics of isotope exchange reactions of iodine in some meta and para derivatives of iodobenzene. *J. Gen. Chem. USSR* **49**:1823-1827.
222. Tarle, M., R. Padovan, and S. Spavenli. 1978. Radioiodination of iodinated estradiol-17-diphosphates. *J. Labelled Comp. Radiopharm.* **15**:7-21.
223. Petzold, G., and H. H. Coenen 1981. Chloramine-T for "no-carrier-added" labelling of aromatic biomolecules with bromine-75, 77. *J. Labelled Comp. Radiopharm.* **18**:1319-1336.
224. Wilbur, D. S., K. W. Anderson, W. E. Stone, and H. A. O'Brien. 1982. Radiohalogenation

- of non-activated compounds via aryltrimethylsilyl intermediates. *J. Labelled Comp. Radiopharm.* 19:1171-1181.
225. Wilbur, D. S., and K. W. Anderson. 1982. Bromine chloride from N-chlorosuccinimide oxidation of bromide ion. Electrophilic addition reactions in protic and aprotic solvents. *J. Org. Chem.* 47:358-359.
226. Flanagan, R. J., B. C. Lentle, D. G. McGowan, and L. I. Wiebe. 1981. α -Halostilbenes related to diethylstilbestrol. *J. Radioanal. Chem.* 65:81-94.
227. Harbottle, G., and N. Sutin. 1959. The Szilard-Chalmers reaction in solids. *Adv. Inorg. Chem. Radiochem.* 1:267-314
228. Ford, P., R. J. Flanagan, L. I. Wiebe, I. Koslowsky, and P. Eu. Unpublished results.
229. Yacyshyn, H., D. R. Tovell, J. Samuel, E. E. Knaus, L. I. Wiebe, and D. L. Tyrrell. Manuscript in preparation.
230. Lee, Y. W., J. B. Giziewicz, E. E. Knaus, and L. I. Wiebe. 1984. Tumor uptake of radiolabelled pyrimidine bases and pyrimidine nucleosides in animal models: VII. [2- 14 C]-5-ethyl-1-(2'-deoxy- β -D-ribofuranosyl)uracil. *Int. J. Radiat. Isot.* 35:1063-1066.
231. Wasternak, C. 1981. Degradation of pyrimidines and pyrimidine analogs - pathways and mutual influences. *Pharmac. Ther.* 8:629-651.
232. Haddad, P. R., and A. L. Heckenberg. 1981. Determination of inorganic anions by high-performance liquid chromatography. *J. Chromatogr.* 300:357-394.
233. Anders, M. W. 1982. Aliphatic halogenated hydrocarbons. p. 29-49. In Jakoby, W. B., Bend, J. R., and Caldwell, J. (ed.), Metabolic basis of detoxification. Metabolism of functional groups. Academic Press, New York.
234. Prusoff, W. H., J. J. Jaffe, and H. Gunther. 1960. Studies in the mouse of the pharmacology of 5-iododeoxyuridine, an analog of thymidine. *Biochem. Pharmacol.* 3:110-121.
235. Rosowsky, A., J. E. Wright, G. Steele, and D. W. Kufe. 1981. Thymidine 5'-O-pivaloate: evidence for prodrug action in rat and rhesus monkey *Cancer Treat. Rep.* 65:93-99.
236. Ensminger, W. D., and A. Rosowsky. 1979. Thymidine 5'-O-pivaloate. A prodrug derivative of thymidine with potential application in high-dose methotrexate therapy. *Biochem. Pharmacol.* 28:1541-1545.
237. Lee, Y. W., J. Samuel, E. E. Knaus, and L. I. Wiebe. Unpublished results.
238. Sinkula, A. A., and C. Lewis. 1973. Chemical modifications of Lincomycin: synthesis and bioactivity of selected 2,7-dialkyl carbonate esters. *J. Pharm. Sci.* 62:1757-1760.
239. Mercer, J. R. 1985. Synthesis and evaluation of radiolabeled 5-halo-1-(2'-fluoro-2'-deoxy- β -D-ribofuranosyl)uracil analogs as non-invasive tumor diagnostic radiopharmaceuticals. Ph.D Thesis, University of Alberta, Edmonton, Canada.
240. Fox, J. J., C. Lopez, and K. A. Watanabe. 1981. Pyrimidine nucleosides: chemistry, antiviral and potential anticancer activities, p. 27-40. In F. G. De las Heras and S. Vega

(ed.), Medicinal Chemistry Advances. Pergamon Press, Oxford.

241. Philips, F. S., A. Feinberg, T.-C. Chou, P. M. Vidal, T. L. Su, K. A. Watanabe, and J. J. Fox. 1983. Distribution, metabolism, and excretion of 1-(2-fluoro-2-deoxy- β -D-arabinofuranosyl)thymine and 1-(2-deoxy-2-fluoro- β -D-arabinofuranosyl)-5-iodocytosine. *Cancer Res.* 43:3619-3627.
242. Misra, H. K., E. E. Knaus, and L. I. Wiebe. Manuscript in preparation.

APPENDIX

A. Yield Calculation for the $^{81}\text{Br}(n, \gamma)^{82}\text{Br}$ Nuclear Reaction

The formula for the yield calculation for a nuclear reaction is given by the equation

$$A = N_1 \phi \delta [1 - \exp(-\lambda t)]^\dagger$$

where A = the radioactivity in Bq, N_1 = the number of nuclei in the target ϕ = the flux of bombarding particle (n per cm^2 per s) δ = cross section in cm^2 and $[1 - \exp(-\lambda t)]$ is correction term for the decay of the produced radionuclide during the production reaction.

The value of N_1 is determined by the formula

$$N_1 = W \Theta N(A) / \text{MW}$$

where W = the weight of the target in g, Θ = the isotopic abundance of the target nuclei in the target material, and $N(A)$ = Avagadro's constant (6.02×10^{23} per mol) and MW = molecular weight.

For 1 mg of NH_4Br (97.8% ^{81}Br enriched)

$$N_1 = 0.001 \times 0.978 \times 6.02 \times 10^{23} / 99 = 5.947 \times 10^{18}$$

All bromine irradiations were carried out at a neutron flux of 1×10^{12} n cm^{-2} s^{-1} for 4 h. The cross section for conversion of ^{81}Br to ^{82}Br (including ^{82}Br generated from ^{82}Br) is estimated to be 5.8×10^{-24} cm^2 † Therefore theoretical yield of ^{82}Br obtained from 1 mg of NH_4Br by $^{81}\text{Br}(n, \gamma)^{82}\text{Br}$ reaction is

$$A = 5.947 \times 10^{18} \times 10^{12} \times 5.8 \times 10^{-24} [1 - \exp(-0.784)] = 2.6 \times 10^6 \text{ Bq}$$

○ Direct neutron activation of BVdU was carried out using a natural abundance bromine (Θ for $^{81}\text{Br} = 0.4931$) containing sample at a neutron flux of 1×10^{12} n cm^{-2} s^{-1} for 4 h. Theoretical yield for 1 mmol may be calculated using the formulae given above.

$$A = 6.02 \times 10^{20} \times 0.4931 \times 5.8 \times 10^{-24} [1 - \exp(-0.784)] = 1.3 \times 10^4 \text{ Bq}$$

† Data taken from C. M. Lederer, and V. S. Shirley (ed.), Table of isotopes, 7th edition. Wiley Interscience, New York.